

This electronic thesis or dissertation has been downloaded from the King's Research Portal at <https://kclpure.kcl.ac.uk/portal/>



## **Generation of deeply inspirable clouds from dry powder mixtures.**

Kassem, Nuha Mohammed

The copyright of this thesis rests with the author and no quotation from it or information derived from it may be published without proper acknowledgement.

### **END USER LICENCE AGREEMENT**



**Unless another licence is stated on the immediately following page** this work is licensed

under a Creative Commons Attribution-NonCommercial-NoDerivatives 4.0 International

licence. <https://creativecommons.org/licenses/by-nc-nd/4.0/>

You are free to copy, distribute and transmit the work

Under the following conditions:

- Attribution: You must attribute the work in the manner specified by the author (but not in any way that suggests that they endorse you or your use of the work).
- Non Commercial: You may not use this work for commercial purposes.
- No Derivative Works - You may not alter, transform, or build upon this work.

Any of these conditions can be waived if you receive permission from the author. Your fair dealings and other rights are in no way affected by the above.

### **Take down policy**

If you believe that this document breaches copyright please contact [librarypure@kcl.ac.uk](mailto:librarypure@kcl.ac.uk) providing details, and we will remove access to the work immediately and investigate your claim.

**GENERATION OF DEEPLY INSPIRABLE CLOUDS  
FROM DRY POWDER MIXTURES**

**A THESIS SUBMITTED IN PARTIAL FULFILMENT OF  
REQUIRMENTS FOR THE AWARD OF THE DEGREE OF  
DOCTOR OF PHILOSOPHY**

**BY**

**NUHA MOHAMMED KASSEM**

**1990**

**DEPARTMENT OF PHARMACY  
KING'S COLLEGE  
UNIVERSITY OF LONDON**

**BEST COPY**

**AVAILABLE**

Poor text in the original  
thesis.

Some text bound close to  
the spine.

Some images distorted

**VOLUME CONTAINS CLEAR OVERLAYS**  
**OVERLAYS SCANNED SEPERATELY AND**  
**OVER THE RELEVANT PAGE.**



## **Abstract**

### **Generation of deeply inspirable clouds from dry powder mixtures**

Dry powder aerosols are widely accepted as an effective means of drug delivery to the lungs. They are generally formulated by mixing the cohesive, micronised drug with larger carrier particles. Redispersion of the drug particles from agglomerates or carrier surface during inhalation is the most critical factor which governs the availability of the medicament to the lungs. This will depend on the mechanical stability of the powder mix and the way this is influenced by the adhesion characteristics between the drug and the carrier and the external forces required to break up the bonds formed between adhering particles.

The external forces are provided by two components: the inspiratory flow rate and the turbulence created within the inhaler as air flows through it.

To study the influence of inspiratory flow rate an apparatus was developed to permit physical characterisation of an aerosol cloud generated at flow rates ranging between 60-200 l/min, employing the principle of isokinetic sampling to collect a representative fraction of the generated aerosol. Isokinetic conditions were verified using laser doppler anemometry.

The effect of turbulence on the characteristics of an inspirable cloud was investigated and an inhaler was designed to provide high levels of turbulence with minimum resistance to air flow thus resulting in efficient de-aggregation of the powder components and allowing the patient to inhale with minimum effort.

The characteristics of an inspirable cloud were found to be highly dependent on the carrier surface properties, the particle size of both the drug and the carrier, the presence of ternary components in the mix, the drug to carrier ratio and the nature of the electrostatic charges induced on the powder component.

Since the carrier surface properties were found to be of great importance, modification of the surface of lactose was undertaken to produce a carrier with a low surface rugosity. A great increase in the respirable dose was observed with the formulation comprising the modified carrier even at low air flow rates.

Preliminary in vivo evaluation of the novel formulation and the new inhaler were performed by assessing the lung function of asthmatic patients before and after administration of the medicament. The novel formulation with a modified carrier was superior to a commercial formulation and the basic design of the inhaler proved to be efficient in redispersing the powder components.

## **ACKNOWLEDGEMENT**

I wish to express my sincere gratitude to my supervisor, Professor D. Ganderton, for initially suggesting this project , and for his guidance, help and encouragement during the course of this work.

A two years ORS award is also gratefully acknowledged.

I am very grateful to Dr. M. Yianneskis and Dr. K. Suen, at the Mechanical Engineering Department of King's College, for allowing me to use equipment for laser doppler anemometry and their help during this part of my work. Similarly, thanks are due to Dr. J. Moxham and Dr. Ann Ward at the Thoracic Medicine Department of King's College Hospital, for their help in the clinical study and for providing facilities . My thanks also go to Dr. J. Staniforth, at the Pharmacy Department of Bath University, for allowing me to use equipment for electrostatic charge determination and for the useful discussion.

Thanks are also due to, Dr. K. Ho for his initial support and the staff of the Chelsea Department of Pharmacy for their assistance.

Thanks must also go to Dr. T. Brain of the Electron Microscopy Unit for the courteous provision of so much of his time.

Finally, I am deeply indebted to my father for his financial support and to my mother, Majed, sisters and brothers for their encouragement and their moral support throughout my years of study.

**To my parents and Majed**



## **List of contents**

Title

Abstract

Acknowledgement

List of figures

List of tables

### **1 *Introduction***

#### **1.1 Physiology of the respiratory tract**

##### **1.1.1 Air flow through the respiratory tract**

#### **1.2 Inhalation therapy for respiratory diseases**

##### **1.2.1 Respiratory diseases**

##### **1.2.2 Drug treatment of respiratory diseases**

##### **1.2.3 Inhalation therapy for systemic diseases**

#### **1.3 Deposition mechanisms of inhaled particles**

##### **1.3.1 Impaction**

##### **1.3.2 Sedimentation**

##### **1.3.3 Diffusion**

##### **1.3.4 Interception**

##### **1.3.5 Electrostatic forces**

#### **1.4 Factors affecting deposition**

##### **1.4.1 Physiological factors**

##### **1.4.2 Physical properties of aerosols**

#### **1.5 Inhalation delivery systems**

##### **1.5.1 Nebulizers**

##### **1.5.2 Metered dose inhalers (MDIs)**

##### **1.5.3 Powder inhalers**

#### **1.6 Efficiency of inhalation delivery systems**

#### **1.7 Evaluation of inhalation aerosols**

- 1.7.1 *In vitro* evaluation
- 1.7.2 *In vivo* evaluation
- 1.8 Scope of the Thesis
  
- 2 ***Design and evaluation of an apparatus for sampling and characterizing an aerosol cloud***
  - 2.1 Introduction
  - 2.2 Materials and methods
    - 2.2.1 Preparation of capsules
      - Micronization of salbutamol sulphate
      - Particle size analysis
      - Classification of lactose
      - Preparation of powder mixtures
      - Filling of the capsules
    - 2.2.2 Development of an HPLC method for the determination of salbutamol sulphate
      - Method development
      - HPLC system components
      - HPLC conditions
      - Preparation of internal standard solutions
      - Preparation of standard solutions
      - Determination of salbutamol sulphate content in powder mixtures
  - 2.3 Results
    - 2.3.1 Particle size analysis
    - 2.3.2 Moisture content
    - 2.3.3 Content uniformity of the powder mixture
    - 2.3.4 HPLC analysis of salbutamol sulphate

## **2.4 Generation and sampling of an aerosol cloud**

### **2.4.1 The cascade impactor**

### **2.4.2 Apparatus A**

- 1. Design of Apparatus A**
- 2. Evaluation of Apparatus A:  
aspiration efficiency determination**

### **2.4.3 Results and discussion**

- 1 Aspiration efficiency**
- 2 Throat deposition**
- 3 Material losses**

### **2.4.4 Apparatus B**

- 1. Design of Apparatus B**
- 2. Evaluation of Apparatus B:  
aspiration efficiency determination**

### **2.4.5 Results and discussion**

- 1 Aspiration efficiency**
- 2 Material losses**

### **2.4.6 Flow visualization**

- 1 The laser anemometer optics**
- 2 Velocity and turbulence measurements**

### **2.4.7 Results and discussion**

## **3 *The effect of airflow, inhalation device and formulation variables on the inspirable characteristics of a cloud***

### **3.1 Introduction**

### **3.2 Materials and methods**

#### **3.2.1 Characterization of powders**

- 1 Classification of carriers
  - 2 Particle size analysis
  - 3 Flow properties of powders
  - 4 Tensile strength measurement
  - 5 Moisture content
  - 6 Carrier surface characterization
- 3.2.2 Preparation of capsules
- 3.2.3 Evaluation of powder aerosols
- 3.2.4 Determination of salbutamol sulphate deposited  
at various stages
- 3.3 The effect of the external forces on the  
characteristics of an inspirable aerosol cloud
  - 3.3.1 The effect of air flow rate  
Results and discussion
  - 3.3.2 The effect of turbulence
    - 1 Change in nozzle diameter
    - 2 Grid inserts
    - 3 Resistance to air flow  
Results and discussion
- 3.4 The effect of the adhesion properties of a powder  
mixture on the characteristics of an inspirable aerosol cloud
  - 3.4.1 The effect of carrier surface properties
  - 3.4.2 The effect of drug particle size
  - 3.4.3 The effect of drug concentration
  - 3.4.4 The effect of a ternary component
  - 3.4.5 The effect of carrier size
- 3.5 Electrostatic properties of powders
  - 3.5.1 Theoretical considerations



- 3.5.2 Electrostatic charge measurement
- 3.5.3 Results and discussion
- 3.6 Conclusions

#### ***4 Clinical assessment of a novel powder aerosol formulation and a newly designed inhalation device***

- 4.1 Introduction
- 4.2 Materials and methods
  - 4.2.1 Formulation
    - 1 Preparation of the novel powder aerosol formulation
    - 2 A commercial salbutamol formulation
    - 3 Microbiological test
  - 4.2.2 Inhalation devices
  - 4.2.3 Patient selection
  - 4.2.4 Study design
  - 4.2.5 Determination of the amount of drug retained in the inhalers
  - 4.2.6 Analysis of results
- 4.3 Results and discussion
  - 4.3.1 Formulation
  - 4.3.2 Inhalers
  - 4.3.3 The amount of drug retained in the inhalers
  - 4.3.4 Subjective results
- 4.4 Conclusions

#### ***References***

#### ***Appendix***

<b>List of Tables</b>	<b>Page No.</b>
<b>1.1</b> Autonomic classification of bronchodilator drugs.	<b>27</b>
<b>1.2</b> The mean fractional deposition for $^{99m}\text{Tc}$ labelled particles of SCG following inhalation from four dry powder inhalers.	<b>64</b>
<b>2.1</b> The approximate cut-off diameter for various stages of the cascade impactor.	<b>88</b>
<b>2.2</b> The diffuser and sampling tube characteristics at different flow rates in Apparatus A.	<b>91</b>
<b>2.3</b> The percentage of aerosol cloud sampled at various flow rates.	<b>95</b>
<b>2.4</b> The percentage of drug deposited at various stages and the aspiration efficiency at different points across the diffuser at flow rate of 150 l/min and a carrier size of 60-180 $\mu\text{m}$ .	<b>104</b>
<b>2.5</b> The percentage of drug deposited at various stages and the aspiration efficiency at different points across the diffuser at flow rate of 150 l/min and a carrier size of <40 $\mu\text{m}$ .	<b>105</b>
<b>2.6</b> The percentage of drug deposited at various stages and the aspiration efficiency at different points across the diffuser at a flow rate of 60 l/min and a carrier size of <40 $\mu\text{m}$ .	<b>106</b>
<b>2.7</b> The percentage of drug deposited at various stages and the aspiration efficiency at different points across the diffuser at a flow rate of 60 l/min and a carrier size of 60-180 $\mu\text{m}$ .	<b>107</b>
<b>2.8</b> Values of Reynold's Number at different flow rates in Apparatus A.	<b>108</b>
<b>2.9</b> The diffuser and sampling tube characteristics at different flow rates in Apparatus A.	<b>111</b>

<b>2.10</b>	<b>The percentage of drug deposited at various stages and the aspiration efficiency at different points across the diffuser at a flow rate of 150 l/min and a carrier size of 60-180<math>\mu</math>m.</b>	<b>116</b>
<b>2.11</b>	<b>The percentage of drug deposited at various stages and the aspiration efficiency at different positions near the walls of the diffuser at a flow rate of 150 l/min and a carrier size of 60-180<math>\mu</math>m.</b>	<b>117</b>
<b>2.12</b>	<b>The percentage of drug deposited at various stages and the aspiration efficiency at different points across the diffuser at a flow rate of 150 l/min and a carrier size of &lt;40<math>\mu</math>m.</b>	<b>118</b>
<b>2.13</b>	<b>The percentage of drug deposited at various stages and the aspiration efficiency at different points near the walls of the diffuser at an air flow of 150 l/min and a carrier size of &lt;40<math>\mu</math>m.</b>	<b>119</b>
<b>2.14</b>	<b>The percentage of drug deposited at various stages and the aspiration efficiency at a flow rate of 60 l/min with two carrier sizes.</b>	<b>120</b>
<b>2.15</b>	<b>Values of Reynold's Number within the diffuser at different flow rates in Apparatus A.</b>	<b>121</b>
<b>2.16</b>	<b>The principal characteristics of the LDA.</b>	<b>124</b>
<b>3.1</b>	<b>The flow properties of the carriers.</b>	<b>145</b>
<b>3.2</b>	<b>The percentage of drug deposited at various stages at different flow rates using unclassified lactose as a carrier.</b>	<b>150</b>
<b>3.3</b>	<b>The effect of different levels of turbulence generated by changing the nozzle diameter on the pattern of drug deposition at various stages.</b>	<b>156</b>



<b>3.4</b>	<b>Effect of inserting grids of various mesh spacing at different positions within the inhaler of 10mm nozzle diameter on the percentage of drug deposited at various stages.</b>	<b>159</b>
<b>3.5</b>	<b>Effect of inserting grids of various mesh spacing at different positions within the inhaler of 5mm nozzle diameter on the percentage of drug deposited at various stages.</b>	<b>160</b>
<b>3.6</b>	<b>Surface roughness (rugosity) of the carriers.</b>	<b>167</b>
<b>3.7</b>	<b>Effect of drug size on the pattern of drug deposition at various flow rates.</b>	<b>179</b>
<b>3.8</b>	<b>Effect of carrier size and air flow rate on the pattern of drug deposition at various flow rates.</b>	<b>194</b>
<b>3.9</b>	<b>Mean specific charges of different powders measured after flow on a perspex chute</b>	<b>204</b>
<b>3.10</b>	<b>Mean specific charges of different powders measured after flow on a brass chute.</b>	<b>205</b>
<b>3.11</b>	<b>Triboelectric series of different powders flow on a perspex chute.</b>	<b>206</b>
<b>3.12</b>	<b>Triboelectric series of different powders flow on brass chute.</b>	<b>206</b>
<b>3.13</b>	<b>Mean specific charges of powder mixtures measured after flow on a perspex chute.</b>	<b>207</b>
<b>3.14</b>	<b>Mean specific charges of powder mixtures measured after flow on a brass chute.</b>	<b>208</b>
<b>3.15</b>	<b>The sign of charge produced on the surface of different powders after flow on different materials.</b>	<b>209</b>
<b>4.1</b>	<b>Patient's characteristics.</b>	<b>225</b>



<b>List of Figures</b>	<b>Page No.</b>
<b>1.1 Schematic representation of the human respiratory tract.</b>	<b>21</b>
<b>1.2 Chemical structures of sympathomimetic bronchodilators.</b>	<b>28</b>
<b>1.3 Metabolism of isoprenaline.</b>	<b>30</b>
<b>1.4 Chemical structures of anticholinergic bronchodilators.</b>	<b>32</b>
<b>1.5 Chemical structures of Khellin and SCG.</b>	<b>35</b>
<b>1.6 Schematic representation of the mechanisms of particle deposition in the respiratory tract.</b>	<b>44</b>
<b>1.7 Schematic representation of the theoretic deposition of particles in the pulmonary tree as computed by Landahl.</b>	<b>50</b>
<b>1.8 A plot of the cumulative size distribution curve.</b>	<b>52</b>
<b>1.9 A log-probability distribution plot.</b>	<b>52</b>
<b>1.10 Design of some commercial dry powder inhalers.</b>	<b>60</b>
<b>1.11 Mean cumulative dose response curve following inhalation of terbutaline using the "Turbohaler" and salbutamol using the "Rotahaler".</b>	<b>64</b>
<b>2.1 Isokinetic sampling and anisokinetic sampling conditions.</b>	<b>74</b>
<b>2.2 Chemical structures of salbutamol and salmefamol.</b>	<b>79</b>
<b>2.3 Particle size distribution of salbutamol sulphate.</b>	<b>81</b>
<b>2.4 Calibration curve of salbutamol sulphate.</b>	<b>84</b>
<b>2.5 A typical salbutamol sulphate chromatogram.</b>	<b>85</b>
<b>2.6 Sampling configurations.</b>	<b>86</b>
<b>2.7 Andersen 1 CFM sampler and a schematic cross section.</b>	<b>87</b>
<b>2.8 Ideal and actual impaction efficiency curve shapes.</b>	<b>87</b>
<b>2.9 Apparatus A.</b>	<b>92</b>
<b>2.10 The "Rotahaler" inhalation device.</b>	<b>93</b>
<b>2.11 Diagram depicting wall losses due to overshoot of particles near jet entry.</b>	<b>102</b>

<b>2.12 Apparatus B.</b>	<b>110</b>
<b>2.13 Sampling points near the walls of the diffuser.</b>	<b>113</b>
<b>2.14 Optical arrangement of the laser doppler anemometer.</b>	<b>123</b>
<b>2.15 Signal processing system of the LDA and the output.</b>	<b>126</b>
<b>2.16 Schematic diagram of the modified flow configuration.</b>	<b>127</b>
<b>2.17 Schematic representation of the experimental condition.</b>	<b>128</b>
<b>2.18 Profiles of axial mean and r.m.s. velocities of the gas at an air flow of 150 l/min.</b>	<b>133</b>
<b>2.19 Profiles of axial mean and r.m.s. velocities of the gas and particles at an air flow of 150 l/min.</b>	<b>134</b>
<b>2.20 Profiles of axial mean and r.m.s. velocities of the gas and particles in the presence of the inhaler.</b>	<b>135</b>
<b>2.21 Time- resolved record of particle velocity after breaking of capsule.</b>	<b>136</b>
<b>3.1 The relation of log tensile strength to packing fraction for three powder samples.</b>	<b>144</b>
<b>3.2 Effect of air flow rate on the amount of drug deposited on stages 3-7 using unclassified lactose.</b>	<b>150</b>
<b>3.3 Designed inhaler.</b>	<b>153</b>
<b>3.4 Scanning electron micrographs of different carriers.</b>	<b>165</b>
<b>3.5 Scanning electron micrographs of regular lactose and recrystallized lactose.</b>	<b>166</b>
<b>3.6,7 Effect of surface properties of different carriers on the characteristics of an inspirable cloud at flow rates of 60 and 150 l/min.</b>	<b>169</b>
<b>3.8 Scanning electron micrographs of the mixtures formed by mixing the drug with different carriers.</b>	<b>170</b>

<b>3.9,10</b>	<b>Effect of surface properties of regular lactose and recrystallized lactose on the characteristics of an inspirable cloud at flow rates of 60 and 150 l/min.</b>	<b>172</b>
<b>3.11</b>	<b>Scanning electron micrographs of the powder mixture formed by mixing the drug with regular lactose and recrystallized lactose.</b>	<b>173</b>
<b>3.12</b>	<b>Scanning electron micrographs of micronized salbutamol sulphate.</b>	<b>176</b>
<b>3.13</b>	<b>Particle size distribution of the two micronized batches of salbutamol sulphate.</b>	<b>177</b>
<b>3.14,15</b>	<b>Effect of drug concentration in the powder mix on the characteristics of an inspirable cloud using carrier size of 63-90µm at flow rates of 60 and 150 l/min.</b>	<b>182</b>
<b>3.16,17</b>	<b>Effect of drug concentration in the powder mix on the characteristics of an inspirable cloud using a carrier size of &lt;20µm at air flow rates of 60 and 150 l/min.</b>	<b>183</b>
<b>3.18</b>	<b>Scanning electron micrographs of different ratios of salbutamol and the carrier.</b>	<b>185</b>
<b>3.19,20</b>	<b>Effect of the presence of ternary components in the powder mix on the characteristics of an inspirable cloud at air flow rates of 60 and 150 l/min.</b>	<b>189</b>
<b>3.21</b>	<b>Effect of air flow rate on the amount of drug deposited on stages 3-7.</b>	<b>193</b>
<b>3.22</b>	<b>Scanning electron micrographs of coarse and fine lactose.</b>	<b>196</b>
<b>3.23</b>	<b>a. Electron energy level of a metal material showing the Fermi level and work function.</b>	<b>200</b>
	<b>b. Development of contact potential between material A&amp;B.</b>	



<b>3.24</b>	<b>Front elevation of Faraday well for determining static charge on powder particles.</b>	<b>201</b>
<b>4.1</b>	<b>Lung function spirogram.</b>	<b>216</b>
<b>4.2</b>	<b>Spirometric trace of expiratory volume-time curve.</b>	<b>218</b>
<b>4.3</b>	<b>Spirometric trace of expiratory flow-volume curve.</b>	<b>218</b>
<b>4.4</b>	<b>Newly designed inhaler and the Rotahaler.</b>	<b>222</b>
<b>4.5,6</b>	<b>The mean changes in FEV1 following inhalation of the novel formulation and Ventolin.</b>	<b>227</b>
<b>4.7,8</b>	<b>The mean changes in <math>V_{\max}^{30}</math> following inhalation of the novel formulation and Ventolin.</b>	<b>228</b>
<b>4.9,10</b>	<b>The mean changes in FEV1 following inhalation with the new inhaler and the Rotahaler.</b>	<b>229</b>
<b>4.11,12</b>	<b>The mean changes in <math>V_{\max}^{30}</math> following inhalation with the new inhaler and the Rotahaler.</b>	<b>230</b>
<b>4.13,14</b>	<b>A comparison between the actual dose delivered from the new inhaler and the Rotahaler.</b>	<b>232</b>
<b>4.15,16</b>	<b>A comparison between the actual dose delivered of the novel formulation and Ventolin.</b>	<b>233</b>
<b>4.17</b>	<b>FEV1 values for each patient following inhalation of either the novel formulation or Ventolin using the Rotahaler.</b>	<b>238</b>
<b>4.18</b>	<b><math>V_{\max}^{30}</math> values for each patient following inhalation of either the novel formulation or Ventolin using the Rotahaler.</b>	<b>239</b>
<b>4.19</b>	<b>FEV1 values for each patient following inhalation of either the novel formulation or Ventolin using the new inhaler.</b>	<b>240</b>
<b>4.20</b>	<b><math>V_{\max}^{30}</math> values for each patient following inhalation of either the novel formulation or Ventolin using the new inhaler.</b>	<b>241</b>



<b>4.21</b>	<b>FEV1 values for each patient following inhalation of the novel formulation using either the new inhaler or the Rotahaler.</b>	<b>242</b>
<b>4.22</b>	<b>V<sub>max</sub>30 values for each patient following inhalation of the novel formulation using either the new inhaler or the Rotahaler.</b>	<b>243</b>
<b>4.23</b>	<b>FEV1 values for each patient following inhalation of Ventolin using either the new inhaler or the Rotahaler.</b>	<b>244</b>
<b>4.24</b>	<b>V<sub>max</sub>30 values for each patient following inhalation of Ventolin using either the new inhaler or the Rotahaler.</b>	<b>245</b>
<b>4.25</b>	<b>Questionnaire response to:</b> <b>Did either of the treatments have any taste?</b> <b>Do you have any comments on both treatments?</b>	<b>247</b>
<b>4.26</b>	<b>Questionnaire response to:</b> <b>Which inhaler do you prefer to use?</b>	<b>248</b>
<b>Appendix</b>		
	<b>Profiles of axial mean and r.m.s. velocities of the gas at an air flow of 200 l/min.</b>	<b>271</b>
	<b>Profiles of axial mean and r.m.s. velocities of the gas at an air flow of 100 l/min.</b>	<b>272</b>
	<b>Profiles of axial mean and r.m.s. velocities of the gas at an air flow of 60 l/min.</b>	<b>273</b>
	<b>Profiles of axial mean and r.m.s. velocities of the gas and particles at an air flow of 200 l/min.</b>	<b>274</b>

## **Chapter one**

### **I n t r o d u c t i o n**

## **Introduction**

Airborne particles are present throughout the environment. They exist in many different forms, such as dusts, fumes, mists, smog, fog or smoke. These suspended microscopic particles are examples of aerosols. Inhalation is a primary route by which these foreign substances may enter the body and therefore airborne particles (aerosols) constitute a major cause of respiratory disease. However, other types of aerosols are being used increasingly in a beneficial role for the assessment of lung structure and function and hence for diagnosis and, ultimately, the topical treatment of respiratory disorders.

The administration of therapeutic agents to the large surface area of the bronchial tree by inhalation of airborne particles has the important advantage that the drug is applied close to the target tissue. As a result, the drug often begins to act very rapidly and dissipation of its effect due to pharmacokinetic factors is minimized. The effective dose is therefore small, with a reduction in the incidence of systemic side-effects.

There is an increased interest in the inhalation route as a means of introducing pharmacological agents systemically providing that the drug in question is absorbed via the airways without being metabolised (Newman & Clark, 1985)

For better understanding of the aerosol behaviour this chapter will briefly review some aspects of lung physiology and anatomy and the major respiratory disorders and therapy. Aerosol deposition and generation as a means of drug delivery and the methods of their evaluation will be discussed.

## **1.1 The physiology of the respiratory tract**

The respiratory tract can be divided into three main zones:

1. The upper airways which include the nasal passages, mouth, pharynx and larynx. Its main purpose is to conduct air, swallowing, air conditioning, smelling, speech and filtration.
2. The tracheobronchial airways or conducting airways which comprise the trachea, the bronchi, the bronchioles and the terminal bronchioles. Its function is air conduction and filtration.
3. The pulmonary region or the alveolated region where oxygen and carbon dioxide are exchanged between inspired air and the blood.

A schematic representation of the human respiratory tract is shown in Figure 1.1.

The lung divides dichotomously for about 23 generations until it reaches the alveolar sacs, which number approximately 300 million and cover some  $70\text{-}80\text{m}^2$  in the average adult human lungs. Distributed over this surface is 80ml of blood in the alveolar capillaries, through which oxygen is exchanged. Thus the respiratory bronchioles and alveoli provide the greater surface for absorption of the inhaled particles than the other parts of the respiratory tract.

The airway walls consist of epithelium, smooth muscles, cartilage and glands in a framework of connective tissue (Hale *et al*, 1968). A series of horseshoe ring cartilages located in the tubular structure of the airways keeps the trachea open, this cartilagenous support in the walls decreases in size and gradually disappears as



the airways branch further. The last generation of small bronchi contains little cartilage, whereas the bronchioles are distinguished from the bronchi by the absence of cartilage.

The epithelium of the airways is composed of ciliated and goblet cells, together with columnar epithelial and basal cells. Situated between the basal membrane of the epithelium and the cartilage of larger airways are mucous glands, ducts of which open on to the epithelial surface. These glands are absent in bronchioles. The ciliated epithelium, the goblet cells and the glands are essential parts of the mucociliary clearance mechanism that help eliminate foreign matter from the lungs.

The smooth muscle network is arranged in the airway walls to allow changes of width as well as of length. The amount of smooth muscle increases in the small bronchi and it occupies the largest fraction of the wall thickness in the terminal bronchioles.

Secretory cells without cilia (Clara cells) occur in bronchioles and increase in number towards the terminal bronchioles and it is believed that they contribute to the production of surfactants. Mast cells are found around the airways and in the pleura of the human lungs.

Nerve fibres, ganglia and possible sensory elements are present in the airway walls. The function of the nerves is primarily concerned with the efficient control of ventilation under varying conditions, and protection of the lung in terms of cough, bronchoconstriction and mucus secretions. The lower respiratory tract is innervated by the autonomic nervous system through branches of the vagus nerve and thoracic sympathetic ganglia. Parasympathetic vagal stimulation causes bronchoconstriction as the acetylcholine

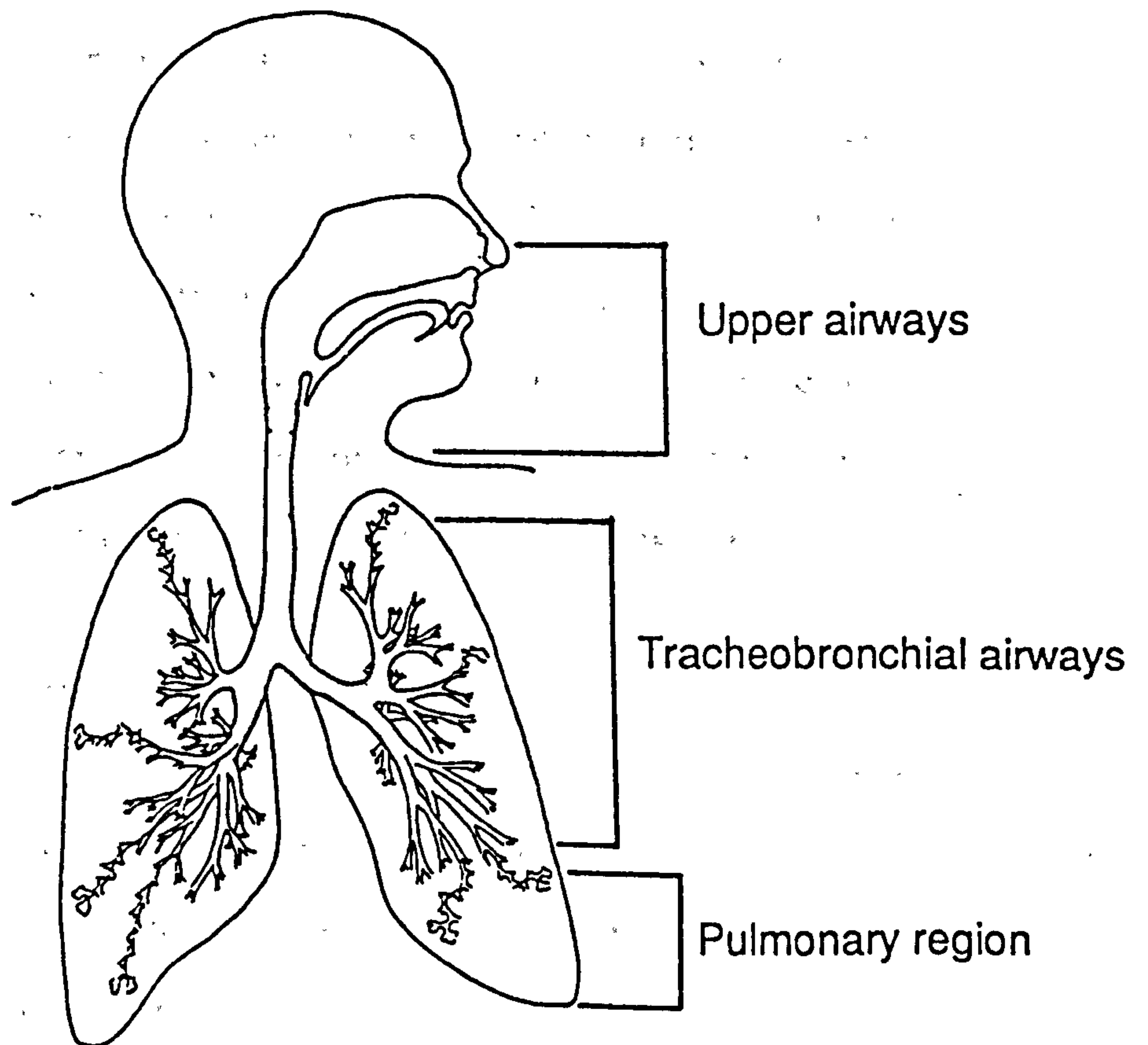


**Fig 1.1** Schematic representation of the human respiratory tract

released from postganglionic nerve endings stimulate receptors on target cells. Cholinergic ganglia are found throughout the tracheobronchial tree and they have been established and studied in man (Nadel & Barnes, 1984)

The sympathetic innervation of human airways reaches the most peripheral parts. Two types of adrenoceptors have been demonstrated: alpha receptors, stimulation of which produces bronchoconstriction and beta receptors which are subdivided into  $\beta$ -1 and  $\beta$ -2 receptors.  $\beta$ -1-receptors are mainly present in the heart and they mediate cardiac stimulation.  $\beta$ <sub>2</sub>-receptors mediate smooth muscle relaxation in the bronchi and blood vessels. Circulating adrenaline released from the adrenal medulla activates alpha or beta adrenoceptors and produces bronchodilation because beta-receptors outnumber alpha receptors in the airway walls.

#### **1.1.1 Air flow through the respiratory tract**

The design of the respiratory tract is optimal so as to maximize alveolar ventilation and to minimize airflow resistance.

Airflow dynamics in the tracheobronchial tree have been studied extensively employing models of the human airways. The nature of airflow within the respiratory tract is of great importance in determining the fate of inhaled particles. Flow dynamics in the human airways vary with the inspiratory flow rate and local airway geometry. Relatively high airflow velocities are normally present in the airways even in quiet breathing and airflow in the trachea and bronchi is turbulent at a certain stage during the breathing cycle. The constricted entrance of air to the trachea via the larynx increases the degree of turbulence. However, as air progresses



down the respiratory tract, the overall cross sectional area increases resulting in laminar flow beyond the first few generations. However, branching affects flow patterns and flow irregularities over several more generations are possible.

In the pulmonary region, bulk flow is almost non-existent, relying primarily on gaseous diffusion.

Variation in lung morphology and airway dimensions with aging and pathologic processes have been reported. Therefore, the local linear velocity of the air stream within the tracheobronchial tree will be determined by the airway anatomy and the inspiratory flow rate.

Inspiratory flow rates in normal human adults can be as high as 300 l/min, whereas in a child or in certain disease states, flow rates are much lower. Recently, it was reported that patients with mild asthma can achieve a peak inspiratory flow rate of up to 200 l/min (Richardset *al*, 1987).

## **1.2 Inhalation therapy for respiratory diseases**

Treatment of respiratory diseases by inhaled remedies is a form of therapy which has been used for many years in several parts of the world. Early methods involved primarily the inhalation of volatile aromatic substances with a mild irritant action, such as menthol, thymol and eucalyptus, or the inhalation of anticholinergic alkaloids derived from burning the leaves of plants such as *Atropa belladonna* and *Datura stramonium*.

Nowadays inhalation therapy has, however, become the most widely used system for drug delivery in the management of both acute and chronic asthma (Shenfield & Paterson, 1973). In addition,



inhalation therapy is used in the treatment of other obstructive airway diseases, such as chronic bronchitis.

### **1.2.1 Respiratory diseases**

#### **Asthma**

The word asthma( $\alpha\sigma\theta\mu\alpha$ ) is derived from a Greek word meaning difficulty in breathing. From a diagnostic point of view, asthma is a disease characterized by wide variations in resistance to airflow in pulmonary airways over short periods of time (Scadding, 1987). The pathophysiological features can be divided into muscle spasm, airway inflammation with oedema and mucous hypersecretion (Hogg, 1982). However, the relative importance of these abnormalities varies with the disease state. Spasm of the bronchial smooth muscles can occur rapidly in response to a provocative stimulus and can be easily and completely reversed by drugs that relax smooth muscles. Respiratory mucous accumulation and oedema formation are likely to require more time to develop. These disorders are usually the major cause of death in asthma since they might be irreversible.

#### **Chronic bronchitis and emphysema**

These are inter-related conditions normally referred to as chronic obstructive airway disease. The main clinical symptoms associated with these diseases are breathlessness accompanied by wheeze, cough and sputum.

The mechanism of bronchial narrowing in these diseases differs from that in chronic asthma. It is mainly due to mucous gland hypertrophy in the bronchial epithelium, excessive mucous

production, and airway collapse resulting from abnormal enlargement of the gas-exchanging air spaces distal to the terminal bronchiole, thus interfering with the mechanism of blood oxygenation.

The value of bronchodilator agents in these diseases is limited in comparison with their effect in bronchial asthma because the contribution of bronchospasm to ventilatory impairment is small compared with the effect of inflammatory changes in the bronchial mucosa and obstruction by excessive bronchial secretions.

### **1.2.2 Drug treatment of respiratory diseases**

#### **Bronchodilators**

Bronchodilators generally act rapidly to relieve bronchospasm. They can produce a substantial increase in pulmonary function by dilating the central and peripheral airways (McPhillips , 1985 ). They also appear to exert a prophylactic effect if taken on a regular basis (Paterson *et al*, 1979). Bronchodilator drugs classification can be thought of in terms of autonomic pharmacology of bronchial smooth muscles which provides a useful framework for understanding the wanted and unwanted effects of many of the most valuable bronchodilators. The wanted effect is the relaxation of the bronchial smooth muscles and subsequent bronchodilation. The unwanted effects arise from the action of these drugs on other receptors which produce different effects ( Table 1.1).

#### **1. Sympathetic bronchodilators**

$\beta$ -adrenergic agents are widely used as maintenance therapy in asthma and bronchitis. These compounds act by stimulating the



adrenergic receptors on smooth muscle cells in the airway walls, thus increasing the cellular concentration of cyclic AMP (cyclic 3', 5' - adenosine monophosphate) which influences the activity of phosphokinase which, in turn, is responsible for further enzyme stimulation to give the final cellular activity, manifested by relaxation in the smooth muscle fibres and subsequent bronchodilation. Adrenaline was the first sympathomimetic agent to be used as a bronchodilator in 1910. Its chemical structure (Figure 1.2a) shows it to be a catecholamine. Adrenaline is ineffective when taken by mouth because it is largely inactivated by monoamine oxidase present in the gastrointestinal tract. In asthma, the usual routes of administration are by inhalation of a nebulised solution or by subcutaneous or intramuscular injection. This compound was followed by the introduction of isoprenaline (Figure 1.2b) in 1940. The structural changes of isoprenaline alters the pharmacological properties to almost exclusive  $\beta$ -receptor activity. This compound is administered mainly by inhalation from metered dose inhalers or from nebulisers, since it is almost ineffective when administered orally due to enzymatic conjugation to an inactive sulphate derivative during its passage of the gut wall (Figure 1.3). Intravenous administration of this compound leads to the formation of 3-O-methyl isoprenaline due to its metabolism by catechol-o-methyl transferase (COMT). The resulting compound is active, but due to its non-selectivity at the  $\beta$ -receptors, its use is limited by the cardiovascular side-effects. Therefore, the inhalation route is preferred since it appears to provide adequate bronchodilation in a dosage small enough to cause minimum cardiac stimulation.

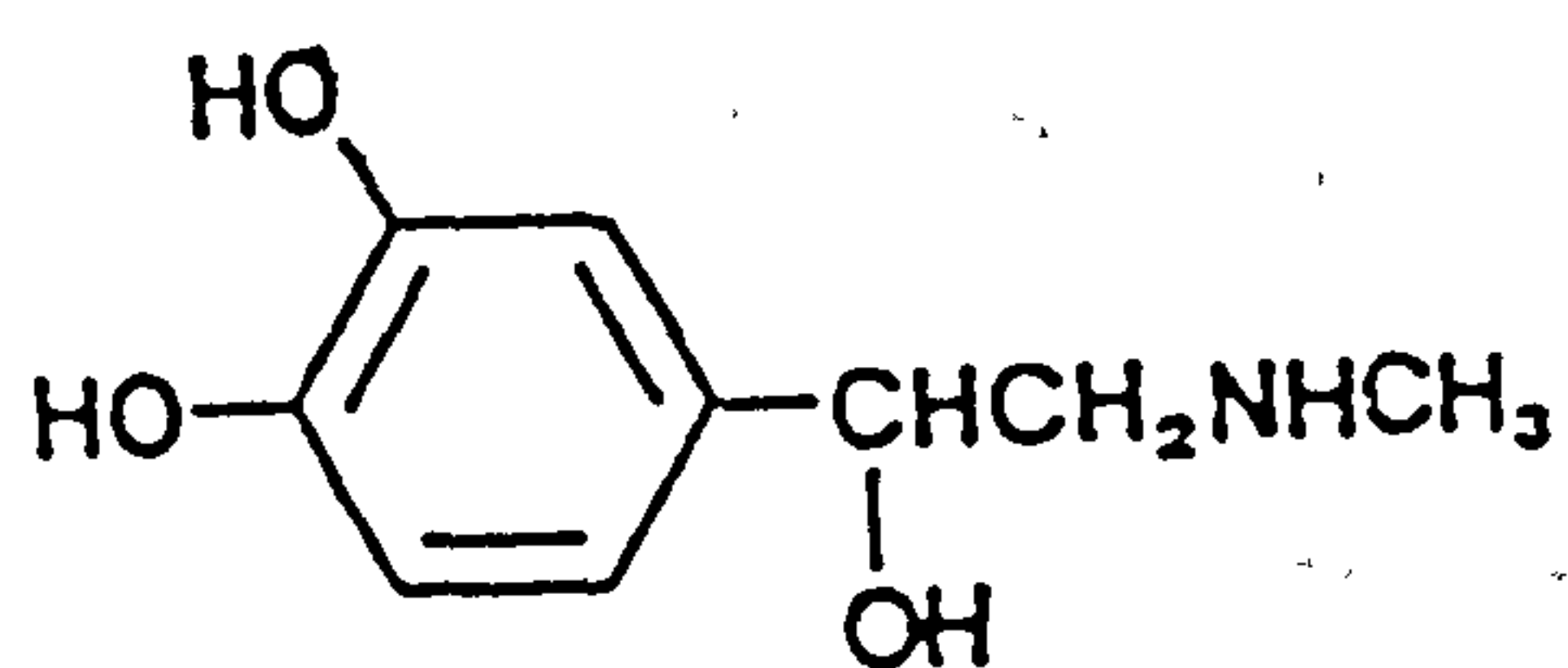
**Table 1.1**

**"Autonomic" classification of bronchodilator drugs**

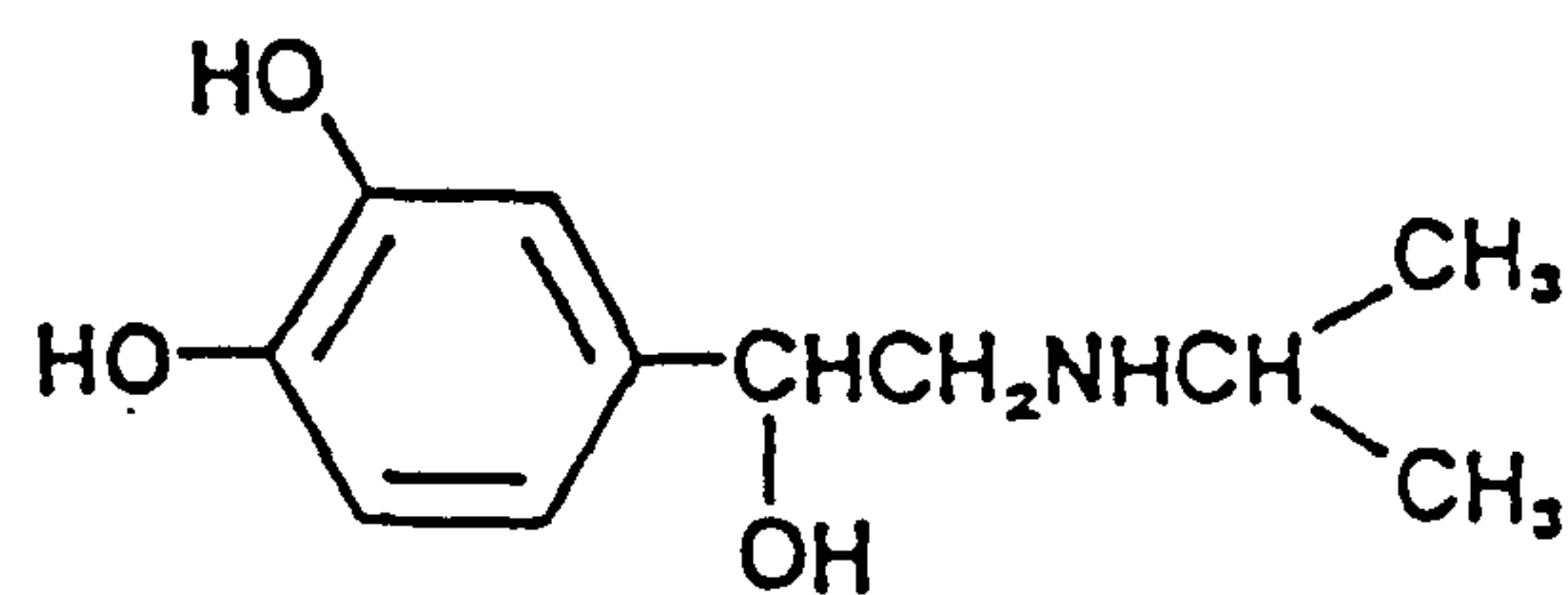
<b>Autonomic action</b>	<b>Drug</b>	<b>Nature of action and unwanted effects</b>
<b>Sympathetic (Adrenergic)</b>	<b>Adrenaline</b>	<b>Relaxation of bronchial</b>
	<b>Ephedrine</b>	<b>smooth muscle (<math>\beta_2</math>-effect)</b>
		<b>Unwanted alpha and beta-1 effects such as</b>
		<b>hypertension, tachycardia, cardiac arrhythmias, headache, palpitation and tremor.</b>
	<b>Isoprenaline</b>	<b><math>\beta_2</math>-bronchodilation.</b>
	<b>orciprenaline</b>	<b>Unwanted <math>\beta</math>-1 effects such</b>
	<b>Isoetherine</b>	<b>as palpitation, tachycardia, headache and skin flushing</b>
	<b>Selective <math>\beta_2</math></b>	<b><math>\beta_2</math>-bronchodilation</b>
	<b>sympathomimetics</b>	<b>Unwanted <math>\beta_2</math>-effects</b>
	<b>such as terbutaline</b>	<b>for instance</b>
	<b>and salbutamol)</b>	<b>muscle tremor and tachycardia</b>
<b>Anticholinergic Drugs</b>	<b>Atropine</b>	<b>Bronchodilation due to</b>
	<b>Ipratropium</b>	<b>para-sympathatic blockade.</b>
	<b>bromide</b>	<b>Unwanted effects such as dry mouth and airways</b>



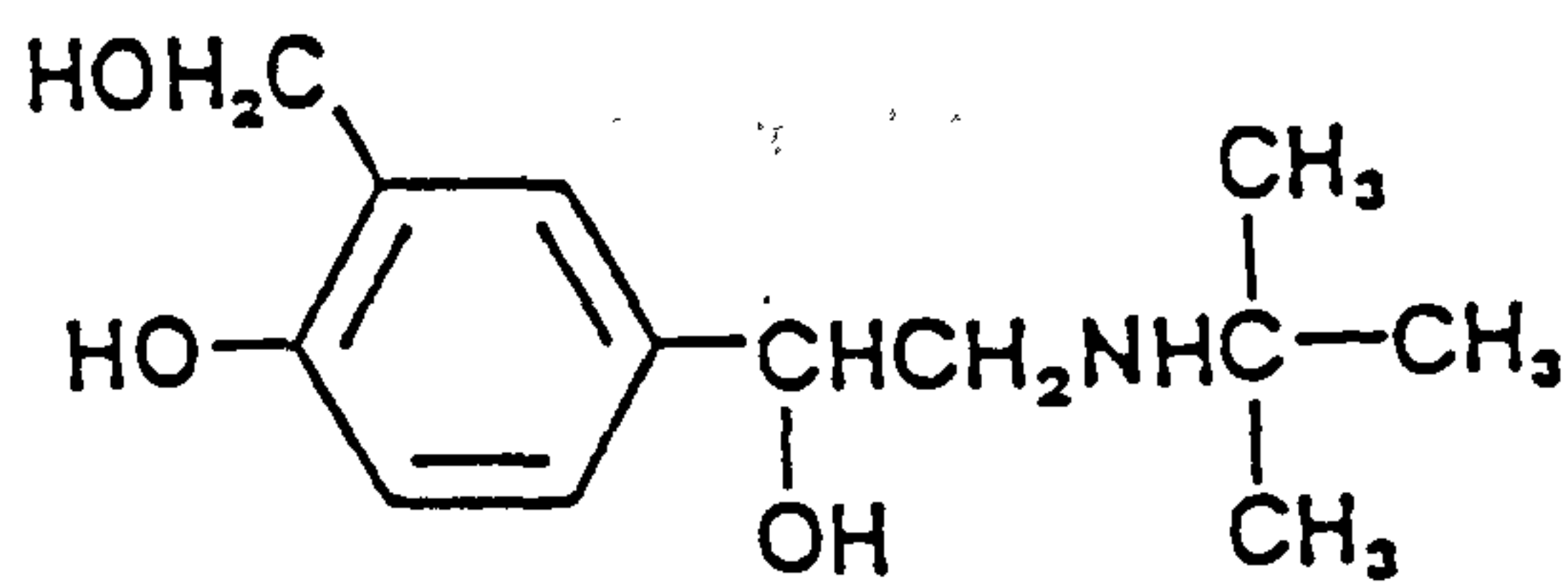
Fig 1.2 Sympathomimetic bronchodilators



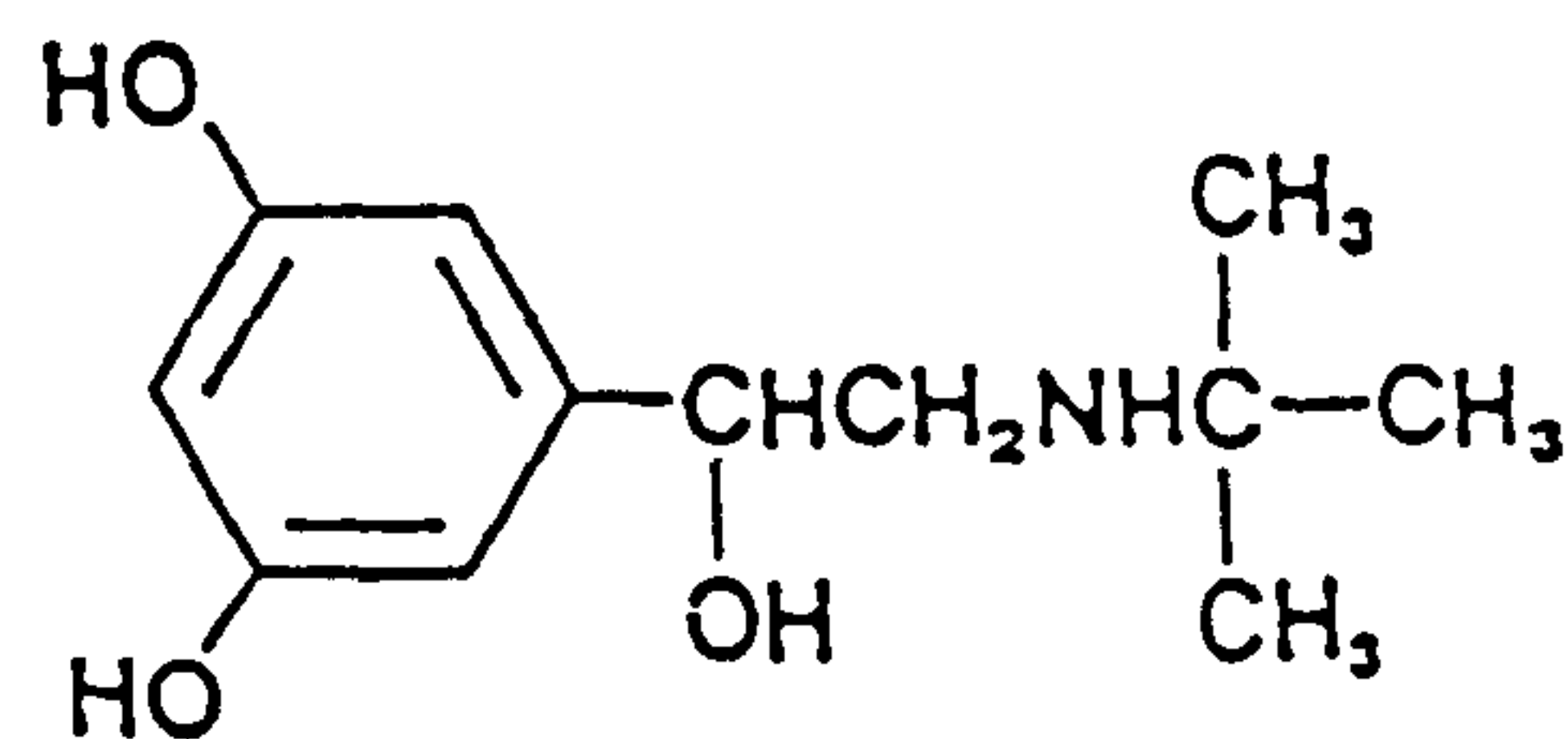
a. Adrenaline



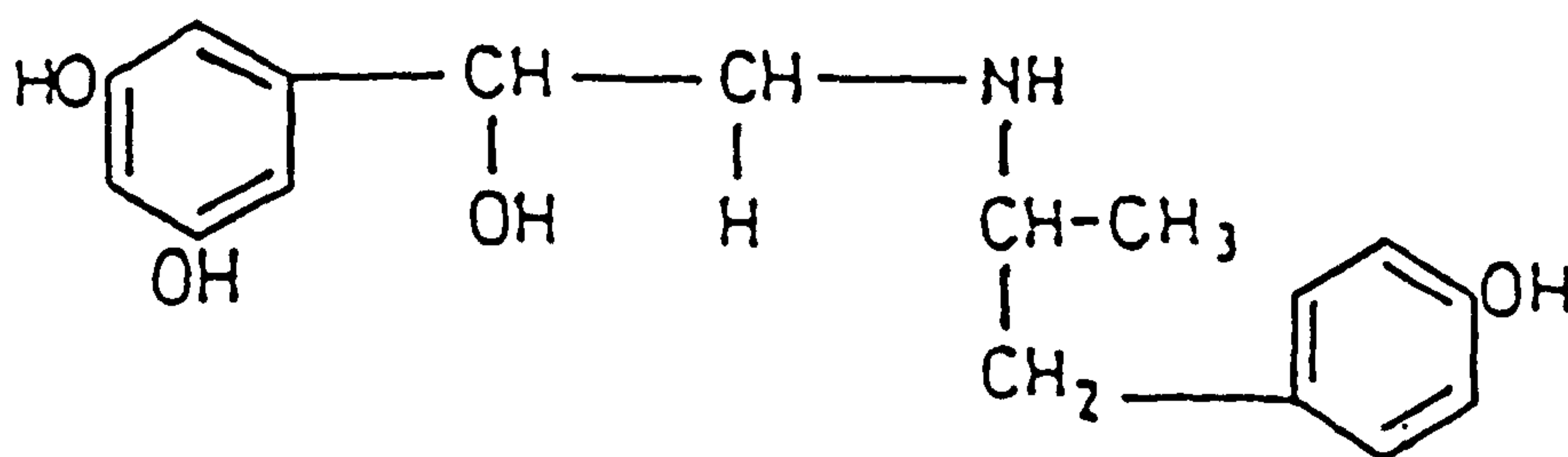
b. Isoprenaline



c. Salbutamol



d. Terbutaline



e. Fenoterol

In 1960's, a rise in asthma mortality associated with the increasing use of bronchodilator aerosols was observed (Speizer *et al*, 1968). Although the actual cause has not been identified, tolerance to the effect of isoprenaline has been described in animals and humans, (Conolly *et al*, 1971). Cross-tolerance between  $\beta$ -receptor stimulants is a recognized phenomenon, leading to the possibility that  $\beta$ -receptor desensitisation due to tolerance from excessive use of  $\beta$ -adrenergic stimulants in patients with asthma might upset a hypothetical balance between constrictor and dilator influences on bronchomotor tone and thus aggravate bronchoconstriction (Benoy *et al*, 1975). Thus, there was great awareness of the potential danger of sympathomimetics after this epidemiological evidence.

The use of isoprenaline aerosols has declined since the introduction of the selective  $\beta_2$ -sympathomimetic bronchodilators (Woolcock, 1977). These compounds offer a longer duration of action and fewer cardiovascular side-effects.  $\beta_2$ -sympathomimetic bronchodilators have the same basic structure as isoprenaline with alteration of the aromatic hydroxyl group which prolongs the duration of action. Additionally, substitution on the amine head provides greater  $\beta_2$ -selectivity Figure (1.2c, d, e). Therefore, cardiovascular side-effects are reduced, although skeletal muscle tremor is sometimes observed. These drugs can be administered either orally or by inhalation. However, the inhalation route is preferable since it increases the therapeutic index by permitting a reduction in the total dose of drug administered while maintaining a useful bronchodilator effect. Bronchodilators delivered from inhalation aerosols are effective in doses of few hundred

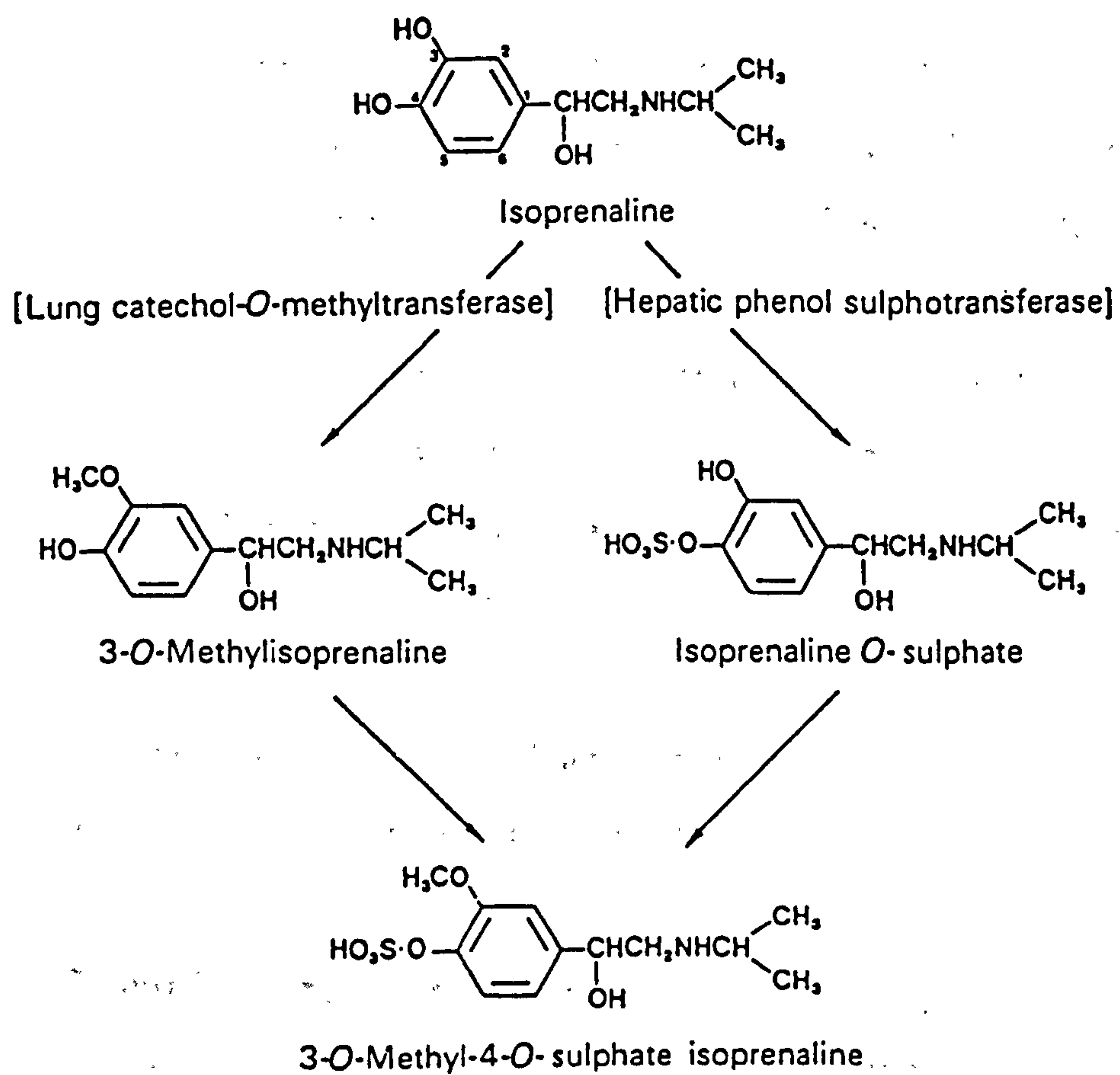


**Fig 1.3** Metabolism of isoprenaline

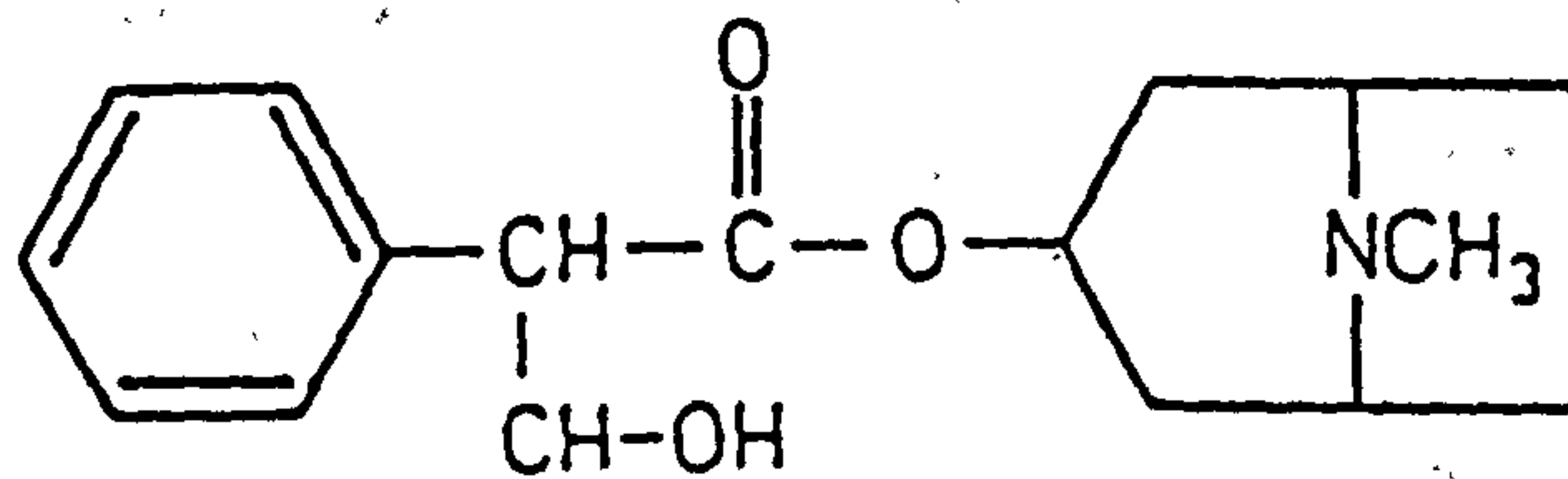
micrograms, of which only about 10% reaches the lungs, whereas a comparable oral dose would be of few milligrams (Larson & Svedmyr, 1977). Heel *et al*( 1978) found that a higher incidence of side effects was associated with the oral administration of fenoterol than when a drug was given by inhalation. Inhaled bronchodilators produce a noticeable effect almost immediately and a peak effect after 15-30 minutes (Hetzel & Clark, 1976); whereas the same drugs given orally do not reach peak effect for 2-3 hours (Clark, 1979). Similar duration of action was obtained for these bronchodilators whether given orally or by inhalation. Bronchodilators administered intravenously have a rapid onset of action, but compared to inhalation they lead to high incidence of systemic side effects (Paterson *et al*, 1979). However (Hetzel & Clark, 1977) found that a 100-200 $\mu$ g inhaled salbutamol can give the same peak bronchodilation effect as 250 $\mu$ g intravenously, and additionally the aerosol has a longer duration of action.

## **2. Anticholinergic bronchodilators**

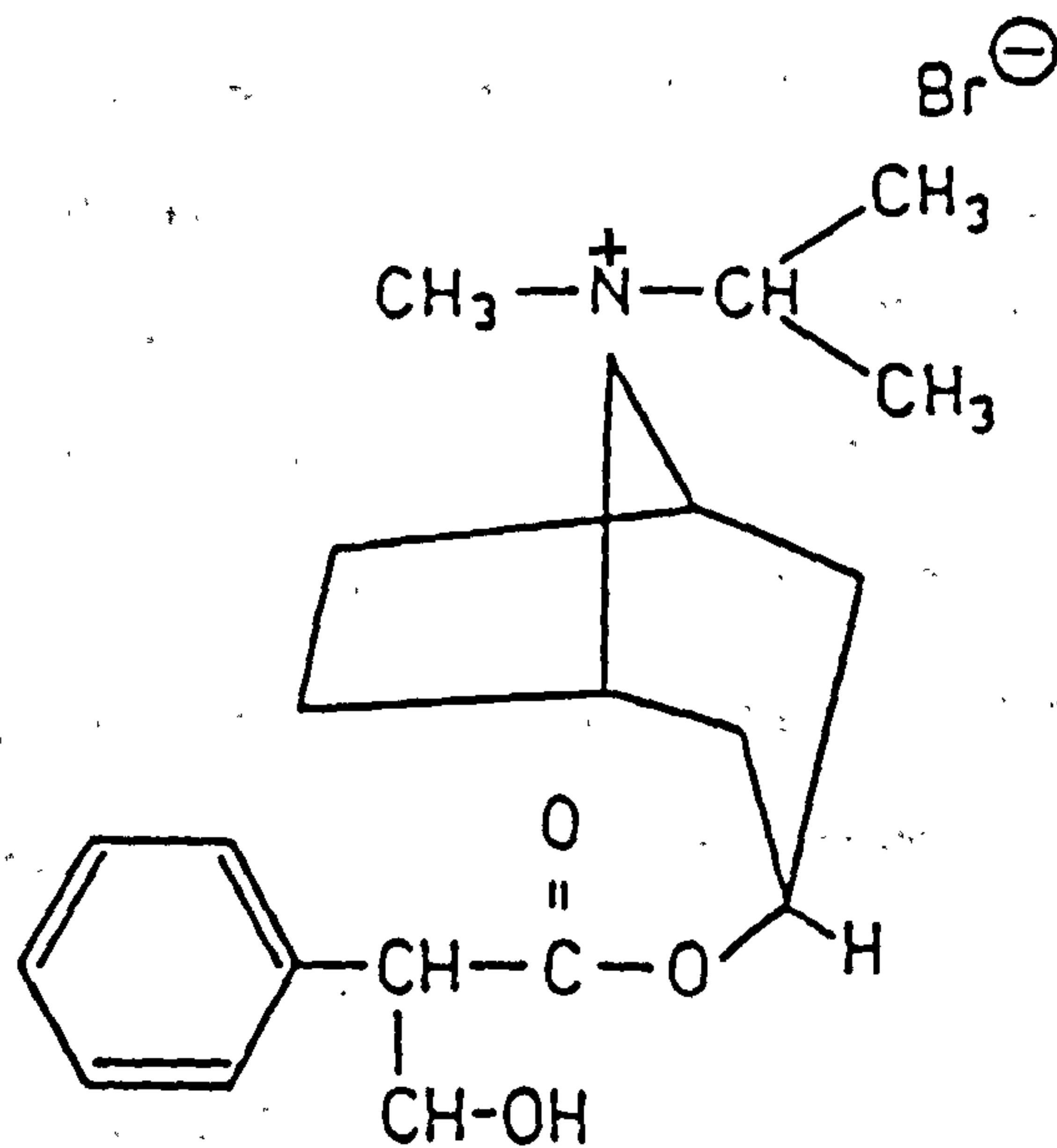
Bronchodilation may be achieved by blocking the muscarinic action of acetylcholine. Pharmacological studies using atropine as a parasympathetic blocking agent in patients with asthma and obstructive lung diseases have confirmed the importance of parasympathetic pathways (Yu *et al*, 1972). However, the intolerable side-effects of atropine make it impractical to use. Recently, a synthetic anticholinergic agent ipratropium bromide, has been developed. This compound is a quaternary isopropyl-substituted derivative of atropine (Figure 1.4), and is said to have some degree of bronchoselectivity particularly when administered



**Fig 1.4** Anticholinergic bronchodilators



a. Atropine



b. Ipratropium bromide

by the inhalation route (Deckers , 1975). Oral absorption of this compound is poor, which tends to reduce the likelihood of side-effects arising from the swallowed portion of the aerosol dose. Ipratropium bromide has none of the undesirable CNS effects of atropine. The onset of action is somewhat slower than the selective  $\beta_2$ -sympathomimetic agents, but the duration of action is as long or even longer. Until recently this drug did not appear to have any advantage over the selective  $\beta_2$ agonists but studies have shown that in chronic bronchitis, ipratropium bromide (80 $\mu$ g) has a comparable bronchodilator effect to salbutamol (200 $\mu$ g) (Douglas *et al*, 1979).

### **3. Methyl xanthines**

These agents such as aminophylline and theophylline have proved to be potent bronchodilators. The mechanism by which they relax the bronchial smooth muscle is unknown. However, one possible explanation might be the inhibition of the enzyme phosphodiesterase, which cleaves c-AMP, thus resulting in an intracellular accumulation of c-AMP. These compounds are usually administered either orally or intravenously. As aerosols they have been found to have less bronchodilator effect than  $\beta$ -agonists, and their bitter taste and the narrow therapeutic index make it difficult to formulate these drugs for inhalation.

### **Sodium cromoglycate (SCG)**

Cromolyn sodium (disodium cromoglycate) is a prophylactic anti-asthmatic agent which has been widely used in Britain since 1968. Structure-activity correlation studies based on Khellin, a naturally occurring substance in a plant *Ammi Visnaga*, with

muscle relaxing properties, led to the synthesis of the bis-cromone cromolyn sodium (Figure 1.5).

The precise mode of action of cromolyn sodium is still unclear, although the drug is known to inhibit the release of secretory granules containing chemical mediators such as histamine and SRS (slow releasing substances of anaphylaxis) from mast cells following antigen challenge of tissues sensitised with specific IgE-antibodies, which initiate the asthmatic reaction (Brompton Hospital Medical Research Council Collaborative Trial, 1972). Forman and Garland (1976) have suggested that this mechanism might occur by preventing calcium ion transport across the mast cell membrane which is necessary for mediator release from the cell.

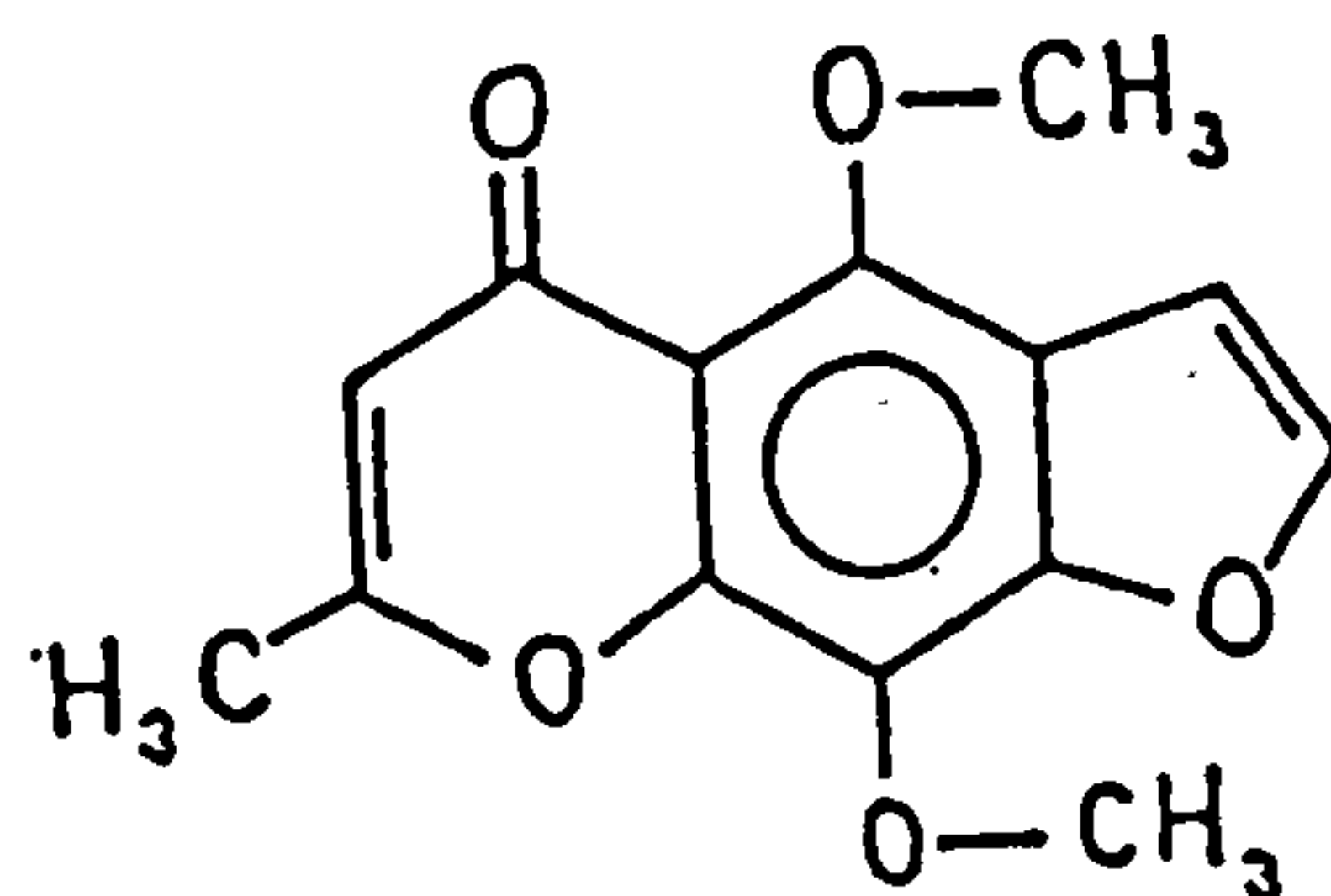
The oral absorption of SCG is poor (Walker *et al*, 1972), therefore administration via the respiratory tract is necessary for its action on the airway mucosa. Powder inhalers were developed for its administration (Bell *et al*, 1971). Metered dose inhalers and nebulizers have also been used.

The major application of cromolyn sodium is a prophylactic treatment of asthma induced by exercise (Davies , 1968) or specific allergens. Studies have shown that sodium cromoglycate provides effective control of asthma in 65-75% of patients (Godfrey *et al*, 1975). However, it has no bronchodilator action, and therefore it is not used in the management of acute attacks of asthma.

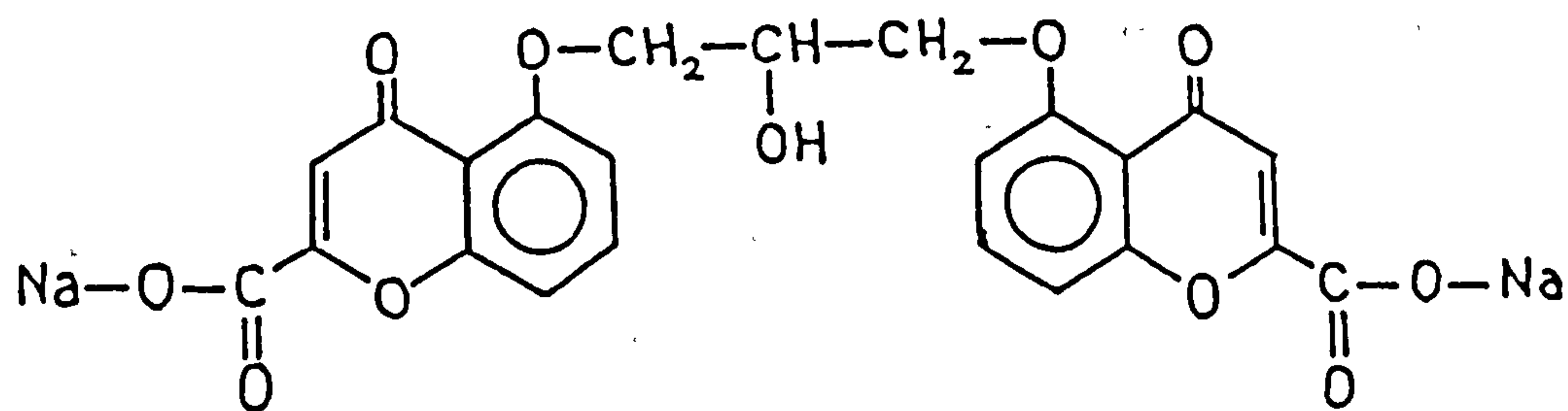
### **Corticosteroids**

Corticosteroids are added to the therapeutic regimen of asthmatics when other measures have failed to relieve the symptoms and

Fig 1.5



Khellin



Sodium cromoglycate



improve pulmonary function. Corticosteroids are used in the management of acute and chronic asthma. It is believed that these compounds probably act by decreasing airway resistance via an antiinflammatory effect. Systemic treatment with corticosteroids is associated with suppression of the hypothalamic-pituitary-adrenal axis. This serious side effect is related to some extent to the high dosage administered. Inhaled corticosteroids given in smaller doses may significantly reduce the undesirable effects and still control the symptoms of asthma. However, oropharyngeal candidiasis and hoarseness have been observed in few patients.

### **Antibiotics**

Because respiratory diseases are often accompanied by chest infections, antibiotics are often prescribed. The use of antibiotic aerosols began in 1940. Aerosolized penicillin was used in the treatment of cystic fibrosis, and some short term benefit was noted (Agnese & Anderson, 1946). Rose *et al* (1970) used colistin aerosol in patients with chronic bronchopulmonary disease with gram-negative organisms in their sputum and a significant reduction in the sputum bacterial count was reported. Recently many studies have been conducted using nebulized carbenicillin, gentamicin, tobramycin and ceftazidime in the treatment of patients chronically infected with *P. aeruginosa* (Hodson, 1988). Renewed interest in the drug pentamidine has led to its widespread application in aerosol form to treat and prevent *Pneumocystis carinii* pneumonia in immunosuppressed patients.

## **Water and saline aerosols**

These are often used in an attempt to liquify secretions and enhance their removal from the lungs post operatively, or to mobilize tenacious secretions in patients with chronic respiratory diseases.

### **1.2.3 Inhalation therapy for systemic diseases**

The use of aerosols to deliver drugs for systemic therapy would appear to offer many advantages over other routes of systemic administration. The enormous surface area of the lungs provides a vast capillary interface for the absorption of substances that can penetrate into the alveolar region. A study of the use of ergotamine tartrate in the management of recurrent vascular headaches revealed that the average onset of response for patients taking oral tablets was 1½ to 3 hours, whereas the response to oral inhalation in the same individual ranged between 10 to 30 minutes (Speed, 1960).

Additionally, the constant pH and the nature of the enzymes in the respiratory region, all provide a good possibility for drug absorption, and reduce the extent of drug degradation or inactivation by the degradative enzymes in the liver and GIT (Gonda *et al*, 1978).

Metabolic reactions can take place in the lung. These include: hydrolysis, o-methylation and mixed function oxidation. However, the metabolic pathway in the airways differs qualitatively and quantitatively from that of orally and intravenously administered drugs. Additionally, the role of the pulmonary tissues in metabolizing aerosolised drugs is not yet clearly defined.



Heparin by inhalation is another drug which has been proposed for systemic anticoagulation (Jaques *et al*, 1976). Intrapulmonary heparin resulted in an anticoagulant effect for up to 14 days after inhalation of a single large dose. The peak anticoagulant effect was not observed until the next day. The lengthening of clotting time increased with dosage. Examination of the lungs, body fluids and tissues showed that heparin was cleared rapidly from the lung and enters a body cellular compartment from which it is slowly released to plasma. No evidence was found of haemorrhage or any heparin-related pathological change indicating either immediate or long-term toxic effects in the lung or other tissues.

Insulin, prepared as metered dose inhaler and inhaled by rabbits exhibited rapid peak plasma concentration after absorption from the lungs (Jones *et al*, 1988).

Administration of these two compounds via the inhalation route offer the potential advantages of simple and apparently safe route of administration. Additionally, the inhalation route might have a potential in administering other peptides which are decomposed in the GIT if administered orally.

Given these advantages, it may seem surprising, that the availability of systemic inhaled products is very limited. This reflects the fact that the progress in this field has not reached a point where an accurate dose of the drug can be specifically "targeted" to an absorption site in the lung. The limiting factors controlling accurate delivery of drug particles into the lower respiratory tract include the physiological factors related to the patient, the physical properties of the aerosol and the efficiency of the inhalation delivery systems. These factors are further discussed below.



### **1.3 Deposition mechanisms of inhaled particles**

Deposition is a process by which inhaled particles carried in an air stream separate from the flow streamlines and contact a respiratory tract surface from which there is no rebound or resuspension . Particles which remain suspended in the tidal air throughout the respiratory cycle are exhaled.

Due to the anatomy and physiology of the respiratory tract, particles deposit at various sites within the bronchial tree by several mechanisms. Figure 1.6 illustrates the five possible mechanisms by which significant deposition might occur: impaction, sedimentation, diffusion, interception and electrostatic precipitation. However, the first two are the predominant deposition mechanisms in most cases.

#### **1.3.1 Impaction**

The inhaled air follows a tortuous path through the branching airways. Each time the air changes direction, the momentum of particles carried by the air stream tends to keep them on their established trajectories, which can cause them to impact on airway surfaces.

If a particle is moving at a velocity,  $V$ , in the absence of gravity, the drag forces will bring it to a stop. Thus the trajectory motion of the particle is a balance between the inertial and resistant forces. The resistant force is given by Stoke's law, and a 'stop distance'  $x$ , can be calculated.

$$x = V \cdot \frac{V_t}{g} \quad (1.1)$$

where  $V_t$  is the settling velocity and  $g$  is the gravitational constant.

The aerosol particle will have a velocity of magnitude  $u \sin \theta$  as it changes its direction by an angle  $\theta$ . Hence the particle moves a total distance of:

$$x = \frac{(u \sin \theta) V_t}{g} \quad (1.2)$$

For a particle travelling in an airway, the stop distance  $x$  can be compared with the radius,  $R$  of the airway. A dimensionless function, the Stoke's number (Stk) is related to the probability of deposition by impaction, where

$$\text{Stk} = \frac{P d^2 V}{18 \eta R} \quad (1.3)$$

$P$  is the particle density

$d$  is the particle diameter

$V$  is the air velocity

$\eta$  is the air viscosity

$R$  is the airway radius

The higher the value of Stoke's number, the more readily particles will diverge from the airflow streamlines. Therefore, with large particles whenever the convective airflow is fast or turbulent as in the upper airways, or changing direction at bifurcations between successive airway generations, deposition by impaction is the most likely mechanism forming "hot spots" particularly on the carinal ridges of bifurcations. Consequently, this mechanism causes the major portion of aerosol deposition on mass basis.

### 1.3.2 Sedimentation

This mechanism of deposition is a time dependant process, in which small airborne particles settle in airways under the influence of gravity, during either breath-holding or slow tidal breathing.

Due to gravity, an airborne particle with density ( $P_p$ ) greater than that of air ( $P_a$ ) experiences a downward force ( $F$ ) given by:

$$F = v(P_p - P_a)g \quad (1.4)$$

where  $v$  is the volume of the particle. The particle accelerates downwards and reaches its terminal velocity when the retarding force due to its motion through the air just balances its weight. For a spherical particle Stoke's law can be used to predict the retarding force  $F_r$ :

$$F_r = 3\pi d\eta V \quad (1.5)$$

where  $V$  is the velocity of the particle.

At terminal velocity,  $V_t$ , the downward force is equal to the retarding force, therefore:

$$V_t = \frac{(P_p - P_a)d^2 g}{18\eta} \quad (1.6)$$

Stoke's law is valid for unit density particles of 1 to  $40\mu\text{m}$  in diameter settling in air. Correction factors can be included to extend the useful range for particles 0.001 to  $200\mu\text{m}$  in diameter (Mercer 1973). For particles of large diameter, the retarding force is increased by the inertial effects of accelerating a mass of gas to push it aside. With a small diameter particle, the retarding force is



less than that predicted by Stoke's law because the particle is comparable in size to the mean free path of air molecules and can slip between molecules.

Deposition by sedimentation takes place mainly in the small airways and alveolar spaces where the rapid increase in the cross sectional area gives low air velocity, and where large particles will rarely penetrate.

### 1.3.3 Diffusion

When the terminal velocity of the particles falls below 0.001 cm/sec, which for unit density spheres is equivalent to the diameter of  $\sim 0.5\mu\text{m}$ , deposition by diffusion becomes more effective than sedimentation.

Particles less than one micrometer in size undergo a random motion in air caused by the impact of gas molecules. This brownian motion increases with decreasing particle size, and becomes an effective mechanism for particle deposition in the lung as the root mean square displacement approaches the size of the airspace.

The root-mean square displacement( $\Delta$ )is given by:

$$\Delta = \sqrt{6Dt} \quad (1.7)$$

where

t is the time

D is the diffusion coefficient of the particles which can be expressed as,

$$D = \frac{KT}{3\pi\eta d} \quad (1.8)$$

where

$K$  is the Boltzmann constant

$T$  is the absolute temperature

$\eta$  is the gas viscosity

$d$  is the particle diameter

This mechanism is therefore, important for submicron particles. However, therapeutic aerosols are usually of larger sizes and this mechanism is responsible for only a small percentage of total lung deposition.

#### **1.3.4 Interception**

This mechanism is usually significant only for fibrous particles. It occurs when the trajectory of a particle brings it close enough to the airway wall so that the edge contacts the surface even though the particle's centre of gravity might lie in the convective air streamline relatively distant from the wall.

#### **1.3.5 Electrostatic forces**

Deposition of particles with high electrical mobility results from image charges induced on the surfaces of the airways (Chan & Yu, 1982 ). Particles produced by high velocity dispersion of solid or liquid material can have substantial electric mobilities (John 1980), and if their generation is followed immediately by inhalation before the rapid neutralization in the atmosphere, this mechanism might contribute considerably to aerosol deposition.

### **1.4 Factors affecting deposition**

The respiratory tract acts as a series of filters for inhaled particles.

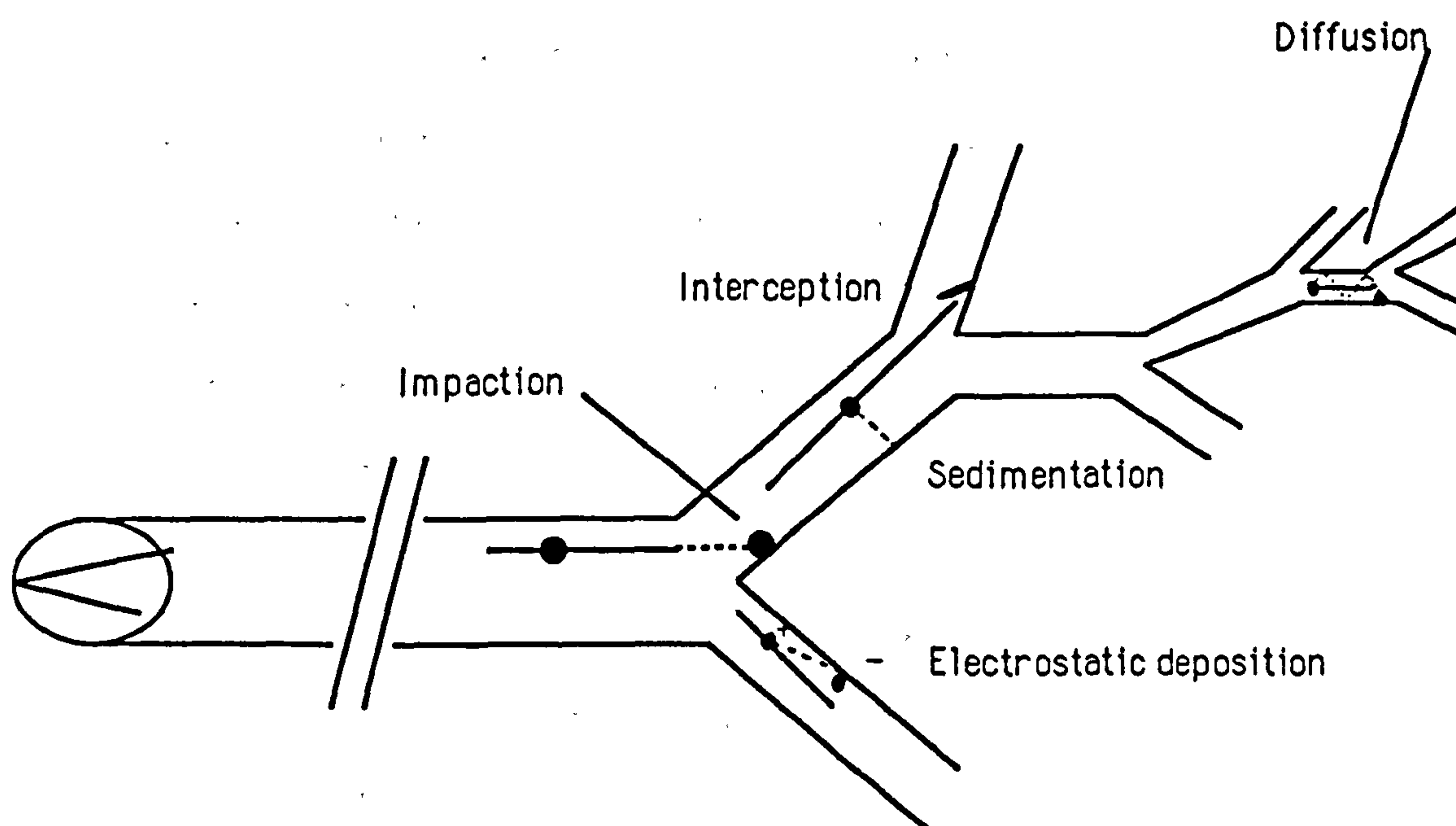


Fig 1.6 Mechanisms of particle deposition in respiratory tract airways



The deposition pattern of the inspired aerosol can be influenced by two major factors:

#### **1.4.1 Physiological factors**

The anatomical structure of the respiratory tract along with the mode of inhalation plays a significant role in the determination of the deposition mechanism of inhaled particles. The most important features of inhalation are the flow rate, the inhaled volume and the breath-holding time after inhalation (Newman *et al* , 1983). At high inspiratory flow rates, drug penetration into the lungs will be minimal due to the impaction of particles in the throat and the proximal part of the tracheobronchial tree.

Newman *et al* (1981, 1982), studied the response to a dose of a bronchodilator and the pattern of deposition as assessed by radioactive tracer techniques following carefully controlled and systematically varied inhalation manoeuvres from a pressurized metered dose inhaler. The studies demonstrated that metered dose aerosols should be inhaled slowly and steadily at about 30 l/min. Faster inhalation of approximately 80 l/min is less effective since more aerosol impacts in the oropharynx and is unable to penetrate into the lungs. Other workers have confirmed the value of inhaling slowly. Lawford and McKenzie (1981) found a greater bronchodilator response to fenoterol in a metered dose inhaler (MDI) following inhalation at 64 l/min than that at 192 l/min.

There are different opinions as to the point in the inspiratory process at which actuation of a metered dose inhaler should occur. Riley *et al* (1976, 1979) found that an isoprenaline MDI was more

effective when actuated at a high lung volume i.e 80% vital capacity (VC) compared to low lung volume, 20% VC. However Newman *et al* (1981, 1982) in a study carried out with terbutaline sulphate indicated that, provided the inhaler was activated during inspiration, no difference in efficacy was observed as a function of the point in the inspiratory phase at which actuation took place. The variations in the results may be attributed to the difference between the two studies. Riley *et al* performed their study on patients with mild airflow obstruction and used a very slow inhalation flow rate whereas Newman *et al* performed their study at higher flow rates.

A period of breath-holding after inhalation increases the probability of peripheral deposition, since it allows time for the particles to settle on the airways by gravitational sedimentation. Several groups of workers have established that a period of 5 to 10 seconds was found to enhance the clinical response and seemed both necessary and sufficient to give maximal bronchodilation.

The correct mode of inhalation for powder inhalation aerosols was unclear until clinical studies showed that a higher response was attained at high inspiratory flow rates. In a study carried out using a fenoterol powder, there was a significant increase in response when children inhaled as fast as possible compared with very slow inhalation of 16-19 l/min. However, breath-holding pause of 10 seconds after the inhalation had no significant effect on bronchodilation (Padersen and Steffensen, 1986).

Auty *et al* (1987) examined the respiratory deposition of SCG as reflected by its plasma concentration and urinary excretion, and



found that a higher plasma concentration was achieved at high inspiratory flow rates and that a peak inspiratory flow rate around 160 l/min probably represented optimal inhalation rate. No direct link between plasma concentration and clinical effect was established in this study.

However, the above observations were confirmed later by Richard *et al* (1988), who found that both inspiratory flow rate and the area under the plasma concentration time curve correlated well with the degree of protection afforded against AMP-induced bronchoconstriction. In this study, a link between inspiratory flow rate, plasma concentration and clinical effect was established. The increased protection at high inspiratory flow might be attributed to both an increase in the amount of drug delivered to the lungs and a more peripheral deposition.

Marked differences in deposition between individuals were observed. The intersubject variability may be due to anatomical and physiological variation (Heyder *et al*, 1982). Pitchard *et al* (1986) demonstrated the difference in regional deposition of inhaled particles in the 2.5-7.5  $\mu\text{m}$  size range for a particular inspiratory flow rate between men and women. This difference was attributed to the dimensions of the airways and the size of the lung which varies with age, height and sex.

Respiratory diseases influence the distribution of inhaled particles. Bronchoconstriction or obstruction of airways leads to diversion of flow to non-obstructed airways. The remaining healthy airways and alveoli may be increasingly exposed to inspired particles.



Narrowing of airways by mucus, inflammation or bronchial constriction can increase linear airflow velocities, thus enhance inertial deposition and cause more central deposition patterns (Lourenco *et al*, 1972 and Lauber *et al*, 1986). Svartengren *et al* (1989) have reported that a small degree of bronchoconstriction induced in humans, can markedly diminish the fraction of alveolar deposited particles in the lung.

#### 1.4.2 Physical properties of aerosols

The most important physical property influencing pulmonary deposition is the particle size of the aerosol cloud. Theoretically, inhalation aerosols may be targeted to a particular lung deposition site by governing the particle size.

From equations 1.3 and 1.6, it can be seen that impaction and sedimentation depend on the product density-diameter<sup>2</sup> ( $Pd^2$ ). Therefore ( $Pd^2$ ) can be used to predict the deposition site and collection efficiency. The square root of this product is known as the aerodynamic diameter of the particle ( $D_a$ ). This diameter is used to describe the effective size of particles moving in an air stream (The Task Group on Lung Dynamics, 1966). It can be defined as the diameter of a unit density sphere with the same settling velocity as the particle in question (Agnew, 1984).

$$D_a = d P^{1/2} \quad (1.9)$$

Particle size may continually change throughout the duration of a breath. Volatile aerosols or water droplets may evaporate leaving smaller particulates. Conversely, hygroscopic materials may grow dramatically in size as they pass from ambient relative humidity to

greater than 99% RH in the respiratory tract, particularly if the particles are water soluble. Water will condense on the particle until the vapour pressure on the surface of the particle equals that of the surrounding air in the respiratory tract. This will result in the particle growing in size thereby altering the deposition pattern. This effect is of considerable practical importance since the majority of inhalation aerosols are hygroscopic to some extent.

Lam *et al* (1984), pointed out that the particle size of inhaled salbutamol increased slightly during inspiration thus enhancing its deposition in the upper respiratory tract. Therefore the predicted dose of the drug that reaches the lower respiratory tract will be less than the non-hygroscopic aerosols of the same size.

The importance of particle size in inhalation aerosols results from the ability of the different diameters and branching airways of the respiratory tract to act as an efficient size separator. Mathematical models have been proposed for calculating the extent of retention of particulate matter of various sizes in the average adult human lungs. A schematic representation of the theoretical deposition of particles in the pulmonary tree as computed by Landhal is shown in Figure 1.7 ( Mitchell,1960).

The ideal size for therapeutic aerosols however is not known precisely. Davies *et al* (1976), estimated the size to be between 0.5-7.0 $\mu$ m. Particles larger than 7.0 $\mu$ m cannot penetrate beyond the trachea; whereas particles smaller than 0.5 $\mu$ m are probably exhaled.

Curry *et al* (1975) found a greater response to sodium cromoglycate when administered in a size of 2.0 $\mu$ m compared with particle sizes

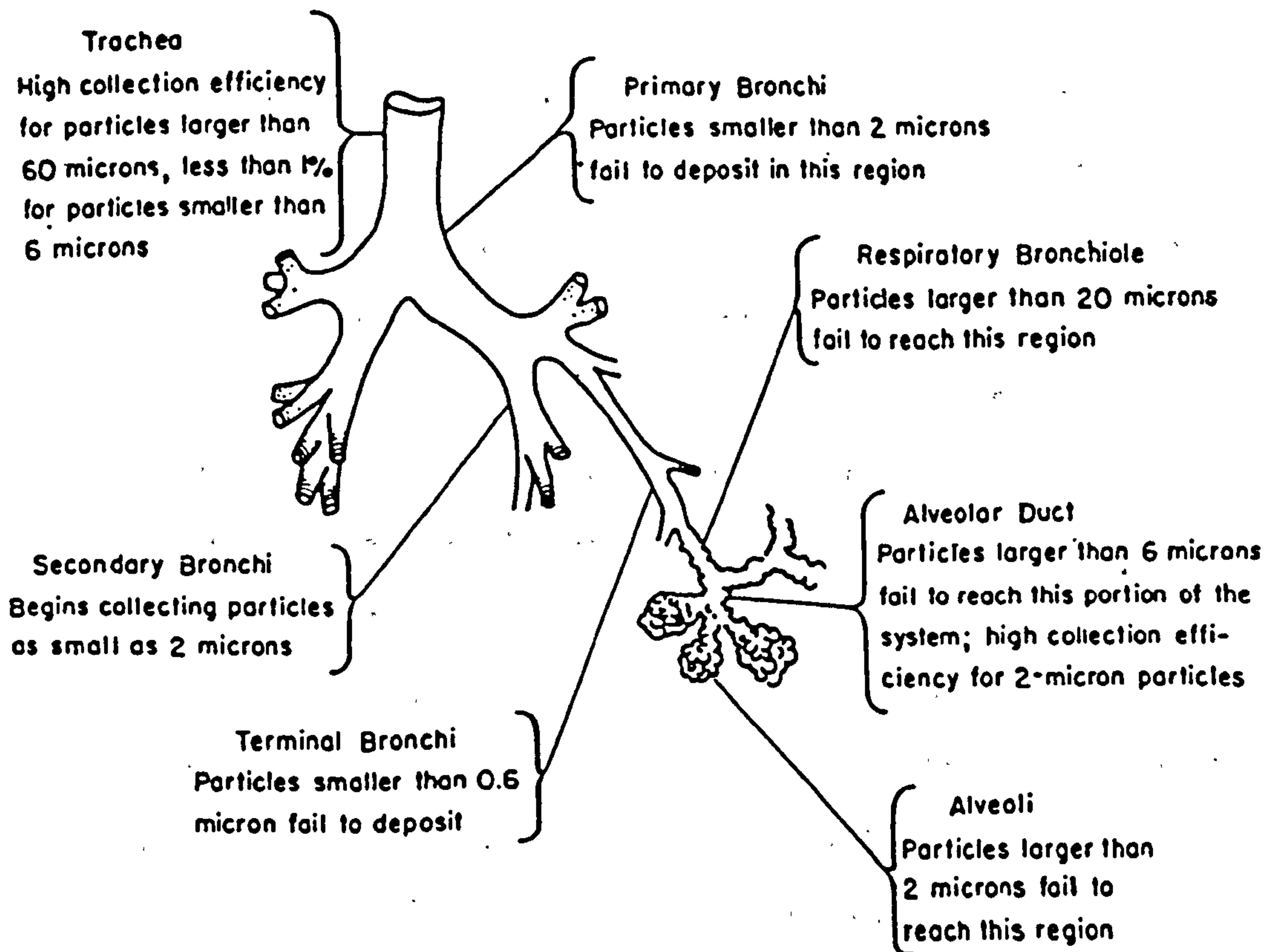


**Fig 1.7** Schematic representation of the theoretic deposition of particles in the pulmonary tree as computed by Landahl



of 6.0 and 11.7 $\mu\text{m}$ . This observation was confirmed by Rees *et al* (1982), who reported a greater bronchodilation response to terbutaline sulphate particles of diameter less than 5.0 $\mu\text{m}$  compared with inhaled particles in the size range of 5-10 $\mu\text{m}$  or 10-15 $\mu\text{m}$ . On the other hand, a similar deposition pattern was observed for 3.2 $\mu\text{m}$  and 6.4 $\mu\text{m}$  radioactively labelled Teflon particles (Newman *et al*, 1984).

Most aerosols are polydisperse and have a wide range of sizes. Because of the wide range and the fact that the physical properties of aerosols are strongly dependent on particle size, it is necessary to characterize these size distributions by statistical means. Distribution data are commonly plotted in a cumulative form (Figure 1.8). The geometric median diameter is the diameter corresponding to 50% on the plot such that 50% of all particles are above and below this value. If the cumulative curve is a straight line on the log-probability plot, the distribution is log-normal (Figure 1.9). The size range can be expressed by a geometric standard deviation (GSD) which is the diameter ratio at 84.1% and 50% or at 50% and 15.9%. This value is a measure of dispersity and corresponds to the standard deviation ( $\pm$  S.D.) of the median diameter of the curve. The distribution pattern of deposited particles and the subsequent clinical response may be dependent on the fate of few particles carrying a high proportion of the total mass. It is therefore more appropriate to express these distributions in terms of mass or volume (Mass Median Diameter MMD).

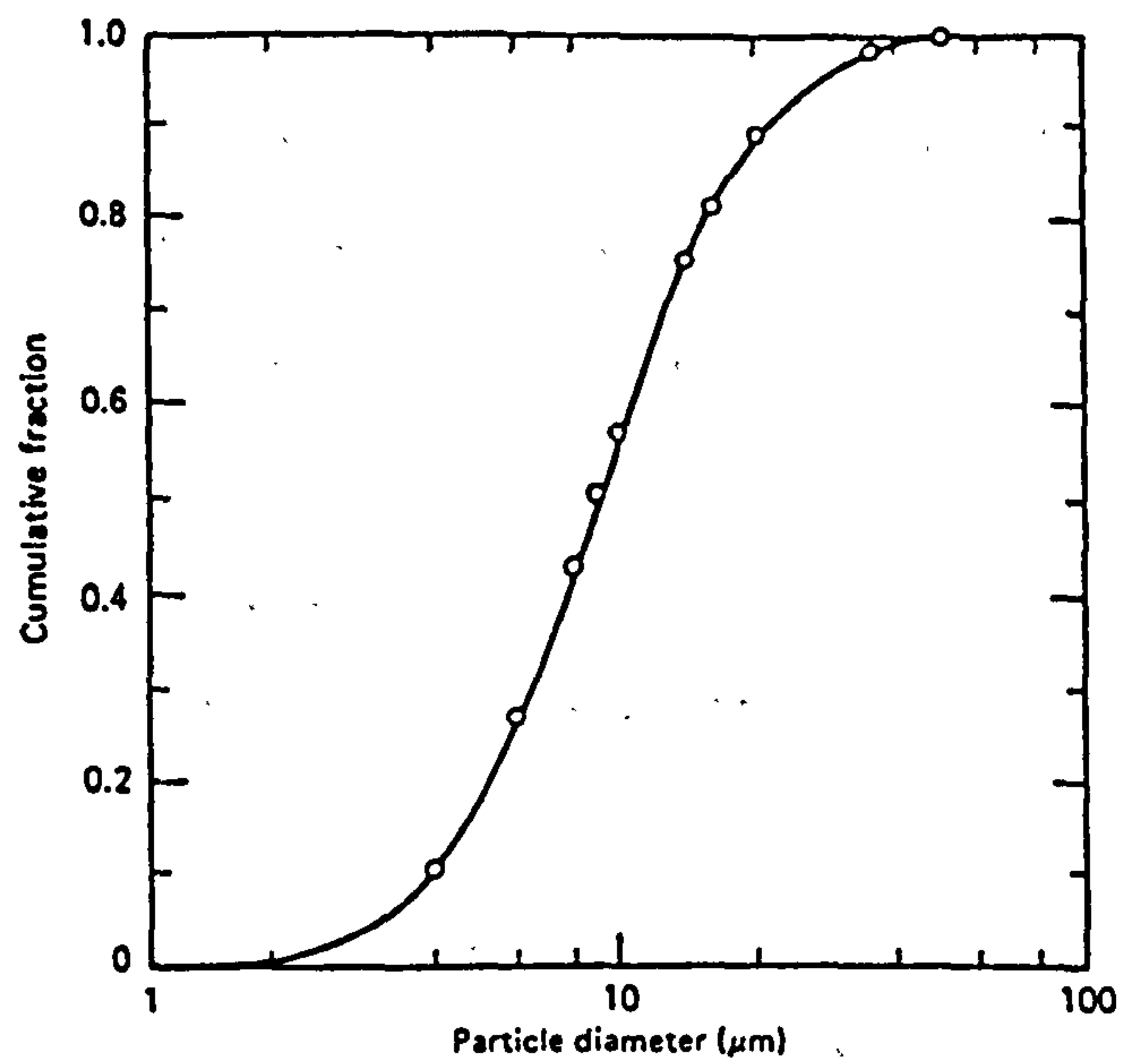


Fig 1.8 Cumulative distribution curve

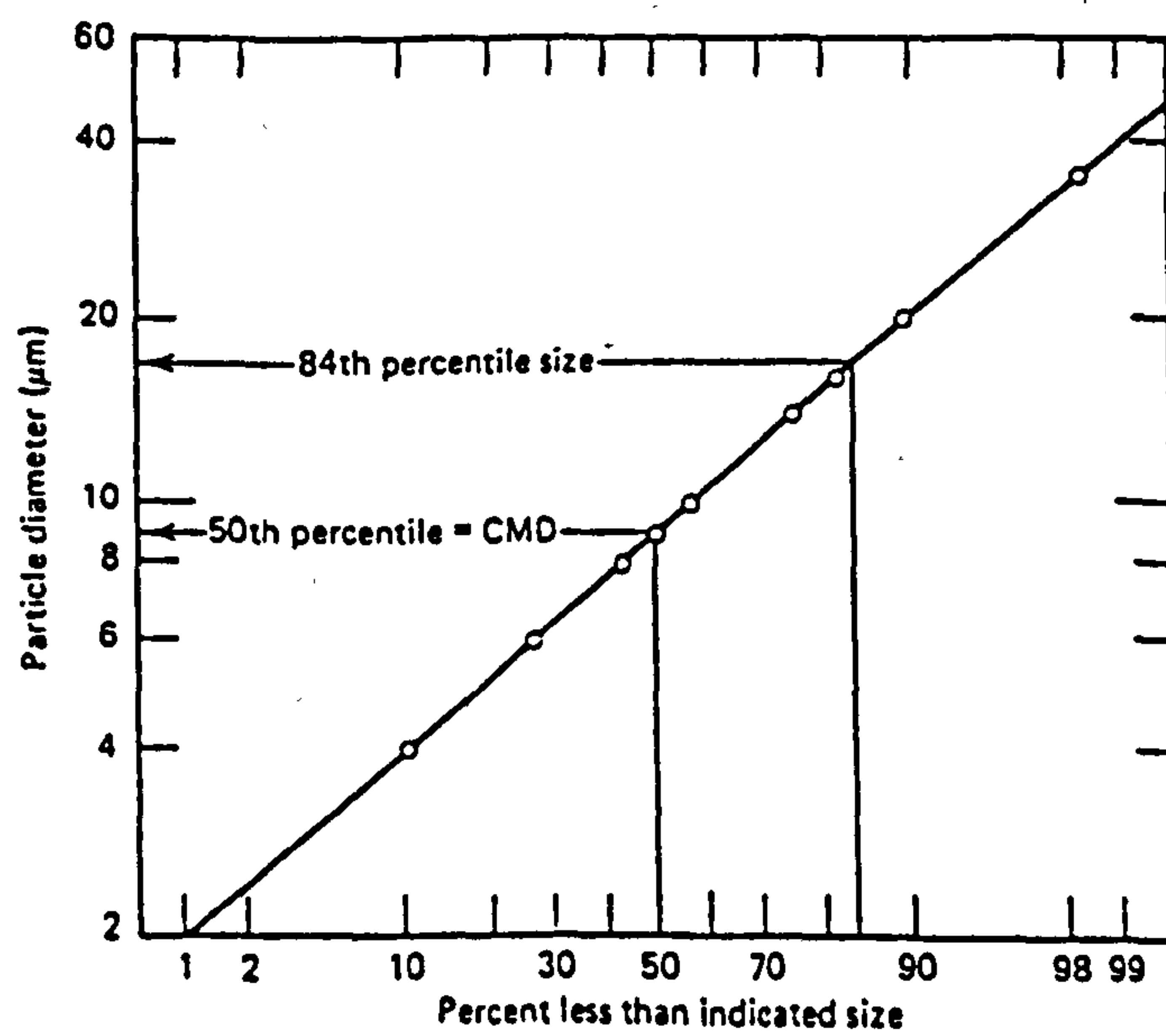


Fig 1.9 Log - probability graph

## **1.5 Inhalation delivery systems**

For more than a century inhaled remedies were delivered to the respiratory airways by inhalation of hot aromatic vapours via reed pipes or by smoking cigarettes made from leaves of plants containing the therapeutic agent (Miller, 1973).

However, in the modern era of aerosol therapy, three types of delivery system have been developed: nebulizers, pressurized metered dose inhalers (MDI) and dry powder inhalers (insufflators).

For patient use the ideal aerosol delivery system should be easy to use, portable, unobtrusive, inexpensive and enable precise quantities of the medicament to be delivered directly to the lungs.

### **1.5.1 Nebulizers**

The conversion of an aqueous solution into a mist of fine particles is a process known as nebulization. To achieve this process two types of nebulizers can be used:

1. Jet nebulizers are the most commonly used nebulizers. They work on the Venturi principle. They are driven by gas, either air or oxygen, which is forced through a jet. This creates an area of low pressure which draws up the drug solution into the fast moving gas stream, where it breaks up into small droplets. Larger droplets are trapped on a baffle and fall back into the solution for renebulization.

The major factor governing nebulizer performance is the flow of the compressed air used to generate the aerosol. Aerosol size is inversely proportional to the compressed gas flow rate (Davis S S 1978, Clay *et al*, 1983).



2. Ultrasonic nebulizers use high frequency sound waves produced from a piezoelectric transducer. The vibrations are focused on the surface of the liquid to generate the aerosol spray.

A wide range of nebulizers is commercially available. However, the output and particle size varies considerably between the different types (Newman *et al*, 1986, Clay *et al* , 1983 and Ho, 1988). Nebulizers are flexible devices in that a wide range of medicaments may be administered. Large doses are normally dispensed by these devices, thus they are useful in acute severe attacks of asthma. However, nebulizers are the least portable of the inhalation devices. Therefore, they are mainly used for hospital treatment and increasingly in domiciliary use. Patients receiving this treatment, do, however, require comprehensive instructions regarding sterilization of the nebulizer, storage of the drug and maintenance of the compressor.

### 1.5.2 Metered dose inhalers (MDIs)

The introduction of MDIs over 30 years ago was a significant innovation in inhalation therapy. New medicaments have been introduced into this type of device in the meantime but the basic aerosol system has remained substantially the same. Preparations usually consist of solutions or suspensions of one or more active ingredients held under pressure in a suitable propellant or a mixture of propellants. Propellants, such as chlorofluorohydrocarbons, are liquified gases and mixtures of these may be used to obtain optimal solution properties and desirable pressure, delivery and spray characteristics. Pressurised inhalers may contain suitable auxiliary

substances such as solvents, solubilising agents, suspending agents and lubricating agents to prevent clogging of the valves (British Pharmacopoeia, 1988). They are intended to be inhaled in controlled amounts and are delivered by the actuation of an appropriate metering valve.

The generated aerosol cloud contains drug particles in an envelope of surfactant or co-solvent and propellant. The size distribution of the emitted aerosol is not precisely known. Hiller *et al* (1978) noted that the size distribution of MDI aerosols does not necessarily conform to log-normal modelling and a multi-modal distribution was observed. In more recent work, Bouchikhi *et al* (1988) obtained a multi-modal distribution, however, a different aerodynamic profile was observed, which is a function of physico-chemical properties related to the formulation and the environmental conditions.

On actuation of the MDI, rapid initial vaporization of the propellant occurs. This breaks up the liquid stream into filaments then droplets. The particle velocity exceeds the inspiratory flow rate, thus a large number of particles are impinged onto the oropharynx. A rapid cooling due to heat transfer during propellant evaporation promotes condensation of water vapour onto the droplets. The resultant particle size therefore might be larger than the micronized drug particles. The determination of size together with velocity is necessary for this type of aerosol, since both factors can affect lung penetration. MDIs are widely favoured since they are highly portable, inexpensive and represent a convenient method for multi-dose delivery.



However, there are many inherent disadvantages associated with these systems. Clinical research over the years has shown that there is an optimum way for the MDI to be used but it has become increasingly clear that a large proportion of patients do not employ this technique effectively.

The most common problem is the inability to synchronise aerosol release with inspiration (Crompton , 1982b). To solve this problem, several inhalation aids have been developed. A spacer fitted to the mouthpiece of a conventional MDI is believed to cause a delay between actuation and inhalation thus reducing the need for co-ordination (Koing , 1985). Recently, a breath-actuated MDI (Aerolin Autohaler) was developed (Crompton , 1988). This device requires minimum patient involvement to ensure that drug delivery is synchronous with inhalation. It is believed that the new inhaler functions reliably at inspired flow rates of around 28 l/min.

A drawback of the MDI delivery system is their content of chlorofluorocarbon propellants. There has been some controversy about their toxicity, the possibility of causing bronchoconstriction and potential arrhythmogenic effects (Thiessen & Pedersen, 1980). In addition, the use of these substances has been greatly criticized owing to the possible destruction of the ozone layer in the atmosphere (Maugh , 1984) and increasing the "green-house" effect.

### **1.5.3 Dry powder inhalers**

Dry powder inhaler systems provide clear advantages over other delivery systems. Because of their convenience and portability, they are widely accepted by both patients and clinicians as an effective means of drug delivery to the lower respiratory tract. The clear



advantage of dry powder systems is that the inspirational effort of the patient leads to entrainment of the drug powder in the inhalation air stream. Therefore these devices can be of great importance, particularly to those who have difficulty in co-ordinating the actuation of MDI with the intake of breath (Crompton , 1982a).

The product consists primarily of a device from which the drug powder is dispensed and a means of containment of the drug system. A balance between effective delivery of the medicament to the lower respiratory tract, and patient convenience and acceptability depends strongly on two elements:

1. The formulation.
2. The design of the device.

The drug particles are presented in respirable fractions, i.e.  $5\mu\text{m}$  or less in diameter. However, this involves problems of powder fluidisation, flow and dispersion. Additional complication may arise if a potent drug substance is to be used in doses of few micrograms. Therefore, an inert soluble carrier, commonly lactose, is included in the dry powder formulations to facilitate the fluidisation process. However, for the drug to penetrate into the respiratory tract, it has to be dispersed as single particles. In this respect the construction of the device affects the type of air flow within the inhaler air channels and the ability of the system to both empty the powder reservoir and redisperse the powder mixture as separate components.

To describe the nature of airflow in the air channels, Reynold's Number can be employed.

$$\text{Reynold's Number} = dVP/\eta$$

where

$d$  is the tube diameter

$V$  is the air velocity

$P$  is the air density

$\eta$  is the air viscosity

The use of this dimensionless parameter allows the differentiation between laminar and turbulent flow and quantifies the level of turbulence in a tube. If Reynold's Number is greater than 2000, then the flow is turbulent. A value less than 2000 indicates laminar flow.

Over the past two decades, particular emphasis has been given to the development and production of different powder inhaler devices. The first invention was the "Spinhaler" (Fisons Ltd) shown in Figure 1.10a for inhalation of cromolyn sodium (Bell *et al*, 1971). In this design, a gelatin capsule containing the powder mixture is inserted into a rotor and pierced. As the patient inhales, the revolution of the rotor causes high-frequency vibration in the capsule wall. The powder is fluidised within the capsule and the vibrations cause the drug to be dispensed into the inhaled air stream through the perforations.

In 1977, a new dry powder device the "Rotahaler" (Allen & Hanbury's Ltd) was introduced (Hallworth, 1977), initially for salbutamol (Duncan *et al*, 1977) and subsequently for beclomethasone dipropionate (Carmichael *et al*, 1978). The construction of this device (Fig 1.10b) is fairly simple compared to the "Spinhaler". The capsule "Rotacap" is inserted into the end of the inhaler. As one end is turned, the capsule is separated into two halves. The part containing the powder drops into a chamber and the drug particles are



dispensed into the air stream as the patient inhales through the device. In another powder inhaler, "Berotec" inhaler (Boehringer Ingelheim), the drug is inhaled through the pierced holes of a stationary capsule contained in a very narrow chamber (Fig 3.10c).

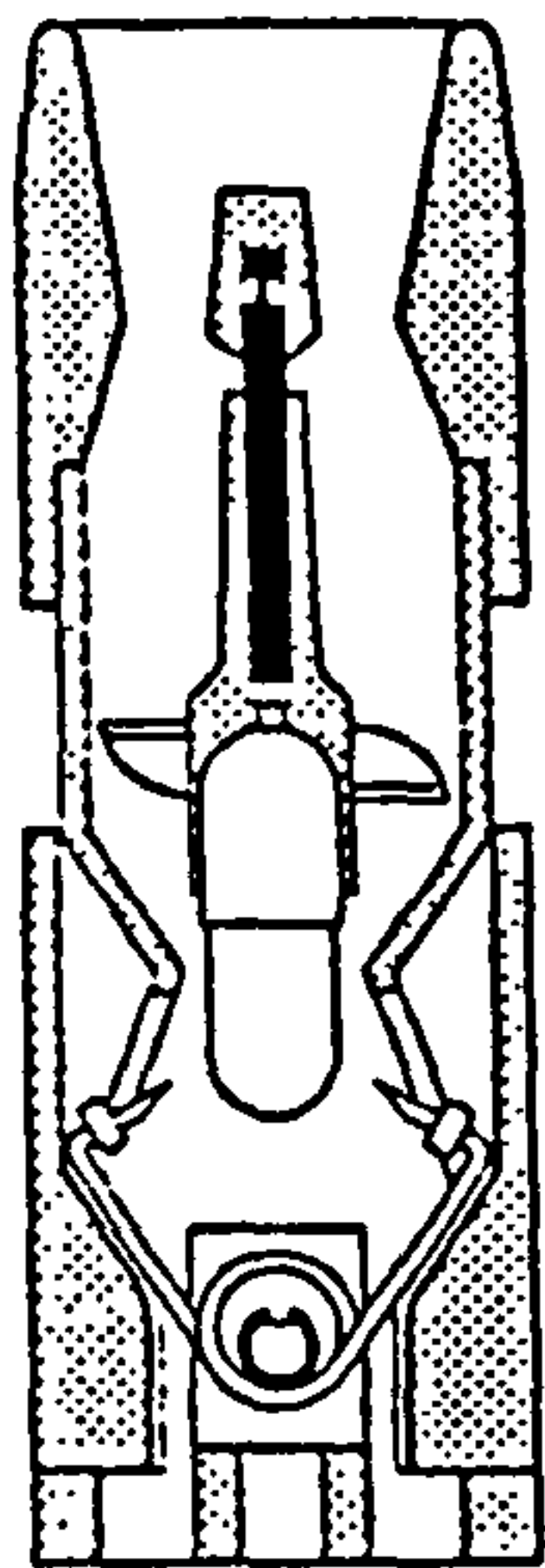
These devices are based on the inhalation of a pre-packed unit doses which are inserted into the device prior to inhalation. Reloading the inhaler can be very inconvenient to the patient especially in acute attacks of asthma. Therefore, over the last few years, new devices have been developed to improve the patient acceptability. In these improved delivery systems, the required dose is metered from a reservoir.

The "Diskhaler" (Allen & Hanbury's Ltd) was designed to have similar efficiency to the "Rotahaler". In this reloadable device, a disc containing eight foil blisters of drug is inserted into the device. The inhaler is made ready for inhalation by lifting the mouthpiece cover. The blisters are pierced by means of a needle and the drug is dispensed into the inhaled air stream. The doses are numbered, making it possible for the patient to know how many doses remain.

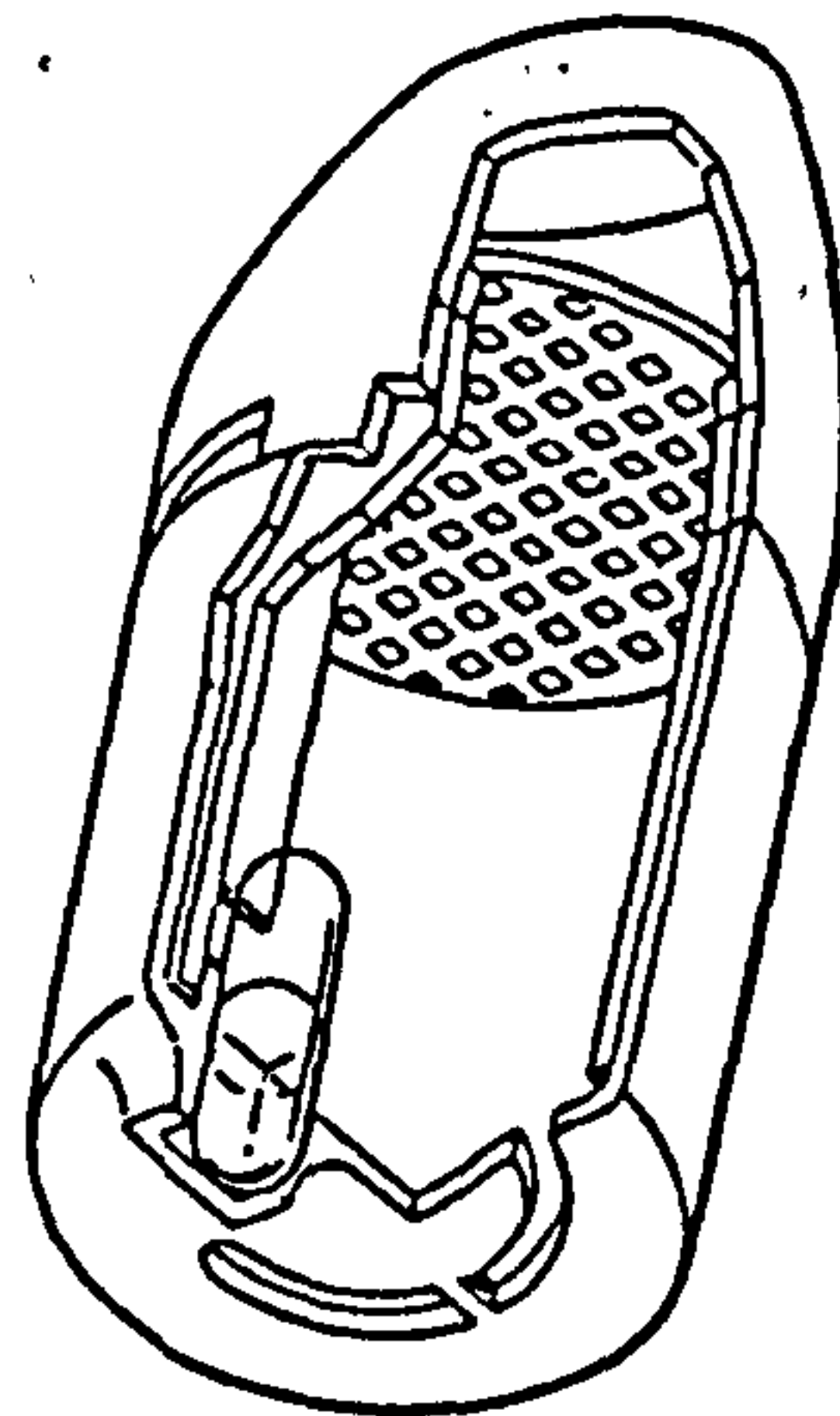
More recently, a multi-dose powder inhaler the "Turbohaler" (Astra Pharmaceuticals) was introduced for administration of terbutaline sulphate (Fig1.10d). The "Turbohaler" is unique in that it is a metered dose inhaler which is not pressurized and is free from additives. The device is disposable after its 200 doses have been used and has visual warning signal when only 20 doses are left in the inhaler. The device is simply operated by twisting the turning grip at the bottom of the inhaler. The drug flows from a reservoir down onto a dosing disc with



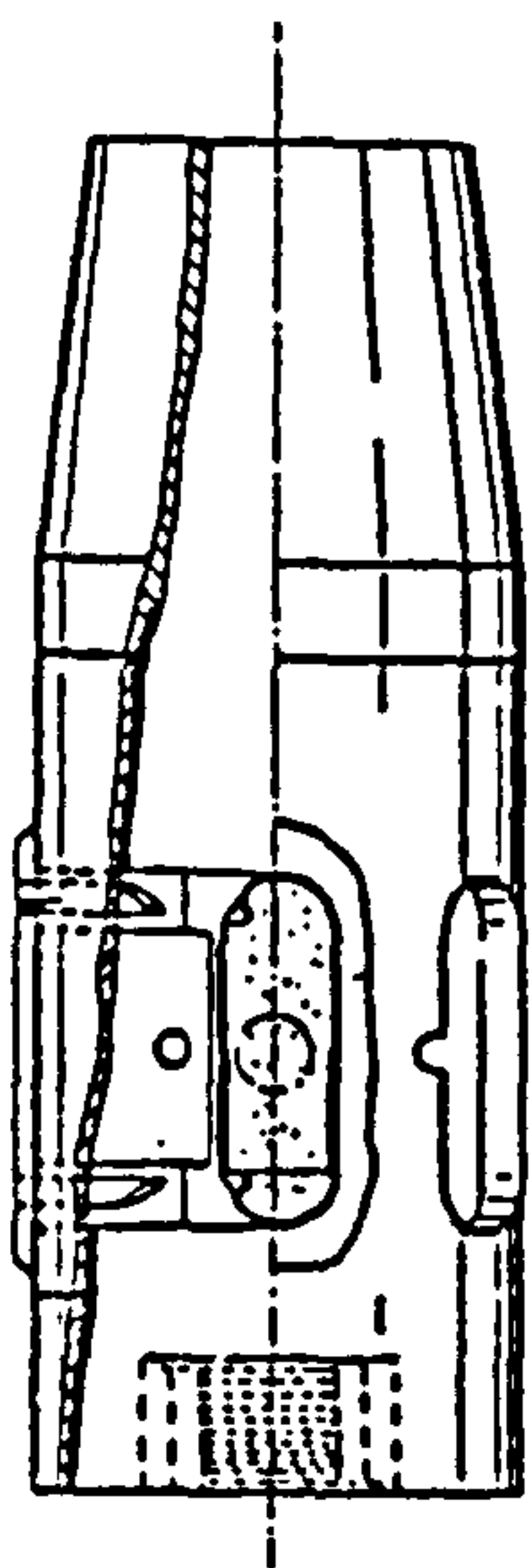
**Fig 1.10**



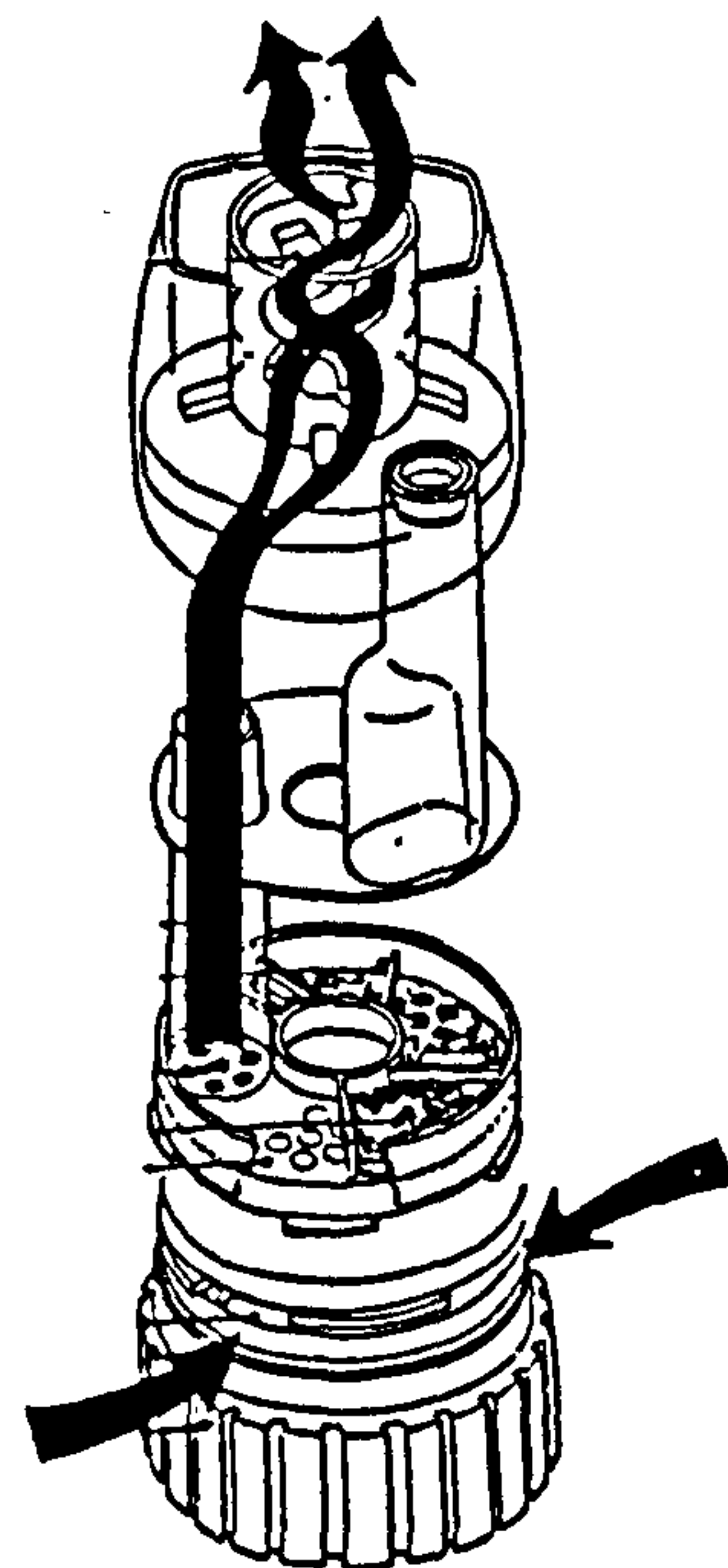
**(a) Spinhaler**



**(b) Rotahaler**



**(c) Berotec inhaler**



**(d) Turbohaler**

fine holes. The holes are filled up and a metered dose is made available for inhalation as the inhalation air stream enters the channel into the dosing unit (Wetterlin , 1988).

Encouraging results have been obtained in clinical trials performed to compare the efficiency and acceptability of these devices with other inhalation delivery systems. Dry powder inhalers seem to be more attractive and are now an established alternative to MDIs and nebulizers.

### **1.6 Efficiency of inhalation delivery systems**

With the range of inhalation devices, a question may arise as to which of these delivery systems is superior in terms of the clinical response produced. For this purpose clinical studies were carried out comparing the performance of the available devices and investigating whether switching a patient to an alternative type of inhalation device would produce the same response.

A comparison between nebulized salbutamol and salbutamol from a metered dose inhaler was performed by Jenkins *et al* (1987) who reported that there was no significant difference in the efficiency of the two delivery methods.

In a more recent study comparing the effectiveness of equal doses of salbutamol administered by a nebulizer and by a "Rotahaler", it was observed that salbutamol inhaled via a "Rotahaler" is just as effective as the same dose inhaled from a nebulizer in producing bronchodilation. Furthermore, the "Rotacaps" offered an advantage of being more portable than a wet nebulizer (Assouffi & Hodson, 1989)

Other studies have been performed to investigate the efficiency of a dry powder inhaler in comparison with a pressurized MDI. It was found that the powder dose of salbutamol administered via a "Rotahaler" has to be doubled in order to produce the same response as that from the MDI (Hetzel *et al*, 1977 and Muittari *et al*, 1979). However, in recent investigation, an equal dose of ipratropium bromide inhaled via a pressurized MDI produced the same effect as when inhaled via a powder inhaler, "Atrovent" (Boehringer Ingelheim) (Salorinne *et al*, 1988). A comparable clinical effect was also observed for terbutaline administered by a pressurized MDI and by a multi-dose powder inhaler the "Turbohaler" (Parsson *et al*, 1988). Both "Atrovent" inhaler and the "Turbohaler" appear to release the same amount of the respective drugs as the MDI, whereas, with the "Rotahaler" above, double the dose was required for equipotency. This suggests that the type of powder inhalation device and the nature of the powder formulation might have a great influence on the efficiency of powder aerosols.

In a study in children, fenoterol administered by a powder inhalation device was found to be superior to that by an MDI (Chambers *et al*, 1980). The difference observed in this study was attributed to the incorrect inhalation technique used when inhaling from a MDI, which emphasises the importance of synchronization.

A comparison between various powder inhalation devices was carried out by Vidgren *et al* (1987), who showed that the respirable fraction of SCG achieved from various devices was significantly different (Table 1.2). The difference was attributed to the construction of the device. In a more recent work Bogaard *et al* (1989), found no



significant difference in clinical response of terbutaline administered via a "Turbohaler" and an equipotent dose of salbutamol administered by a "Rotahaler" (Figure 1.11). The "Turbohaler" was superior in its ease of use since it is a multi-dose system and requires only a relatively low inhalation flow for activation such as 33 l/min which was proved to give a good response (Parsson *et al*, 1988), whereas it was observed that at flow rate of 30 l/min, there was barely any rotation of the capsule in the "Rotahaler" and emptying was erratic (Svedmyr *et al*, 1982).

All the above studies confirm that there is probably little difference in the clinical efficiency between the various devices providing that they are handled correctly. Each type of the inhalation devices has its own advantages and disadvantages. Therefore, the choice of the device will mainly depend on the patient's disease state. For instance, nebulizer treatment can be ideal in acute severe asthmatic attacks where co-ordination of actuation with inhalation as required with MDIs might be difficult, or high inspiratory flow rates cannot be achieved to actuate a powder inhaler. On the other hand, for routine use, patient convenience and acceptability are important. Therefore, more portable devices seem to be more suitable. However, the availability of the various types of devices makes it possible for all patients to benefit from inhalation therapy which is superior to other therapeutic dosage forms in the treatment of lung diseases.

### **1.7 Evaluation of inhalation aerosols**

There seems to be little doubt that therapeutic aerosols must reach the lungs in sufficient quantities in order to attain a therapeutic

Table 1.2 The mean fractional deposition of <sup>99m</sup>Tc - labelled particles of SCG following inhalation from four dry powder inhalers

Inhaler	Fraction from the dose %		
	Lungs	Upper airways	Device
Spinhaler	11.5	30.9	57.6
I.S.F	16.4	44.0	39.6
Berotec	16.0	59.0	25.0
Rotahaler	6.2	50.1	43.8

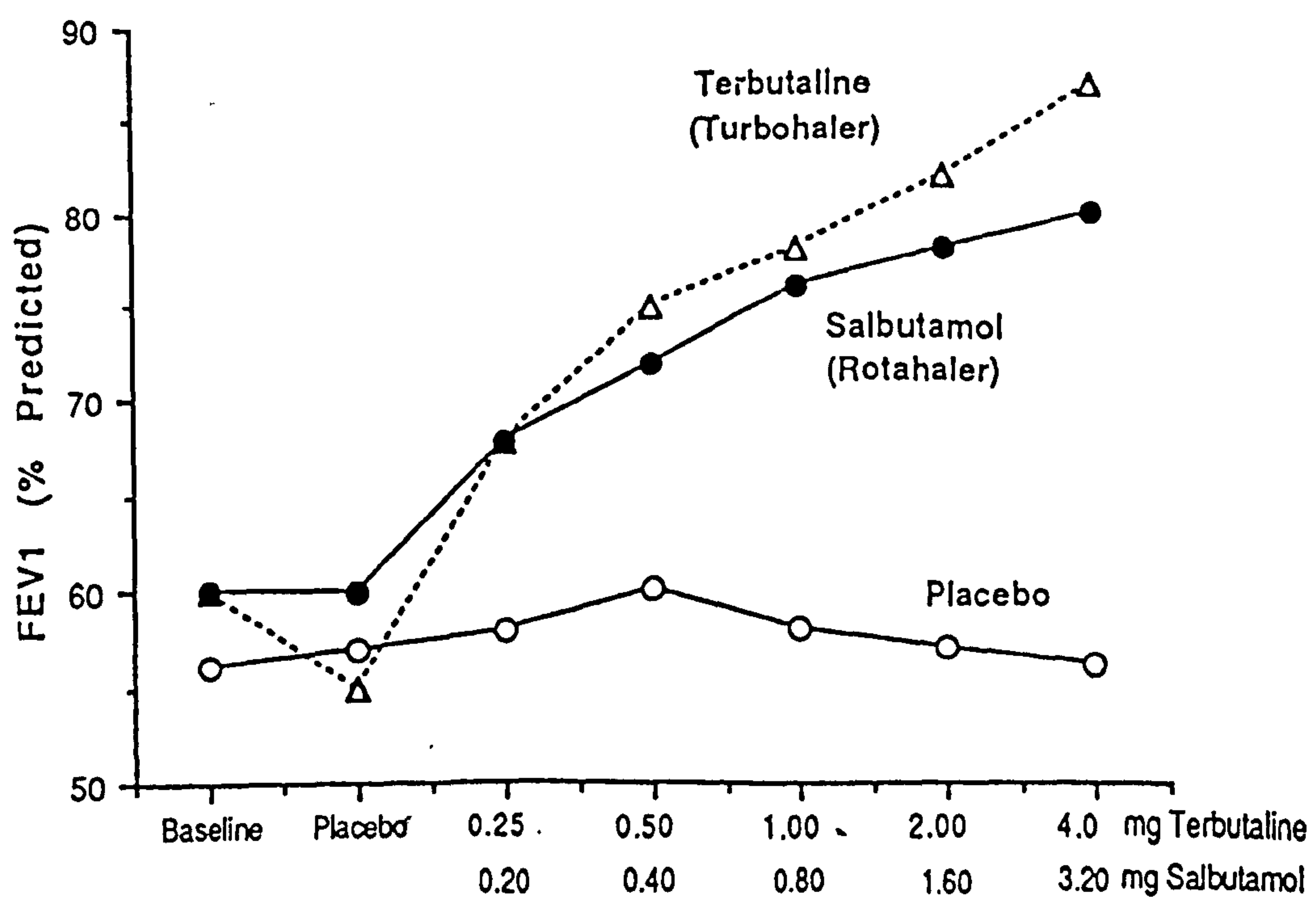


Fig 1.11 Mean cumulative dose-response curves following inhalation of terbutaline using a Turbohaler and salbutamol using a Rotahaler

principle that the light scattered by a particle is a direct function of its size. Davies *et al* (1980 a,b) employed the " Royco" particle size analyser which measures the projected area diameter of the particles and provides rapid counts of large number of particles. More recently laser Fraunhofer diffraction size analysers were introduced which offer even more potential for rapid measurement.

Aerodynamic size distribution can be measured employing the single particle aerodynamic relaxation time (SPART) analyser. In this technique particles are subjected to acoustic oscillation, and the aerodynamic diameter is directly related to the phase lag between particle oscillation and acoustic field oscillation (Hiller *et al*, 1978, 1980). The limitations for the light scattering technique is that it requires extreme aerosol cloud dilution and thus large particles are lost and the initial droplet size changes during passage through the air before the measurement is made. This presents problems of representative sampling. Additional limitations include lens aberration, background stray light and electric fields which can produce disturbances in the collection of signals. Using this method it is not possible to distinguish drug particles from foreign or excipient particles or from other drugs in combination drug products.

One of the indirect methods which has been explored for sizing airborne particles is the one based on inertial separation.

Impaction models which are intended to simulate the behaviour of the respiratory tract have been used (Kirk, 1972, Karig *et al*, 1973 & Sciarra & Cutrie, 1978) to compare the likely respiratory penetrability of aerosols. These models are very simple compared to the actual anatomical configuration of the human respiratory tract and give a poorly defined



size cut-off characteristics.

Other impactors which have been developed basically for use in work places for collection and sizing airborne particulate matter to assess the potential health hazards from air contaminants have been employed for evaluation of therapeutic aerosols. Hallworth and Andrews (1976) used a number of conventional cascade impactors which utilise the relationship between velocity and mass. The value of this method is that a mass distribution of the aerosol is given directly in terms of aerodynamic diameter which describes the behaviour of inhaled particles within the respiratory tract. The quantity of collected materials in an impactor can be determined chemically or physically; a procedure which is time consuming. A simplified twin-impinger (Hallworth *et al*, 1978; Hallworth and Westmoreland, 1987) was subsequently developed for more rapid quality control processing of inhalation pharmaceuticals. This device is included in the British Pharmacopoeia (1988) as an official method for characterizing inhalation aerosols. The twin-impinger has proved to give a good correlation with the clinical performance of therapeutic aerosols (Padfield *et al*, 1983).

Thus, the respirable fraction determined *in vitro* may vary depending on the technique used. Therefore, if any of these techniques gives the real respirable fraction can only be determined by referring to clinical trials.

### **1.7.2 *In Vivo* methods:**

Deposition of therapeutic aerosols may be difficult to predict

accurately based on *in vitro* models. *In vivo* studies are essential to characterize the mode of deposition and hence the clinical response. For bronchodilators the simplest method for detecting the penetration of drug particles into the lungs is by assessing the lung function before and after administration of the medicament.

Valuable information on the deposition of drugs in the respiratory tract may also be obtained from pharmacokinetic studies. The amount of drug and its metabolites in plasma and urine can be compared after both inhalation and oral intake (Walker *et al*, 1972 and Fuller & Collier, 1983).

Radioaerosol methods using gamma-ray emitting radionuclides are the most practical means of assessing both total and regional deposition of therapeutic aerosols. Inhaled gamma labelled particles can be detected externally by means of a gamma camera since gamma rays can penetrate the tissues of the body. Chemical labelling of antiasthmatic agents with gamma-ray emitting radionuclides is very difficult, since these compounds rarely contain an element with a suitable radionuclide. The only successful labelling achieved was with the bronchodilator ipratropium bromide-labelled with a gamma-emitter  $^{77}\text{Br}$  (Spiro *et al*, 1984).

Inert labelled particles have been used as a model for the prediction of the deposition of inhaled particles.  $^{99\text{m}}\text{Tc}$  has been found useful for labelling the inert materials. Teflon particles have been shown to be particularly suitable since they are biologically inert and insoluble in body fluids. Newman *et al* (1982) have studied the deposition of radioactive pressurized aerosols using these particles. More recently physical labelling of MDIs was achieved by the addition of  $^{99\text{m}}\text{Tc}$  to a canister containing the drug suspended in a

liquified propellant (Kohler *et al*, 1988 and Summers *et al*, 1989). In this technique the drug is not directly labelled but the distribution of the activity can be assumed to represent the distribution of the drug. Deposition from nebulizers were also studied using radiolabelled vehicles (Clay *et al*, 1987)

To assess deposition patterns from powder inhalation aerosols, two novel methods for physical labelling of the dry powder were developed. In the first method, Vidgren *et al* (1987) labelled SCG particles using a spray drying technique. In the second method described recently by Newman *et al* (1989), the radionuclide  $^{99m}\text{Tc}$  dissolved in chloroform was added to a spheronized formulation of terbutaline sulphate and the chloroform was allowed to evaporate leaving radiolabelled particles. However, these two methods cannot be used to study deposition from all dry powder aerosols. Both spray drying and spheronization will change the physical properties of the drug particles and thus formulations containing mechanically micronized particles will have different inspirable characteristics.

Therefore, until other techniques are available for labelling mechanically micronized particles which are normally present in the powder aerosols, direct detection of powder aerosols, within the lungs is not feasible and other *in vivo* techniques have to be employed.



## **1.8 Scope of the thesis**

The importance of inhalation, in particular that associated with dry powder inhalation, in the treatment of various respiratory diseases has been discussed in the preceding introduction. Studies on the major factors which influence the efficiency of powder inhalation aerosols are not well documented in the literature. The possible variables which might affect the fate and efficacy of the aerosol cloud in the respiratory tract are the formulation variables, the device and the patient (see Section 1.7).

Recent clinical studies have shown that the patient's inspiratory flow rate is a major factor governing pulmonary deposition (Auty *et al* 1987, and Richard, *et al*, 1988). However, *in vitro* evaluation of dry powder inhalation aerosols in terms of inspiratory effort is not possible using the available techniques. The following work was structured under the following headings to study the efficiency of dry powder aerosols in relation to these variables:

1. Development of an apparatus which permits physical characterisation of an aerosol cloud generated at various flow rates employing the principle of isokinetic sampling to collect a representative fraction of the generated aerosol.
2. Assessment of the effect of formulation variables and a device on the characteristics of an inspirable cloud using the concept of mechanical stability of powder mixtures and the way this is influenced by factors which affect the adhesion properties between the drug and the carrier.
3. *In vivo* evaluation of a novel dry powder aerosol formulation and a device.

## **Chapter two**

### **Design and evaluation of an apparatus for sampling and characterising an aerosol cloud**

## 2.1 Introduction

In nature, solid particles such as dust are conveyed into the atmosphere as air flows over a layer of powder. At low air velocities, particles become detached from the surface and are carried by the turbulent air flow. However, at high flow velocities, not only the particles are carried away but the whole aggregates are torn out and disintegrated by the current of air (Fuchs, 1964). This is the principal mechanism by which dry powder inhalation aerosols are conveyed into the inhalation air stream of the patient.

Aerosols produced by dry powder inhalers are polydisperse. As described in section 1.6.3, drug particles in the formulation are normally present in a respirable size together with a suitable carrier of a coarser size. Upon fluidisation, the aerosol cloud will consist of, a mixture of single fine drug particles, drug agglomerates of various sizes and coarse carrier with some drug particles still adhering to its surface. The size distribution of the generated cloud will mainly depend on the flow velocity of the air stream. This is in agreement with clinical studies which have indicated that the extent of pulmonary deposition is highly dependent on the inspiration rate (Auty *et al*, 1987, Richard *et al*, 1987, Dolovich *et al*, 1988). This, in turn, depends upon the patient's disease state and age.

There have been no reports in the literature of *in vitro* studies carried out to predict the clinical performance of dry powder aerosols at flow rates exceeding 60 l/min despite the much higher inspiratory flow rates attainable by normal human lungs and even by mild asthmatics (Richard *et al*, 1987).



Previous workers (Bell *et al*, 1971, Chowhan *et al*, 1977, Hallworth & Westmoreland, 1987, Vidgren *et al*, 1987) have employed inertial separation methods to assess the physical characteristics of the whole aerosol cloud. However, although this technique has great relevance to the behaviour of the inhaled particles in the respiratory tract, the use of inertial impactors in this way is limited by their low operational flow speeds. Operating the impactors or impingers at different flow rates requires re-calibration of the impaction stages which fractionate the cloud. This process is very tedious and time consuming. Furthermore, operating the impactors at high flow rates may not be feasible, since increasing the suction flow rate within an impactor will increase the velocity within each stage.

Solid particles will hit the impaction surfaces at a very high velocity and part of the kinetic energy of the particle will be dissipated and part is converted elastically to kinetic energy of rebound. If the rebound energy exceeds the adhesion energy, the particles will bounce away from the surface thus leading to errors in the particle size distribution.

Similarly, operating the liquid impingers at high flow rates may cause severe rippling and excessive turbulence in the liquid as air impinges on its surface. Consequently, the liquid vortex shape and the jet liquid surface spacing will be inconsistent resulting in an inefficient particle size separation.

Therefore, to study the behaviour of powder inhalation aerosols generated at various flow rates, there is a need to develop an apparatus which overcomes these difficulties.

In occupational hygiene and environmental air monitoring, a wide

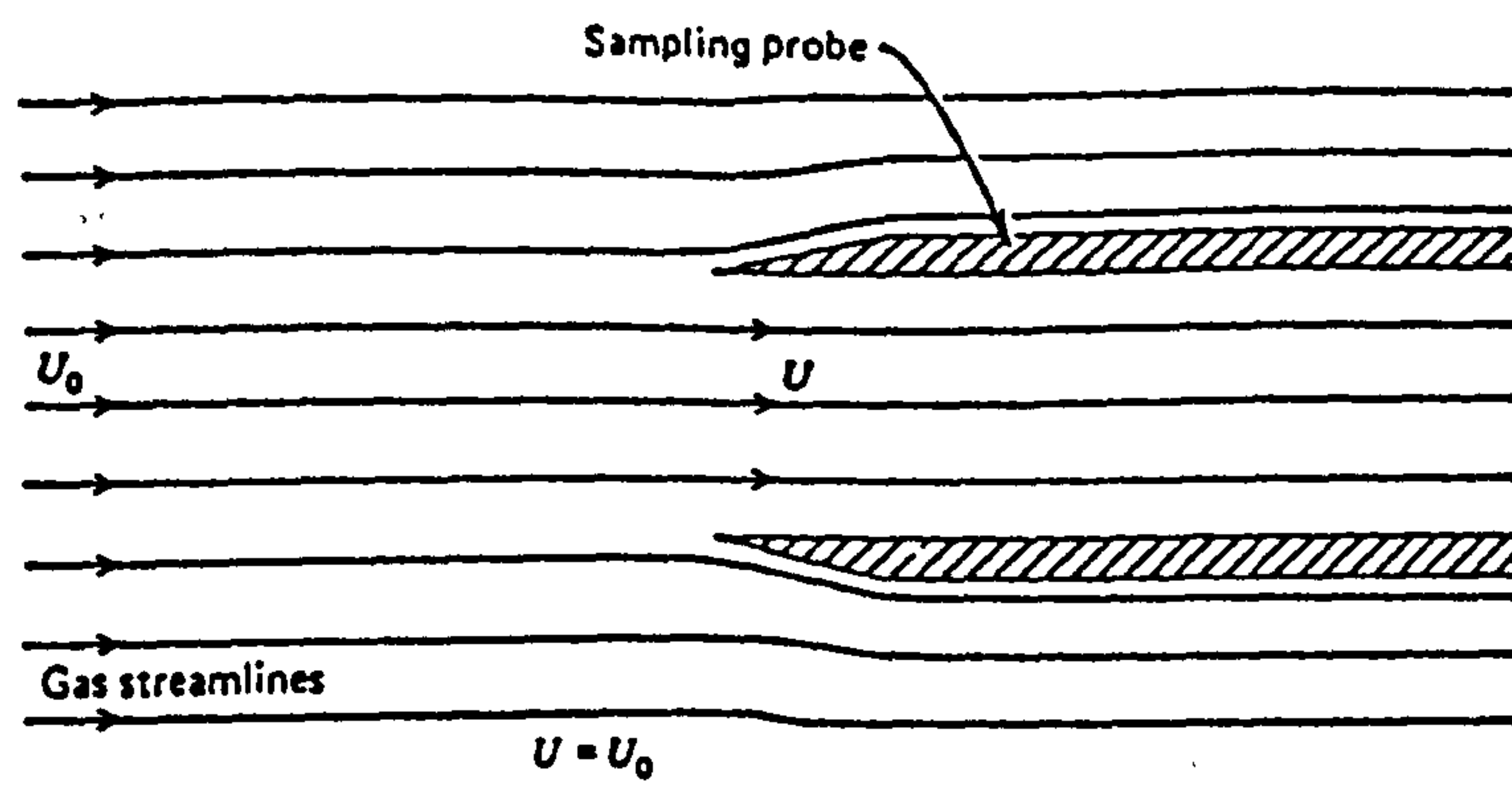
range of dust sampling configurations are employed for the determination of the concentration of airborne dust in a flowing air stream. In these dust samplers only a portion of the dust laden air is aspirated and collected by a measuring device. Therefore, a difficulty may arise in removing a sample which is representative of the gas stream. This can only be achieved if the velocity of aspiration into the sampling tube,  $U$ , is equal to the free stream velocity,  $U_0$ , at that point (Figure 2.1a). This is known as isokinetic sampling.

Under isokinetic conditions there is no disturbance of the gas streamlines and the concentration of airborne particles inside the sampling tube will be the same as that in the undisturbed flow upstream. Failure to sample isokinetically (anisokinetic sampling) may result in distortion of the particle size distribution and misrepresentation of the concentration. Anisokinetic sampling occurs when the sampling velocity differs from that of the gas stream. This will disturb the gas streamlines causing some particles to be deflected from their original direction of motion and hence the quantity of particles entering the sampling tube will differ from that entering under isokinetic conditions. The sample may contain either an excess or a deficiency of large particles depending on the conditions of sampling (see Figure 2.1c and d).

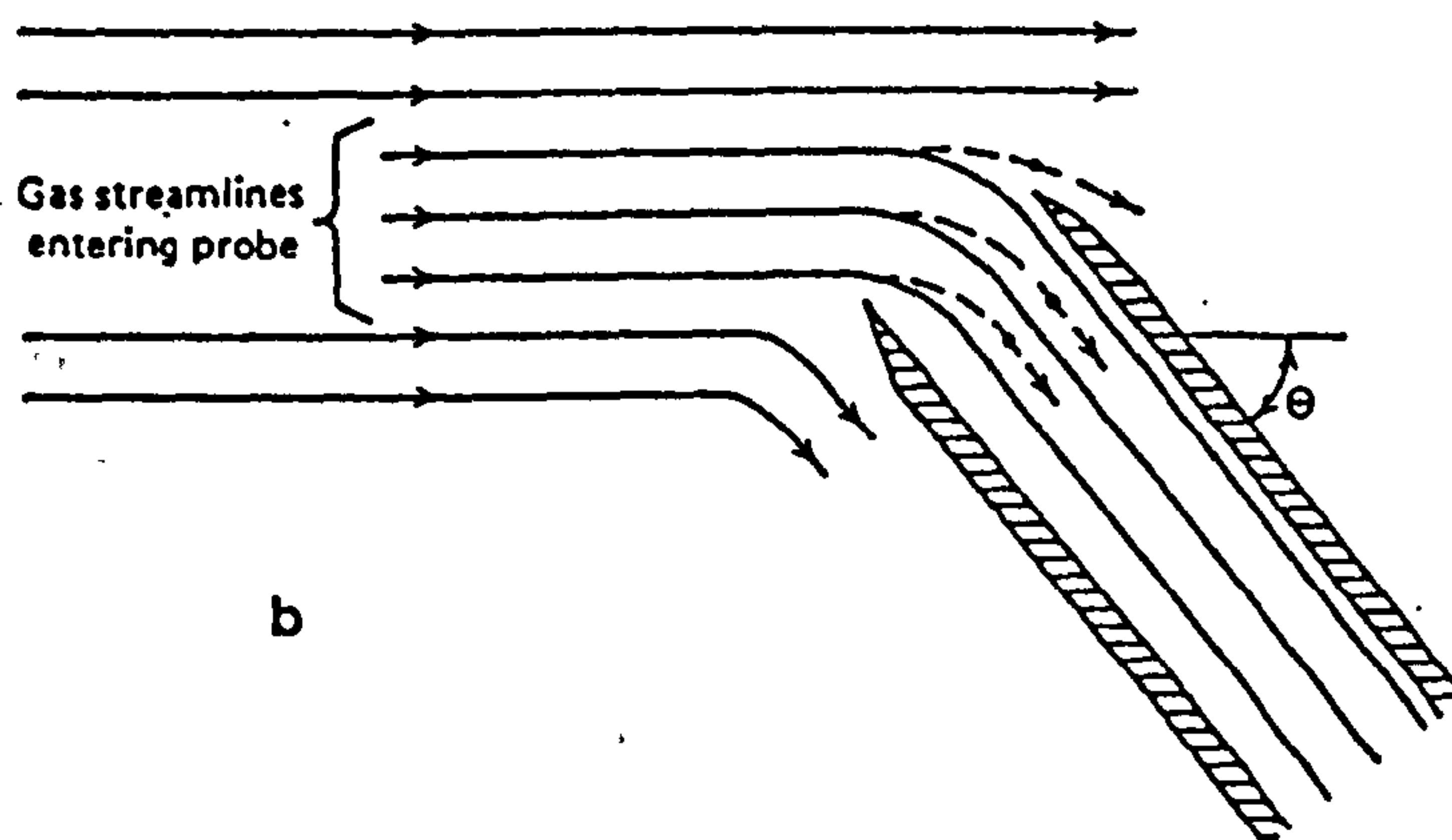
Anisokinetic sampling might also occur if the sampling tube is not aligned with the gas flow streamlines (Figure 2.1b).

In the present study, the principle of isokinetic sampling was employed to develop an apparatus where a cloud generated at various flow rates, can be sampled isokinetically and fractionated using a cascade impactor.

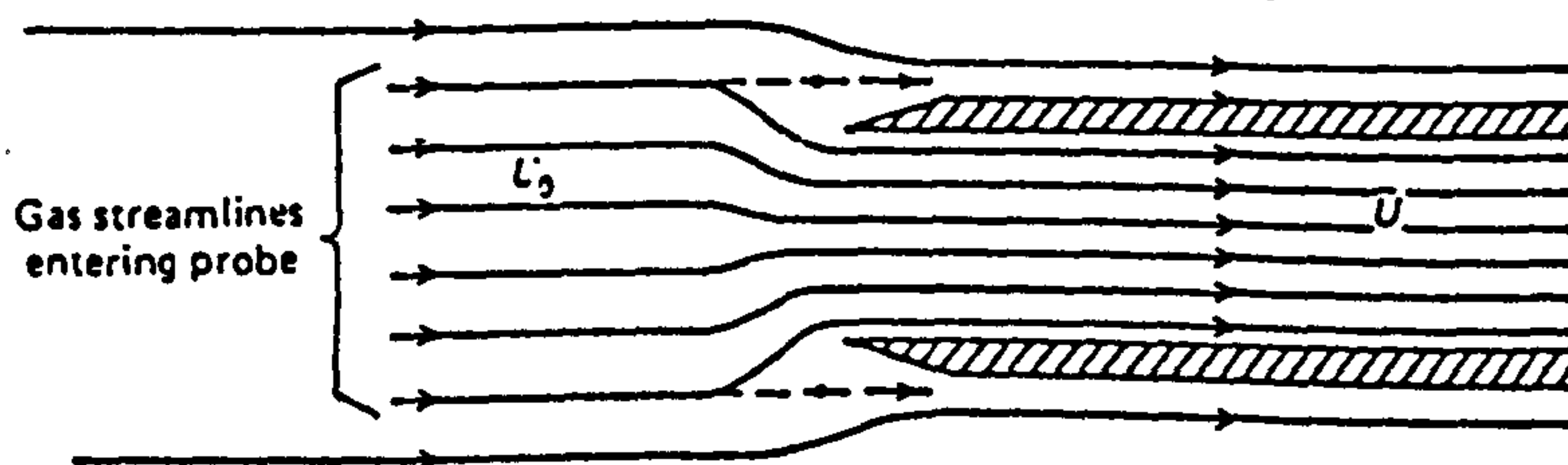
Fig 2.1



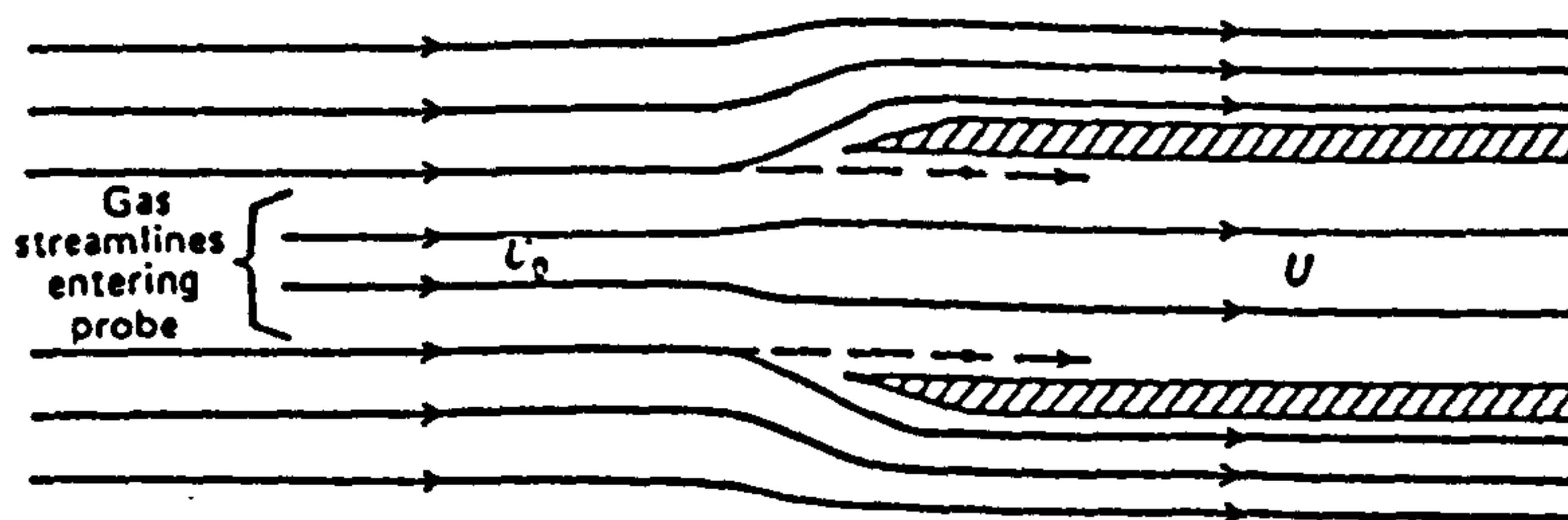
a. Isokinetic sampling



b



c



d

Anisokinetic sampling

b. Misalignment,  $\theta \neq 0$  , c.  $U > U_0$  , d.  $U < U_0$



The guidelines for isokinetic sampling from a ducted aerosol flow are stipulated by Fissan *et al* (1987). However, sampling aerosols by this technique may cause many sampling errors as a result of aerosol transport to the site of analysis.

This chapter discusses the development of sampling configurations and their suitability to isokinetic sampling. Aspiration efficiency, which refers to the effectiveness with which airborne particles are transported from the aerosol cloud outside the sampler and through the sampling tube, will be used as a means of evaluating the isokinetic sampling conditions. Additionally, flow visualization using laser doppler anemometry will be employed.

## **2.2 Materials and methods**

### **2.2.1 Preparation of capsules**

#### **Micronization of salbutamol sulphate**

Salbutamol sulphate was micronized using an air jet mill (Fryma Jet Mill, J M 80) at a powder feed rate of 5g/min and an air pressure of 7.5 bar. The moisture content was measured using an infra-red moisture balance at 100°C. The micronized drug was stored in a light resistant container in a vacuum desiccator over silica gel.

#### **Particle size analysis**

The particle size of the micronized drug was measured using scanning electron microscopy (SEM). The powder sample was mounted on the SEM stump and dispersed with a soft hair brush to break any agglomerates. Several photomicrographs were produced by scanning fields, selected randomly. The size was determined from the photomicrograph by tracing the perimeters of the

individual particles on a graphic tablet connected to a computer. A total of 500 particles were measured to obtain a size distribution.

#### **Classification of lactose**

Lactose monohydrate (Lactochem Pharmaceuticals) was classified into narrow size fractions. Air Alpine jet sieve was fitted with sieves to obtain size fractions of 125-180 $\mu$ m, 63-90 $\mu$ m and to give a powder all of which passed a 40 $\mu$ m mesh. This powder was classified into the range of particle sizes from 20-40 $\mu$ m, <20 $\mu$ m and <10 $\mu$ m using a centrifugal air classifier (Alpine "zig-zag" classifier). The powder was dried in an oven overnight at 100°C. The powder samples were stored in a vacuum desiccator over silica gel.

#### **Preparation of powder mixtures**

Samples of drug-lactose were prepared in a ratio of 1:67.5, according to the commercial "Ventolin" formulation, by mixing the micronized drug and the classified lactose with a spatula. The homogeneity of the mixtures was verified by the assay of ten 30mg samples by HPLC (see Section 2.2.2).

#### **Filling of the capsules**

Hard gelatin capsules (size 3) were filled with  $27.4 \pm 1.4$ mg of the powder mixture so that each capsule contained 400 $\mu$ g drug. The filling was performed manually.

### **2.2.2 Development of an HPLC method for the determination of salbutamol sulphate**

The basic HPLC method employed for quantifying salbutamol

sulphate was provided by Glaxo, and used benzyl biphenyl as an internal standard, a mobile phase of 76:24 v/v methanol and ammonium acetate solution (0.013M) and a reversed phase column packed with octadecylsilane.

The following modifications were introduced: salmefamol was selected as an internal standard. It has a chemical structure similar to that of salbutamol (Figure 2.2) differing only in the substitution on the amine head. The longer hydrocarbon chain of salmefamol makes it less polar than salbutamol and thus, can be separated using a reversed phase chromatography. Therefore, modification of the mobile phase was essential for the separation. The revised mobile phase consisted of methanol and 0.013M ammonium acetate in a ratio of 65:35 v/v. This provided the best peak separation of the drug and the internal standard.

#### **The HPLC system components**

The HPLC system consisted of the following: a pump, a multiple wavelength UV detector (Cecil instruments model C 2112), a reversed phase column (C-18  $\mu$ -Bondapack, 30cm x 3.9mm i.d), an integrator, a printer and an autosampler.

#### **HPLC conditions**

Flowrate:	0.8ml/min
Detector sensitivity:	0.02 AUF
Detector wavelength:	276nm
Injection volume:	40 $\mu$ l



### **Preparation of the internal standard solution**

Salmefamol was dissolved in the mobile phase to obtain a solution having a concentration of 0.0025mg/ml. This concentration gave a peak area ratio of drug to internal standard of 0.5-10.

### **Preparation of the standard drug solutions**

An accurately weighed quantity of salbutamol sulphate (10.0mg) was transferred to a 100ml volumetric flask, dissolved in the internal standard solution, and made up to volume to obtain a 0.1mg/ml drug concentration.

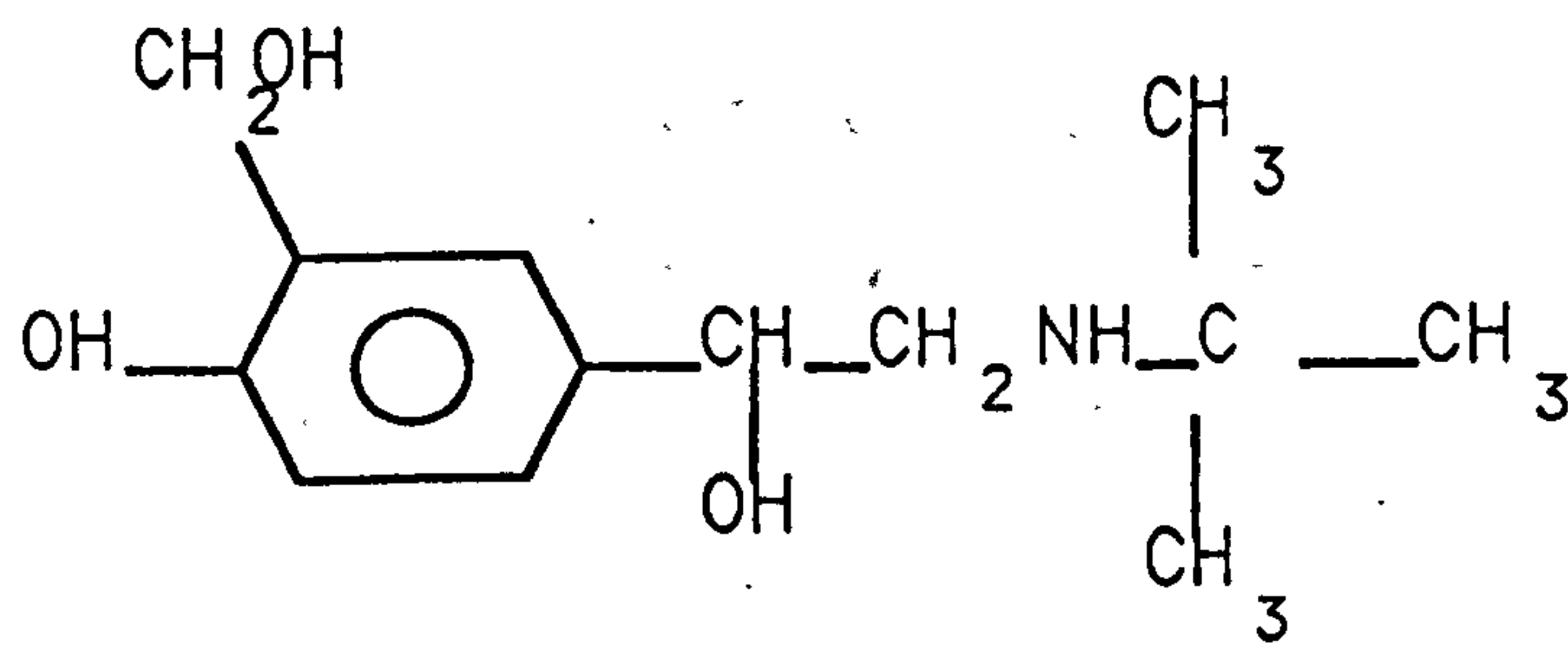
A 1, 2, 3, 4, 5 and 6ml aliquot of this solution were pipetted into 20ml volumetric flasks and made up to volume using the internal standard solution. The mobile phase was pumped through the column. Injection of each of the standard solutions was made in triplicate. The retention times for salbutamol sulphate and salmefamol were 4.7 and 5.8 minutes, respectively. A calibration curve was constructed by plotting peak area ratios of salbutamol to those of the internal standard versus salbutamol sulphate concentration.

The developed HPLC method was reproducible and accurate with a standard deviation of  $\pm 0.026$  based on six consecutive injections.

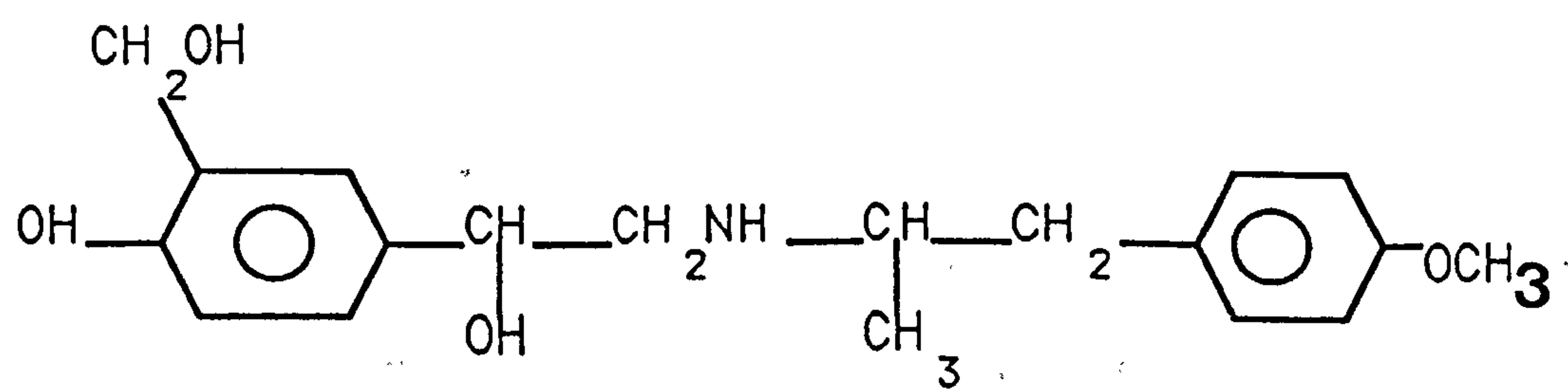
### **Determination of salbutamol sulphate content in powder mixtures**

The salbutamol sulphate content in the powder mixes was determined by accurately weighing a 30mg sample in a 20ml volumetric flask. The sample was dissolved in the internal standard solution. This solution was filtered through a millipore filter (Whatman G F) fitted to a glass syringe and 40 $\mu$ l of this solution

**Fig 2.2**



**(a) Salbutamol**



**(b) Salmefamol**

was injected into the HPLC. No interference from the carrier lactose was observed. The salbutamol content in milligrams was obtained by the following equation:

$$\text{mg salbutamol sulphate} = \frac{\text{AUC S/IS}}{\text{AUC St/IS}} \times \text{Wst} \times \text{dilution factor}$$

where

AUC S/IS is the area under the curve ratio of sample to internal standard

AUC St/IS is the area under the curve ratio of standard to internal standard from calibration curve.

Wst is the weight of standard in mg.

## **2.3 Results**

### **2.3.1 Particle size analysis**

The mass medium diameter of micronized salbutamol sulphate was  $2.8\mu\text{m}$  with a geometric standard deviation of 1.3. The particle size distribution is shown in Figure 2.3.

### **2.3.2 Moisture content**

The moisture content of salbutamol sulphate was found to be 0.8% w/w and was not higher than 0.05% w/w for the lactose samples.

### **2.3.3 Content uniformity of the powder mixtures**

The mixing was found to be homogenous with a coefficient of variation of the sample contents ranging between 1.3-2.3% for the prepared mixtures .

### **2.3.4 HPLC analysis of salbutamol sulphate**

A linear plot of the peak ratios of salbutamol sulphate to those of



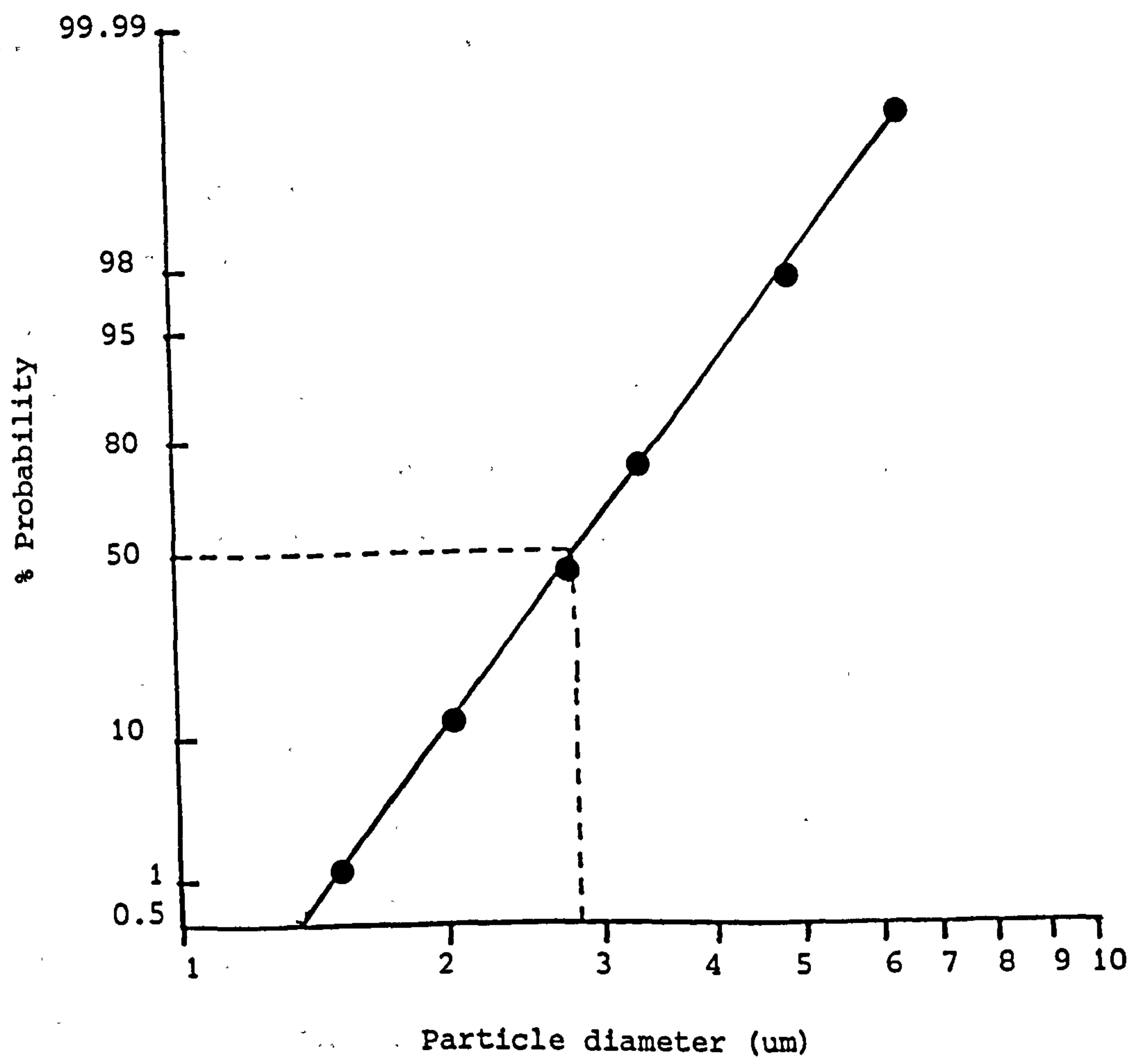


**Fig 2.3** Particle size distribution of micronized salbutamol sulphate

the internal standard versus salbutamol sulphate concentrations was obtained (Figure 2.4) with a correlation coefficient ( $r$ ) of 0.998. A typical HPLC chromatogram is shown in Figure 2.5.

## **2.4 Generation and sampling of a cloud**

In the design of the apparatus which permits in vitro evaluation of dry powder aerosols at various flow rates, it was desired to determine the size distribution and concentration directly using a commercially available cascade impactor.

Since the flow rate of the sampler is fixed and the airflow proposed for cloud generation ranged between 60-200 l/min, two sampling methods were proposed to fulfil the basic requirement for isokinetic sampling.

- 1 Method A: isokinetic sampling configuration that provides a gradual deceleration of the free stream velocity to match the suction velocity within a sampling probe of fixed diameter (Figure 2.6a).
- 2 Method B: isokinetic sampling employing probes the upper diameters of which were adjusted to achieve a suction velocity identical to the free stream velocity in a fixed diameter tube at different flow rates (Figure 2.6b).

The sampling probes used in both configurations were fitted to a cascade impactor operated at an air flow of 28.3 l/min.

### **2.4.1 The cascade impactor**

The cascade impactor (Anderson I CFM ambient) is shown in Figure 2.7. It consists of eight stages, 0 to 7, and a preseparator stage that are held together by three spring clamps and sealed with

O-ring. The preseparator stage is an impaction chamber with 13.25mm inlet orifice and three outlet tubes. Each impactor stage contains multiple precision drilled orifices. The size of the orifices decreases with each succeeding stage, ranging from 2.55mm diameter in stage 0 to 0.25mm in stage 7. Each stage is fitted with a removable impaction plate for collection of the particles. The top two stainless steel collection plates have a 22mm opening in the centre to allow air flow through the centre. Each plate has a curved lip so that the air stream can flow around the edge of the plate to the next stage. The last stage is followed by a filter to capture all particles less than the cut off size of this stage. The impactor is connected to a vacuum pump which draws air through the instrument at a constant flow rate of 28.3 l/min. At this flow rate each impactor stage has a sharp cut off curve which gives the particle diameter having 50% collection efficiency ( $d_{50}$ ) (Figure 2.8). The cut off size is reduced in each stage by decreasing the orifice size and increasing the velocity since the same mass of gas flows through each stage. As the sampled aerosol cloud flows in sequence through successive stages, the captured particles on a given stage represent a range of particle sizes smaller than the cut off size of the previous stage and larger than the cut off size of the given stage. The sequential separation classifies the aerosol cloud into fractions according to their aerodynamic diameters.

The approximate cut off diameter for the various stages of the impactor, according to the manufacturers calibration, is shown in Table 2.1.

To obtain an accurate aerosol size fractionation with the cascade impactor, all the particles striking the collection surface must



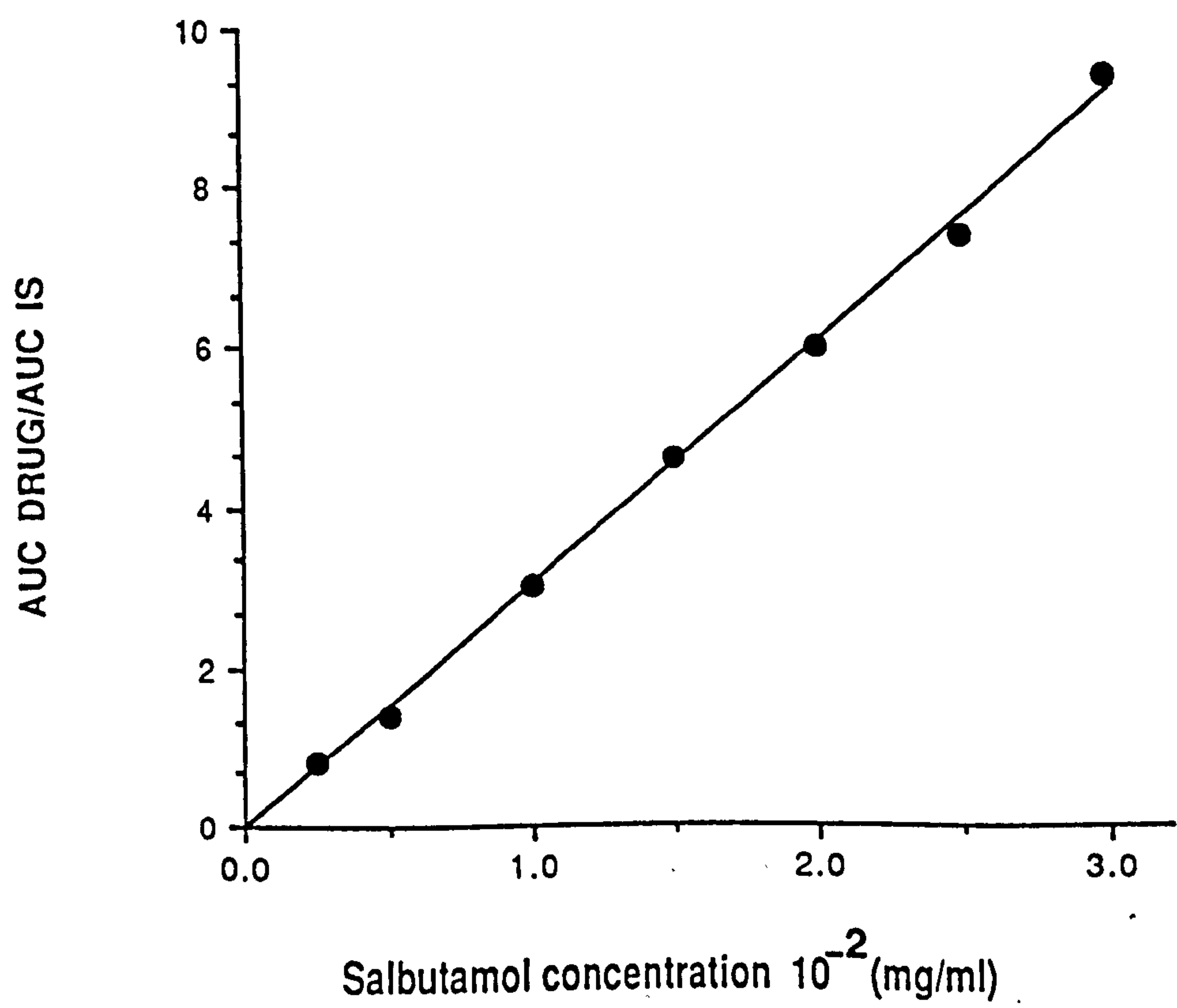
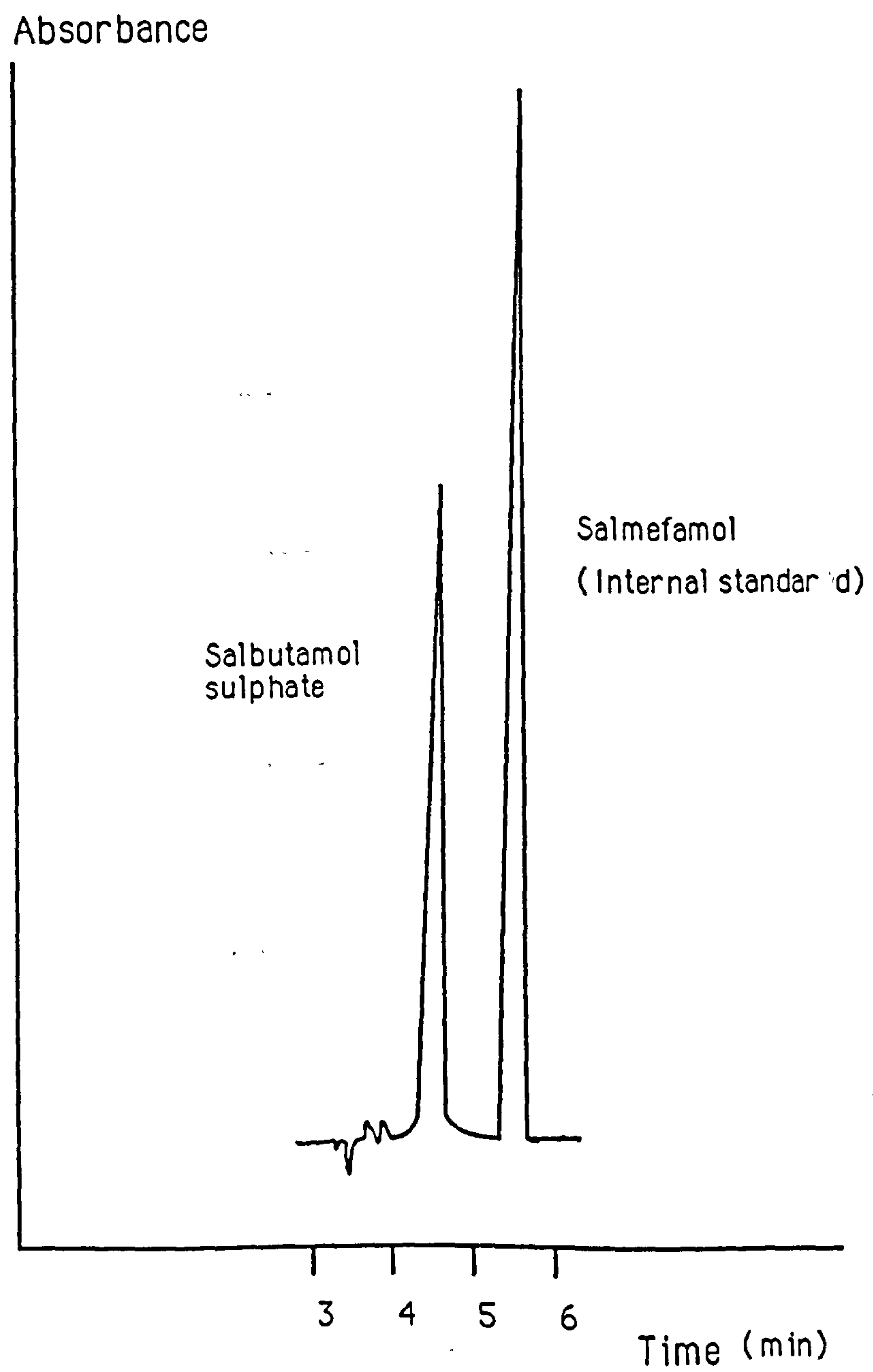


Fig 2.4 Calibration curve of salbutamol sulphate



**Fig 2.5** A typical salbutamol sulphate chromatogram

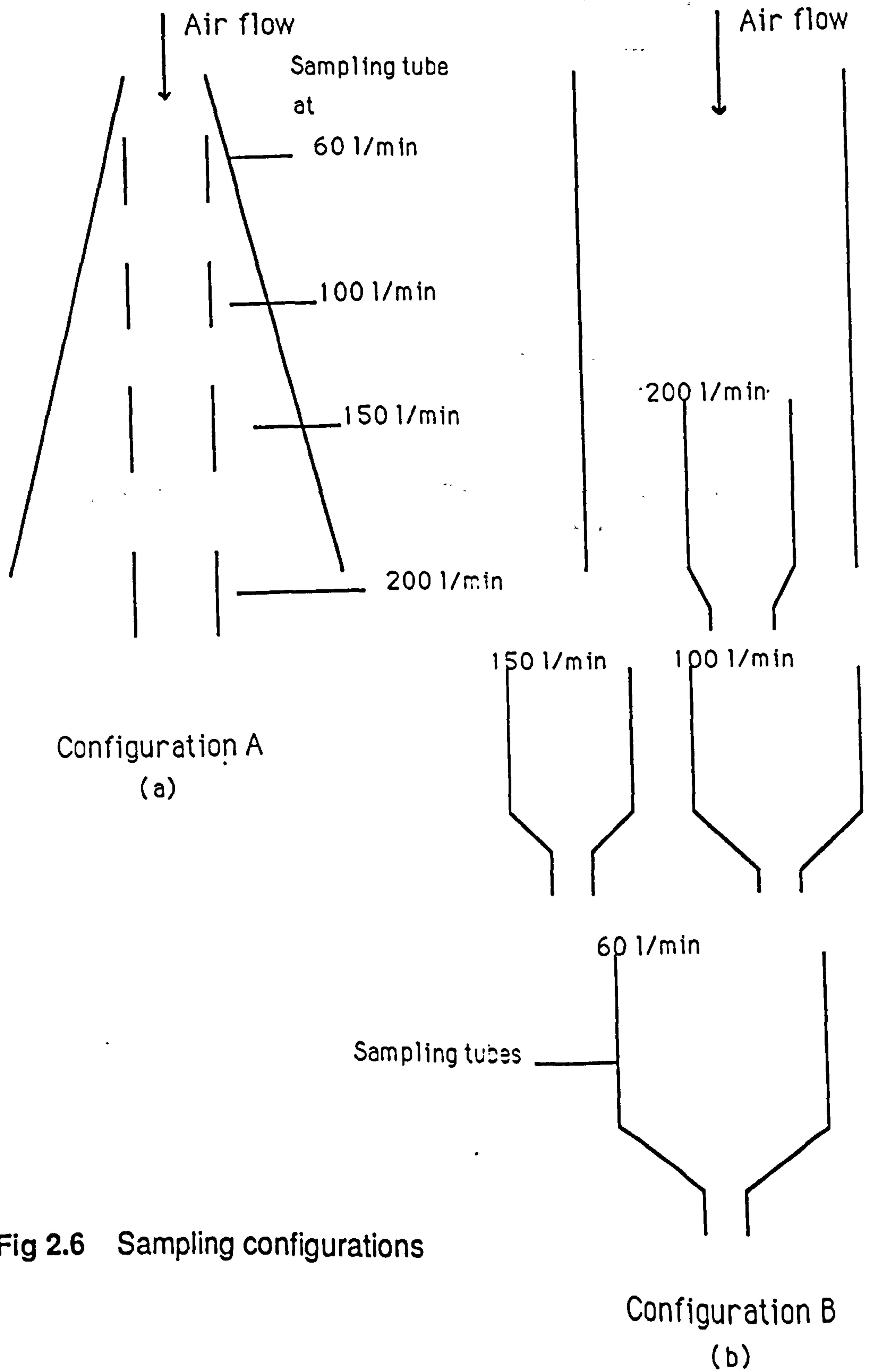


Fig 2.6 Sampling configurations



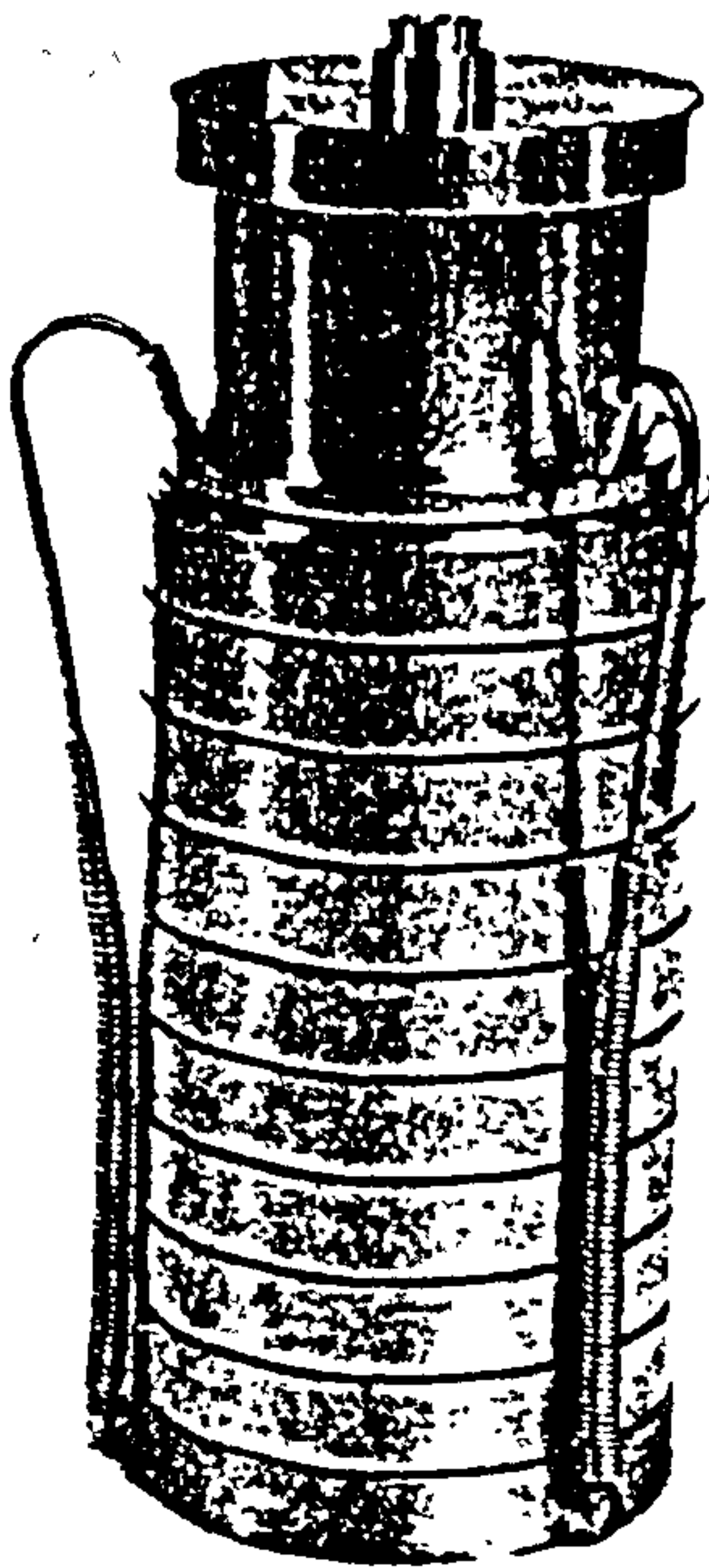
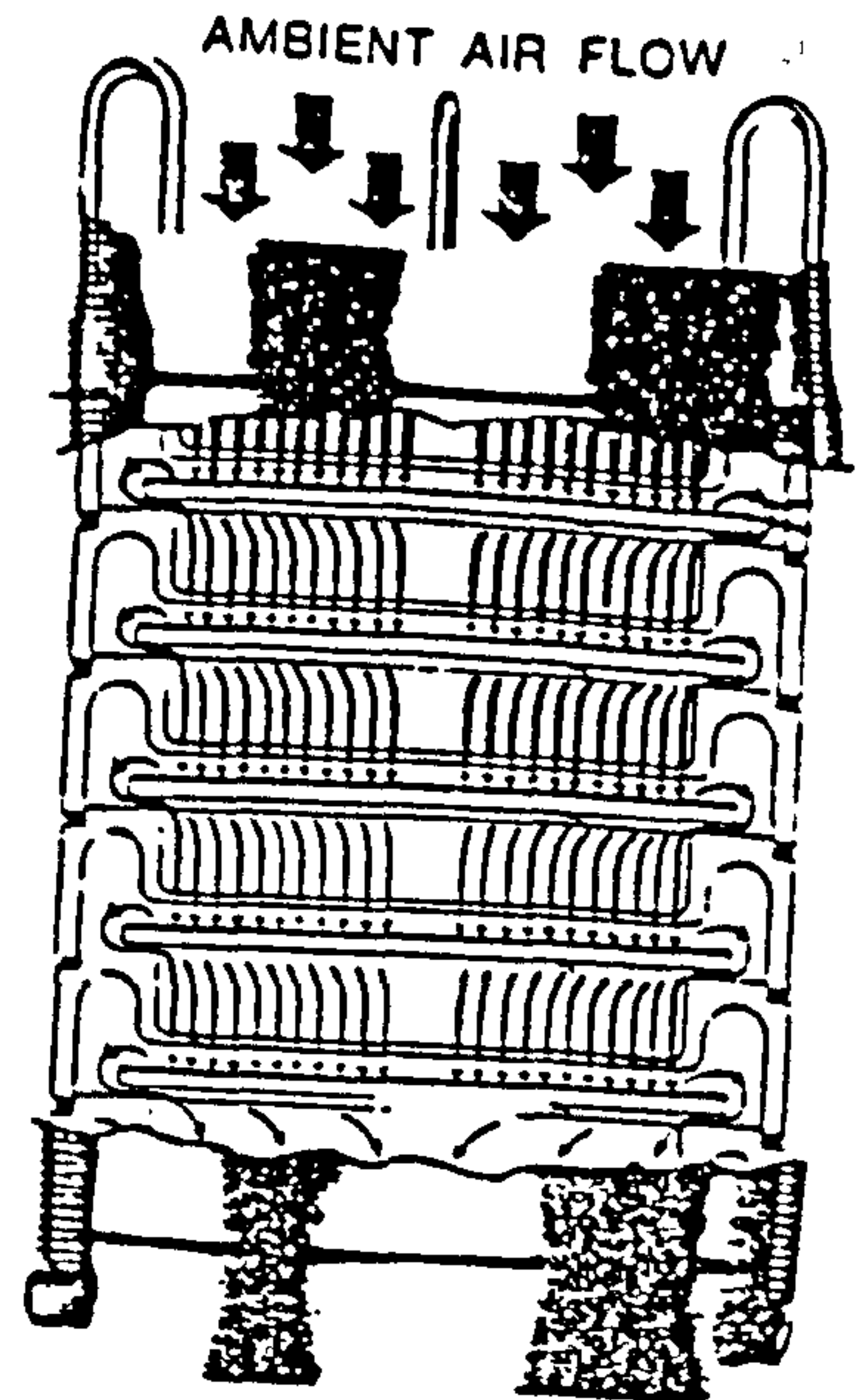


Fig 2.7 Andersen 1 CFM ambient sampler with preseparator



Schematic cross section of the impactor

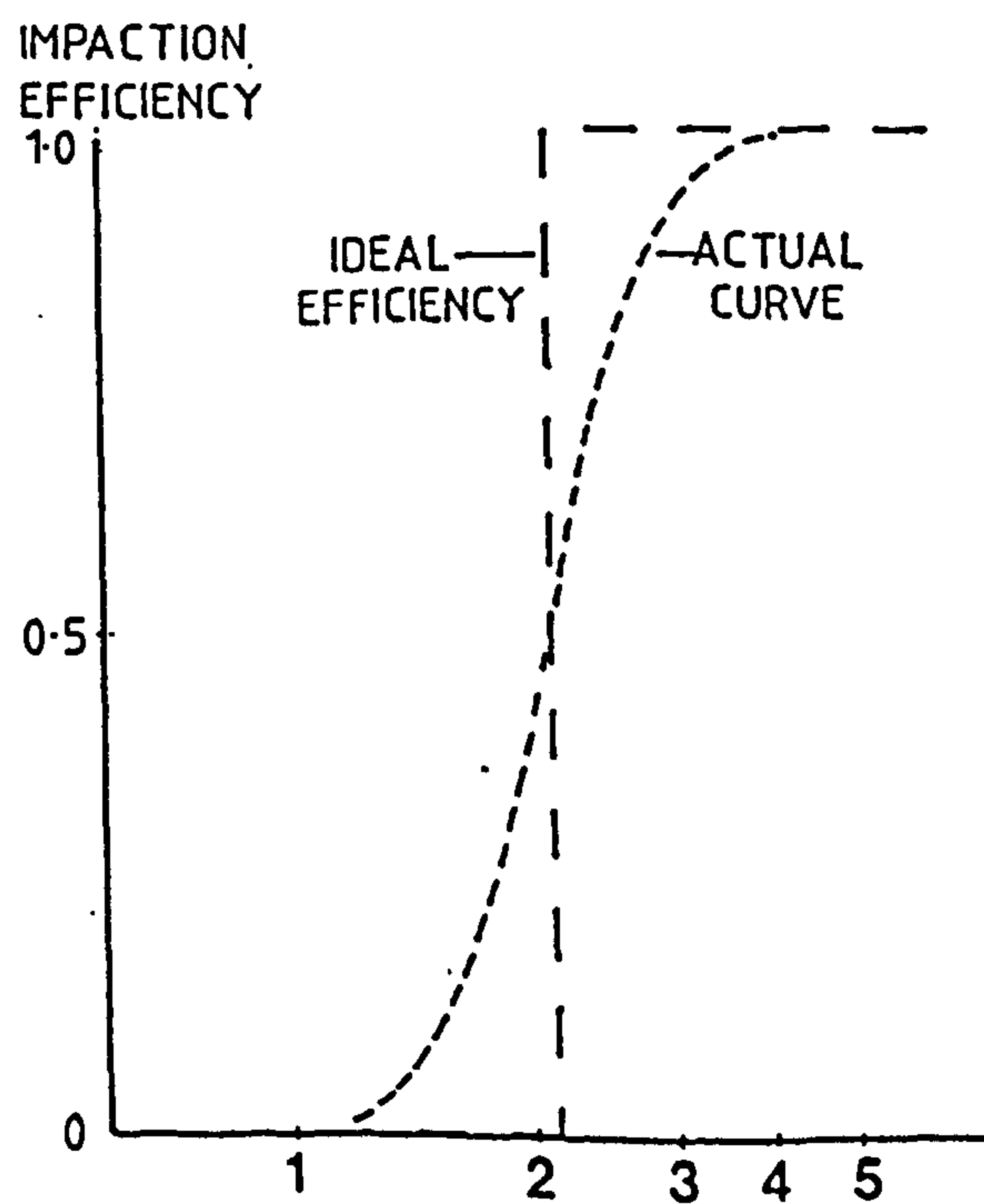


Fig 2.8 Ideal and actual impactation efficiency curve shapes

**Table 2.1      The approximate cut off diameter for various stages of the cascade impactor**

Stage	Cut off size (μm)
Preseparator	>10.0
0	9.0-10.0
1	5.8-9.0
2	4.7-5.8
3	3.3-4.7
4	2.1-3.3
5	1.1-2.1
6	0.7-1.1
7	0.4-0.7
Filter	0-0.4

adhere to it. However, dry solid particles were found to bounce from the surface upon impaction at a high air velocity (Turner and Hering, 1987). Distortion of the size distribution will occur if these particles are collected on subsequent stages (Nurtan *et al*, 1980). Therefore, to absorb the kinetic energy of the impacting particles and avoid re-entrainment, the preseparator stage and the impaction plates were coated with a thin film of 10% solution of silicon oil in hexane. The oil coating was stable and did not blow away as air was drawn through the impactor. This will preserve the shape of the distribution function.

## **2.4.2 Apparatus A**

### **1. Design of Apparatus A**

The apparatus is depicted in Figure 2.9. In this apparatus a commercial powder inhaler device, the Rotahaler ( Allen and Hanbury's Ltd; Figure 2.10), containing an encapsulated dose of the powder mixture was assembled in a line conducting dried-filtered air at a rate up to 200 l/min. The air supply was measured by a variable area flow meter with a flow range of 50-300 l/min (Perflow Instruments, Ltd). On actuation of the device the powder was blown through a glass "throat" of 20mm internal diameter and having a right angled bend. The throat assembly was intended to simulate the oro-pharynx and is commonly included in models built by some investigators to represent the most realistic sampling conditions (Kirk, 1972, Hallworth *et al*, 1976, 1986, Bell *et al*, 1973). The sample stream was then led from the throat to an expansion section which provided a gradual deceleration of the free stream velocity. This section consisted of a smooth conical glass diffuser with a divergent angle of  $90^\circ$ . The angle of the diffuser was



designed to be as small as possible to minimize flow disturbances caused by angles and bends. At different levels within the expansion section samples were drawn into the cascade impactor by means of sharp edged, thin walled, conical sampling tube of 150 mm in length and 21.5 mm internal diameter.

The thin walls and sharp edges reduce sampling errors caused by the finite dimensions of the tube which may disturb the flow field. The sampling tube, aligned parallel to the airflow direction, offers a sharp circular profile and reduces errors caused by non-isoaxial sampling. A minimum length of 150mm was required to facilitate sampling at different positions within the diffuser using the same tube.

To achieve isokinetic conditions, the flow rate in the diffuser ( $Q_0$ ) and in the sampling tube ( $Q$ ) were directly proportional to their respective cross-sectional areas. To calculate the position of the sampling tube within the diffuser at a particular air flow rate, the following equation was employed:

$$\frac{Q}{Q_0} = \left( \frac{D}{D_0} \right)^2 \quad (2.1)$$

where

$D$  is the sampling tube internal diameter and

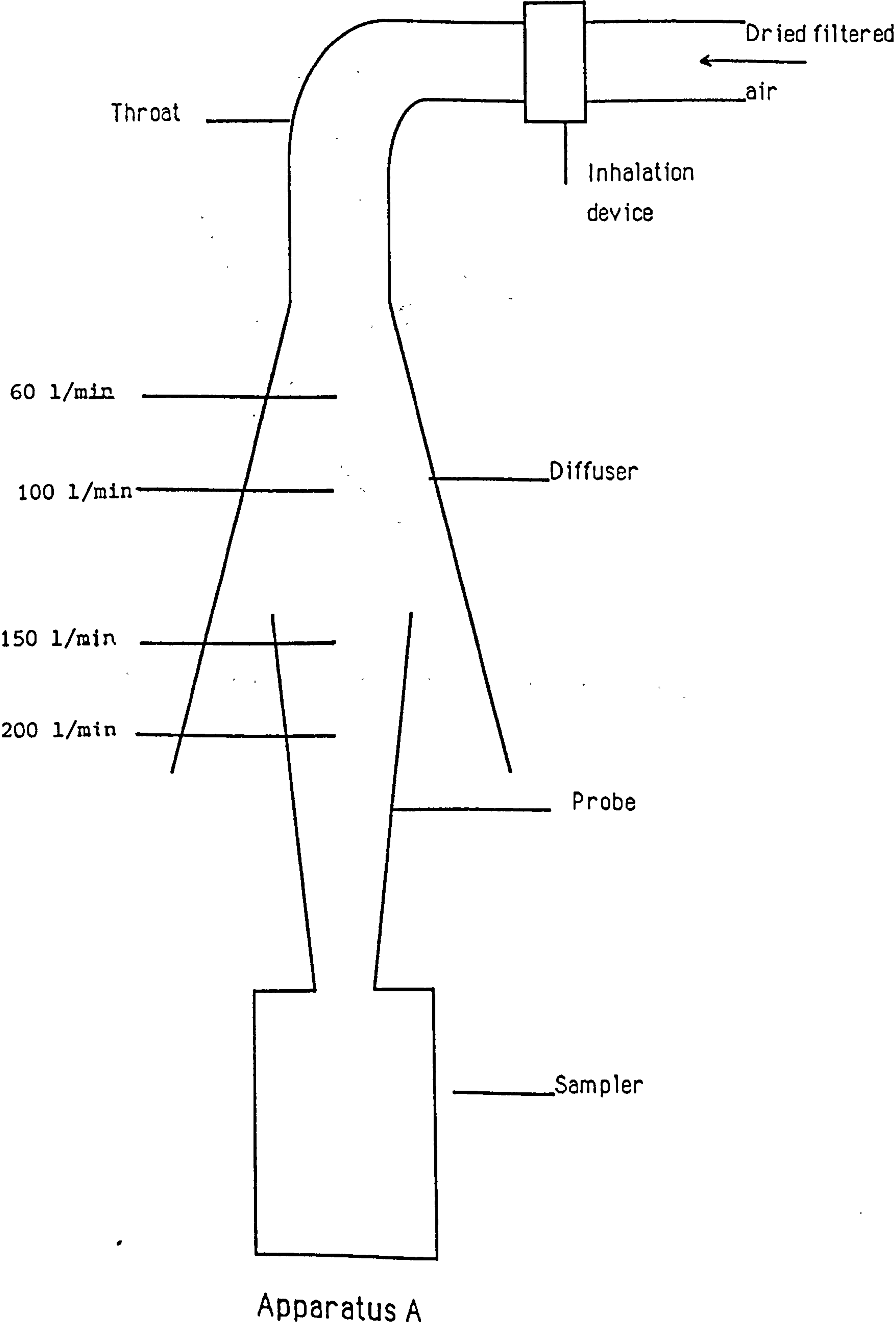
$D_0$  is the diffuser diameter at a particular flow rate.

The position of the sampling tube within the diffuser at different flow rates is shown in Figure 2.9. The diffuser diameter and the air stream velocity at the sampling positions are given in Table 2.2.

**Table 2.2 The diffuser and sampling tube characteristics at different flow rates in Apparatus A**

Qo l/min	Do cm	Q l/min	D cm	U=Uo cm/sec
200	5.71	28.3	2.15	129.9
150	5.00	28.3	2.15	129.9
100	4.04	28.3	2.15	129.9
60	3.10	28.3	2.15	129.9
<p>Qo: Flow rate within the diffuser</p> <p>Do: Diameter of the diffuser at the respective flow rate</p> <p>Q: Flow rate within the sampling tube</p> <p>D: Diameter of the sampling tube</p> <p>U and Uo: The calculated velocities within the sampling tube and the diffuser respectively.</p>				

Fig 2.9



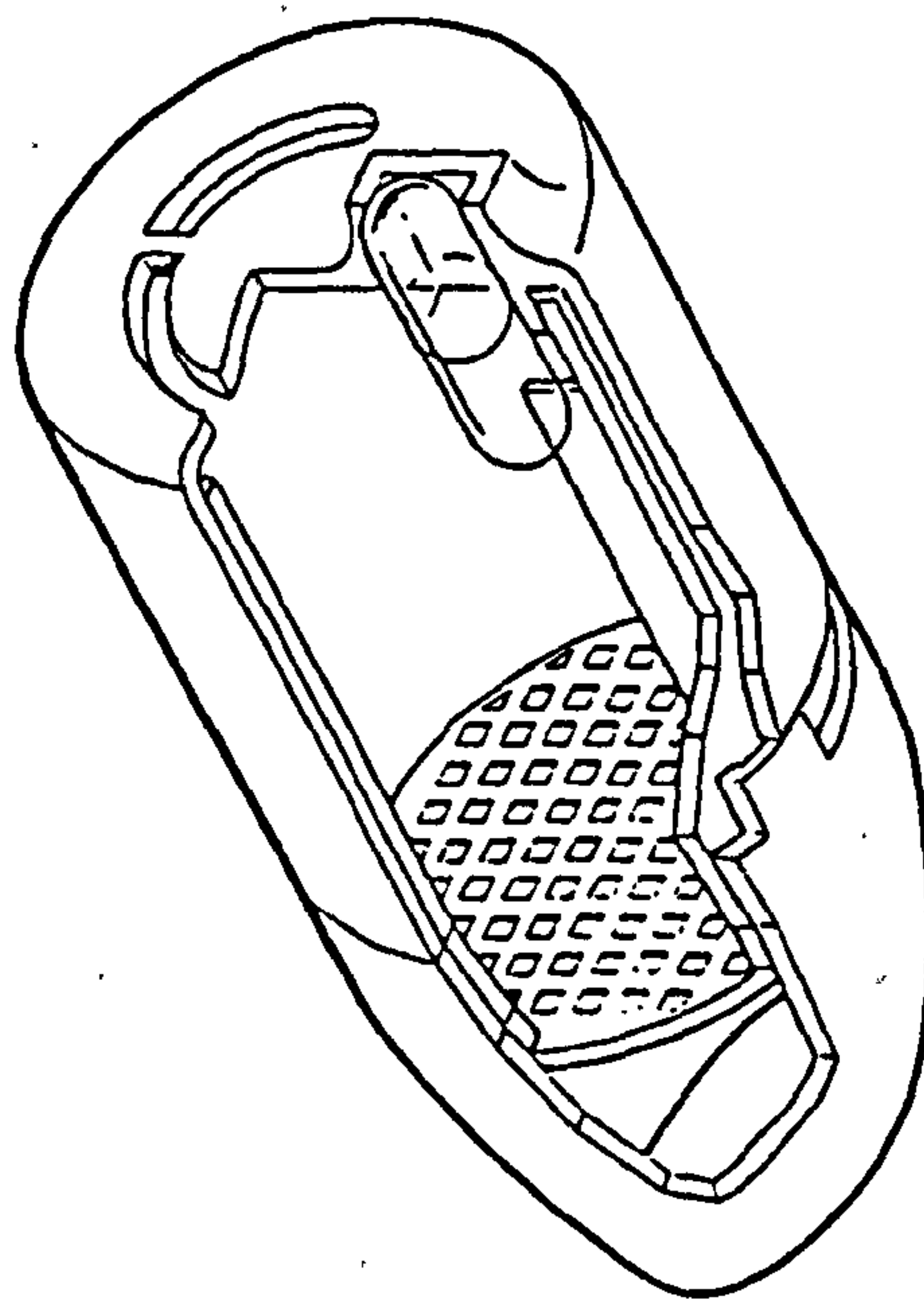


**Fig 2.10** Powder inhaler device (Rotahaler, Allen & Hanbury's,Ltd)



## 2. Evaluation of Apparatus A

### Aspiration efficiency determinations

The aspiration efficiency ( $\eta$ ) can be quantified by determining the ratio of the concentration in the samples ( $C_N$ ) to the concentration in the investigated aerosol ( $C_{No}$ ).

$$\eta = \frac{C_N}{C_{No}} \quad (2.2)$$

This ratio was employed as a means of judging whether a representative sample was removed from the aerosol cloud. A value of one, or close to one, indicates representative sampling.

The aspiration efficiency was determined for powder mixtures with carrier sizes of 60-180 $\mu$ m and <40 $\mu$ m. Sampling was carried out in the following manner:

The apparatus and the cascade impactor were inspected for a tight fit. The vacuum pump was set into operation and the dried-filtered air from the airline was adjusted to the specific flow rate. When steady flow was established, one end of the inhalation device was turned, the capsule was separated into two halves and the contents were dispensed into the air stream. Experiments were conducted at 60 and 150 l/min, each using ten capsules. This number of capsules allowed the collection of sufficient material for analysis on the various stages, but prevented re-entrainment of drug particles from the impactor collection surfaces as a result of the incoming particles impacting on collected particles rather than on the oiled surfaces.

During sampling, only a portion of the generated cloud was

transported into the sampling tube. This portion varies according to the volume of air flowing through the sampling tube and in the annulus around it and is proportional to the respective cross-sectional areas.

The portion of the cloud sampled at various flow rates is given in Table 2.3.

**Table 2.3 The percentage of aerosol cloud sampled at various flow rates**

Flow Rate( l/min)	% of Cloud Sampled
200	14.3
150	18.9
100	28.3
60	47.2

Experiments were carried out by moving the sampling tube to equally spaced sampling points across the diffuser and at different points near the wall of the diffuser. The purpose of these experiments was to investigate the uniformity of the aerosol cloud within the diffuser since the generated cloud was polydispersed.

After sampling was completed, the apparatus was disassembled and the amount of drug deposited in the inhaler and the capsules, the "throat", the preseparator stage, stages 0 to 2, stages 3 to 7 and the filter of the impactor, were separately rinsed with the internal

standard solution and the washings were assayed by the HPLC method described in Section 2.2.2. The stages were combined to collect sufficient material for the analysis. These combinations were made so that the cloud was fractionated into two size fractions: respirable, which was on stages 3 to 7, of size range 0.4-4.7 $\mu$ m and non-respirable, on stages 0 to 2 and the preseparator of size range 4.7-10 $\mu$ m and >10 $\mu$ m, respectively.

The total amount of salbutamol sulphate recovered from the combined stages was calculated and expressed as a percentage of the total dose released.

### **2.4.3 Results and discussion**

#### **1. Aspiration efficiency**

The results of the aspiration efficiency determinations for the powder mixtures with carrier sizes of 60-180 $\mu$ m and <40 $\mu$ m, at different sampling points across the diffuser, are illustrated in Tables 2.4 to 2.7.

The aspiration efficiency differed significantly at the different sampling points ( $P < 0.01$ ). A significant difference was also observed when sampling powder mixtures with different size distributions and at different flow rates.

The aspiration efficiency values were not close to unity in all cases (Tables 2.4 to 2.7). A value greater than one was obtained when sampling a cloud with 60-180 $\mu$ m carrier size at 150 l/min (Table 2.4), whereas a value of less than one was obtained with the finer cloud of <40 $\mu$ m, carrier size, at the same flow rate (Table 2.5). At

a flow rate of 60 l/min, a value of  $<1$  was observed with both carrier sizes (Tables 2.6 and 2.7).

The variation in the collection efficiency between the coarse and fine carrier at 150 l/min, might be explained by the deflection of the gas streamlines away from the centre of the diffuser, as a result of the right angled bend of the "throat". Allen (1975) noted that for the flow of solids in a  $90^\circ$  bend, concentrations are generally higher downstream along the duct wall farthest from the centre of curvature, and are lower along the duct wall nearest the centre of turning. Thus, coarse particles with high inertia persist in their original direction of motion; the amount entering the probe is less dependent on the sampling velocity. However, the fine particles,  $<40\mu\text{m}$ , follow more closely the deflected gas streamlines. Therefore, in this experiment, a reduced aspiration efficiency was observed as a result of the loss of some large particles from the moving air stream. At an airflow of 60 l/min, the sampling position, was moved upstream in the diffuser. At this sampling position the aspiration efficiency dropped significantly to less than one when a cloud comprising coarse carrier particles was sampled. A value still below one was also observed for the smaller size carrier; this value was significantly higher at 150 l/min. The possible reason for this is that at a sampling position 15mm downstream from the divergent angle of the diffuser, disturbances and eddy effects in the airflow are high, although the angle is small.

To minimize these effects, Allen (1975) recommended that a site of eight to ten duct diameters downstream from a disturbance, caused by inlets, outlets, bends and constrictions, should be selected.



Therefore, the low aspiration efficiency indicates that some particles are blown away from the sampling tube as a result of these disturbances. However, the higher aspiration efficiency obtained with the finer carrier may be due to a fraction of the cloud being sampled upstream in the diffuser before complete deflection of the streamlines caused by the right angled bend.

The data in Tables 2.4 to 2.7 reveal that fractions of a particular aerodynamic size distribution were significantly different as the sampling tube was moved to different sampling points across the diffuser. This was observed with the two carrier sizes and flow rates ( $P < 0.01$ ).

This demonstrates that the aerosol cloud was unequally distributed over the cross-section of the diffuser. This non-uniformity is aggravated by the gas turbulence. The turbulence level can be estimated by Reynold's Number; estimated values at various sampling flow rates is given in Table 2.8. The values obtained were greater than 2000 indicating turbulent flow. However, these theoretical values do not adequately describe the effects caused by angles, bends and turbulent fluctuations across the cross-section of the diffuser and therefore underestimate disturbances. This is particularly true with a value close to 2000 indicating low levels of turbulence at a flow rate of 60 l/min.

## **2. Throat deposition**

Since the "throat" was intended to simulate the oro-pharynx, it was of interest to investigate if it has a fractionating effect on the size distribution of the aerosol cloud. This has been assessed by

quantifying the amount retained by the preseparator stage which captures all particles larger than  $10\mu\text{m}$  in diameter. The large fraction captured by this stage indicated that the "throat" was not efficient at removing large particles. The results in Tables 2.4 to 2.7 show that at low air speeds the "throat" was collecting more particles, particularly, when the fine carrier was used. However, the collected fraction was markedly reduced at high air flow rates and when a coarse carrier was employed. These results were surprising since it was expected that at high air velocities and large particle size the impaction efficiency will be greater. This results from the large particles being unable to follow the diverging streamlines at a right angled bend due to their momentum causing impaction on the "throat" according to the theory described in Section 1.6 . This agrees with the findings of Hallworth and Andrews (1976). They observed that "throat" deposition occurs by impingement of the aerosol on the tubular inlet part of the "throat" due to gravitational effect and by inertial impaction of large particles on the right angled bend. Consequently, deposition falls with increasing air flow, as a rapid air flow sweeps the aerosol along the "throat" and minimizes contact with the "throat" wall.

The "throat" in the present experiments was coated with a 10% solution of silicon oil in hexane to facilitate capturing of large particles. This, however, will not remain true following the actuation of the first few capsules since particles will cover the "throat" surface and subsequently the incoming particles impact on the collected particles rather than on the sticky surface. As a result, particle re-entrainment from the "throat" surface will occur and since the "throat" would not have a sharp cut-off ability, the physical

nature of the sampled cloud will vary affecting the principle of collecting a representative sample.

### **3. Material losses**

#### **On the sampling tube**

Losses between the inlet of the sampling tube and the impactor can not be avoided. These losses on the wall of the probe were quantified (Tables 2.4 to 2.7) and were found to be significant at all flow rates and with the two carrier sizes. Numerous mechanisms can operate to remove particles from the aerosol. These mechanisms include: impaction and sedimentation of large particles, diffusion of small particles to the walls and electrostatic interaction. Losses by these mechanisms increase with an increase in tube length (Fissan & Schioientek, 1987).

In apparatus A, the length of 150mm was essential to facilitate sampling of the aerosol cloud at different levels within the diffuser using the same sampling tube. Particles deposited at the internal walls of the tube were removed from the cloud by one or more of the above mechanisms before they can actually be sampled. From the data in Tables 2.4 to 2.7 it was not possible to suggest whether the process was selective for a certain particle size. Therefore, these significant losses cannot be neglected as they reduce the overall sampling efficiency.

#### **On the diffuser**

Although losses on the walls of the diffuser did not exceed 10% (Tables 2.4 to 2.7), particles were observed to deposit mainly on its expansion angle.



Both turbulence and centrifugal effects may contribute to particle removal in bends (Fissan & Schioientek, 1987). Additionally, high inertia particles may also impact on the expansion angle of the diffuser as a result of a change in air flow direction. However, the data available provides no evidence as to whether cloud segregation occurred by selective removal of large particles from the cloud. Furthermore, wall losses were more pronounced with the finer aerosol cloud. These losses cannot be ignored as they may alter the nature of the sampled cloud and hence the collected sample may not be representative of the total aerosol cloud.

#### **Interstage losses**

Loss of particles on the preseparator lid, the jet inlets and the edges of the impactor stages are considered as interstage losses. Greasing the impaction plates was found to considerably reduce these losses.

This phenomenon was recognised by McFerland *et al* (1977) and Rao and Whitby (1978) who noted that all forms of the Anderson impactor have been shown to exhibit interstage losses especially in the few top stages. Interstage losses were found to result from high inertia of particles unable to turn sharply with the air streamlines at the jet inlets or around the plate edges as described in Figure 2.11. Owing to this mechanism, losses preferentially occur for larger particles and the general effect is a bias to small particle size.

However, in the present study, since the quantified interstage losses did not exceed 1.0% of the total dose discharged and since this amount was reproducible in almost all the experiments, losses were



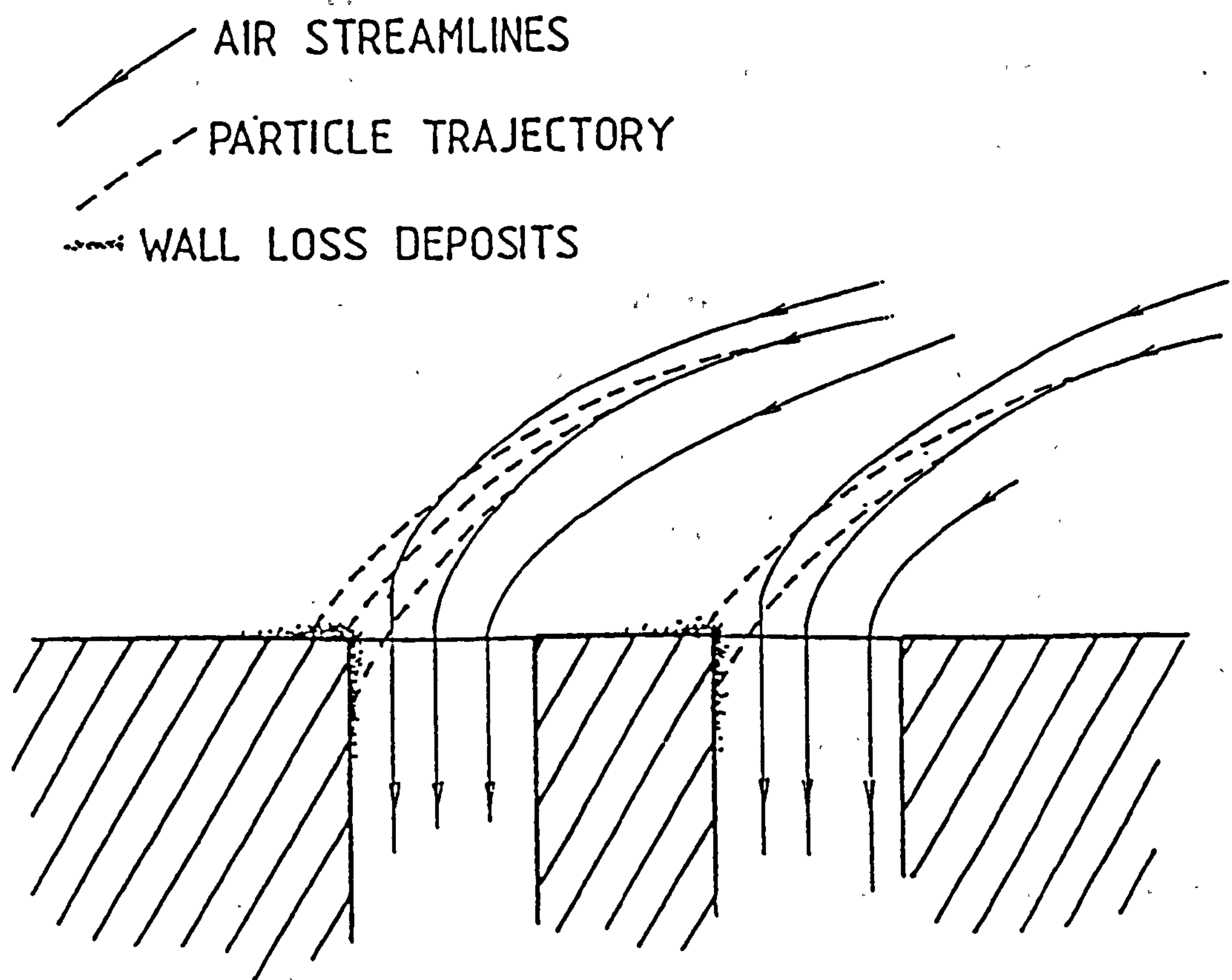


Fig 2.11 Diagram depicting wall loss due to overshoot of particles near jet entry

not considered serious and were not expected to bias the size distribution.

From the above results, it can be concluded that although this apparatus was designed to give isokinetic sampling conditions, the aspiration efficiency values obtained were not acceptably close to unity, indicating that representative sampling was not achieved.

It would appear that the overall performance of the apparatus was not only governed by matching the free stream velocity and the sampling velocity. Other factors appeared to have an effect on aerosol sampling and introduced errors into the system. Turbulence and eddy effects in the air flow pattern created by the right angled bend, made the behaviour of the aerosol flow downstream in the diffuser largely unknown. Furthermore, the transport of the cloud was markedly dominated by the particle properties, such as, inertia of large particles and ability of the small particles to respond to changes in air direction and turbulent fluctuation. Re-entrainment of particles from the "throat" surface and the substantial wall losses on the sampling tube, all affect the overall aspiration efficiency.

Therefore, Apparatus A was considered unsuitable for sampling aerosol clouds generated at various flow rates. Elimination of the observed errors necessitated a total redesign of the apparatus.

**Table 2.4 The percentage of drug deposited at various stages and the aspiration efficiency at different points across the diffuser at a flow rate of 150 l/min and a carrier size of 60-180 $\mu$ m.**

Stage	-r/2	r	+r/2
Device and capsules	15.5 $\pm$ 0.9	16.0 $\pm$ 1.8	17.0 $\pm$ 0.8
Throat	2.9 $\pm$ 0.8	5.3 $\pm$ 1.4	6.1 $\pm$ 1.1
Diffuser	4.4 $\pm$ 0.6	3.9 $\pm$ 0.7	4.7 $\pm$ 0.7
Probe	3.4 $\pm$ 0.9	4.6 $\pm$ 1.1	4.7 $\pm$ 1.8
Preseparator	68.2 $\pm$ 5.9	55.5 $\pm$ 1.7	59.0 $\pm$ 2.2
Stages 0-2	0.3 $\pm$ 0.2	3.3 $\pm$ 0.9	4.8 $\pm$ 0.8
Stages 3-7	4.3 $\pm$ 0.9	11.3 $\pm$ 1.9	9.9 $\pm$ 1.2
Interstage losses	1.0 $\pm$ 0.3	0.7 $\pm$ 0.2	0.5 $\pm$ 0.3
Aspiration efficiency	1.4 $\pm$ 0.10	1.3 $\pm$ 0.09	1.2 $\pm$ 0.08

The results are the mean and standard deviation of six experiments.

The aspiration efficiencies and the depositions at various stages of the impactor differ significantly at  $P < 0.01$  (t-test)

**Table 2.5 The percentage of drug deposited at various stages and the aspiration efficiency at different points across the diffuser at a flow rate of 150 l/min and carrier size of <40 $\mu$ m.**

Stage	-r/2	r	+r/2
Device and capsules	19.0 $\pm$ 1.7	17.0 $\pm$ 0.9	16.6 $\pm$ 1.4
Throat	10.3 $\pm$ 0.9	8.6 $\pm$ 1.7	9.8 $\pm$ 1.9
Diffuser	7.0 $\pm$ 0.4	6.0 $\pm$ 0.6	7.6 $\pm$ 1.0
Probe	5.0 $\pm$ 1.9	4.9 $\pm$ 1.3	4.6 $\pm$ 1.9
Preseparator	30.9 $\pm$ 2.8	25.1 $\pm$ 2.8	36.7 $\pm$ 3.5
Stages 0-2	5.9 $\pm$ 1.2	10.9 $\pm$ 1.8	8.7 $\pm$ 1.1
Stages 3-7	21.2 $\pm$ 1.0	25.9 $\pm$ 2.5	15.4 $\pm$ 1.1
Interstage losses	0.7 $\pm$ 0.3	0.7 $\pm$ 0.9	0.9 $\pm$ 0.5
Aspiration efficiency	0.6 $\pm$ 0.08	0.7 $\pm$ 0.32	0.43 $\pm$ 0.01

The results are the mean and standard deviation of six experiments

The aspiration efficiencies and the depositions at various stages of the impactor differ significantly at P<0.01 (t-test)



**Table 2.6 The percentage of drug deposited at various stages and the aspiration efficiency at different points across the diffuser at a flow rate of 60 l/min and carrier size of <40 $\mu$ m.**

Stage	r	r/2
Device and capsules	25.0 $\pm$ 0.8	23.4 $\pm$ 0.6
Throat	19.2 $\pm$ 2.1	16.1 $\pm$ 0.6
Diffuser	10.5 $\pm$ 1.1	12.6 $\pm$ 0.8
Probe	5.2 $\pm$ 1.2	4.9 $\pm$ 0.9
Preseparator	29.6 $\pm$ 1.5	36.8 $\pm$ 3.0
Stages 0-2	4.7 $\pm$ 0.5	3.2 $\pm$ 0.3
Stages 3-7	5.3 $\pm$ 0.8	3.3 $\pm$ 0.3
Interstage losses	0.8 $\pm$ 0.3	0.9 $\pm$ 0.1
Aspiration efficiency	0.8 $\pm$ 0.04	0.9 $\pm$ 0.06

Sampling was carried out at two sampling points since the diffuser diameter was very small at this flow rate.

The results are the mean an standard deviation of six experiments.

The aspiration efficiencies and the depositions at various stages of the impactor differ significantly at P<0.01.

**Table 2.7 The percentage of drug deposited at various stages and the aspiration efficiency at different points across the diffuser at a flow rate of 60 l/min and carrier size of 60-180 $\mu$ m.**

Stage	r	r/2
Device and capsules	14.5 $\pm$ 0.3	14.9 $\pm$ 0.5
Throat	12.4 $\pm$ 1.3	10.5 $\pm$ 0.9
Diffuser	5.8 $\pm$ 0.2	6.1 $\pm$ 0.7
Probe	7.3 $\pm$ 3.1	2.5 $\pm$ 1.4
Preseparation	5.5 $\pm$ 2.6	60.5 $\pm$ 3.0
Stages 0-2	2.6 $\pm$ 1.2	0.7 $\pm$ 0.4
Stages 3-7	1.6 $\pm$ 0.5	3.5 $\pm$ 0.5
Interstage losses	0.8 $\pm$ 0.3	1.0 $\pm$ 0.3
Aspiration efficiency	0.7 $\pm$ 0.06	0.8 $\pm$ 0.06

Sampling was carried out at two sampling points since the diffuser diameter was very small at this flow rate.

The results are the mean and standard deviations of six experiments.

The aspiration efficiencies and the depositions at various stages of the impactor differ significantly at P<0.01.

**Table 2.8 Values of Reynold's Number at different flow rates in Apparatus A.**

Flow Rate( l/min)	Reynold's Number
200	5031
150	4382
100	3619
60	2857

#### **2.4.4 Apparatus B**

Since isokinetic conditions were not achieved with apparatus A, apparatus B was constructed in the hope that some of the identified problems might be solved.

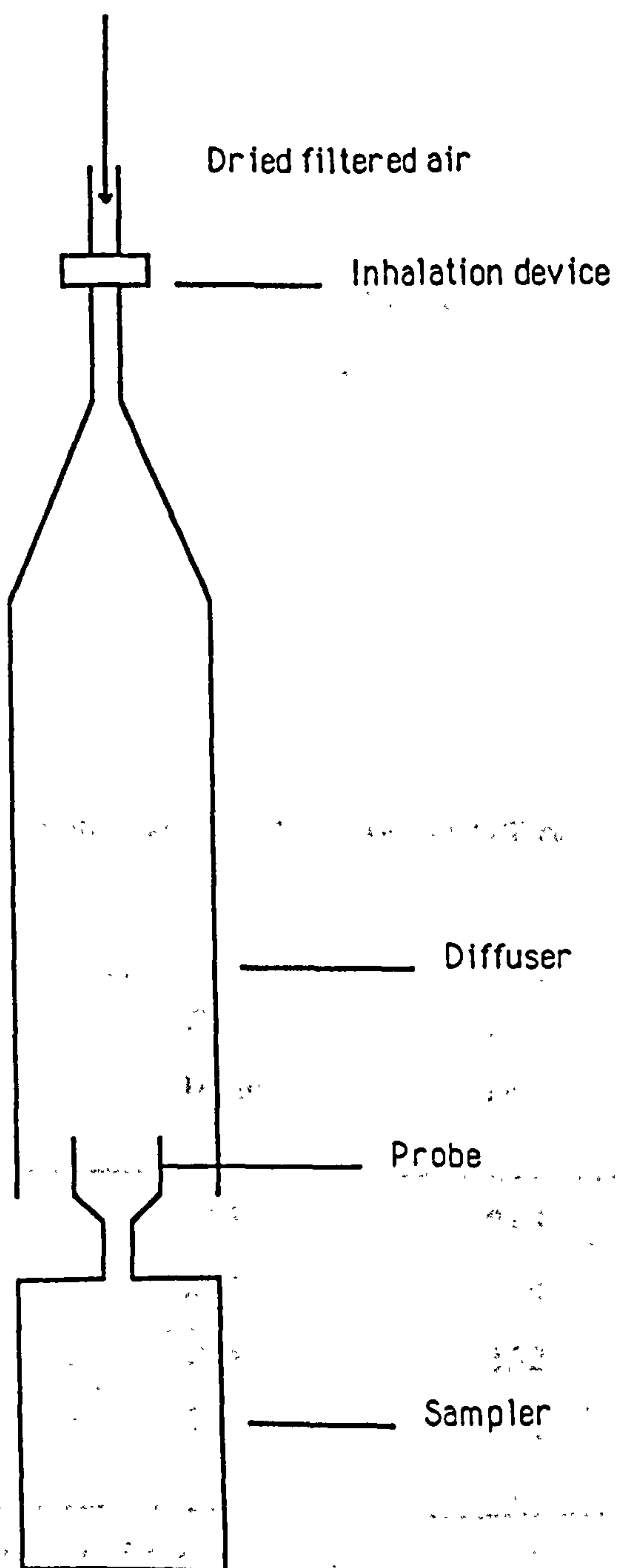
##### **1. Design of Apparatus B**

The apparatus is depicted in Figure 2.12. A powder inhaler device containing an encapsulated dose was assembled in a line conducting dried- filtered air at a flow rate up to 200 l/min. On actuation, the powder was blown into a low angle, vertical glass diffuser 550mm in length with 20mm and 70mm inlet and outlet diameters, respectively. The "throat" was eliminated since the preseparator stage of the impactor captures all particles larger than  $10\mu\text{m}$ , simulating the mouth and oral cavity. The expansion angle of the diffuser was smoother than ( $7^\circ$ ) and the length was extended to five times the diameter. These modifications were intended to improve the airflow pattern and decrease the turbulence as the aerosol cloud travels down the length of the diffuser. At a minimum distance of four diffuser diameters from the expansion angle, samples of the aerosol cloud were continually drawn to a cascade impactor operated at 28.3 l/min, through sharp edged conical probes.

The upper diameter of the probes was calculated so that the volume of air flowing through the probe and in the annulus around it, is proportional to the respective cross sectional areas. Equation 2.1 was used to calculate the probe diameters at different flow rates. The length of these tubes was kept as short as possible to



Fig 2.12



Apparatus B

minimize wall losses.

The characteristics of the sampling probes at different flow rates is given in Table 2.9.

2. Evaluation of Apparatus B

Aspiration efficiency determination

This was determined at air flow rates of 60 and 150 l/min at different sampling positions within the diffuser as described previously in Section 2.4.2.

Table 2.9 The diffuser and sampling tube characteristics at different flow rates in Apparatus B.

Qo	Do	Q	D	U=Uo
l/min	cm	l/min	cm	cm/sec
200	7.00	28.3	2.63	86.6
150	7.00	28.3	3.04	64.9
100	7.00	28.3	3.72	43.3
60	7.00	2.83	4.81	26.0

- Qo: Flow rate within the diffuser
- Do: Diameter of the diffuser
- Q: Flow rate within the sampling tube
- D: Diameter of the sampling tube at the respective flow rate
- U and Uo: Calculated sampling and air stream velocities respectively

## **2.4.5 Results and discussion**

### **1. Aspiration efficiency**

The aspiration efficiency obtained using this apparatus is given in Tables 2.11 to 2.15. No significant difference in the aspiration efficiency values was observed at air flow rates of 60 and 150 l/min for powder mixtures of the same carrier size. However, a variation was observed when powder mixtures of different carrier sizes were used. The aspiration efficiency approached unity with the small carrier size ( $<40\mu\text{m}$ ), whereas a value between 0.75-0.80 was obtained with the coarse carrier (60-180 $\mu\text{m}$ ).

When the sampling tube was moved to different sampling points across the cross-section of the diffuser and near the walls as demonstrated in Figure 2.13, similar aspiration efficiency values were obtained for the fine and coarse carrier (Tables 2.10 to 2.14).

These results demonstrate discrepancies in the overall sampling efficiency between the coarse and fine clouds. This is not surprising, since it has previously been observed that the turbulence of the airstream has little effect on the aspiration efficiency of small aerodynamic particle diameter, but its effect increased with particle size, especially for sizes above 40 $\mu\text{m}$ , due to inertia (Vincent *et al*, 1985). Weiner *et al* (1988) found that turbulence has a pronounced effect on the overall sampling efficiency with the small inlet sampling tubes and the large particle diameter.

The level of turbulence estimated by Reynold's Number at

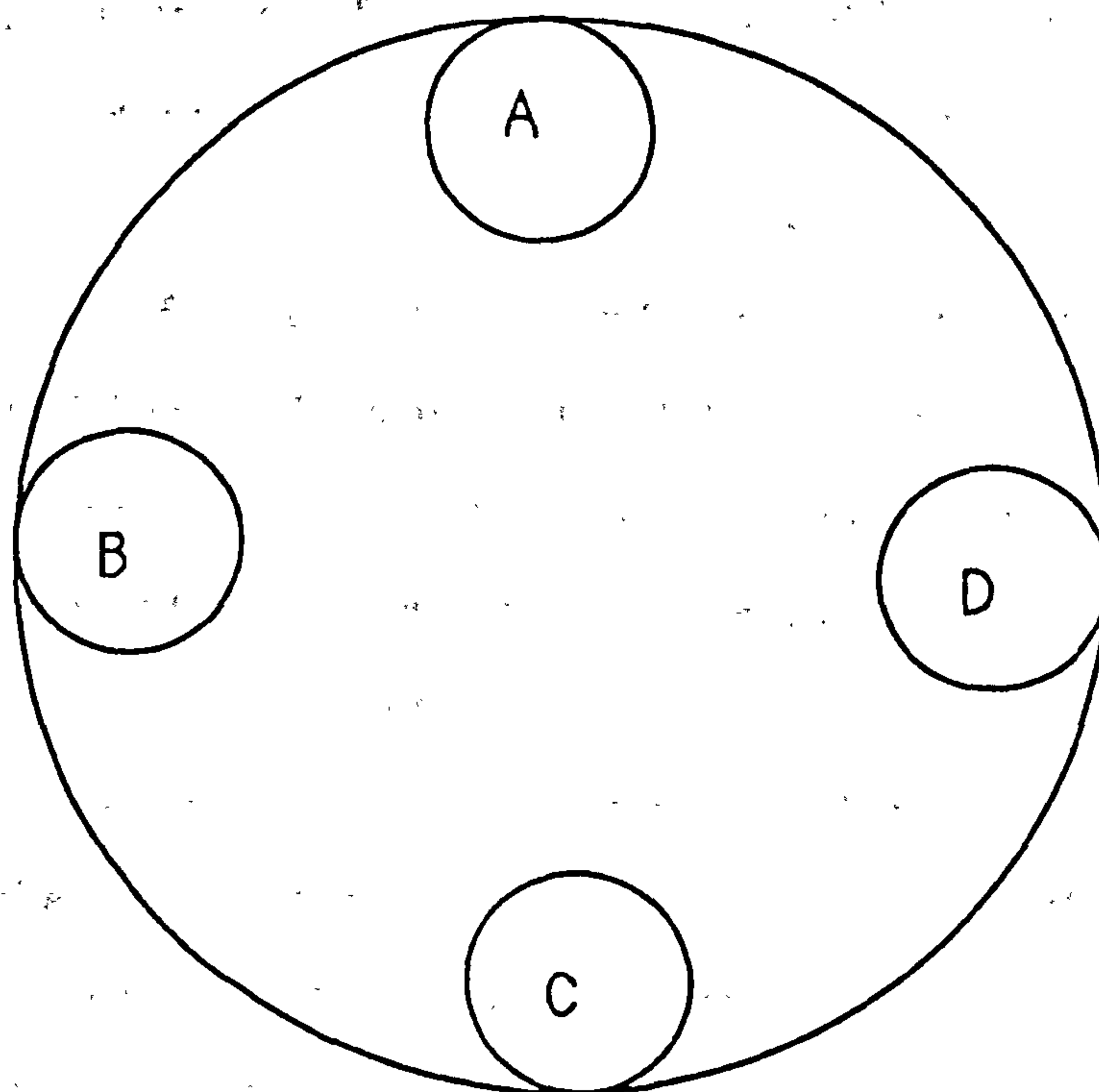


**Fig 2.13**

Sampling points near the wall of the diffuser



different flow rates (Table 2.15) was not appreciably lower than that for Apparatus A . However, in reality, the turbulence was substantially reduced in this apparatus, particularly at the sampling position as a result of sampling at a distance from a site likely to create air flow disturbances.

Comparable aerodynamic size fractions were obtained from various stages of the impactor when sampling at different sampling points within the diffuser (Tables 2.10 to 2.14). This indicates the efficiency of mixing of the aerosol cloud and a uniform distribution of the coarse and fine particles across the diffuser. Vincent (1988) found that the free stream air turbulence tends to smooth out particle concentration gradients as a result of diffusive processes particularly for large particle sizes.

The equal distribution of the cloud in Apparatus B may also be attributed to the fact that samples were drawn into the sampling tube at the same position from the bottom of the diffuser at all flow rates. This will have an advantage of minimizing errors caused by change in the air flow pattern as a result of the diffuser configuration. Additionally, this allows for cloud equilibration as it travels down the length of the diffuser before drawing the samples.

## **2. Material losses**

### **On the sampling tube**

Wall losses were reduced to less than 1% in this apparatus as a result of the shorter length and the larger diameter of the sampling tubes. These losses were considered insignificant .

### **On the diffuser**

Losses on the walls of the diffuser varied with the particle size of the generated cloud. Higher losses were observed with the finer cloud which may be attributed to electrostatic effects. However, these losses were assumed to be non-selective for a certain particle size. This is because the fractions of small and large particles collected when sampling at different points across the diffuser and near the walls were similar, indicating no segregation of the aerosol cloud. Therefore, the core material within the diffuser was considered representative of the total aerosol cloud.

### **Interstage losses**

Interstage losses within the cascade impactor were comparable to those observed previously and did not exceed 1%.

Having completed the above experiments it may be argued that the low aspiration efficiency values obtained with the coarser cloud were due to the difference between the free stream velocity and the velocity within the sampling tube. Air velocities in the presence of suspended particles could be significantly different to those in the absence of particles, especially in turbulent flow (Nouri *et al*, 1987), whereas fluid and particle velocities are identical at low Reynold's Numbers (Yianneskis & Whitelaw, 1984)

Thus to ascertain that the free stream velocity and the velocity within the sampling tube were identical in the absence and presence of particles, a flow visualization experiment was essential to confirm the suitability of the system for isokinetic sampling.

**Table 2.10** The percentage of drug deposited at various stages and the aspiration efficiency at different points across the diffuser at a flow rate of 150 l/min and a carrier size of 60-180 $\mu$ m.

Stage	-r/2	r	+r/2
Device and capsules	14.3 $\pm$ 0.4	15.1 $\pm$ 0.2	14.9 $\pm$ 0.5
Diffuser	2.2 $\pm$ 0.1	2.0 $\pm$ 0.2	1.9 $\pm$ 0.1
Probe	0.9 $\pm$ 0.1	0.3 $\pm$ 0.0	0.8 $\pm$ 0.0
Preseparator	66.5 $\pm$ 1.9	64.3 $\pm$ 1.1	66.4 $\pm$ 2.0
Stages 0-2	1.5 $\pm$ 0.1	1.6 $\pm$ 0.1	1.4 $\pm$ 0.1
Stages 3-7	14.4 $\pm$ 0.9	16.2 $\pm$ 1.2	15.5 $\pm$ 0.9
Interstage losses	0.3 $\pm$ 0.2	0.5 $\pm$ 0.1	0.6 $\pm$ 0.1
Aspiration efficiency	0.8 $\pm$ 0.01	0.8 $\pm$ 0.03	0.8 $\pm$ 0.02

The results are the mean and standard deviation of six experiments.

No significant difference in the aspiration efficiencies and the depositions at various stages of the impactor at  $P < 0.05$ .

**Table 2.11** The percentage of drug deposited at various stages and the aspiration efficiency at different sampling positions near the walls of the diffuser at a flow rate of 150 l/min and a carrier size of 60-180 $\mu$ m.

Stage	Position A	Position B	Position C	Position D
Device and Capsules	15.6 $\pm$ 0.9	16.2 $\pm$ 1.1	13.4 $\pm$ 1.3	14.2 $\pm$ 0.8
Diffuser	2.1 $\pm$ 0.1	1.9 $\pm$ 0.1	2.3 $\pm$ 0.1	2.6 $\pm$ 0.1
Probe	0.4 $\pm$ 0.0	0.7 $\pm$ 0.1	0.5 $\pm$ 0.0	0.3 $\pm$ 0.0
Preseparator	63.3 $\pm$ 2.1	61.7 $\pm$ 2.0	66.6 $\pm$ 2.5	65.0 $\pm$ 1.8
Stages 0-2	1.8 $\pm$ 0.1	1.8 $\pm$ 0.0	2.0 $\pm$ 0.1	1.4 $\pm$ 0.1
Stages 3-7	16.1 $\pm$ 0.7	17.5 $\pm$ 0.9	14.8 $\pm$ 0.4	14.9 $\pm$ 0.7
Interstage losses	0.7 $\pm$ 0.1	0.3 $\pm$ 0.1	0.5 $\pm$ 0.1	1.0 $\pm$ 0.0
Aspiration efficiency	0.8 $\pm$ 0.03	0.8 $\pm$ 0.03	0.8 $\pm$ 0.03	0.8 $\pm$ 0.04

The different sampling points are illustrated in Figure 2.13

The results are the mean and standard deviation of five experiments.

No significant difference in the aspiration efficiencies and the depositions at various stages of the impactor at P<0.05.



**Table 2.12** The percentage of drug deposited at various stages and the aspiration efficiency at different sampling points across the diffuser at a flow rate of 150 l/min and a carrier size of  $<40\mu\text{m}$ .

Stage	-r/2	r	+r/2
Device and capsules	18.9±1.5	17.7±1.1	19.6±0.9
Diffuser	23.1±3.0	24.2±2.4	22.0±3.0
Probe	1.0±0.1	0.9±0.0	0.9±0.0
Preseparator	14.8±1.2	14.2±0.9	15.5±1.1
Stages 0-2	15.5±0.9	14.9±1.4	16.1±1.4
Stages 3-7	26.0±1.1	27.0±1.6	24.9±1.9
Interstage losses	0.8±0.1	1.1±0.1	1.0±0.02
Aspiration efficiency	1.0±0.03	1.0±0.02	1.0±0.03

The results are the mean and standard deviation of five experiments.  
 No significant difference in the aspiration efficiencies and the depositions at various stages of the impactor at  $P<0.05$ .

**Table 2.13** The percentage of drug deposited at various stages and the aspiration efficiency at different sampling positions near the walls of the diffuser at a flow rate of 150 l/min and a carrier size of <40 $\mu$ m.

Stage	Position A	Position B	Position C	Position D
Device and Capsules	17.9 $\pm$ 2.3	17.5 $\pm$ 2.9	20.4 $\pm$ 1.8	18.9 $\pm$ 2.0
Diffuser	22.1 $\pm$ 3.5	23.0 $\pm$ 4.0	21.6 $\pm$ 2.8	20.5 $\pm$ 2.2
Probe	1.0 $\pm$ 0.1	0.8 $\pm$ 0.03	0.6 $\pm$ 0.03	1.0 $\pm$ 0.1
Preseparator	18.4 $\pm$ 1.8	20.0 $\pm$ 0.9	18.9 $\pm$ 1.1	19.7 $\pm$ 1.3
Stages 0-2	14.4 $\pm$ 2.1	16.2 $\pm$ 1.0	13.3 $\pm$ 1.3	15.6 $\pm$ 1.0
Stages 3-7	25.7 $\pm$ 2.0	21.5 $\pm$ 1.3	24.5 $\pm$ 0.9	23.5 $\pm$ 1.1
Interstage losses	6.1 $\pm$ 0.1	0.9 $\pm$ 0.1	0.7 $\pm$ 0.03	0.8 $\pm$ 0.05
Aspiration efficiency	1.1 $\pm$ 0.02	1.0 $\pm$ 0.05	0.9 $\pm$ 0.08	1.1 $\pm$ 0.05

The different sampling points are illustrated in Figure 2.13

The results are the mean and standard deviation of five experiments.

No significant difference in the aspiration efficiencies and the depositions at various stages of the impactor at P<0.05.

**Table 2.14** The percentage of drug deposited at various stages and the aspiration efficiency at a flow rate of 60 l/min with two carrier sizes.

Stage	Carrier size	
	125-180 $\mu$ m	<40 $\mu$ m
Device and capsules	12.1 $\pm$ 0.9	27.3 $\pm$ 2.1
Diffuser	2.1 $\pm$ 0.1	6.1 $\pm$ 1.1
Probe	0.0	0.6 $\pm$ 0.0
Preseparator	81.2 $\pm$ 3.0	46.7 $\pm$ 2.4
Stages 0-2	0.5 $\pm$ 0.0	8.9 $\pm$ 1.4
Stages 3-7	4.0 $\pm$ 0.9	9.9 $\pm$ 1.0
Interstage losses	0.4 $\pm$ 0.1	0.5 $\pm$ 0.0
Aspiration efficiency	0.8 $\pm$ 0.03	1.0 $\pm$ 0.05

The results are the mean and standard deviation of six experiments.

**Table 2.15 Values of Reynold's Number at different flow rates in Apparatus B.**

Flow Rate( l/min)	Reynold's Number
200	1518
150	1315
100	1074
60	833



#### **2.4.6 Flow visualization**

Several techniques have been employed for the measurement of the velocity of suspensions in gases, such as hot-wire anemometry and laser doppler anemometry. The latter offers an advantage over other techniques in that it is non-invasive and measurements can be made without disturbing the flow field. Therefore, this technique was employed to investigate the flow properties in Apparatus B.

Air stream and particle mean velocities and turbulence intensity can be measured experimentally at fixed points using this method. The degree of turbulence,  $u/U$ , where,  $u$ , is the root mean square velocity and  $U$ , is the mean flow velocity, obtained is almost independent of Reynold's Number. The latter describes the overall turbulence and is dependent upon the dimensions of the tube in which the air is flowing and the air velocity. However, the turbulence intensity measured by the laser technique, depends on the fluctuations in air velocities arising from eddies at certain points in the flow field.

##### **1. The laser anemometer optics**

The laser anemometer is shown schematically in Figure 2.14. The laser anemometer was operated with forward scattered light using a 10mW Helium-Neon laser and a rotating diffraction grating which splits the laser beam into two equal intensity beams that are focussed to a cross forming a control volume. A particle moving in this control volume causes a frequency shift of the light scattered by the particles. The scattered light is collected by a photomultiplier. The principal characteristics of the optical system are listed in Table 2.16. The signals from the photomultiplier are processed

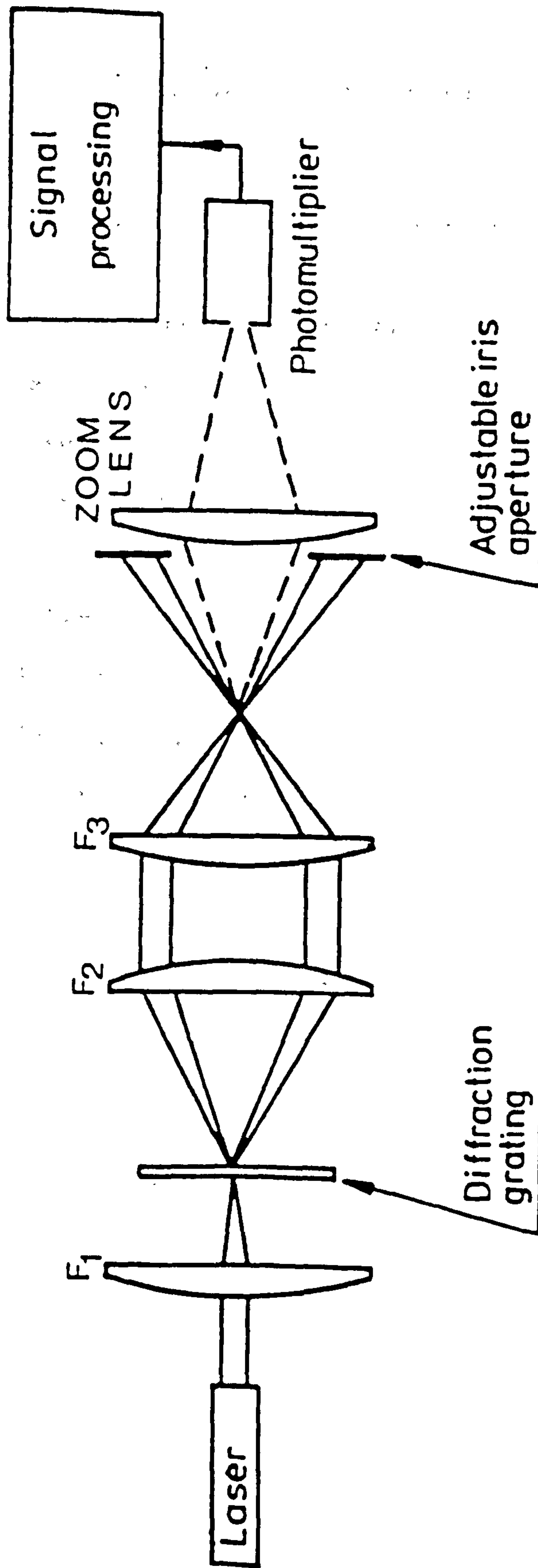


Fig 2.14 Optical arrangement of the Laser-Doppler anemometer

**Table 2.16 The principal characteristics of the laser doppler anemometer**

Laser wavelength, nm	632.8
Frequency-to-velocity conversion constant, m/s/MHZ	4.53
Half-angle between incident beams, degrees	4.0
Focal length of Lens F <sub>1</sub> , mm	200
Focal length of Lens F <sub>2</sub> , mm	500
Focal length of Lens F <sub>3</sub> , mm	200
Beam spacing at Lens F <sub>3</sub> ,mm	28
Intersection volume diameter , μm	95
Intersection volume length , μm	1350
Number of fringes in intersection volume	21
Fringe spacing, μm	4.53
Frequency shift, MHz	0.4

by the frequency counter. The measured frequencies are obtained from the digital output of the counter which is interfaced to a micro-computer, with which the mean and root mean square velocity components are calculated.

The signal processing system and the output are shown in Figure 2.15.

## **2. Velocity and turbulence intensity measurements**

The modifications carried out on the apparatus to perform the necessary experiments are shown in Figure 2.16. The laser anemometer and ancilliary equipment were mounted on a platform, and the apparatus was fitted on a table to minimize vibrations transmitted to the platform. An adjustable table allowed the laser anemometry measurements to be taken at about 5 diffuser diameters from the bottom of the diffuser. Measurements across the diffuser were performed by moving the control volume . This was carried out by moving the optical unit ( $F_3$ ) along an optical bench, re-aligning the photomultiplier and adjusting the iris aperture with each increment (Figure 2.17).

To evaluate the suitability of Apparatus B for isokinetic sampling, it was necessary first to confirm that the free stream velocity ,  $U_0$ , and the velocity by the sampling tube,  $U$ , were identical both in the absence and presence of particles. These experiments were conducted without inserting the inhaler in the flow configuration. However, since the design of the inhaler might introduce some asymmetry to the flow field, experiments were performed with the inhaler inserted to investigate its influence on the airflow pattern.



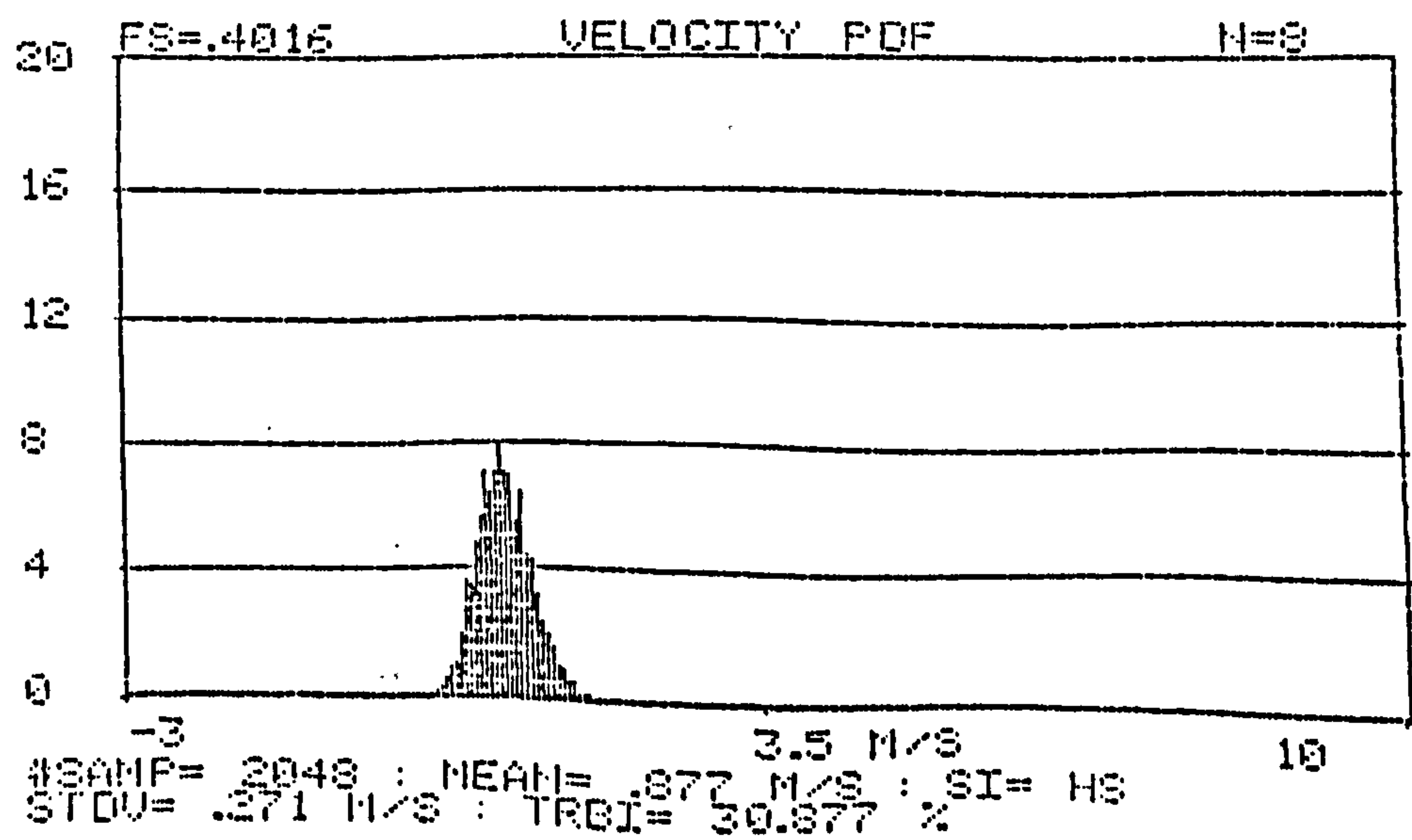
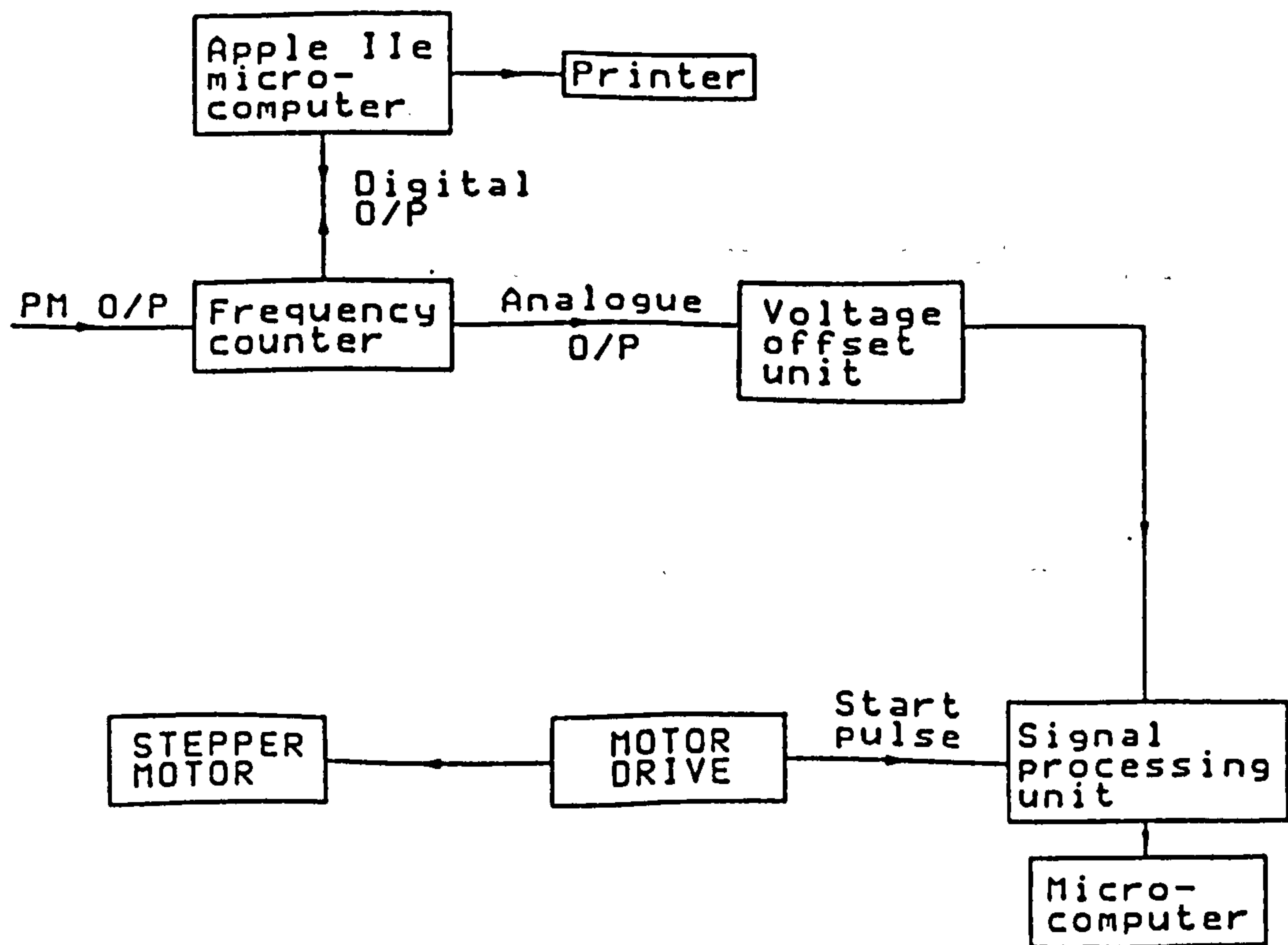


Fig 2.15 Signal processing system of the Laser-Doppler anemometer and the output

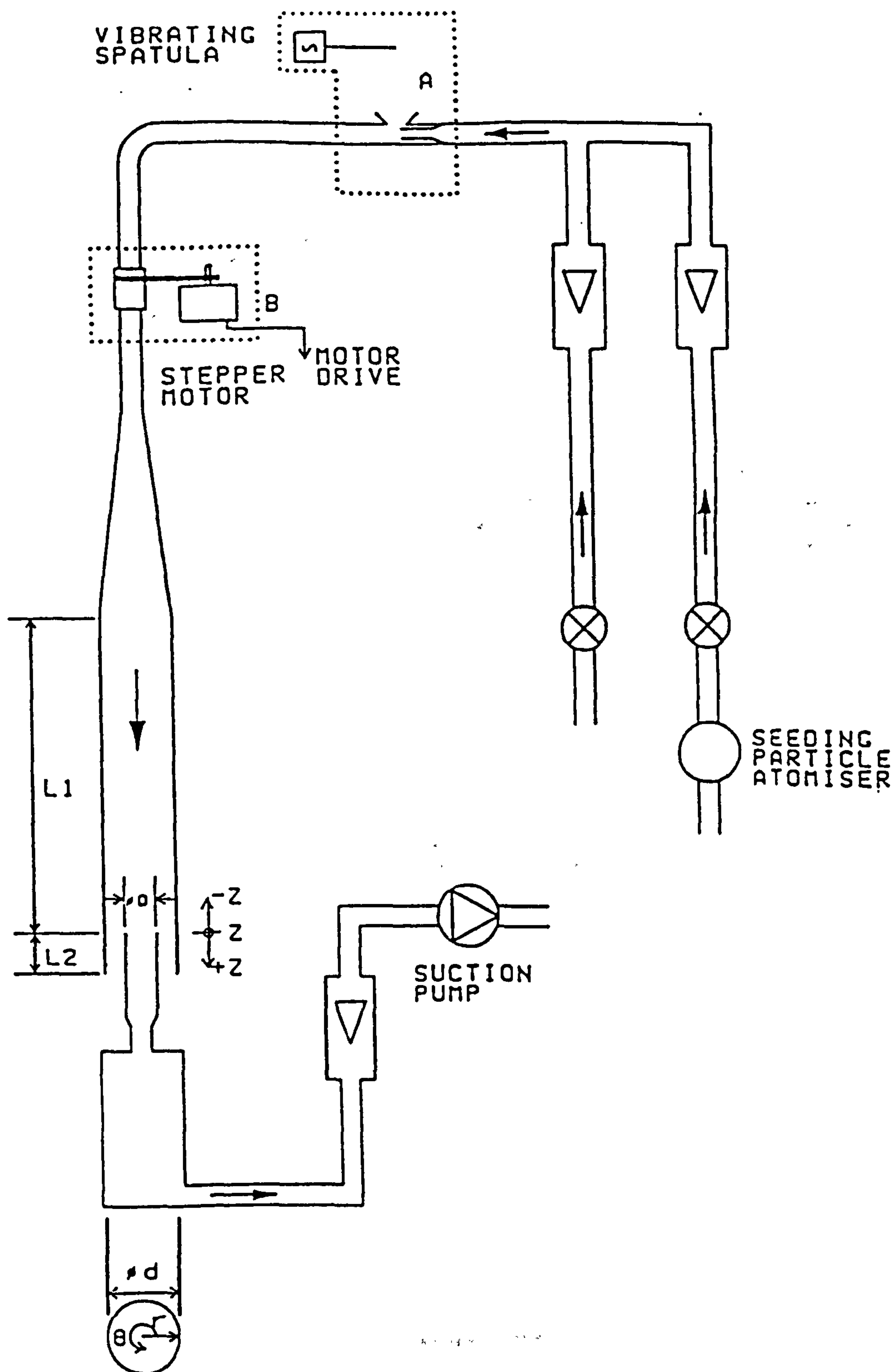


Fig 2.16 Schematic diagram of the modified flow configuration

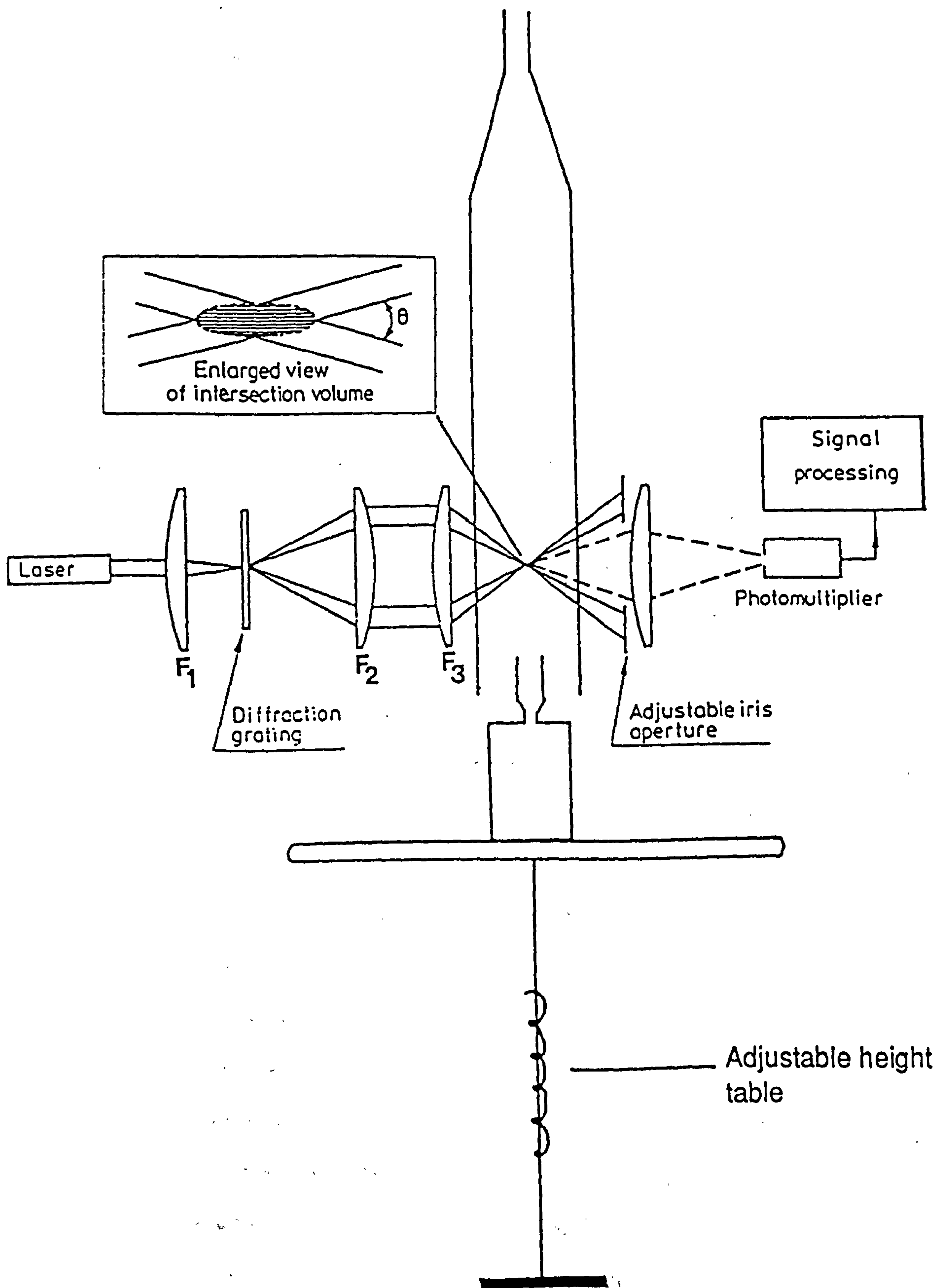


Fig 2.17 Schematic representation of the experimental condition

But since the actual process was a transient release of particles rather than a steady flow, experiments were conducted to measure the particle velocity after breaking the capsule to verify that this does not account to any significant alteration in the sampling process.

These experiments were conducted in the following sequence:

First the mean and root mean square velocities (indicating the turbulence intensity) of the steady airflow through the diffuser, without the inhaler, were measured at 60, 100, 150 and 200 l/min, using silicon oil droplets of  $<2\mu\text{m}$  mean diameter as seeding particles. These droplets, generated by an atomizer, are small enough to follow closely the gas streamlines and thus, the velocity recorded is the velocity of the gas carrying these particles (Yianneskis 1987). Measurements of the steady airflow velocity were made across the diffuser at three axial locations: 110mm upstream from the probe, 10mm upstream from the probe inlet and 10mm downstream from the probe inlet, both inside and in the annulus around it. The sampling tubes were made from perspex to enable optical access.

For the second set of measurements, particle and r.m.s. velocity measurements at flow rates of 150 and 200 l/min were made using clouds of lactose particles of size fractions  $<40\mu\text{m}$  and 60-180 $\mu\text{m}$ . A section of the small pipe (at location A in Figure 2.16) incorporated a convergent nozzle to induce local flow acceleration and a reduction in pressure. At the point of minimum pressure, a small funnel was attached to the pipe wall through which solid particles could be introduced. The flow through the funnel was



measured during each test with a hot-wire anemometer. Particles were gravity fed into the diffuser using a vibrating spatula which has been previously adjusted to introduce particles at approximately 1.6 g/min.

In the third set of experiments, the inhaler was inserted in the diffuser at location B (see Figure 2.16). Measurements were made at 150 l/min for the steady air flow and the solid particle flow, as described above.

In the fourth experiment, the rotating section of the inhaler was coupled to a stepper motor as shown in Figure 2.16. A capsule was loaded with 140mg of powder to maximize the resolution as the particles crossed the control volume. The motor rotated the upper half of the inhalation device to break the capsule and this operation was synchronized with the measurement of particle velocities released at 60 l/min. The rotation of the stepper motor simultaneously triggered the frequency counter measurements. The analogue output of the counter was interfaced to a second micro-computer which was used to calculate the velocity at each recording.

#### **2.4.7 Results and discussion**

Representative measurements for air stream and r.m.s. velocity components at a flow rate of 150 l/min are shown in Figure 2.18. The results obtained at the other flow rates are given in the Appendix . The results indicate that air stream and sampling velocities were similar upstream in the diffuser, upstream before the sampling tube, in and around the sampling tube. The velocity profiles were flat across the diffuser and they were not significantly disturbed by the presence of the probe. The results also indicate that the turbulence intensity was high within the diffuser; however, turbulent fluctuations were uniform across the cross-section. Similar results were obtained at all flow rates.

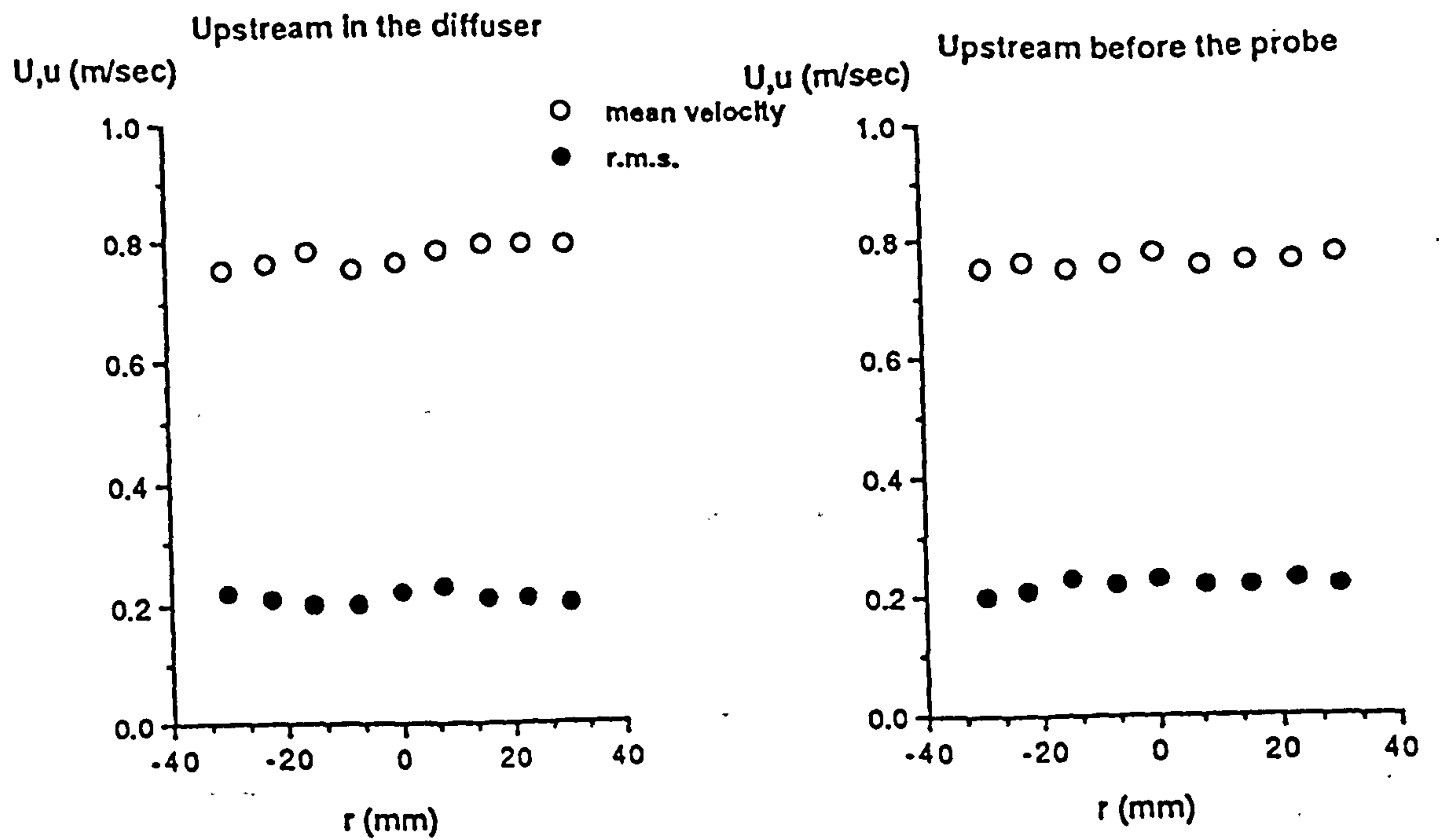
Particle velocities at a flow rate of 150 l/min, from each of the two size fractions 60-180 $\mu$ m and <40 $\mu$ m, are compared with the gas velocities in Figure 2.19. All the measurements made indicated that the particle mean and r.m.s. velocity profiles were similar, upstream before the sampling tube, inside, and in the annulus around it. However, the mean velocities of the large particles are about 0.16m/sec higher than those of the smaller ones, which in turn are about 0.04m/sec larger than those of the air flow. This can be expected as gravity acts in the down flow situation so as to increase the particle velocity. The r.m.s. velocity results shown in Figure 2.19 indicate that there is an increase in turbulence as particle size increases, as well as in comparison to gas flow. The latter results are in agreement with the findings of Lee (1985), who observed that the particle r.m.s. velocity was higher than the

single-phase gas r.m.s. over most of the pipe cross-section for most Reynold's Numbers examined.

Measurements obtained with the inhaler device inserted in the airline at a flow rate of 150 l/min are shown in figure 2.20. The air and particle mean velocities were similar to those shown in Figure 2.19 in the absence of the inhalation device. The profiles were uniform, indicating that the flow recovers soon after its passage through the inhaler and that the asymmetry in its design has no influence on the air flow pattern down stream from the diffuser.

Therefore from these measurements, it was verified that the velocity of the air stream and the particles of the two size fractions were similar at the sampling point. Hence, neither the geometry of the diffuser nor the presence of the inhaler could account for the reduced aspiration efficiency observed for the coarse carrier particles.

The velocity trace obtained by the transient particle release at an air flow of 60 l/min is shown in Figure 2.21. For a short period after breaking the capsule, there were no particles crossing the control volume which was located 10mm above the sampling tube and approximately 500mm downstream of the device. For this reason the velocity record was initiated with a small delay after breaking the capsule. The average velocity value indicated in the trace after the first 0.5 seconds was in agreement with the steady air flow velocity at 60 l/min. This was 0.35m/sec. Therefore, it is suggested that the velocity profiles are not noticeably affected by the transient nature of the process.



U Mean velocity  
u r.m.s. velocity  
r Distance from the centre

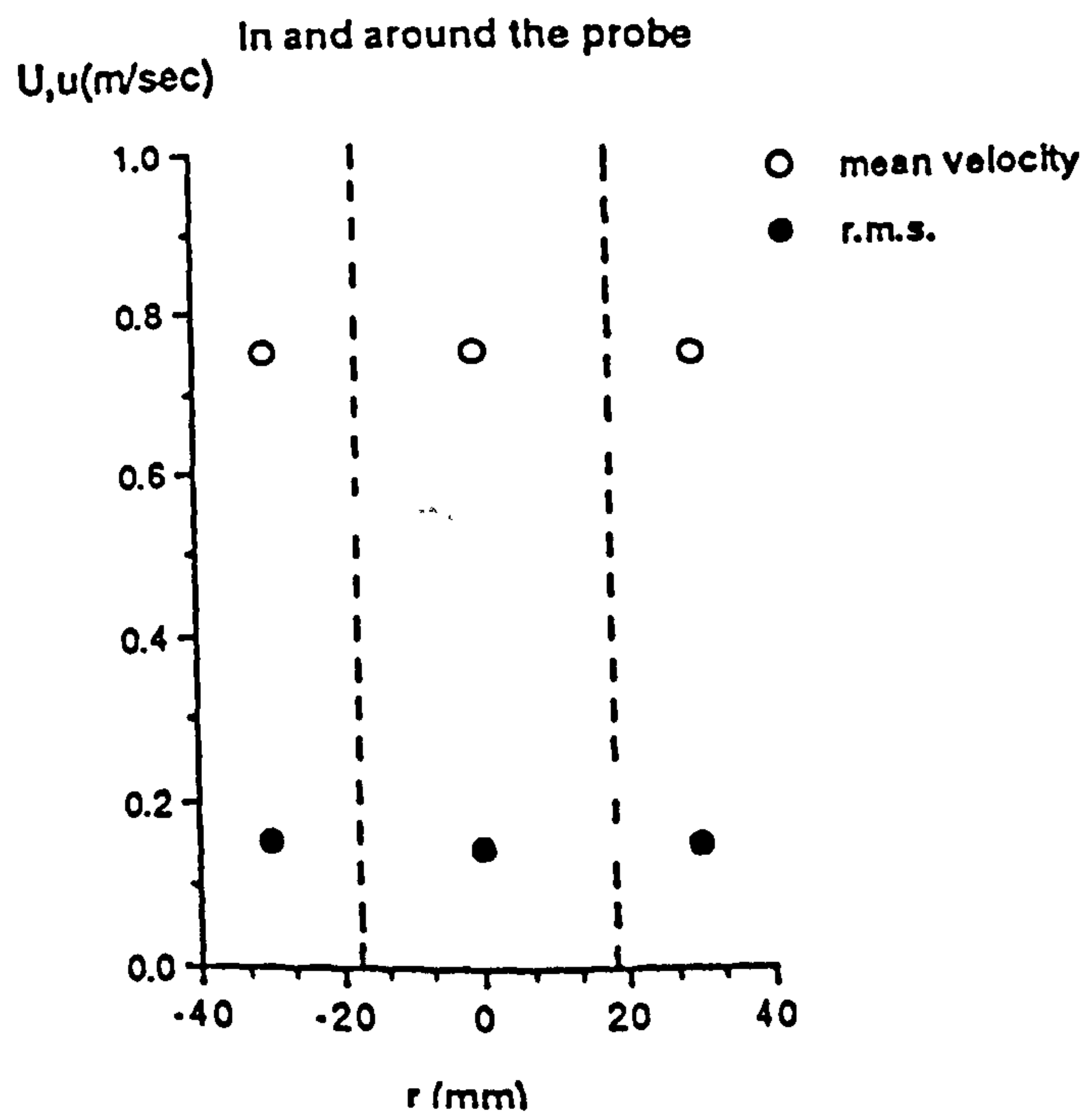


**Fig 2.18** Profiles of axial mean and r.m.s. velocities of the gas at an airflow of 150 l/min



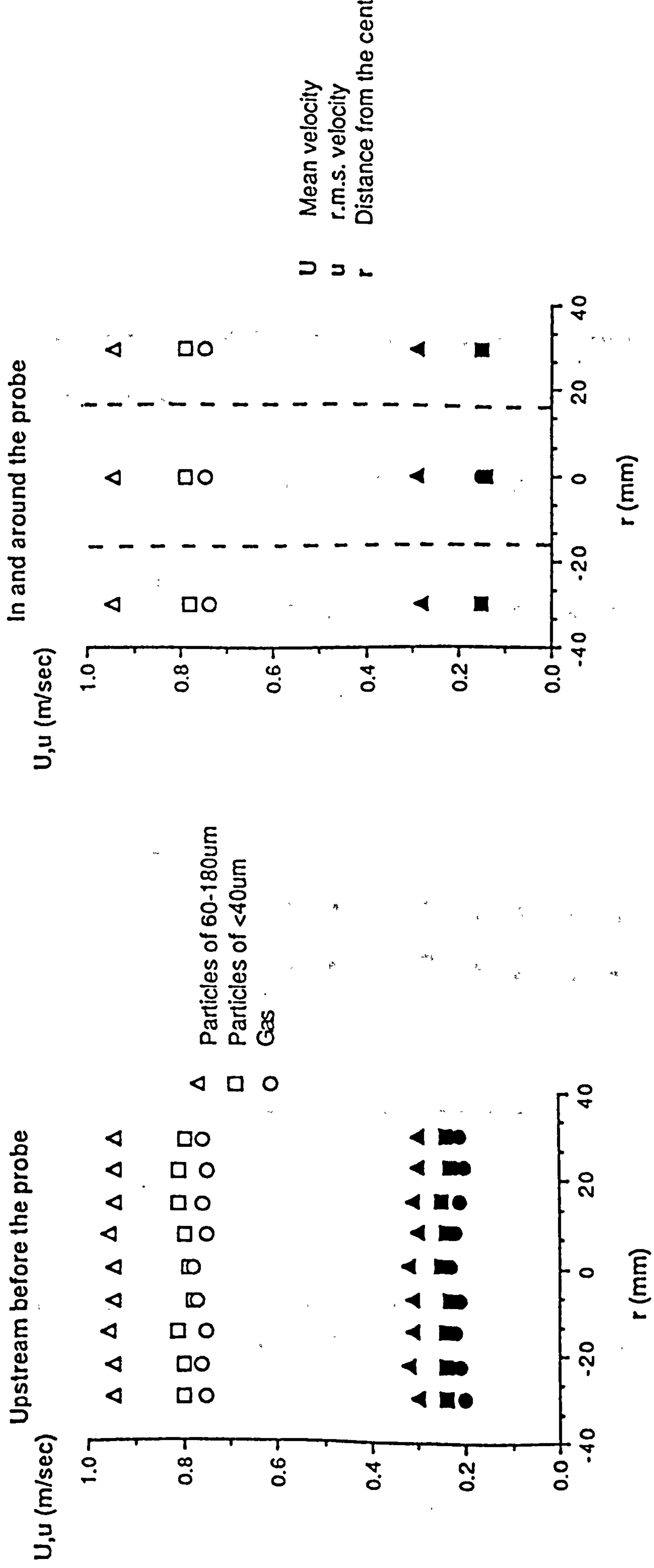


Fig 2.19 Profiles of axial mean (open symbols) and r.m.s. (solid symbols) velocities at an airflow 150 l/min

Gas and particle flow at 150 l/min upstream before the probe in the presence of the Inhaler

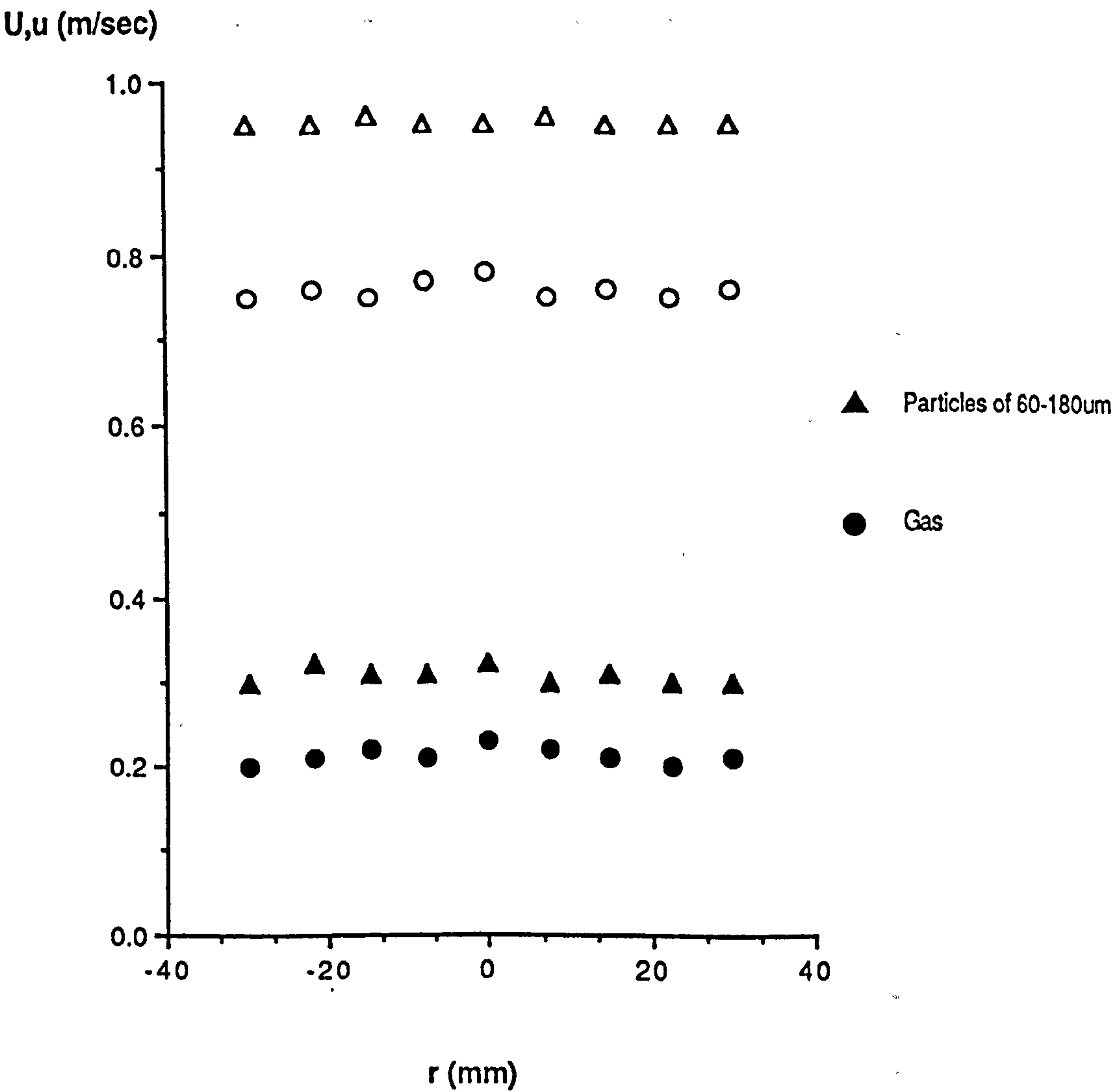
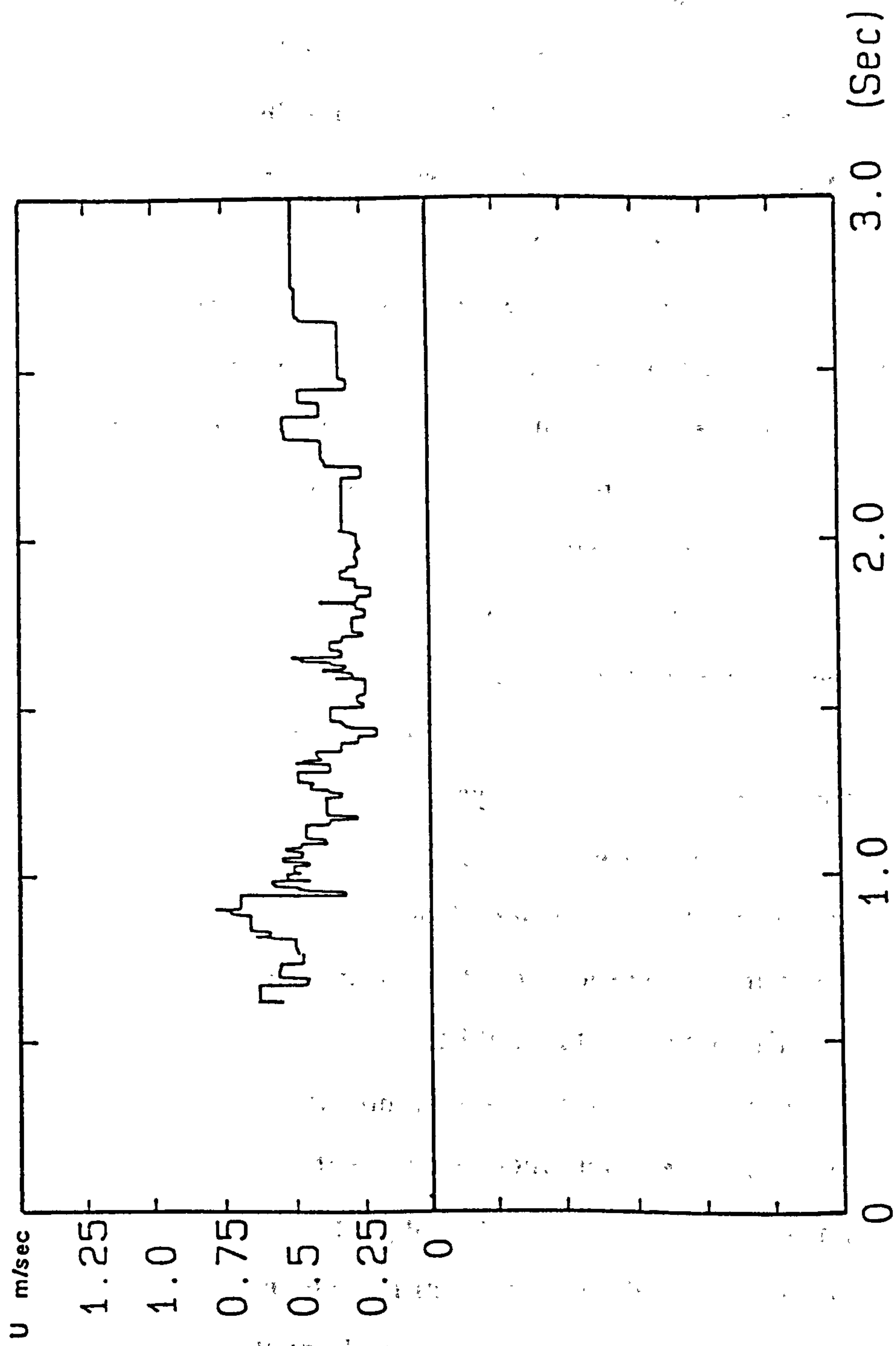
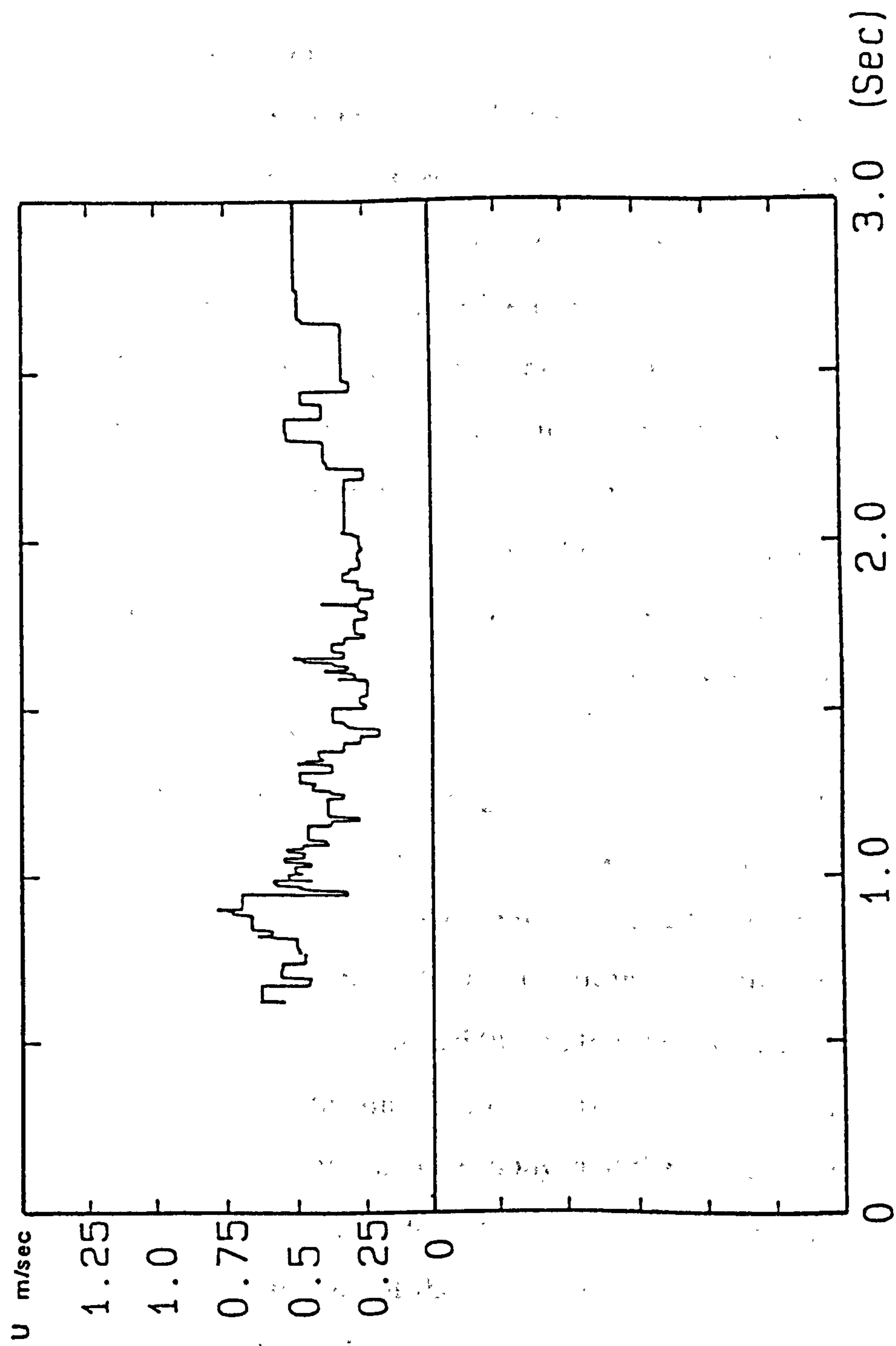


Fig 2.20 Profiles of axial mean (open symbols) and r.m.s. (solid symbols) velocities at an airflow of 150 l/min



**Fig 2.21** Time-resolved record of particle velocity after breaking of capsule



**Fig 2.21** Time-resolved record of particle velocity after breaking of capsule



Having established that the transient nature of the process did not account for any significant alteration in the sampling process and confirmed that the free stream and the sampling velocities were identical under all experimental conditions, it can be concluded that isokinetic sampling conditions have been achieved.

However, these measurements did not explain the reason for the difference in the aspiration efficiency observed for the coarse and fine aerosol clouds. A possible explanation is that particles of unit density and of a radius  $\leq 30\mu\text{m}$  are completely entrained by the conveying gas and are expected to follow the turbulent fluctuations, whereas coarser particles of radius equal to  $100\mu\text{m}$  are found to be only 70% entrained by turbulent fluctuations (Fuchs, 1964). Owing to inertial and gravitational effects large particles move faster than the conveying air stream, thus the level of entrainment is reduced increasing the particle size.

Another possible reason might be related to the dimensions of the sampling tubes. In reality, the thin walled sampling tube does not exist, since the tube walls must have a finite thickness and so present some blockage to the air movement no matter how small.

Vincent *et al* (1982) noted that at the sample orifice the flow may be considered to consist of two parts, the outer one dominated by the flow about the sampler body, and the inner one dominated by the flow into the sampling orifice. This type of flow tends to disturb the gas streamlines at the sampling tube entrance and will depend on the wall thickness. Therefore, particles approaching the entrance of the tube might be subjected to some changes in the direction of air motion. These could cause them to experience inertial forces and so undergo deflection even if the changes were

minor. It would be expected that this effect will be more pronounced for the larger particles. However, having established that the fractionation of the sampled cloud into different aerodynamic size fractions was similar at different sampling points within the diffuser, it is possible to suggest that the sampling process was representative for both size fractions and the devised apparatus is suitable for isokinetic sampling.

By means of isokinetic sampling, Apparatus B permits the evaluation of formulation variables in powder inhalation aerosols in terms of inspiratory effort. This has not been possible in earlier studies which sampled the total aerosol cloud with conventional impactors usually calibrated at flow rates not exceeding 60 l/min.

## **Chapter three**

### **The effect of airflow, inhalation device and formulation variables on the characteristics of a cloud**

## **Introduction**

Mixing fine drug particles with a coarse carrier is the most common way of formulating dry powders for inhalations. The mixture formed can be described as an ordered mixture (Hersey, 1975).

In dry powder aerosols, redispersion of the drug particles from their agglomerates or from the surface of the carrier as single entities during inhalation, is the most critical factor which governs the availability of the medicament to the lungs. This will depend on the mechanical stability of the powder mixture, the way this is influenced by the adhesion characteristics between the drug and the carrier, and the external forces required to break up the bonds formed between adhering particles.

In ordered mixtures, the adhesion characteristics between the drug and the carrier can be influenced by several factors. These include: the surface properties of the carrier, the particle size of the two components, the presence of other components, the relative humidity and electrostatic behaviour. These factors influence the entrapment of fine drug particles within the clefts and pores on the carrier surface and interfere with the strength of the interparticle forces.

High relative humidities result in an increase in the adhesive forces due to capillary action. However, the electrostatic forces, which predominate at low humidities, may increase or decrease the mechanical stability of powder mixtures since powders have different dielectric constants. In powder aerosols, electrical



charges may arise during mixing or may be induced on the powder particles during inhalation as a result of powder bed fluidisation.

Literature reports concerned with the basic principles governing the generation of medical powder aerosols are sparse. The concept of the influence of air flow through the device on its performance as an insufflator was introduced by Bell *et al*, (1971) who also reported the size of the carrier which provides optimum flow properties of the powder. Other workers (Chowhan and Amero, 1977) attempted to introduce possible formulation variables which might improve the performance of dry powder aerosols. They investigated the importance of selecting a proper drug entity in designing powder aerosols. The delivery efficiency of an organic acid and a salt from powder blends, under ambient conditions and following equilibration of the powders under various humidity conditions were compared. Further *in vitro* studies were carried out by Chowhan and Linn (1978) to investigate the effect of the drug dose and the drug to carrier ratio on the delivery efficiency of these drugs. Vidgren *et al* (1987) studied the effect of fine drug particles, produced by two different size reduction methods, on the deposition behaviour of mixtures containing equal proportions of the drug and the carrier.

However, none of the above investigations provided a basic understanding of the powder properties and their behaviour in turbulent air stream. Evaluations were performed at low and fixed flow rates, whereas in reality the cloud might be generated at flow rates which vary according to the patient's disease state and normally higher than those employed. The behaviour of the

aerosol cloud might well differ at different and higher air speeds. Moreover, varying the carrier size and its proportion in the formulation was mainly carried out to improve the flow properties of the powder mixtures at the low flow rates employed. No attempt has been made to relate the behaviour of powder aerosols to the nature of the adhesive forces and the external accelerative forces required to act at the drug-carrier interface to overcome the interparticulate forces.

Therefore in the following study, fundamental knowledge on adhesion was applied to powder aerosols. Formulation variables were varied according to the factors which were expected to affect the adhesion characteristics and for which the force required to redisperse the fine drug particles was altered by changing the flow rate and the turbulence within the inhalation device.

## **3.2 Materials and methods**

### **3.2.1 Characterization of powders**

#### **1. Classification of carriers**

Lactose monohydrate (regular) was classified into different size fractions as described in Section 2.2.1. Milled glass and spray dried lactose (Pharmatose, De Melkindustrie Vegh) were classified by an "Alpine" air jet sieve to obtain a size fraction between 63-90 $\mu$ m. The glass beads were 60 $\mu$ m in size and recrystallized lactose was obtained in the size range of 60-90 $\mu$ m by crystallizing lactose monohydrate under controlled conditions.

## **2. Particle size analysis**

The particle size distribution of the micronized salbutamol sulphate was determined by the method described in Section 2.2.1.

The size distribution of the recrystallized lactose was determined by image analysis optical microscopy. Slides were prepared by dispersing a very small amount of the powder. Fields were selected randomly and the image was projected onto a computer screen. The perimeter of each particle in the field was traced using a graphic tablet; 500 particles were measured to obtain a statistically significant value. The size distribution ranged between 60-90 $\mu$ m.

## **3. Flow properties of powders**

The flow of the carriers was measured by discharge through an orifice. A tube fitted with a circular orifice 5.8mm in diameter was filled with 200g powder and the flow rate was measured by weighing the amount of powder escaping from the orifice in 15 seconds after steady state condition was established. Lactose fractions of <20 $\mu$ m and <10 $\mu$ m were too cohesive for this experiment and a tensile strength test was performed.

Results are shown in Table 3.1.

## **4. Tensile strength measurement**

The tensile strength of micronized salbutamol sulphate and lactose in the size fractions of <20 $\mu$ m and <10 $\mu$ m was measured over a range of packing fractions from 0.1 to 0.6 using a split plate tensile tester (Ajax Ltd).

Figure 3.1 shows the log tensile strength (Nm<sup>-2</sup>) against packing fraction for the three powder samples tested. The results were

found to fit the general equation:

$$\text{Log } T = A_1 P_f + A_2 \quad (3.1)$$

where:  $T$  is the tensile strength,  $P_f$  is the packing fraction and  $A_1$  and  $A_2$  are constants for each sample.

The tensile strength, at any particular packing fraction, decreased in the order:

micronized salbutamol sulphate > lactose (<10 $\mu$ m) > lactose (<20 $\mu$ m)

## **5. Moisture content**

The moisture content was determined for all the powders using an infra-red moisture balance and did not exceed 1.0% w/w. The powders were stored in sealed jars over silica gel.

## **6. Carrier surface characterization**

### **a. Scanning electron microscopy**

Scanning electron microscopy was used to examine the surface texture of the carriers. Photomicrographs of particle surface details are produced in Figure 3.4.

### **b. Surface roughness (rugosity) determination**

The surface roughness ( $R_s$ ) was determined by comparing the external specific surface area obtained by an air permeation method ( $S_o$ ) with the theoretical surface area when the particles are considered as spheres ( $S_d$ ) measured from projected particle diameter:

$$R_s = S_o / S_d \quad (3.2)$$



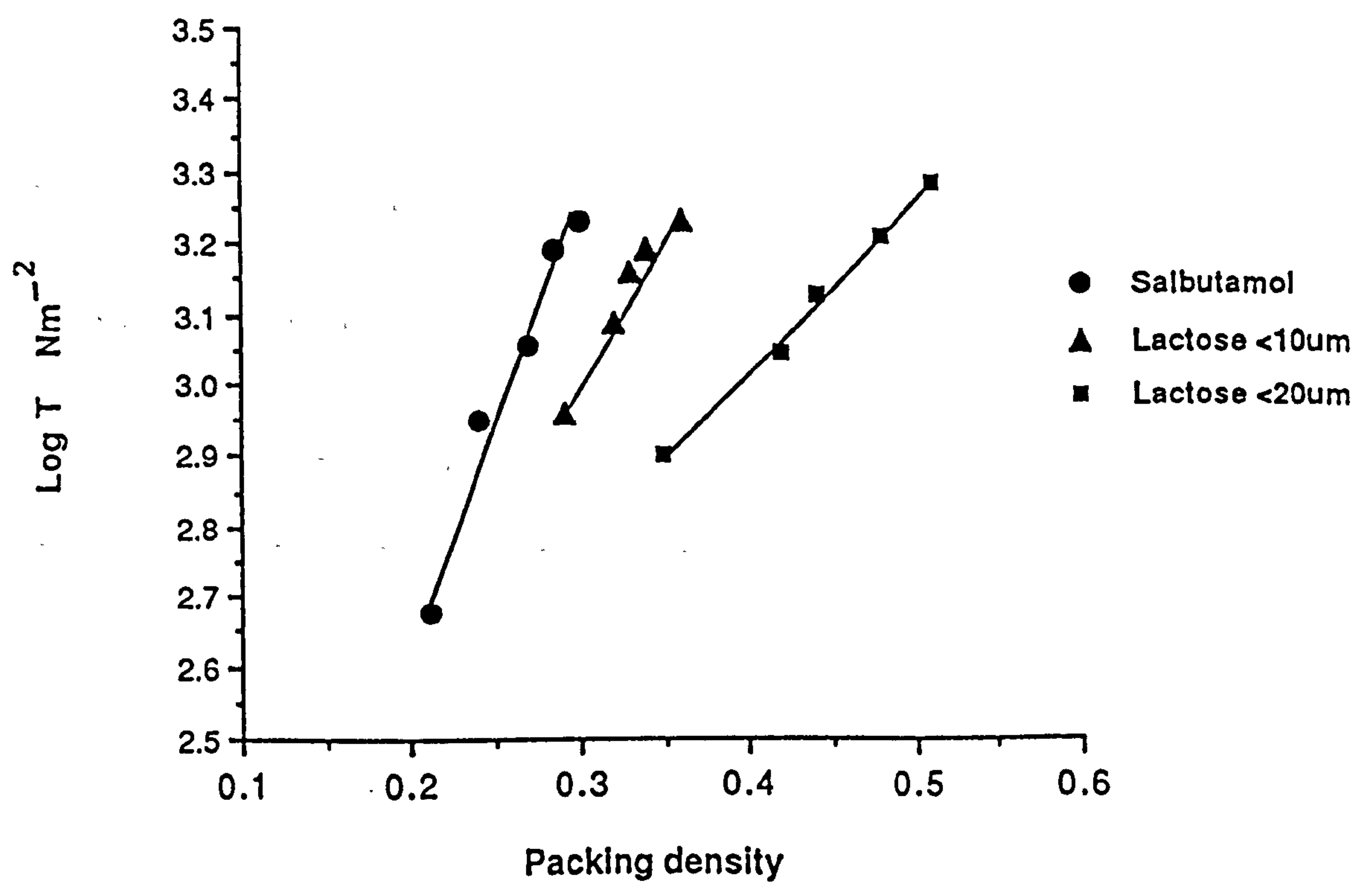


**Fig 3.1** The relation of Log tensile strength to packing fraction for three powder samples

**Table 3.1 The flow properties of the carriers**

Carrier	Flow rate( g/min)
Glass beads (60 $\mu$ m)	419.4
Milled glass (63-90 $\mu$ m)	291.0
Spray dried lactose (63-90 $\mu$ m)	120.0
Regular lactose (63-90 $\mu$ m)	125.2
Regular lactose (125-180 $\mu$ m)	183.0
Regular lactose (20-40 $\mu$ m)	25.7
Recrystallized lactose (60-90 $\mu$ m)	118.0

The determination of the specific surface area by the air permeation method employed a Fisher sub-sieve sizer which measures the ability of air to flow through a packed bed of powder. For a given pressure, flow will depend on the average pore diameter and the total interstitial surface, both characteristics being influenced by the rugosity of the material.

A mass of powder equal to its true density(P) is compressed to a known porosity in the cell of the Fisher sub-sieve sizer. The flow rate through the bed at a fixed pressure differential is transcribed by the instrument to an average particle diameter ( $d_m$ ). This diameter is derived from the specific surface area of the powder ( $S_o$ ) by the following equation:

$$S_o = \frac{6}{d_m P} \quad (3.3)$$

For the calculation of theoretical surface area from microscopic data, the following equations were used:

$$S = \pi d_s^2 \quad (3.4)$$

$$V = \frac{\pi d_v^3}{6} \quad (3.5)$$

where  $d_s$  is the diameter of a sphere having the same surface (S) as the particle and  $d_v$  is the diameter of a sphere having the same volume (V) as the particle.

These two equations can be applied to obtain the surface area ( $S_d$ ) by the relation:

$$S_d = S/V \times P_p \quad (3.6)$$

where  $P_p$  is the true density of the powder.

### **3.2.2 Preparation of capsules**

Blends of salbutamol sulphate and the carriers were prepared and examined by scanning electron microscopy. The mixtures were filled into hard gelatin capsules by the method described in Section 2.2.1.

### **3.2.3 Evaluation of powder aerosols**

Apparatus B, described and evaluated in Chapter 2, was used for the assessment of the dry powder aerosols at various flow rates. The "Rotahaler" was employed for cloud generation unless otherwise specified.

### **3.2.4 Determination of salbutamol sulphate deposited at various stages**

The fractional deposition pattern of salbutamol sulphate was determined by HPLC analysis as described in Section 2.2.2.

## **3.3 The effect of the external forces on the characteristics of an inspirable aerosol cloud**

During inhalation of a powder mixture, the separation force is provided by two components: the inspiratory flow rate and the turbulence created within the inhaler as air flows through it.

These two components are inter-related, i.e, the higher the flow rate, the greater is the turbulence within the inhaler. However, turbulence can also be increased by varying the construction of the inhaler.

In the following study these two components were investigated as follows:



### **3.3.1 Materials and methods**

#### **1. The effect of air flow rate**

To study the influence of the flow rate on the inspirable characteristics of the aerosol cloud, flow rates of 60, 100, 150 and 200 l/min were employed.

An air flow of 60 l/min was the lowest used as this is probably the minimum inspirational flow for an asthmatic patient through a "Rotahaler". Furthermore, lower flow rates may not produce adequate fluidisation of the powder bed within the inhaler. An air flow of 200 l/min was the maximum used since clinical studies have shown that this flow rate is attainable by mild asthmatics.

#### **2. The powder mixture**

Blends of micronized salbutamol sulphate ( $2.8\mu\text{m}$  MMD) and unclassified lactose prepared in a ratio of 1:67.5 were investigated.

### **Results and discussion**

In the following discussion the deposition pattern of salbutamol sulphate fractionated as described in Section 2.4.2 will be interpreted as follows:

The preseparator stage simulates the mouth and the oral cavity. Drug particles captured in this location are present either as drug agglomerates of aerodynamic diameter  $>10\mu\text{m}$  or as a drug adhering on the surface of the coarse carrier.

Stages 0 to 2 simulate capture by the upper respiratory tract. The drug recovered from these stages is either as agglomerates of 5- $10\mu\text{m}$  diameter or as a drug associated with carrier particles of  $<10\mu\text{m}$ .

Stages 3 to 7 simulate the lower part of the respiratory tract. Drug particles deposited on these stages are in the size range of 0.4-4.7 $\mu$ m and are described as respirable.

#### **The effect of air flow rate on the inspirable characteristics of a cloud**

The results of the effect of air flow rate on the drug deposition is shown in Figure 3.2. An increase in the flow rate resulted in an increase in the fraction deposited on stages 3 to 7. For instance at an air flow of 60 l/min, 13.2% of the drug was respirable, in comparison with 27.7% at an air flow of 200 l/min. On the other hand, the amount of drug recovered from the preseparator stage (Table 3.2) indicates that dissociation of the drug from the carrier surface is greater at high air speeds.

Similar results were observed by Kim *et al* (1985) who investigated the influence of air flow rate on the size distribution of sodium cromoglycate powder aerosol generated from a "Spinhaler". Despite the inaccuracy of the sampling technique they adopted, where samples of the aerosol cloud were anisokinetically collected by a cascade impactor, their results indicated that a finer cloud was generated at a flow rate of 80 l/min than at a 50 l/min. The importance of air flow rate lies in the ability of the air stream to create a high level of turbulence within the inhaler, thus breaking up the aggregates and agglomerates into singly dispersed particles that can penetrate deep into the lungs. Additionally, if the force provided by the drag and lift of the air stream on the adherent particles exceeds the force of adhesion, particle detachment from the carrier surface will occur.

**Table 3.2** The percentage of drug deposited at various stages at different flow rates using unclassified lactose as carrier

Flow rate (l/min)	Device	Preseparator	Stages 0-2	Stages 3-7
200	19.2	22.3	8.4	27.7
150	19.9	22.4	8.5	26.7
100	19.9	26.4	11.9	21.5
60	20.3	46.0	10.9	13.2

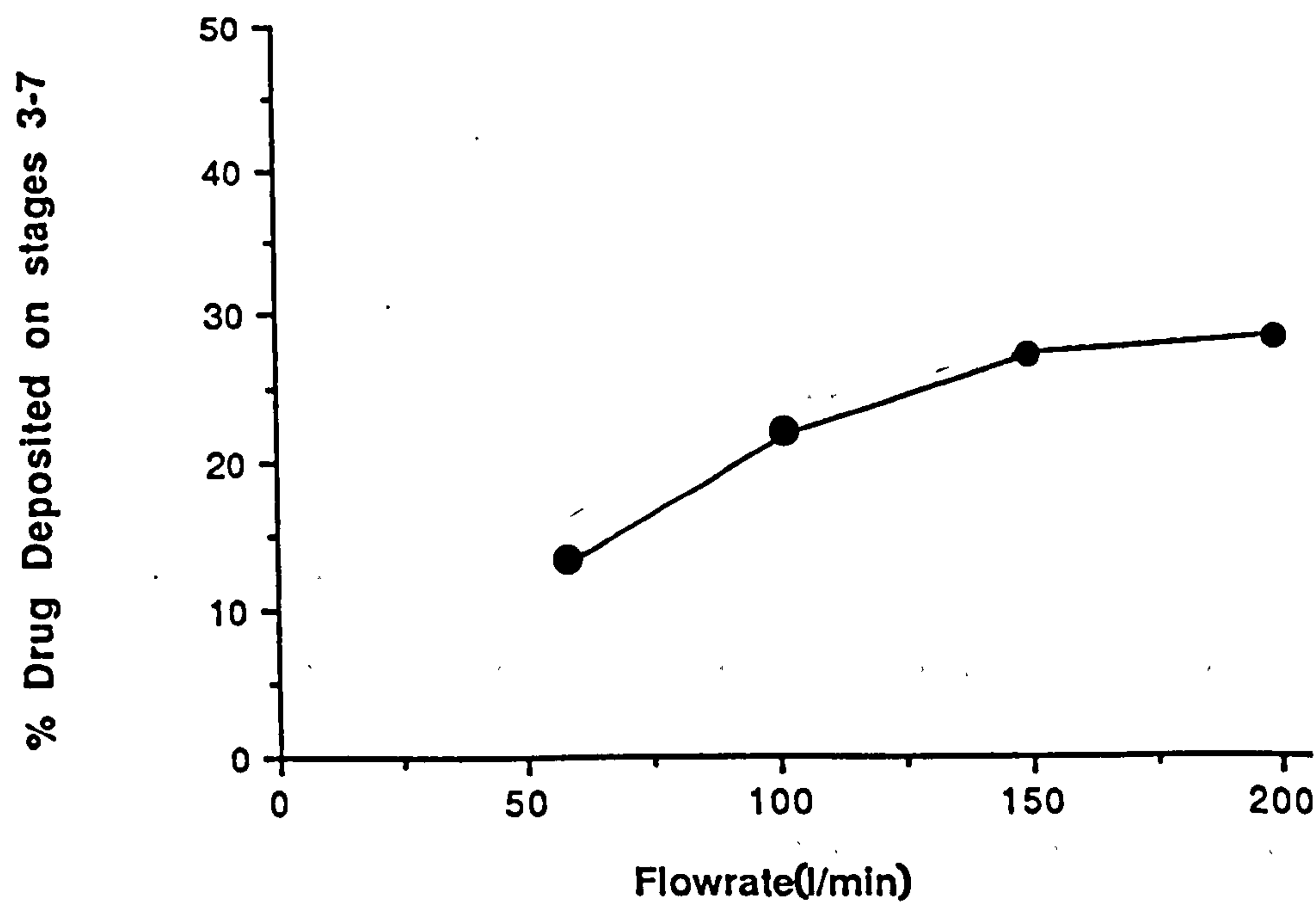


**Fig 3.2** Effect of airflow rate on the amount of drug deposited on stages 3-7 using unclassified lactose

The drag force directed on adherent particles will be determined by the particle size and air velocity employed according to the relation: (Corn & Stein, 1965)

$$F(\text{drag}) = CPV^2D_p^2/2 \quad (3.7)$$

where

C is the drag coefficient of particle

P is the air density

V is the air velocity

and  $D_p$  is the particle diameter

From this relation, it is obvious that high air velocities are needed to detach small adherent particles.

The effect of the air flow rate on the pattern of drug deposition will be illustrated throughout this chapter as all the formulation variables were evaluated at different flow rates. However, most of the subsequent experiments were conducted at 60 and 150 l/min since these two speeds represent a low and somewhat high inspirational efforts.

### 3.3.2 The effect of turbulence

The turbulence level can be increased within the inhaler without varying the air flow rate. In the following study the influence of turbulence was investigated when an aerosol cloud was generated at 60 l/min.

To vary the turbulence as air flows through the inhaler at a constant speed, an inhalation device was designed in a way which facilitates the introduction of nozzles of different diameters and the insertion of grids at different positions. The inhaler is depicted in Figure 3.3.



It consists of a tube with an internal nozzle. A capsule containing a unit dose can be inserted at the end of the inhaler.

#### **The powder mixture**

Blends of salbutamol sulphate ( $2.8\mu\text{m}$  MMD) and lactose ( $63\text{-}90\mu\text{m}$ ) prepared in a ratio of 1:67.5 were investigated.

#### **1. Change in nozzle diameter**

Using the above inhaler to generate the aerosol cloud, it was possible to change the nozzle diameter thus varying the turbulence. Experiments were conducted using nozzles of 20, 15, 12, 10 and 5mm internal diameter. Dispensing of the powder aerosol was performed by sealing the capsule after filling and inserting a thin needle vertically within it. As the end of the inhaler containing the capsule was turned, the needle passing through the body of the capsule was pushed against a shaft within the inhaler causing the bottom of the capsule to break. This procedure was essential to prevent the capsule half containing the powder from being carried by the air stream or blocking the narrow nozzles. The level of turbulence within the nozzles was estimated by Reynold's Number.

#### **2. Grid inserts**

The use of grids or screens is the most common means of inducing turbulence in wind tunnels (Wiener *et al*, 1988). In the following study, grids of 1.0mm and 0.5mm mesh spacing were inserted into the inhaler at position A, B or A and B as shown in Figure 3.3b. Experiments were conducted using nozzle diameters of either 5.0 or 10mm.

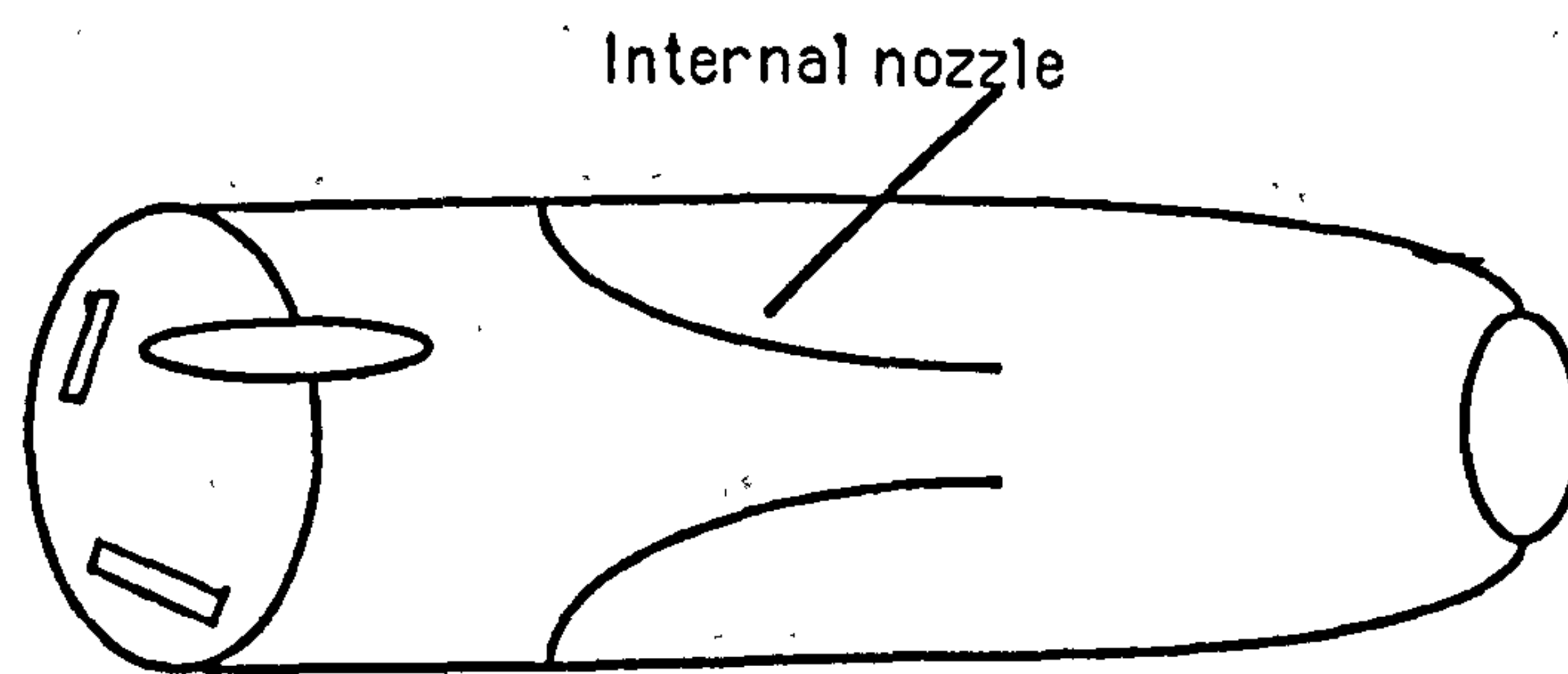


Fig 3.3 a. Designed inhaler

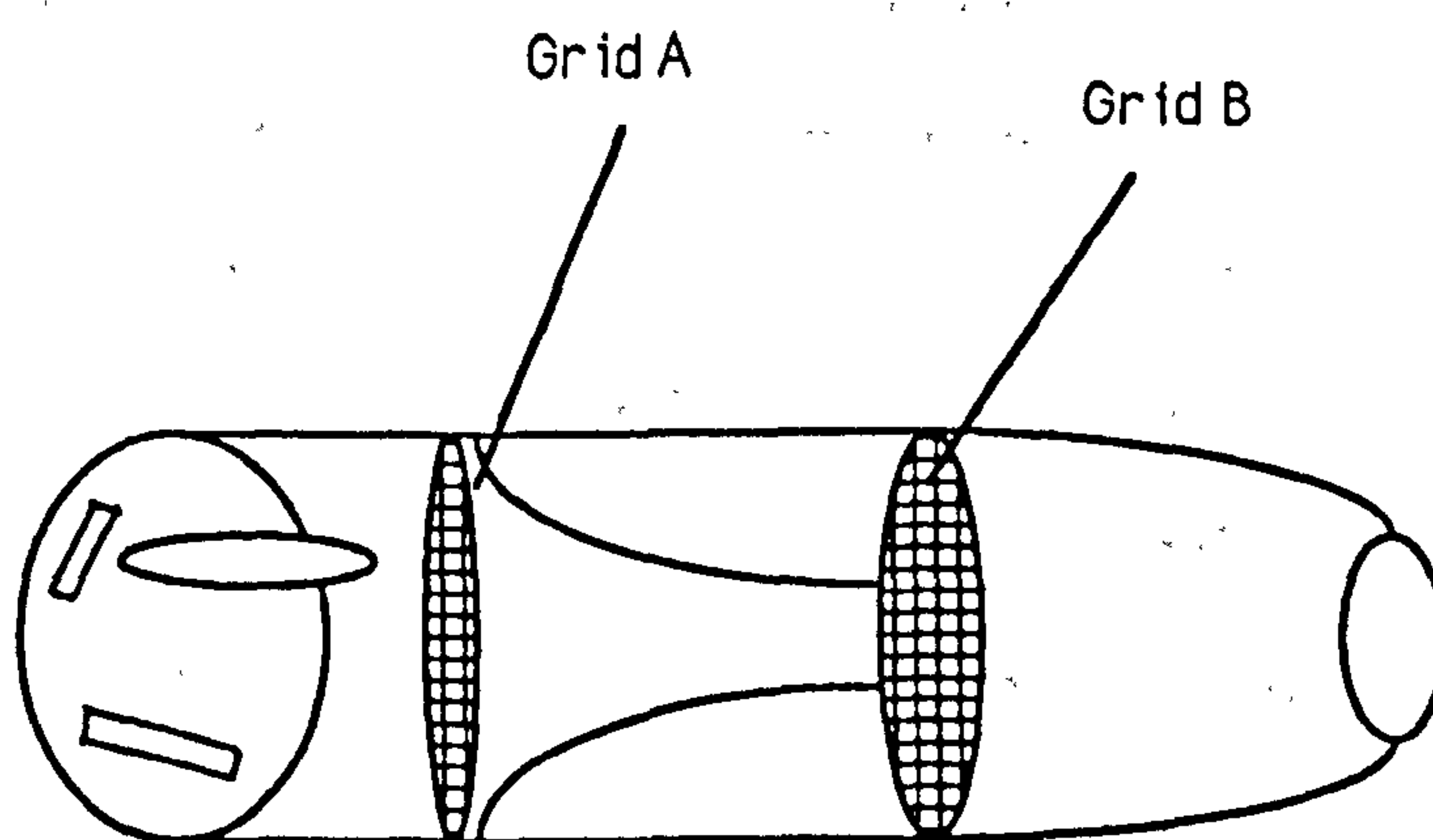


Fig 3.3 b. Inhaler with grids inserted

When a grid was inserted at position A or A and B, dispensing was performed by turning one end of the inhaler which contains the encapsulated dose, separating the capsule into two halves. The part containing the powder dropped into a chamber where it was retained by the grid and the powder was dispensed into the air stream through the nozzle. However, when a grid was inserted at position B, dispensing of the powder was performed as described in the above section to hinder blocking of the narrow nozzles. As air flows through the inhaler, the powder was dispensed to the nozzle and passed through the grid into the air stream.

### **3. The resistance to air flow**

The pressure drop created by the inhaler at all the above configurations was measured using a mercury manometer to determine the resistance of the inhaler to airflow.

### **Results and discussion**

The effect of the different levels of turbulence generated by changing the nozzle diameter on the pattern of drug deposition at various stages is shown in Table 3.3. The pressure drop created by the inhaler at these configurations is also given.

An increase in turbulence resulted in a relatively small increase in the respirable fraction as the nozzle diameter was reduced from 20 to 10mm. When a nozzle of 20mm was used, 1.9% of the drug deposited on stages 3 to 7 compared to 4.9% with a nozzle diameter of 10mm. However, when the nozzle diameter was further reduced to 5mm, 11.3% of the drug was recovered from stages 3 to 7. The amount of drug deposited in the preseparator stage was

inversely related to Reynold's Number. As for the amount of drug retained in the inhaler, a slightly higher amount was recovered with the smaller nozzle diameters. Moreover, the reduction in the nozzle diameter was accompanied by a noticeable rise in the pressure drop created by the inhaler as air flows through it. The pressure drop increased from 0.09 kPa to 1.53 kPa when the nozzle diameter was reduced from 20mm to 5mm, respectively.

Turbulence is directly related to air velocity. In the above experiment the higher air velocities were achieved by decreasing the cross-sectional area of the air channels as air flows at a constant rate of 60 l/min. Therefore, the degree of turbulence is dependent upon the internal dimensions of the inhaler.

The above results indicated that the increase in turbulence provided more effective de-aggregation of the powder mixture. This agrees with the findings of Vidgren *et al* (1987) who demonstrated that the narrower the air channels within inhalation devices, the more efficient is the drug deposition in the respiratory tract. Therefore, a further reduction in the internal dimensions of the inhaler might additionally improve the efficiency of a dry powder aerosol. However, this will lead to an increase in the resistance of the inhaler to air flow and thus to a difficulty to inhale through it at a flow rate which produces optimum drug delivery.

This problem is of great importance particularly with some patients such as children and severe asthmatics. Therefore, there is a need to design an inhaler which provides high levels of turbulence without further increase in the resistance to air flow. This can be achieved by introducing grids of varying mesh size by the way described in Section 3.3.2.



**Table 3.3 The effect of different levels of turbulence generated by changing the nozzle diameter on the pattern of drug deposition at various stages**

% Drug deposition at various stages						
Nozzle diameter (mm)	Reynold's Number	Pressure drop (kPa)	Device	Preseparator	Stages 0-2	Stages 3-7
20	4240	0.093	12.3	85.1	1.0	1.9
15	5660	0.113	8.1	85.8	2.1	3.9
12	7080	0.120	10.3	80.8	0.7	5.1
10	8500	0.147	17.5	78.1	0.6	4.9
5	17000	1.53	15.7	71.9	1.0	11.3

The results of introducing grids are illustrated in Tables 3.4 and 3.5. Inserting grids of 0.5mm and 1.0mm mesh spacing at positions A, B or A and B resulted generally in an increase in the respirable fraction. However, the increase depended on the position of the grids and the size of the mesh. When an inhaler of a 10mm nozzle diameter with the grid inserted at position A was used, a slight increase in the respirable fraction was observed with both the 0.5 and 1.0mm mesh spacing grids (Table 3.4). However, a greater increase in the amount of drug deposited on stages 3 to 7 was noticed when a grid of 0.5mm mesh spacing was inserted at position B. Without a grid, 4.9% of the drug was recovered from stages 3 to 7 in comparison with 11.3% when a grid was inserted at position B. Insertion of grids at positions A and B produced similar results as when the grid was inserted at position B.

When an inhaler of 5.0mm nozzle diameter was used, comparable results as those observed with the 10mm nozzle inhaler were obtained. However, a higher amount of the drug was recovered from stages 3 to 7 (Table 3.5). The major increase in the respirable fraction was observed with the grid inserted at position B; 30% and 50% of the drug deposited on stages 3 to 7 with the 1.0mm and 0.5mm mesh spacing grids, respectively in comparison with 11.3% without a grid and 15% with a grid inserted at position A.

Similar results were obtained when two grids were inserted in the inhaler indicating that the grid at position A had no appreciable effect on the respirable fraction. Additionally, the use of two grids in the inhaler did not contribute to a further increase in the respirable fraction.

The increase in the respirable dose was always associated with a

decrease in the amount of drug recovered from the preseparator stage, indicating a greater dissociation of the drug from the carrier surface. The data in Table 3.5 also indicate that more drug was retained in the inhaler as a result of inserting the grids, particularly at position B or A and B. When an inhaler without a grid was used, 15.7% of the drug was recovered from the inhaler in comparison with 34%, when grids were inserted at these positions.

Therefore, the results suggest that the level of turbulence has increased within the inhaler and was dependent upon the position of the grids and the mesh spacing. Higher turbulence was created with the grid inserted after the nozzle (position B), particularly with the 0.5mm mesh spacing; a respirable fraction of up to 50% was obtained. In contrast, the grid at position A induced only a slight increase in turbulence.

The turbulence produced by the grids was generated through the work done by the air stream against the drag imposed by the grid elements. This type of turbulence is known to be homogenous (Wiener *et al*, 1988). However, although the bar width was smaller with the 0.5mm mesh spacing grid, the turbulence generated was higher. This might be attributed to the larger number of elements composing the grid.

Therefore, the high retention of the drug in the inhalation device observed can be explained in terms of increased contact between the powder mixture and the walls of the inhaler due to turbulence and eddy effects and also the availability of additional surfaces.

From these results it can be concluded that the turbulence created by the inhalation device is of great importance in generating highly inspirable clouds. Turbulence results in a reduction in the laminar

**Table 3.4 Effect of inserting grids of various mesh spacing at different positions within the inhaler of 10mm nozzle diameter on the percentage drug deposition at various stages**

**Grid at position A**

Grid mesh spacing (mm)	Pressure drop (kPa)	Device	Preseparator	Stages 0-2	Stages 3-7
1.0	0.147	20.4	76.1	0.5	5.9
0.5	0.147	22.8	70.4	0.7	6.1

**Grid at position B**

Grid mesh spacing (mm)	Pressure drop (kPa)	Device	Preseparator	Stages 0-2	Stages 3-7
1.0	0.147	23.4	69.0	0.9	6.8
0.5	0.147	18.5	70.0	0.0	11.3

**Grid at position A and B**

Grid mesh spacing (mm)	Pressure drop (kPa)	Device	Preseparator	Stages 0-2	Stages 3-7
1.0	0.147	24.2	69.0	0.0	8.4
0.5	0.147	23.0	63.4	1.3	13.0



**Table 3.5 Effect of inserting grids of various mesh spacing at different positions within the inhaler of 5mm nozzle diameter on the percentage drug deposition at various stages**

**Grid at position A**

Grid mesh spacing (mm)	Pressure drop (kPa)	Device	Preseparator	Stages 0-2	Stages 3-7
1.0	1.53	22.1	66.0	1.3	10.5
0.5	1.53	23.9	61.1	0.0	15.0

**Grid at position B**

Grid mesh spacing (mm)	Pressure drop (kPa)	Device	Preseparator	Stages 0-2	Stages 3-7
1.0	1.53	32.0	38.0	0.0	30.0
0.5	1.53	34.4	14.1	0.8	50.5

**Grid at position A and B**

Grid mesh spacing (mm)	Pressure drop (kPa)	Device	Preseparator	Stages 0-2	Stages 3-7
1.0	1.53	35.0	39.1	0.4	27.6
0.5	1.53	31.3	23.0	0.0	49.9

sublayer at the drug-carrier interface to overcome the interparticulate adhesion forces, resulting in the adherent particles becoming detached.

However, the most interesting observation is that the insertion of grids within the inhaler at different positions, and with varying mesh spacing, did not contribute to a further increase in the pressure drop. This indicates that turbulence can be maximized without an increase in the resistance of the inhaler to air flow.

Therefore, on the basis of this study an inhaler was designed to generate a deeply inspirable aerosol cloud with a minimum effort on the part of the user.

### **3.4 The effect of the adhesion properties of a powder mixture on the characteristics of an inspirable aerosol cloud**

Since the drug and the carrier are normally the only constituents of dry powder aerosols, the formulation might be improved by modifying the relationship between these two components. The following study explored the influence of the factors affecting the adhesion characteristics when such powder mixtures are fluidised for inhalation.

These factors include:

#### **3.4.1 The effect of carrier surface properties**

The surface properties of a carrier play an important role in the adhesion tendency of drug particles (Staniforth *et al*, 1982). Carriers which possess a more porous, rough surface could form stronger interparticulate forces due to the entrapment of the fine drug particles within the surface clefts and indentations. In dry

powder aerosols the penetration of the drug particles into the lungs is largely influenced by the strength of the interparticulate forces.

The stronger the forces the lower the redispersion of the drug from the carrier surface. Therefore, a range of carriers with different surface textures were selected to study the influence of the surface properties on the inspirable characteristics of a cloud.

Particle engineering, which can be defined as the physical or chemical modification of a solid to produce a desired physico-mechanical properties, may also be utilized to produce carriers with different surface properties. Crystallization is the most useful method which yields a wide variety of physical forms with identical chemical properties. Therefore, an attempt was made to produce lactose particles with a surface smoother than that of the commercially available lactose.

## **Materials and methods**

### **1. Crystallization of lactose**

Lactose monohydrate was crystallized under controlled conditions so as to favour the production of crystals having low degree of rugosity. A saturated solution of lactose in water (2:1) was prepared. A water immiscible organic solvent hexane (reagent grade) was added in a proportion 1.5 times the volume of the saturated solution. The mixture was agitated at 500 rpm with a paddle. Acetone (reagent grade) which is miscible with both solvents was then added to the mixture in a proportion which was 5% of the total volume of the other solvents. The partially miscible mixture formed was stirred for 8 to 12 hours during which lactose crystals were produced. After crystal growth, the particles were

filtered and washed with acetone to remove excess mother liquor. The particles were then washed with 60% ethanol/water mixture to reduce the quantity of the very fine particles present and with pure ethanol to facilitate quick drying. The crystals were dried in an oven at 100°C and stored in a vacuum desiccator over silica gel.

## **2. The powder mixtures**

Blends of salbutamol sulphate (2.8 $\mu$ m MMD) and glass beads, milled glass, regular lactose, spray dried lactose or recrystallized lactose, prepared in a ratio of 1:67.5, were investigated.

## **3. Flow rate**

Experiments were conducted at air flow rates of 60 and 150 l/min.

## **Results and discussion**

### **1. Scanning electron microscopy**

Representative photomicrographs of the surface details of glass beads, milled glass, regular lactose and spray dried lactose are shown in Figure 3.4. A marked difference in the surface morphology of the different carriers is illustrated. The spherical glass beads possess the smoothest surface. Milling the glass beads produced regularly shaped particles with some surface discontinuities. However, this surface appears relatively smooth and non-reentrant in comparison with regular lactose. The spray dried lactose showed some fairly large surface cavities. However, the crystallisation of lactose produced particles of smooth appearance with no pores or irregularities when compared to



regular lactose (Figure 3.5).

The surface roughness of the carriers increased in the order:

glass beads < milled glass < recrystallised lactose < regular lactose < spray dried lactose.

## **2. Surface roughness (rugosity)**

The rugosity values for the different lactose carriers is given in Table 3.6.

The rugosity increased in the order:

recrystallised lactose < regular lactose < spray dried lactose.

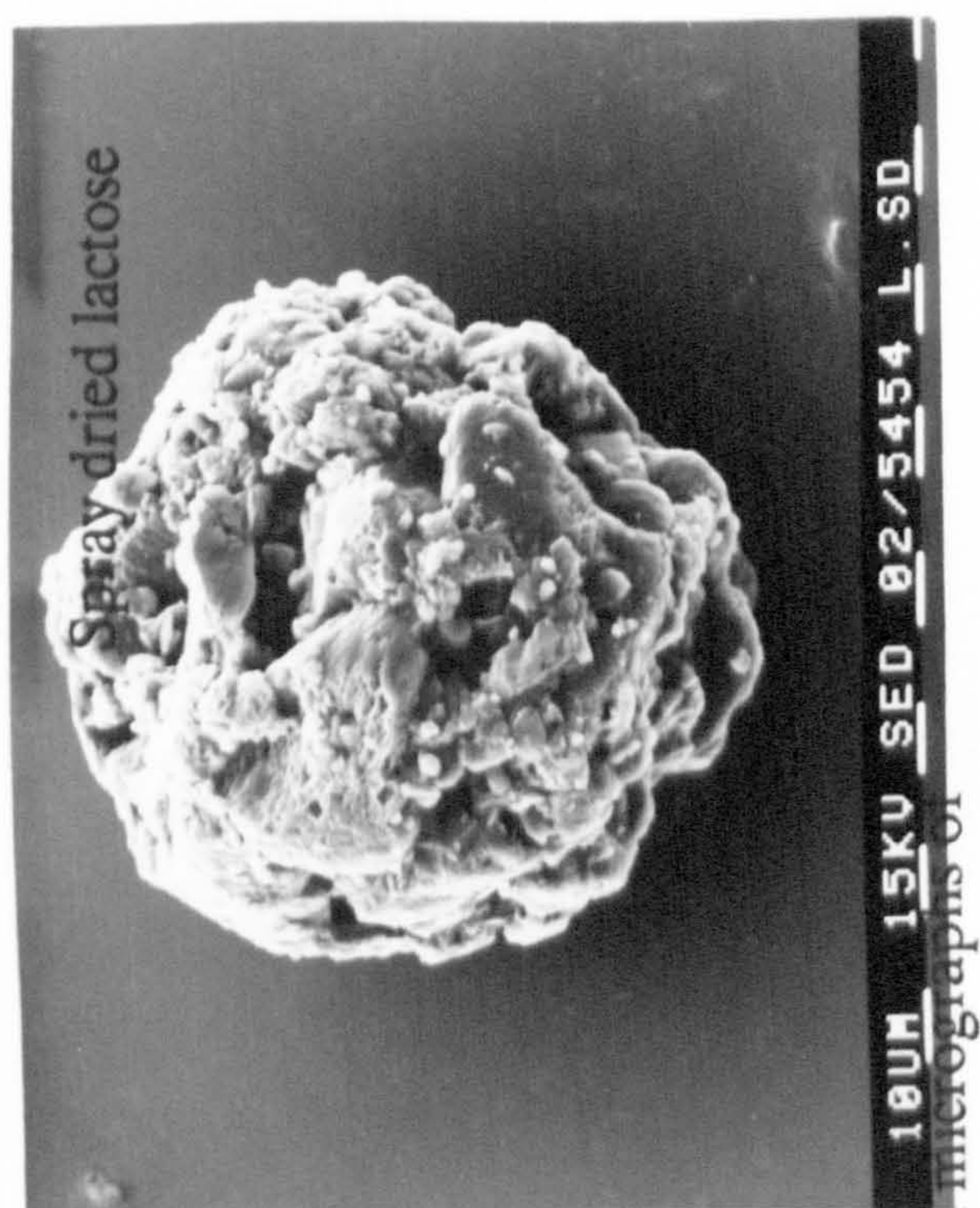
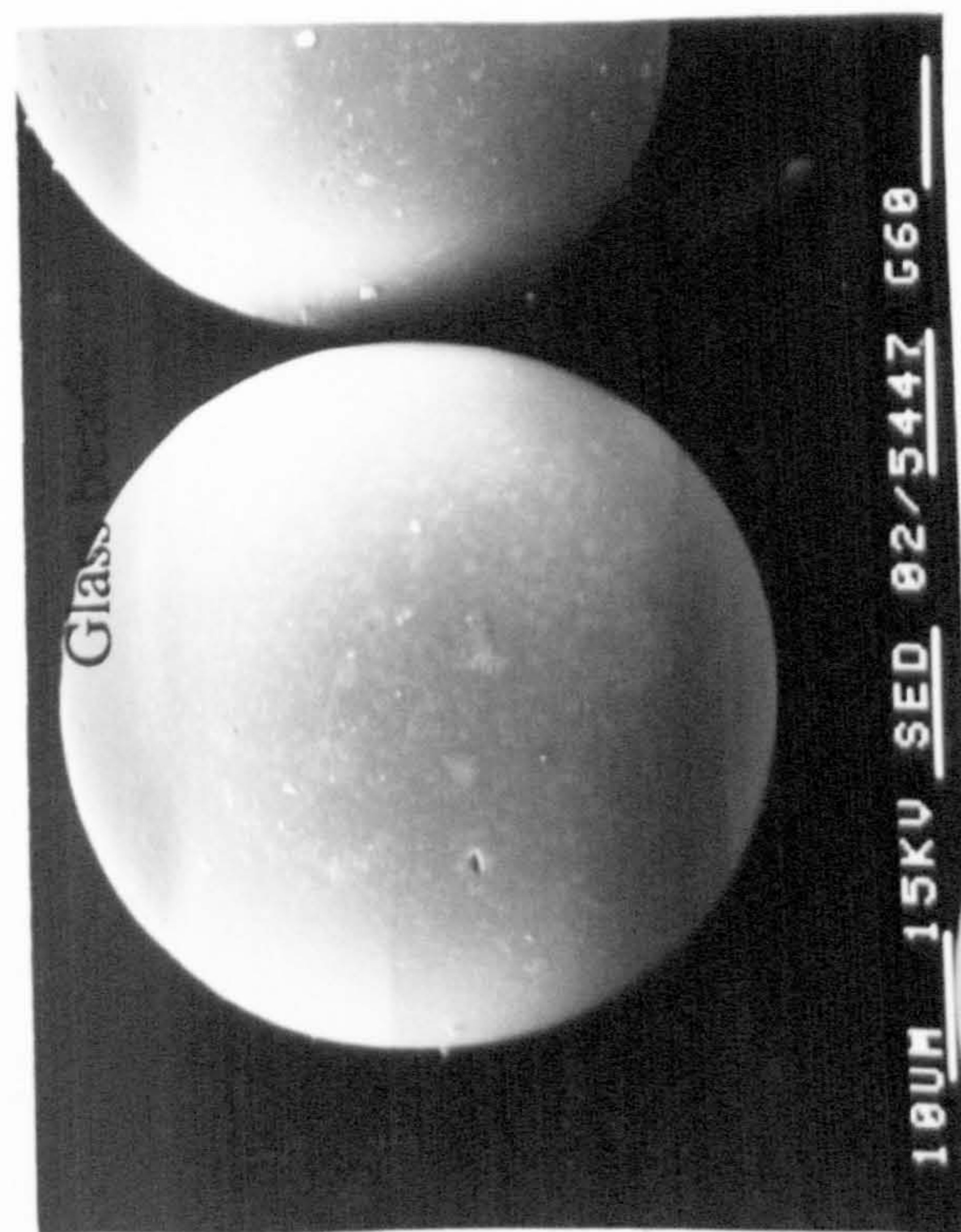
## **3. The effect of surface properties on the characteristics of an inspirable cloud**

The results given in Figures 3.6 and 3.7 show that the change in the surface properties of the carrier has a great influence on the pattern of drug deposition.

The influence of the air flow rate on drug deposition with all carriers is also illustrated. At 150 l/min higher deposition on stages 3 to 7 was observed. Additionally, emptying the inhaler was more efficient at this flow rate compared to that at 60 l/min.

A great variation in the amount of drug retained in the inhaler was also observed between the different carriers. When the spherical glass beads were used as a model carrier in the powder mixture, the amount of drug retained in the inhaler was significantly higher compared with the other carriers investigated. This phenomenon can be explained in terms of the difference in surface morphology. The adhesion of the fine drug particles to the glass beads which have no surface irregularities or a pore structure to entrap the







Glass beads

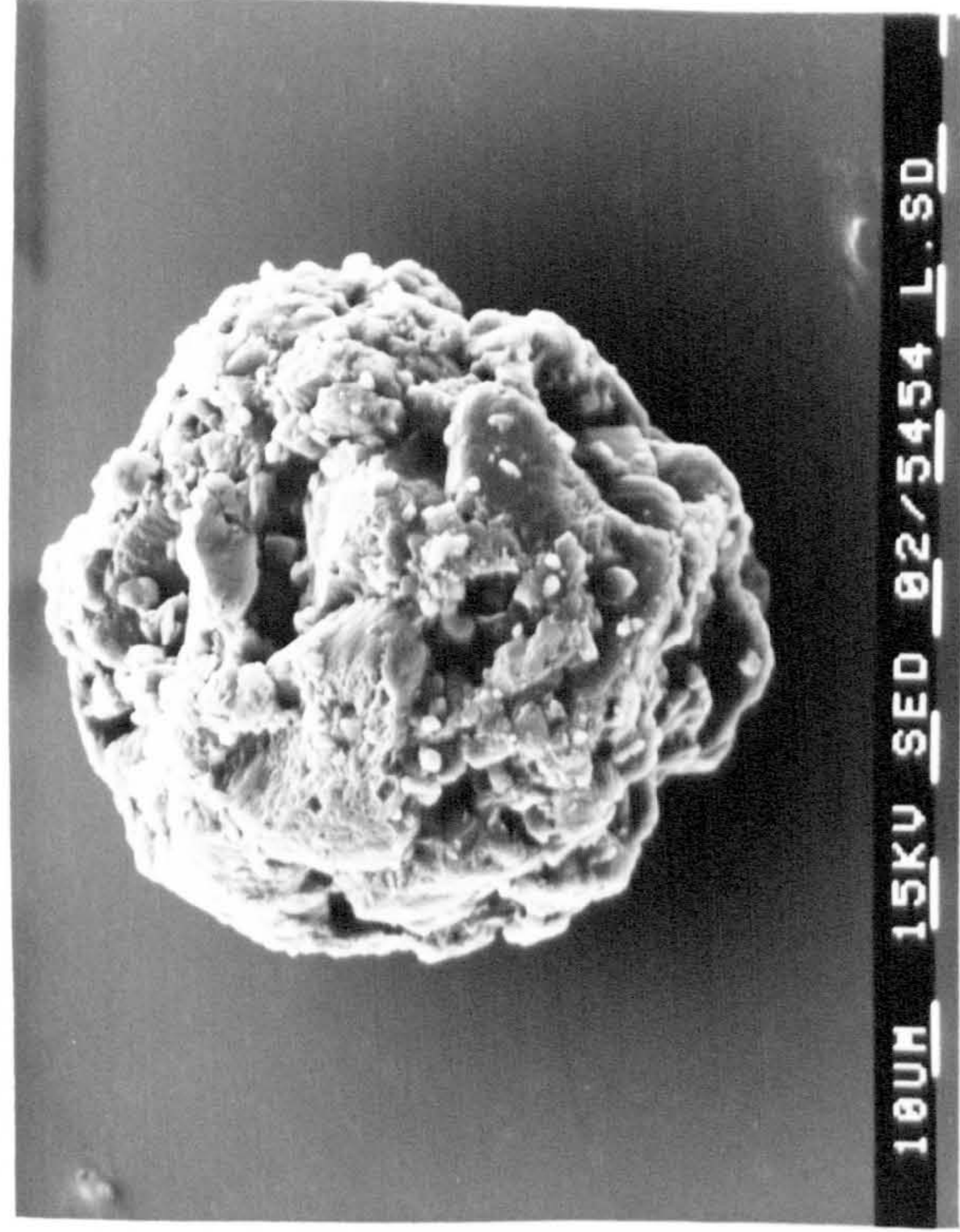
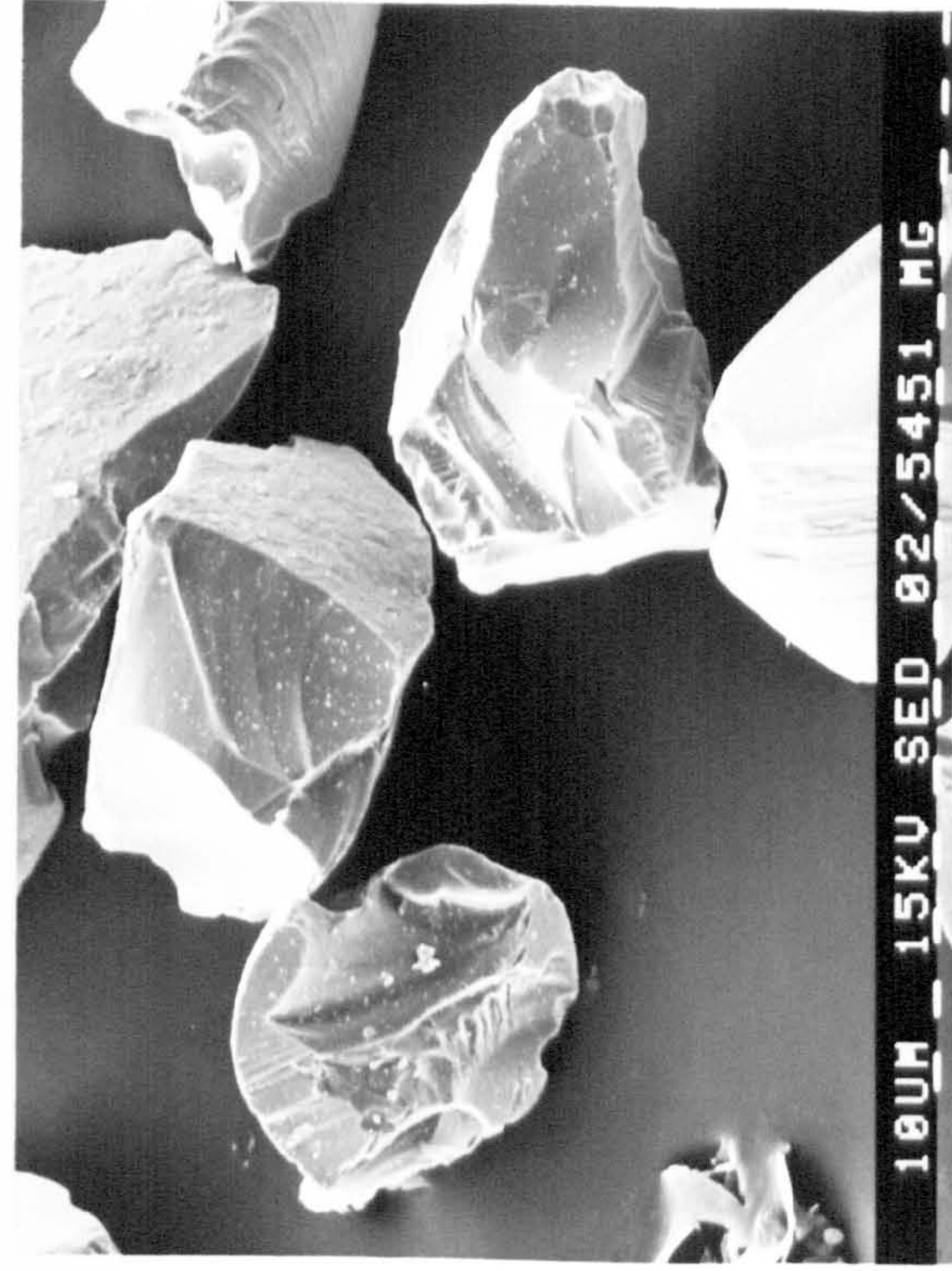
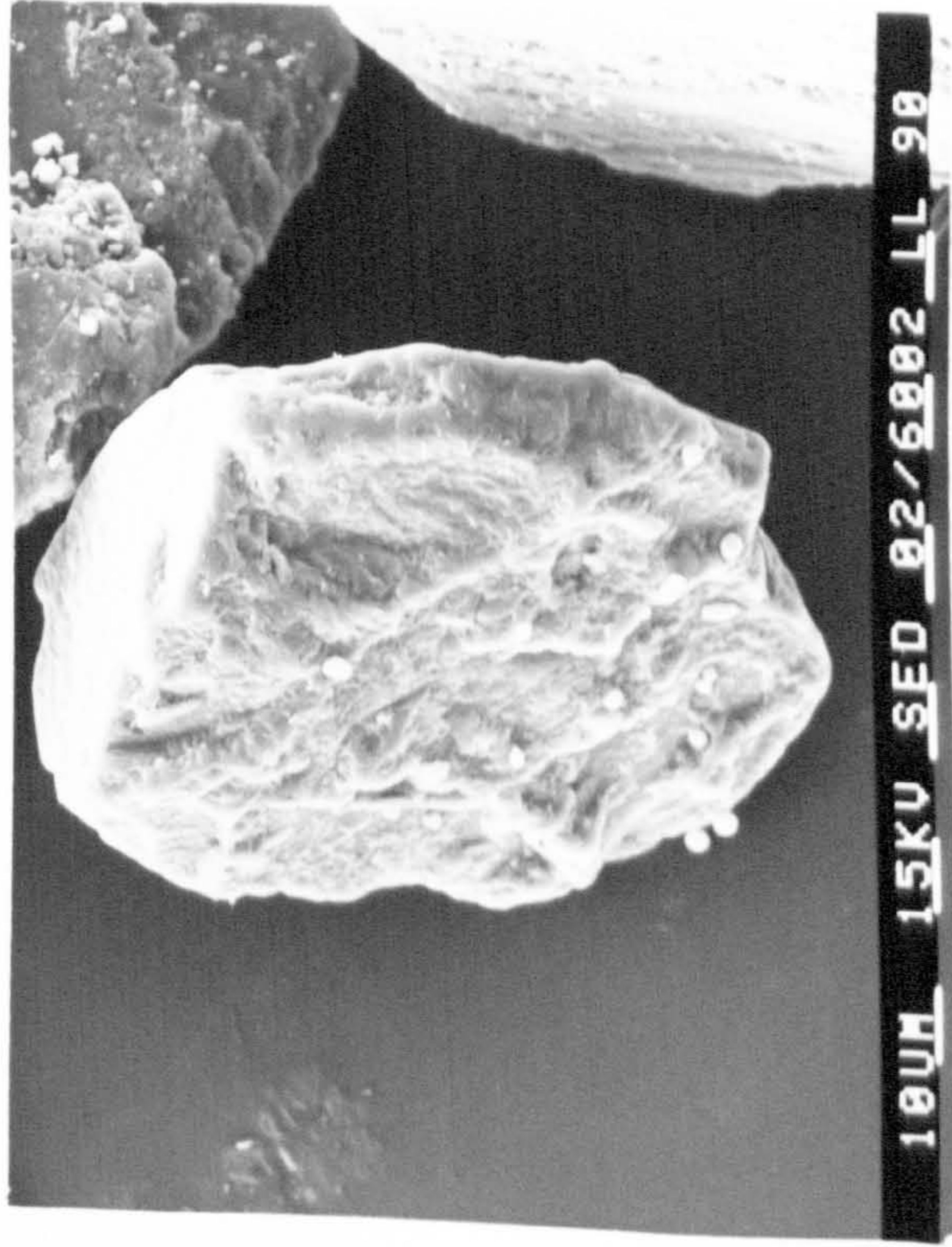
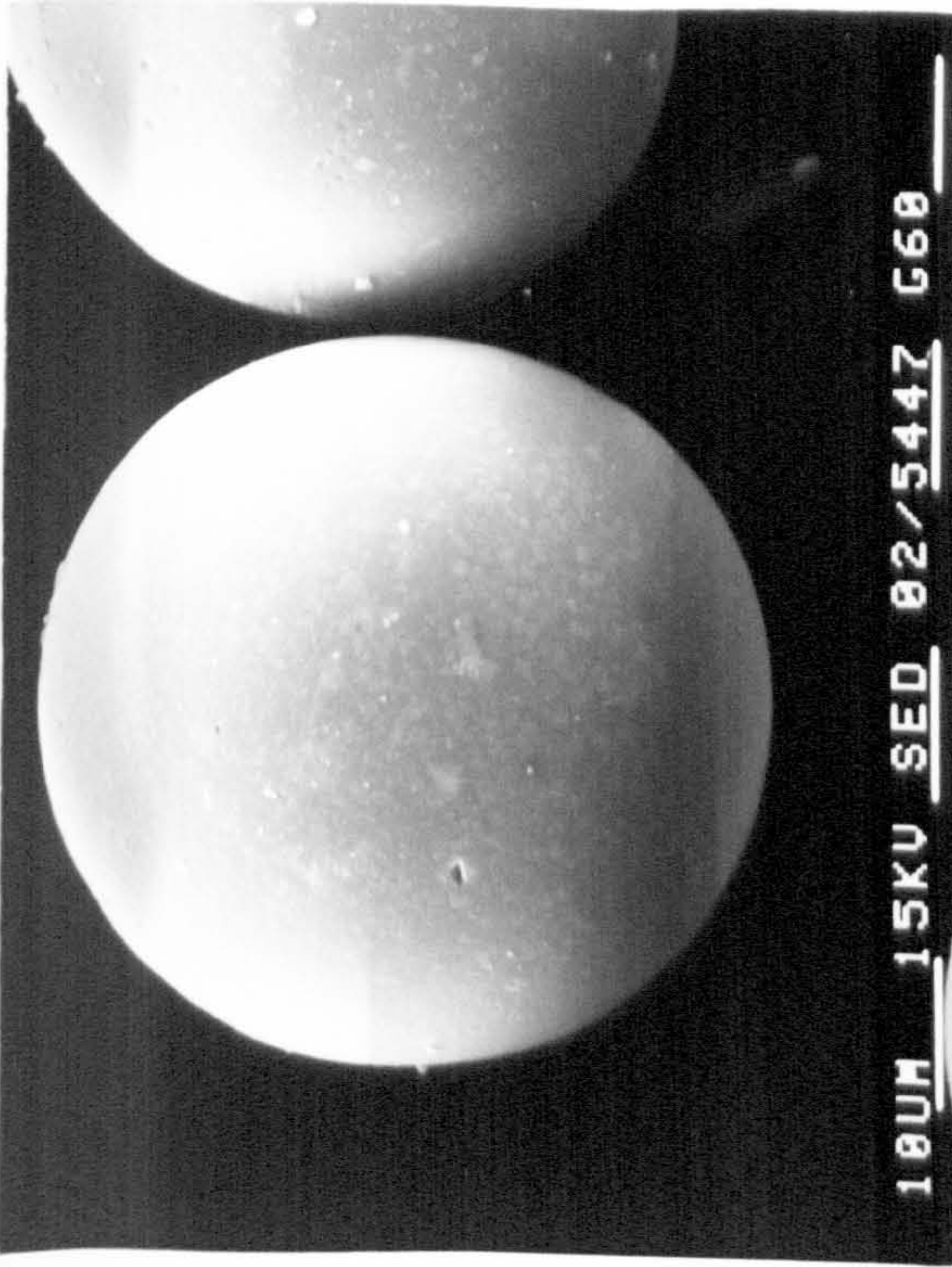
Milled glass

Regular lactose

Spray dried lactose

Fig 3.4 Scanning electron micrographs of







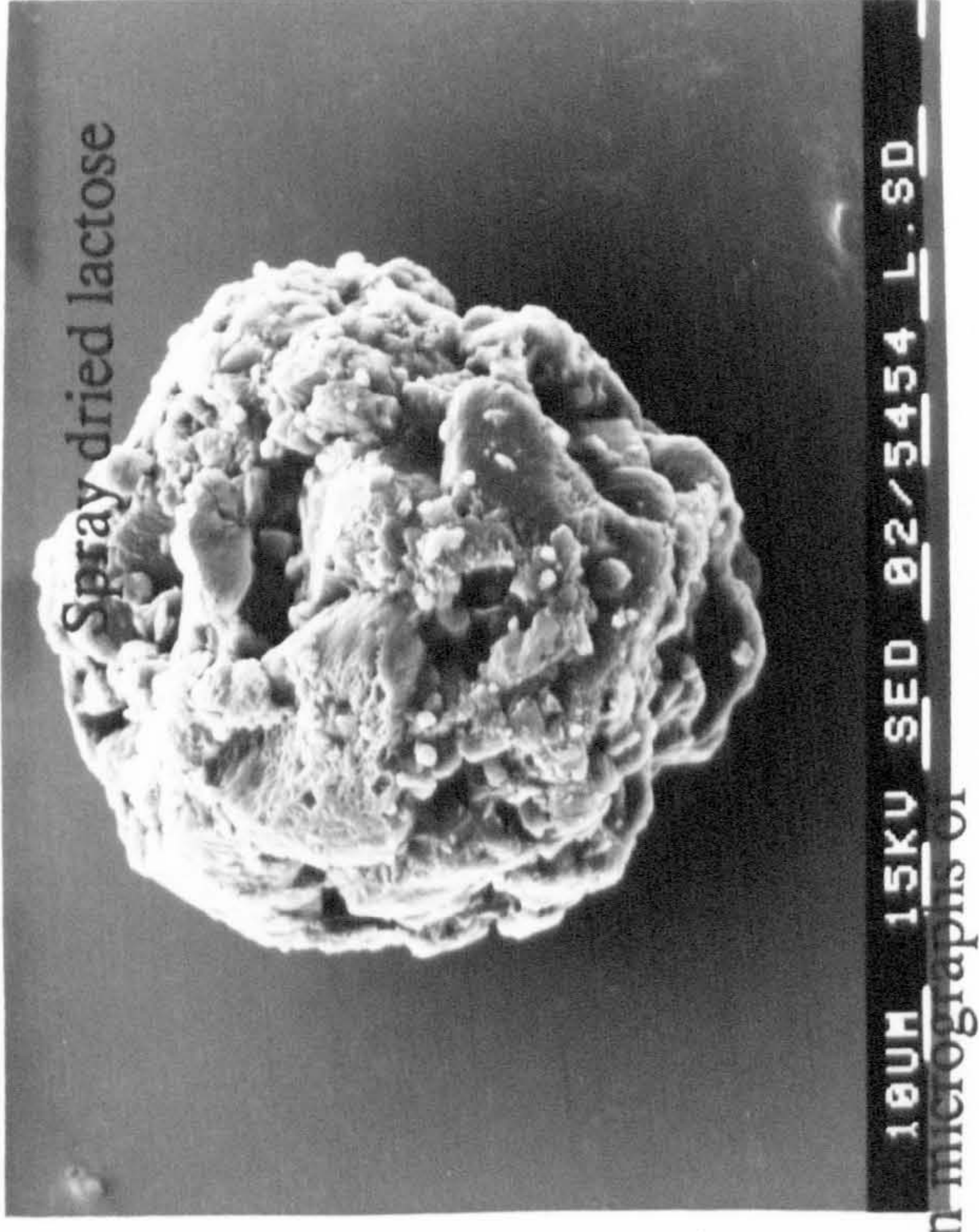
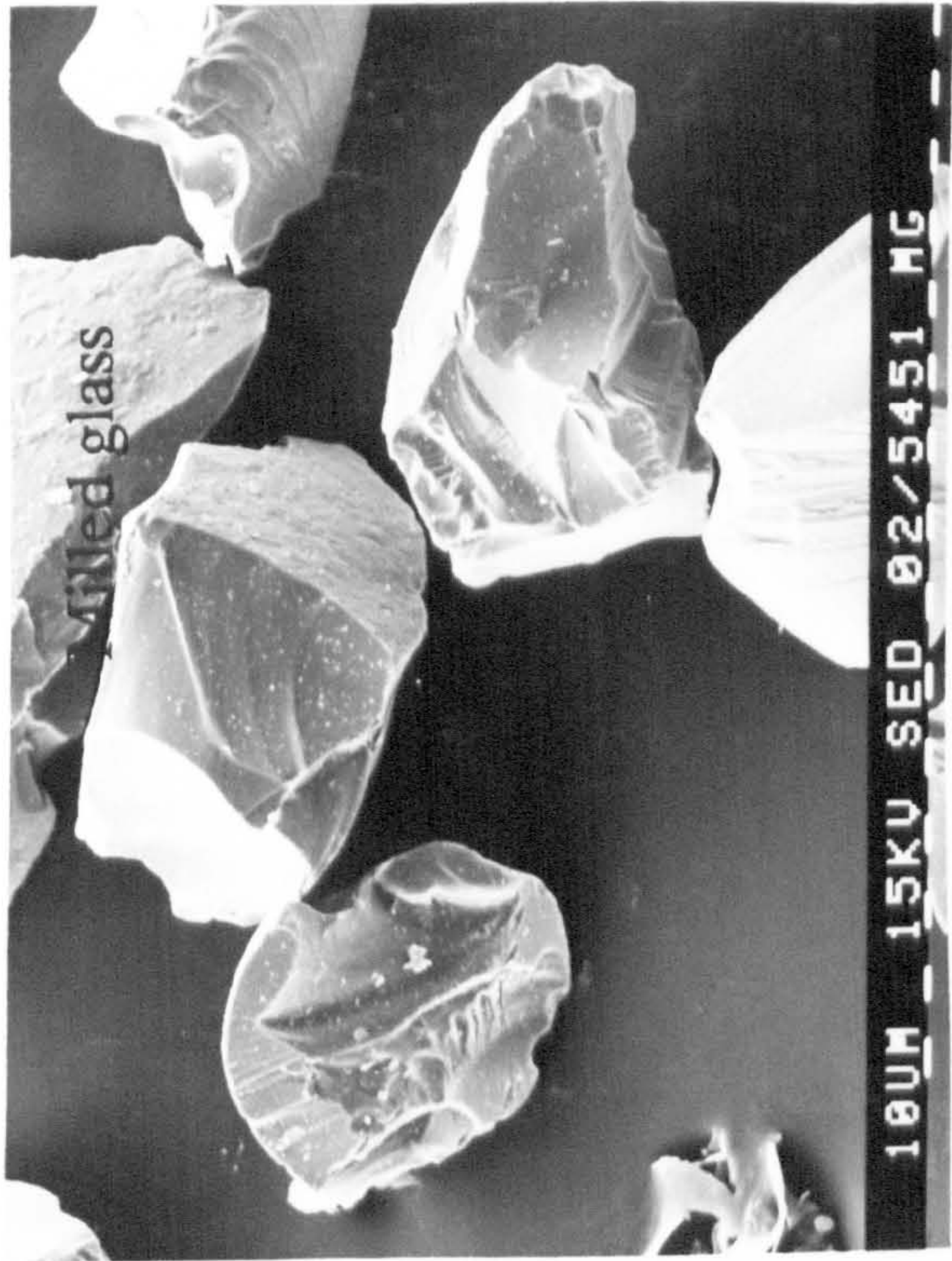
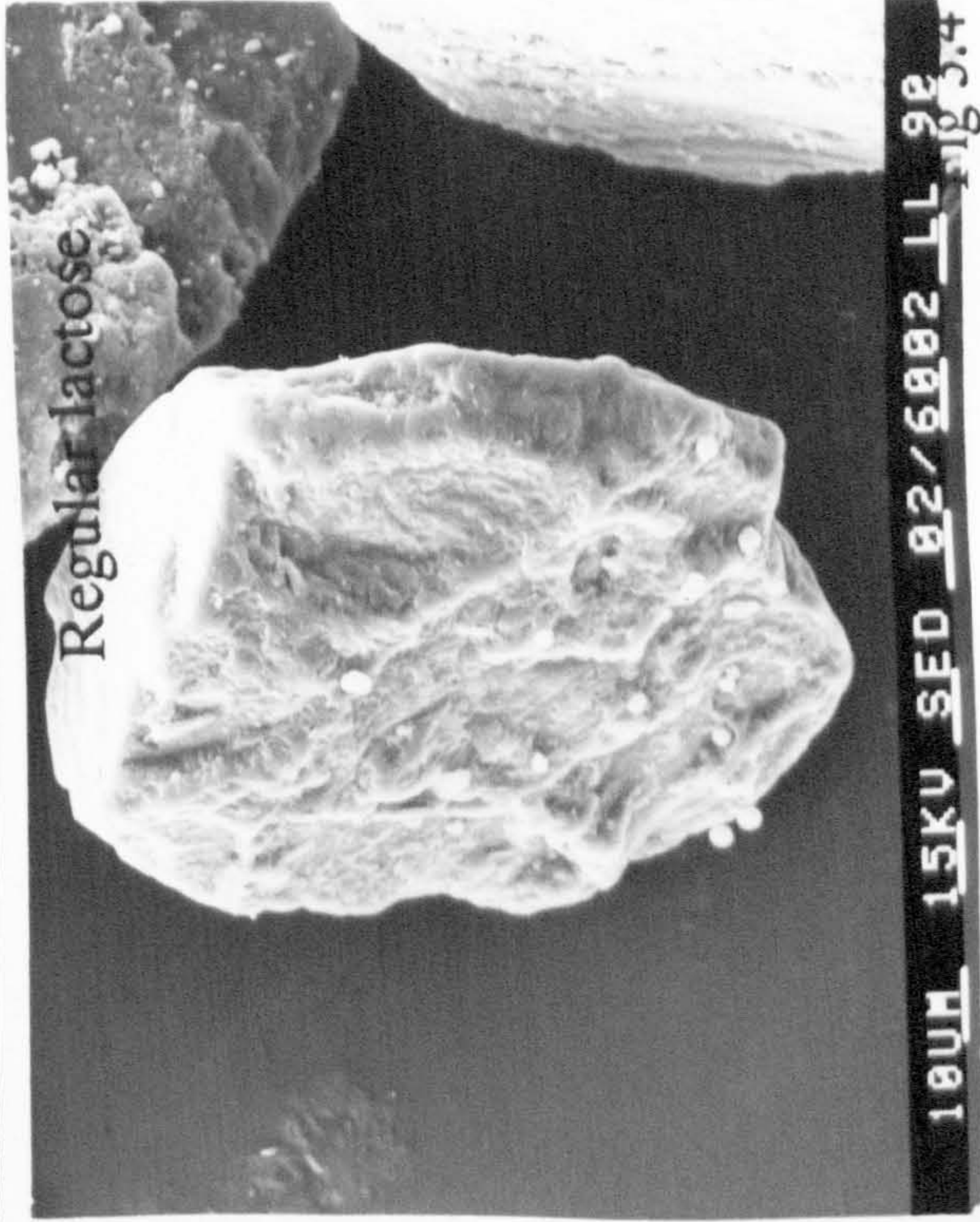
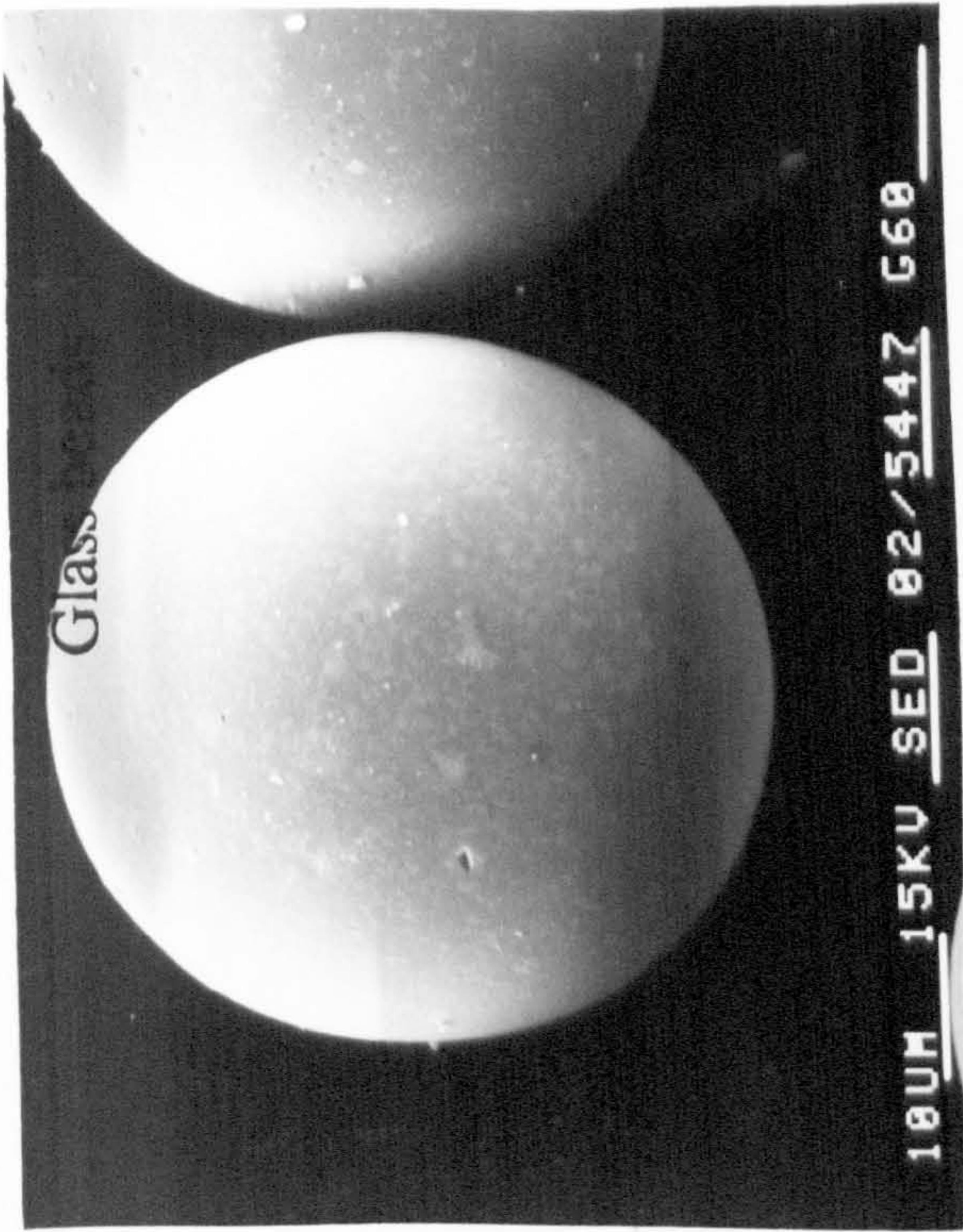


Fig 3.4 Scanning electron micrographs of



Regular lactose

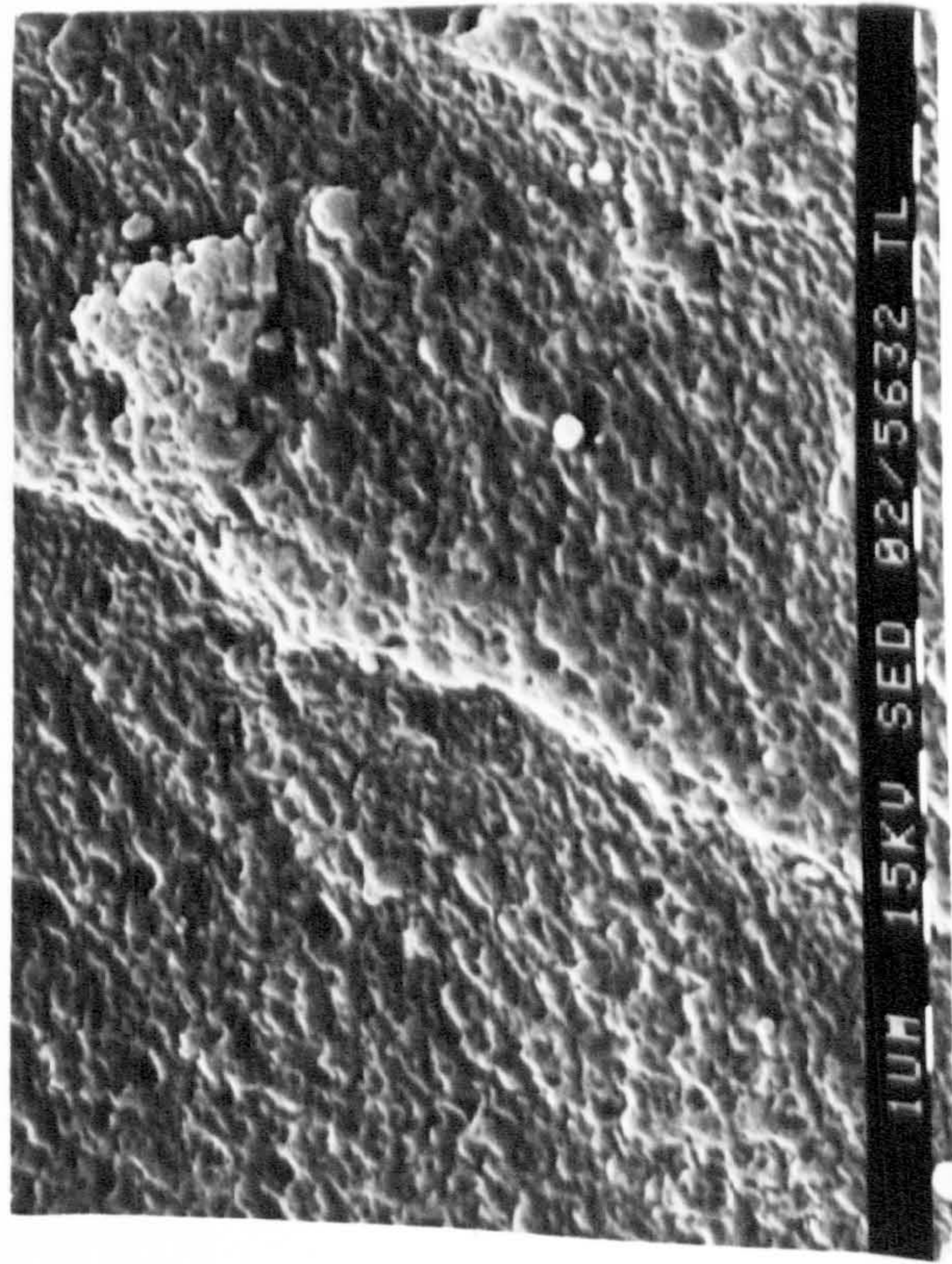
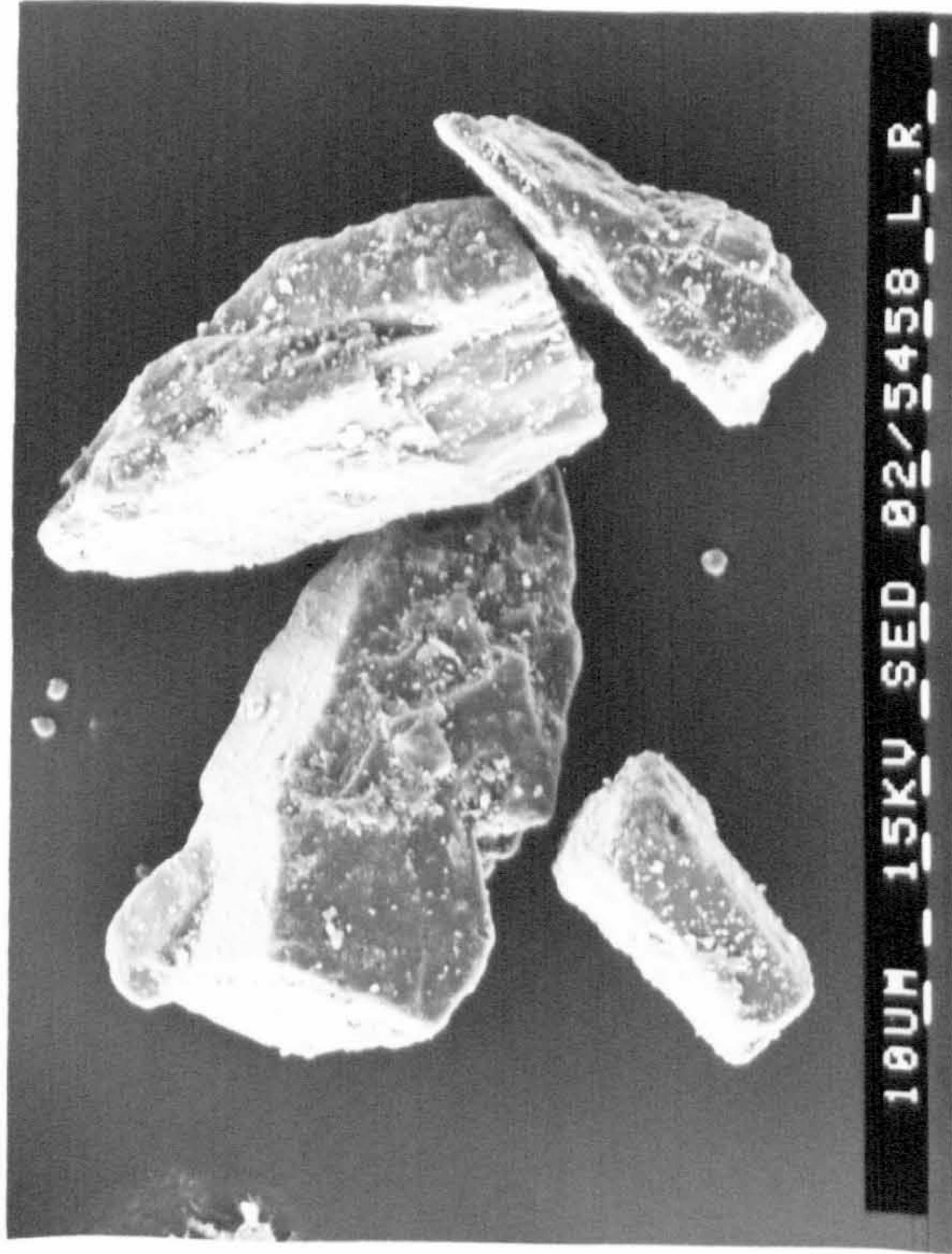
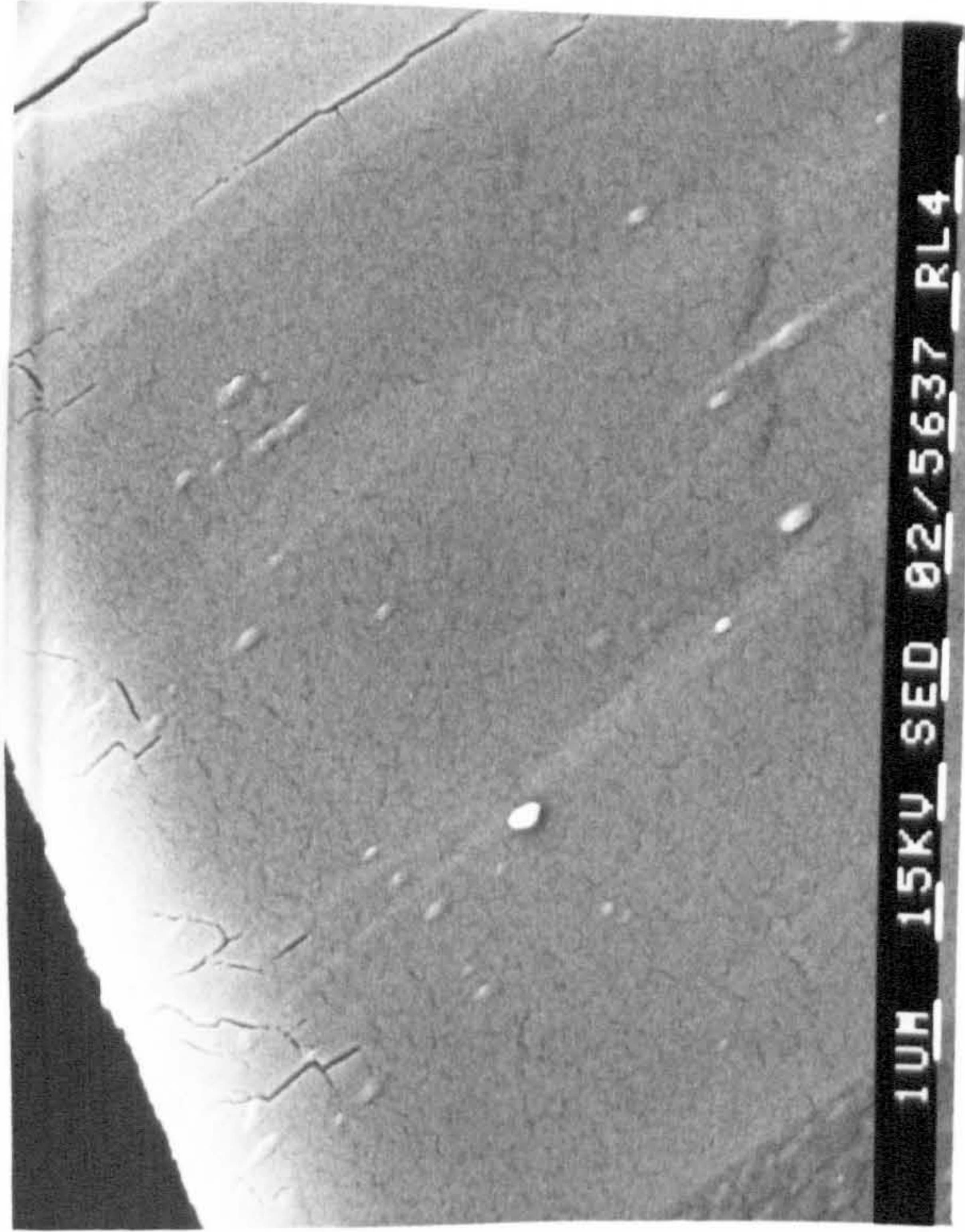
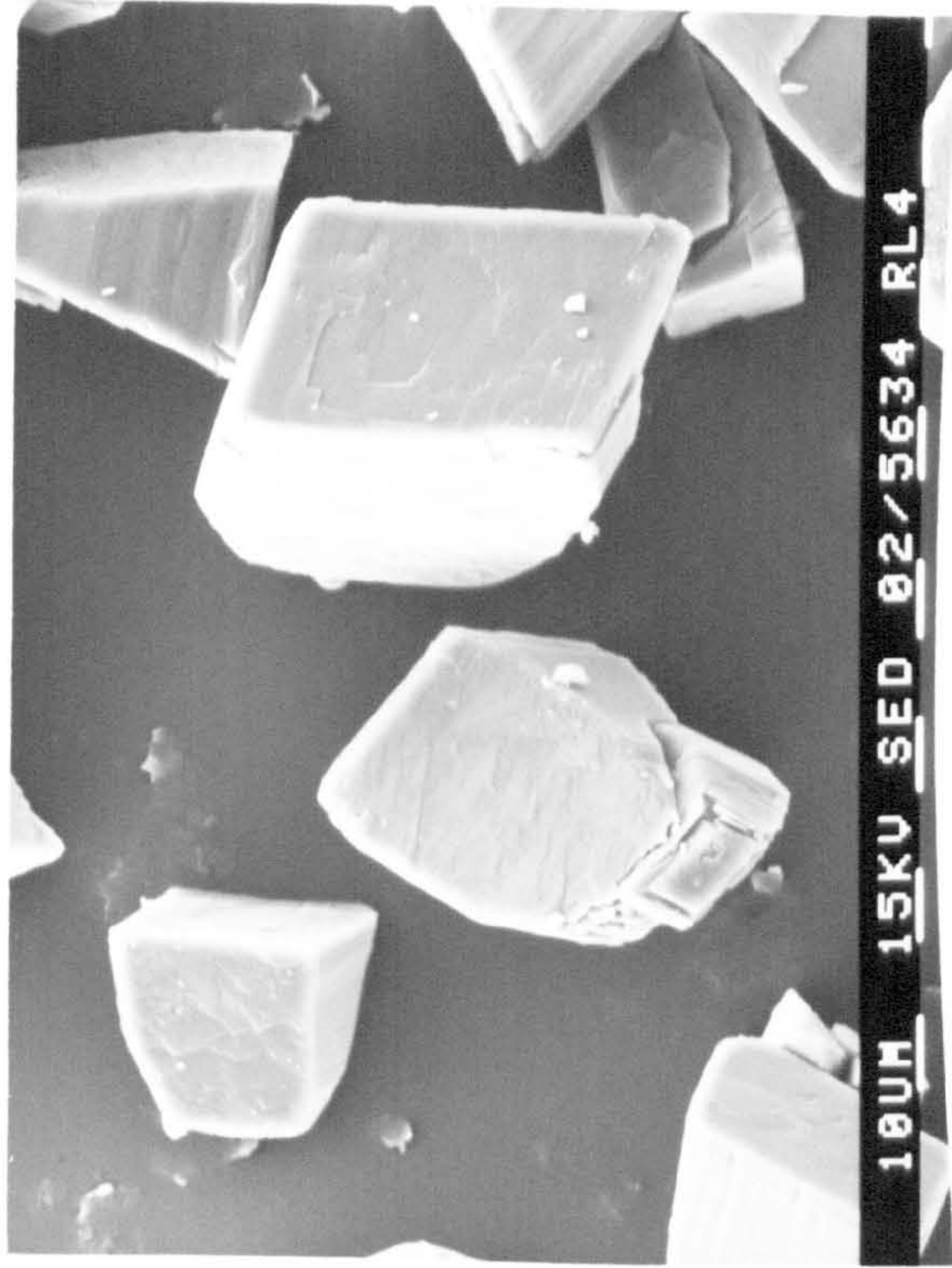
Recrystallized lactose

Surface details of regular  
lactose

Surface details of recrystallized  
lactose

Fig 3.5 Scanning electron micrographs of







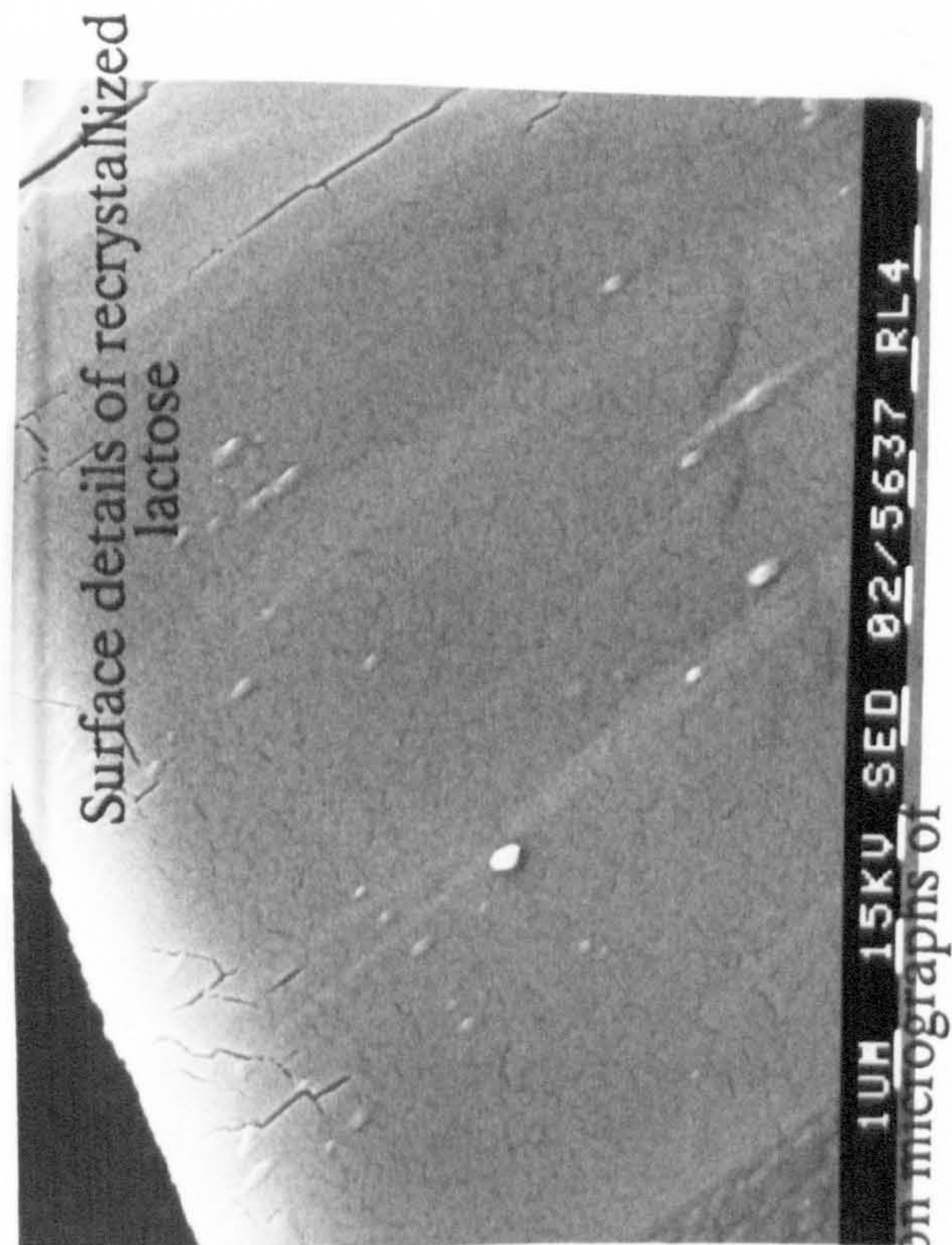
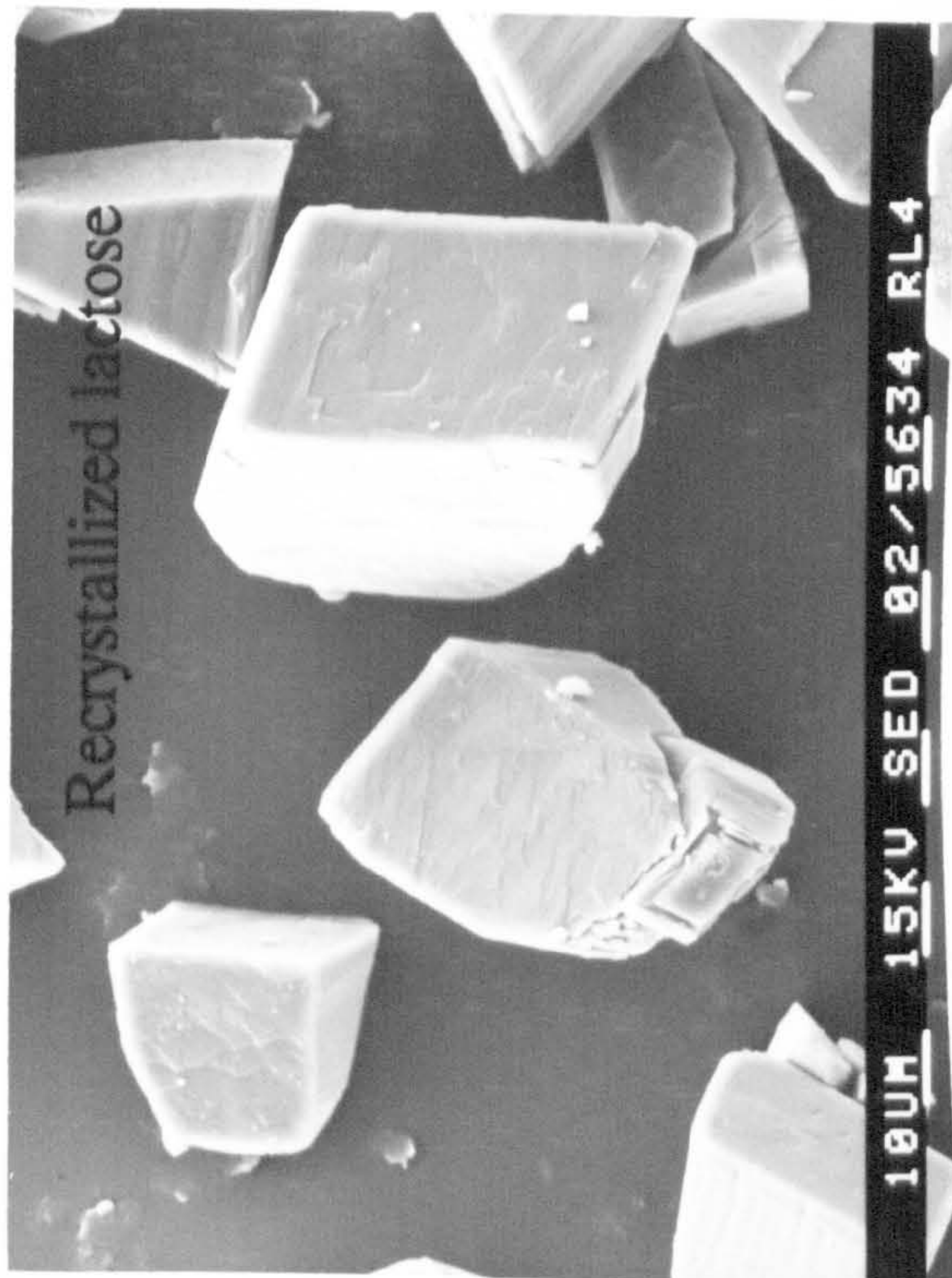
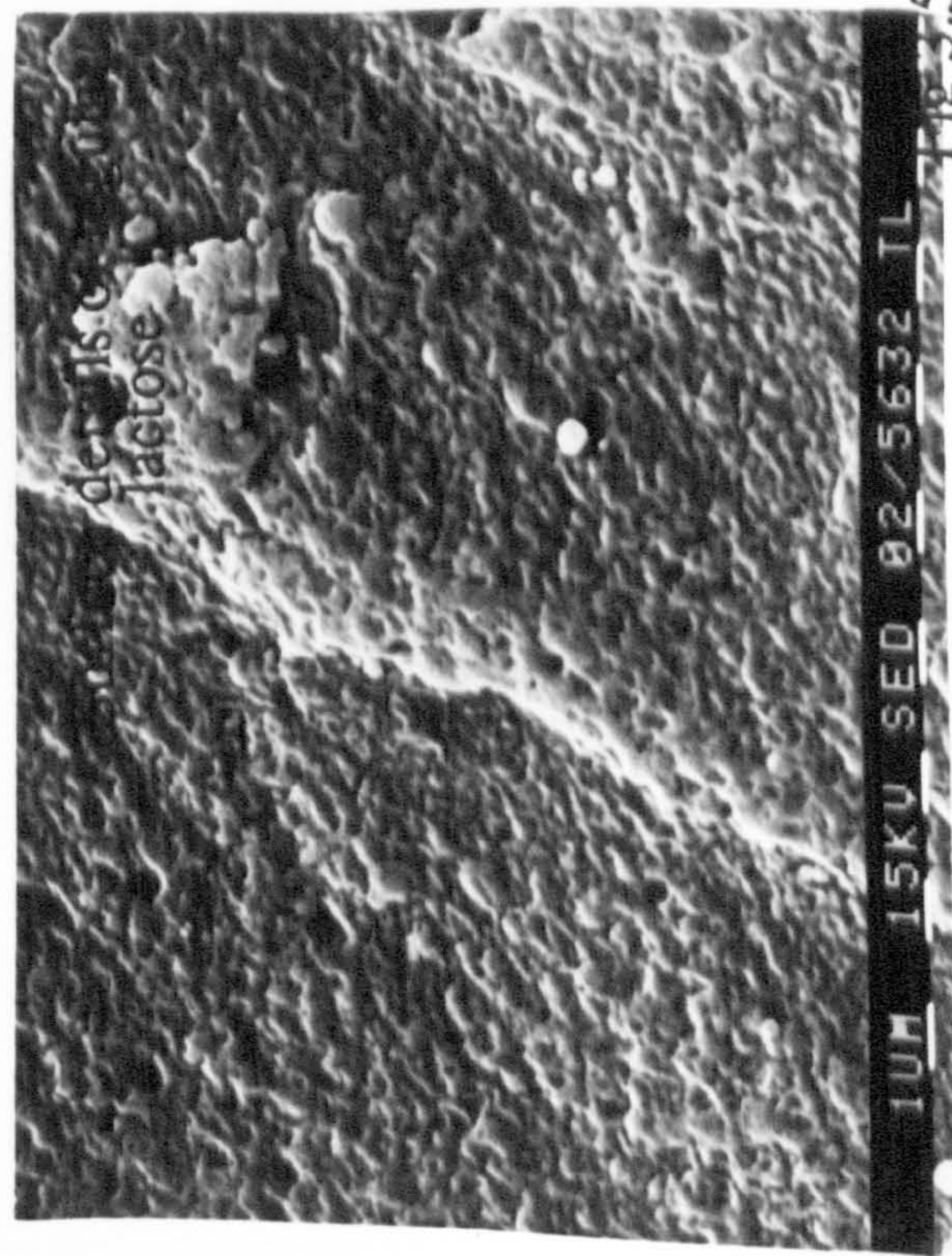
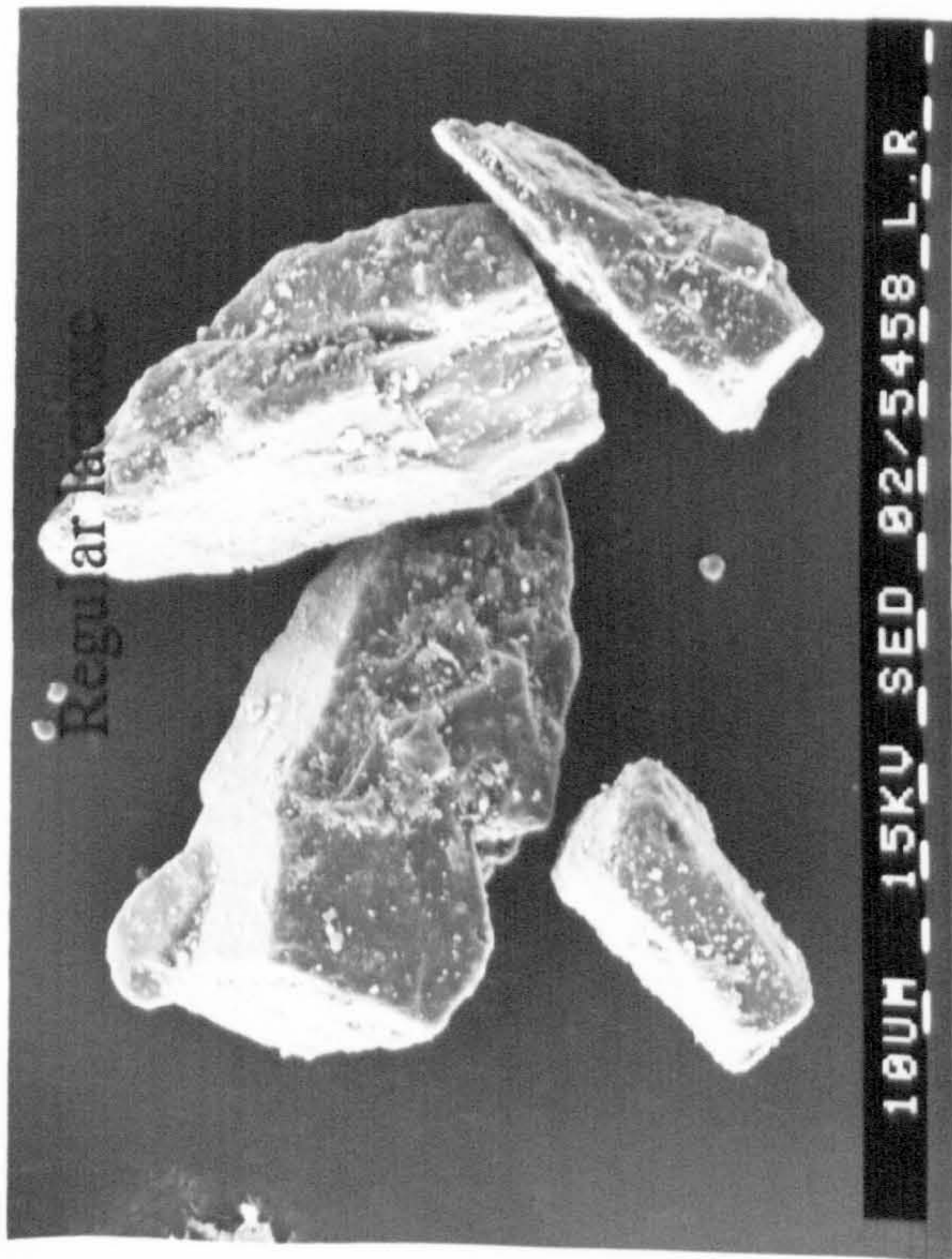


Fig 3.5 Scanning electron micrographs of



**Table 3.6 Surface roughness (rugosity) of the carriers**

Carrier	Rugosity
Regular lactose	2.3
Spray dried lactose	2.6
Recrystallized lactose	1.2

particles (Figure 3.8), results in very weak adhesive bonds.

Therefore, de-mixing is expected to occur with the minimum generated force under normal handling. The detached drug particles then tend to impact onto the walls of the inhaler as a result of their cohesiveness. However, when milled glass was used, the amount of drug retained in the inhaler was smaller since the mixture was less prone to segregation due to the relatively rough surface of the milled glass (Figure 3.8). Furthermore, when regular and spray dried lactose were used as carriers, a much lower fraction was retained in the inhaler indicating that a more stable powder mixture was formed. Although this seems to be an advantage as more drug can be delivered to the patient, the results show that most of the drug was recovered from the preseparator stage and a much lower fraction was deposited on stages 3 to 7. For example, at an air flow of 150 l/min, 55% of the drug was retained in the preseparator and 17% deposited on stages 3 to 7. However, when glass beads and milled glass were used as carriers lower drug deposition in the preseparator stage was observed with a relatively higher respirable fraction (30%).

These results indicate that the smooth surfaces of both the glass beads and the milled glass allow the drug particles to free themselves from the carrier surface more easily. In comparison, the relatively rough surfaces of both regular and spray dried lactose limited the separation of the drug particles from the carrier surface upon fluidisation as a result of the high interparticle forces within these mixtures. However, although the photomicrographs (Figure 3.4) show that the spray dried lactose possess a rougher surface than the regular lactose, the respirable fraction obtained was comparable to that of regular lactose. This can be explained by

# Effect of surface properties of different carriers on the characteristics of an inspirable cloud at different airflow rates

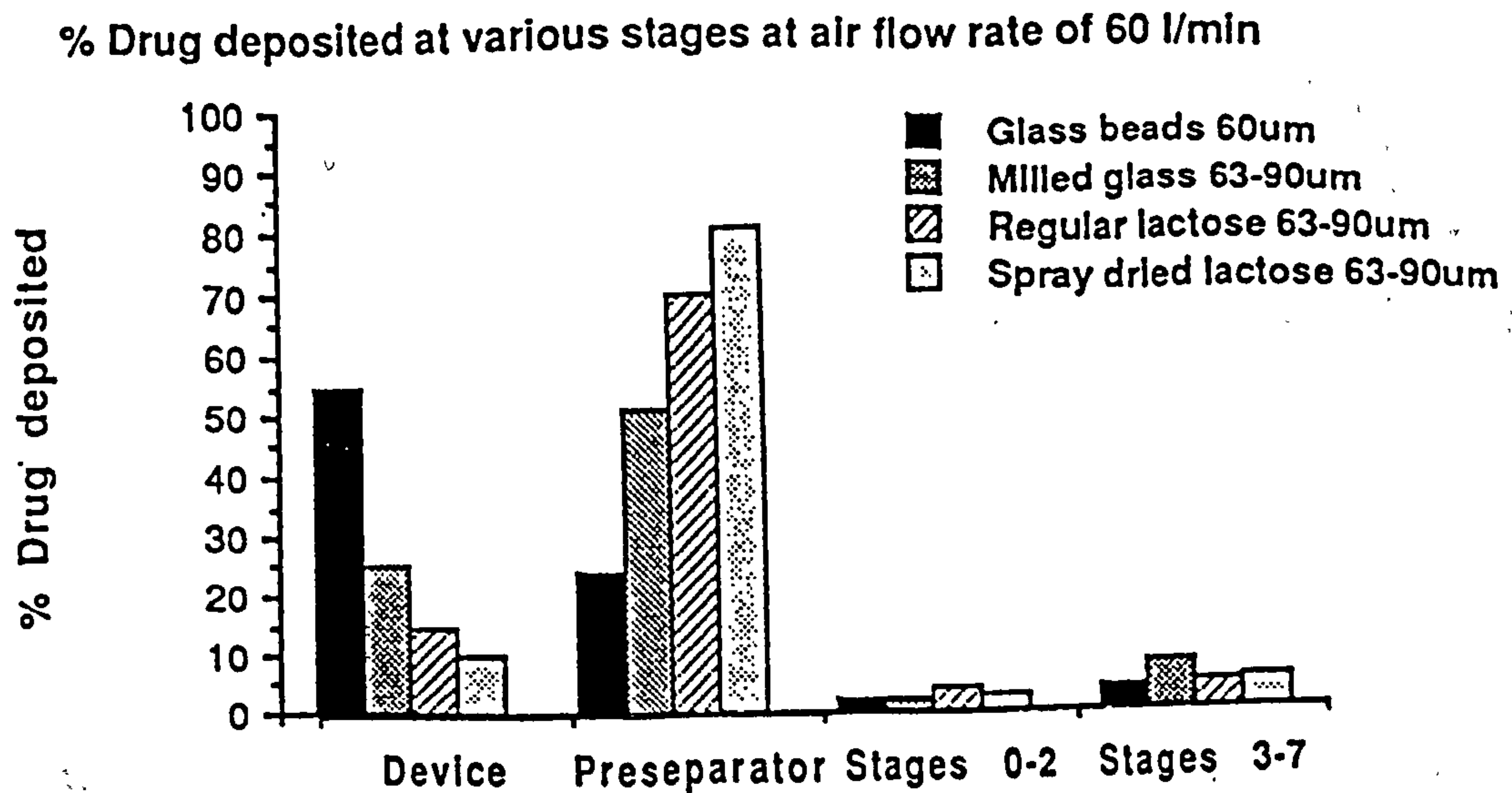


Fig 3.6

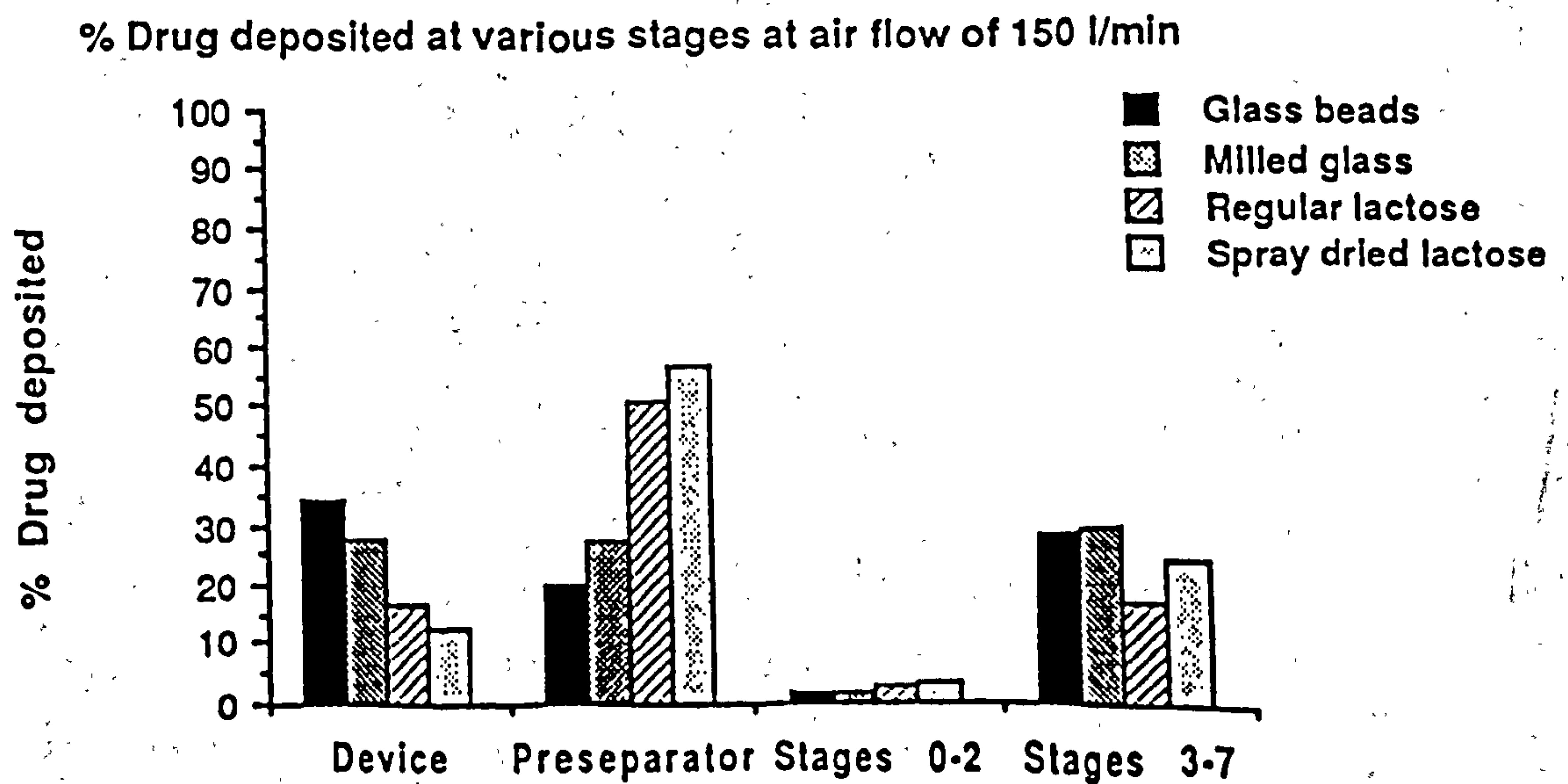


Fig 3.7

L

Glass beads

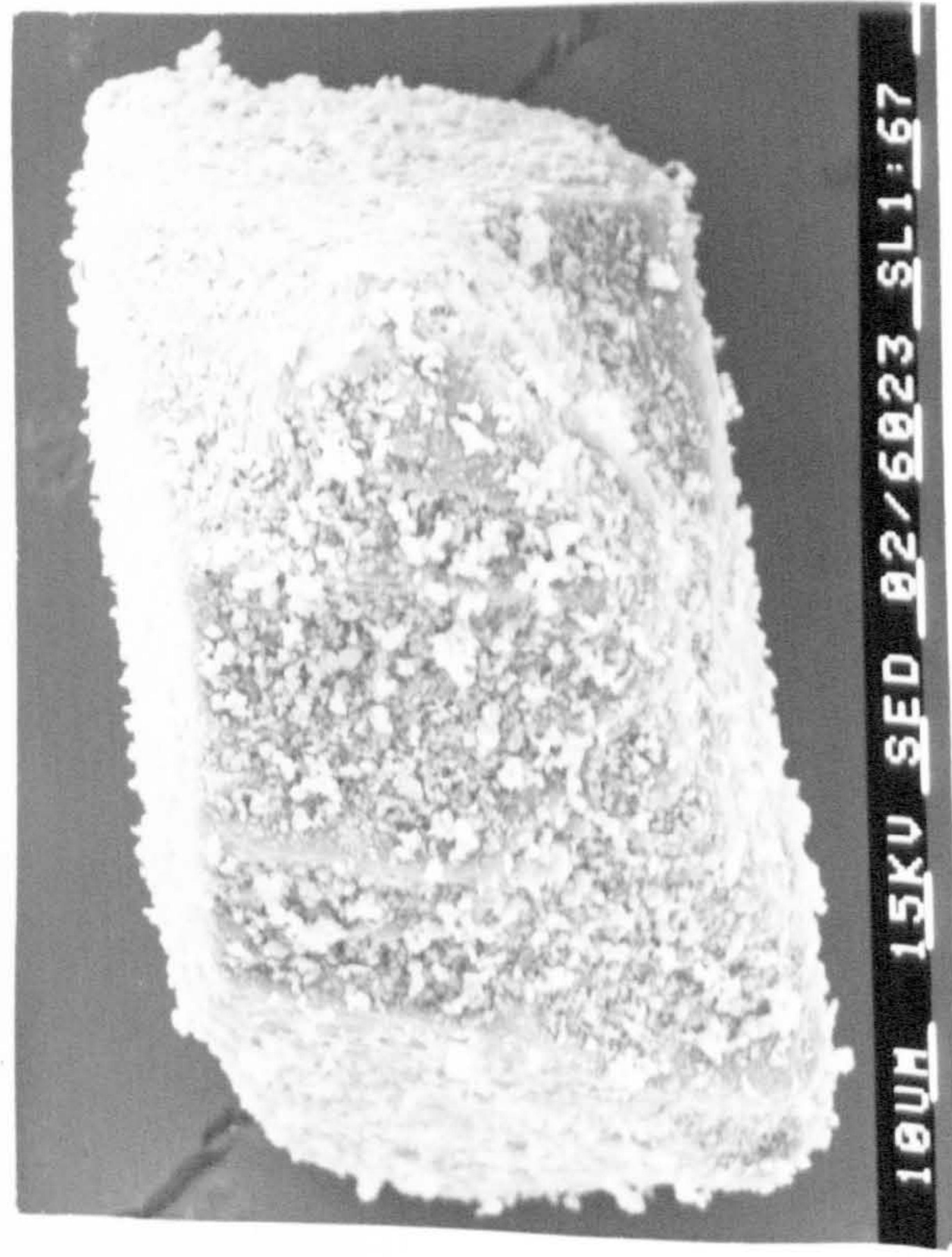
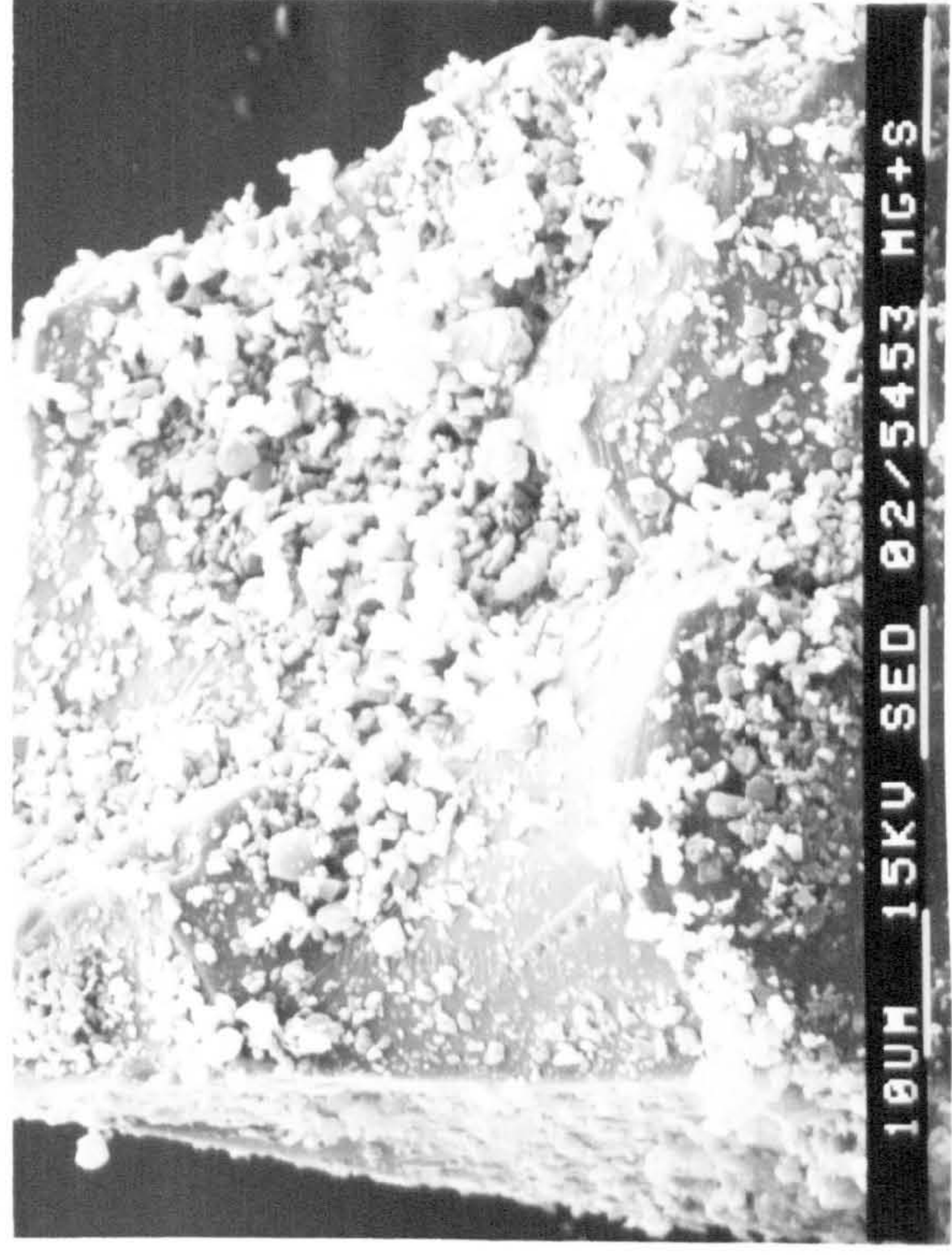
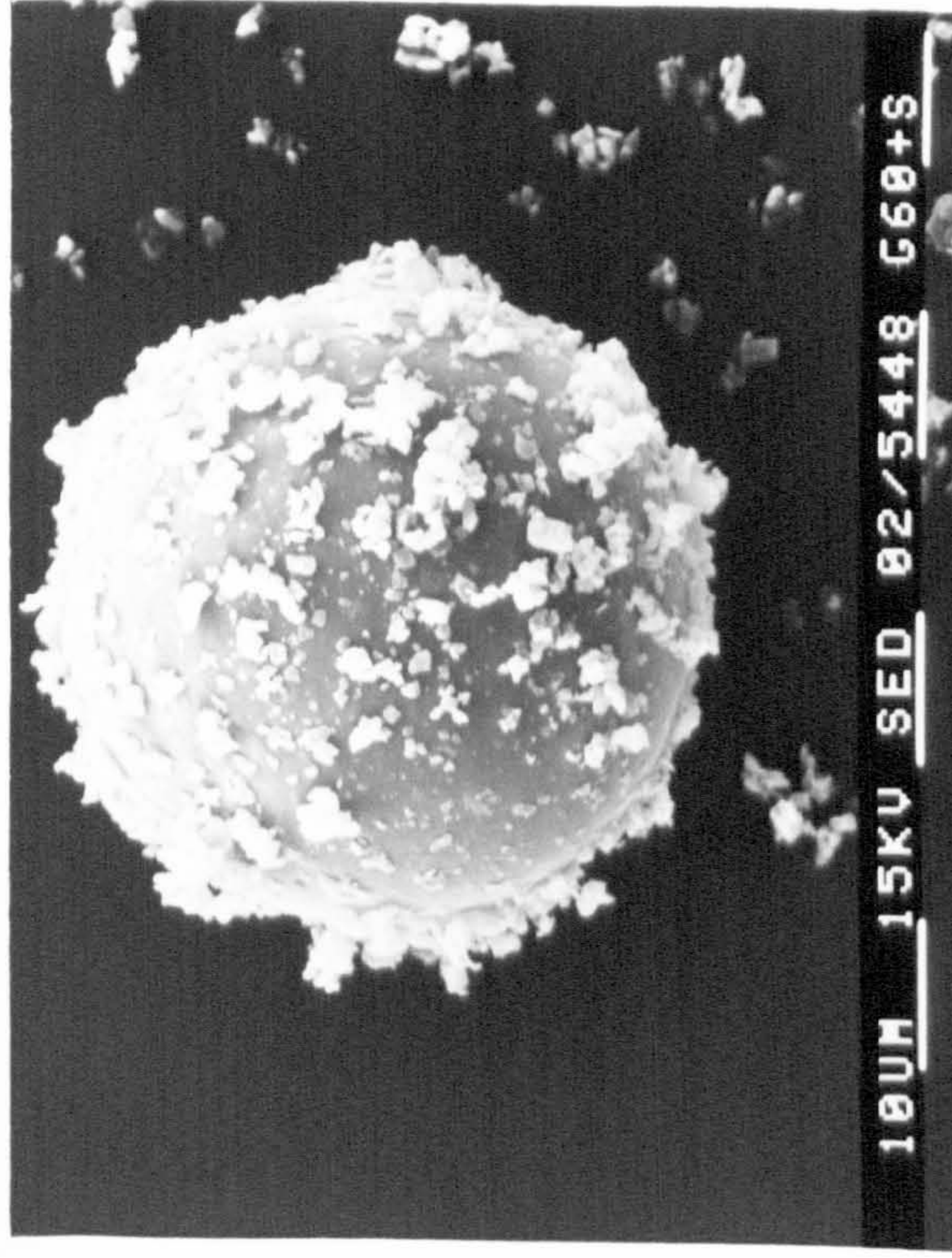
Milled glass

Regular lactose

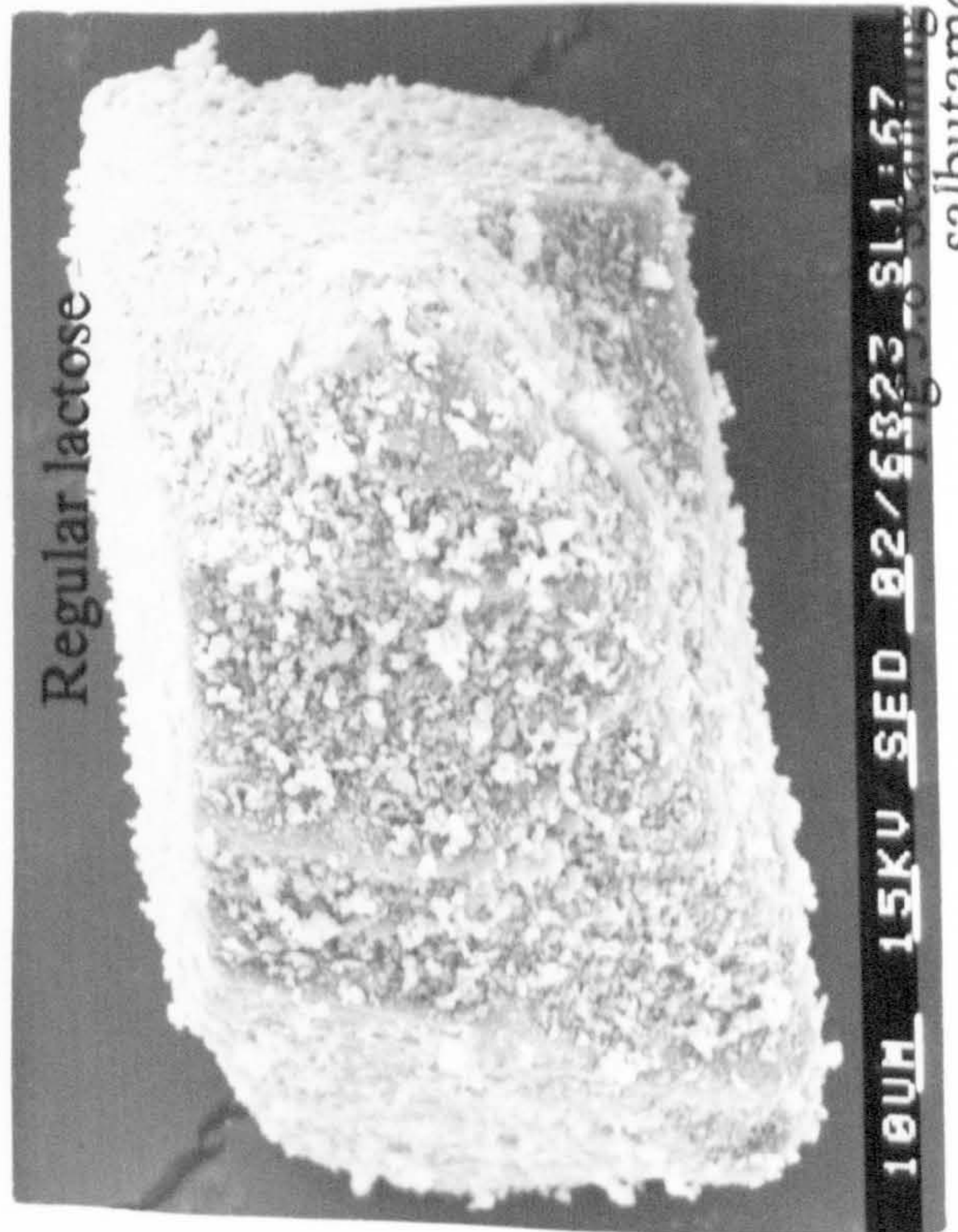
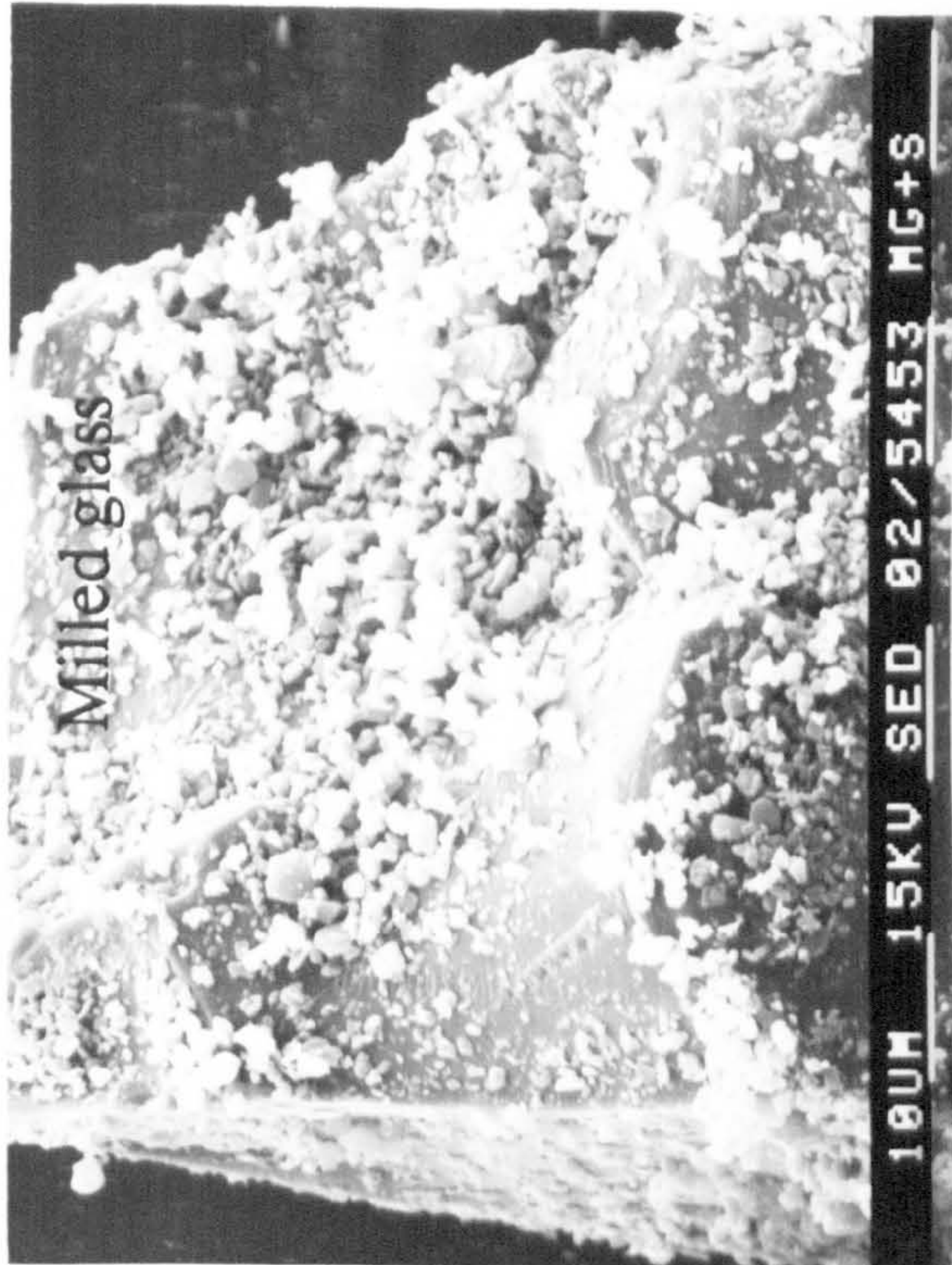
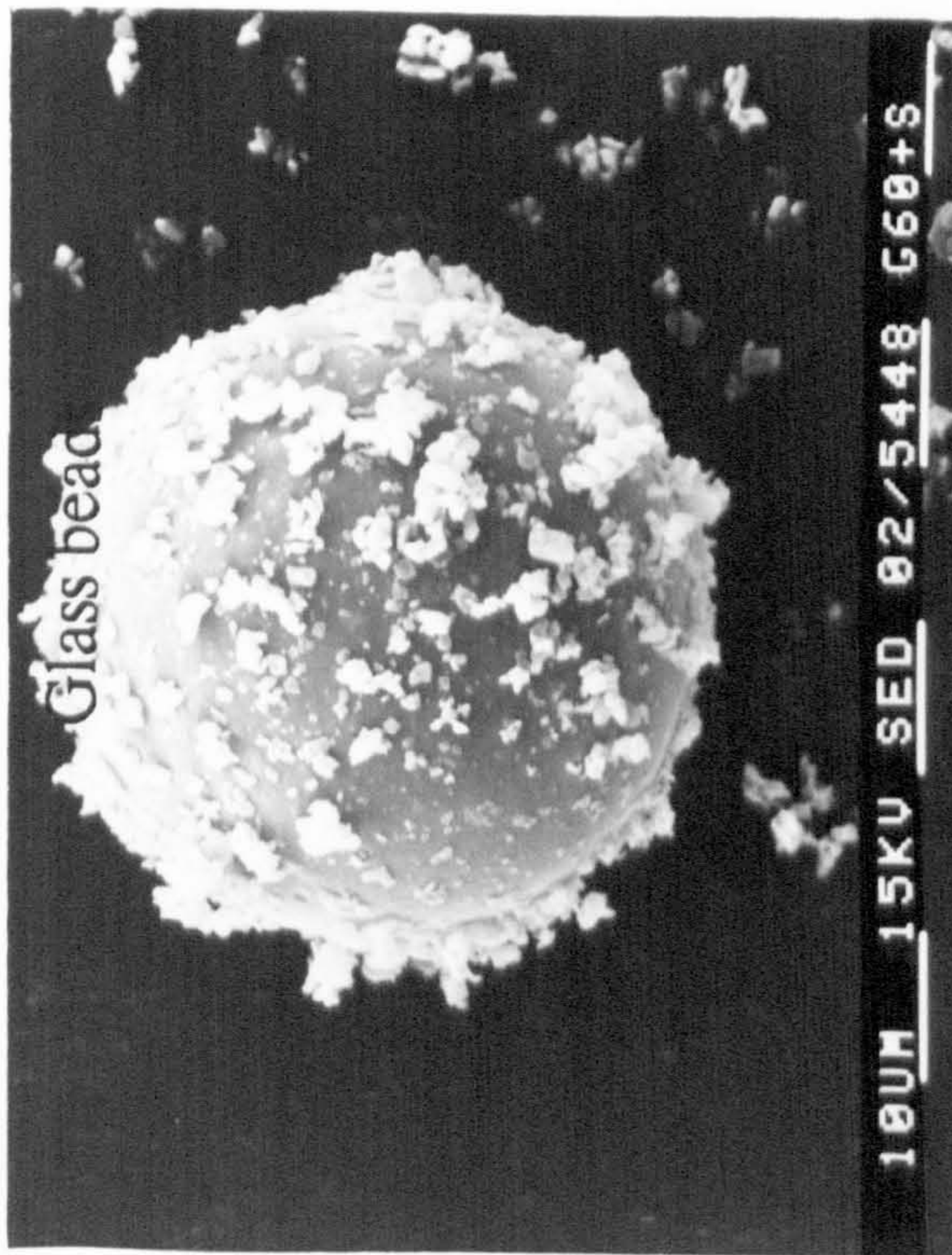
spray dried lactose

Fig 3.8 Scanning electron micrographs of the powder mixtures of salbutamol sulphate with the carriers









Scanning electron micrograph of salbutamol sulphate with the carriers



examining the photomicrographs of the mixtures (Figure 3.8). These show that the drug particles were distributed on the external surface of the spray dried lactose and only very few particles appeared to be adsorbed into the surface cavities.

The above results suggest that a weak association between the drug and the carrier in powder mixtures for inhalation is beneficial. The fine drug particles can redisperse themselves more easily from the carrier surface and penetrate deep into the lungs. However, neither the regular lactose nor the spray dried lactose provide an ideal surface properties.

Recrystallized lactose with lower rugosity than both regular and spray dried lactose resulted in a marked increase in the respirable fraction when used as the carrier (Figure 3.9, 3.10). This increase was accompanied by a decrease in the amount of drug deposited in the preseparator stage, suggesting that the association of the fine drug particles with the carrier surface was reduced. The photomicrographs of the mixture formed by mixing the fine drug particles with the recrystallized lactose (Fig3.10) show that the fine particles were distributed on the carrier surface as a monolayer and no substantial agglomerates were formed. The increase in the respirable fraction was more pronounced at a flow rate of 60 l/min, where an increase from 4% with regular lactose to 23% with recrystallized lactose was observed. In comparison, at 150 l/min the respirable fraction was only increased from 17% to 42% for the regular and recrystallized lactose, respectively.

Therefore, modifying the surface of the lactose resulted in a fewer or weaker sites of adhesion. Moreover, the smooth surface



Effect of surface properties of regular lactose and recrystallised lactose on the characteristics of an inspirable cloud at different airflow rates

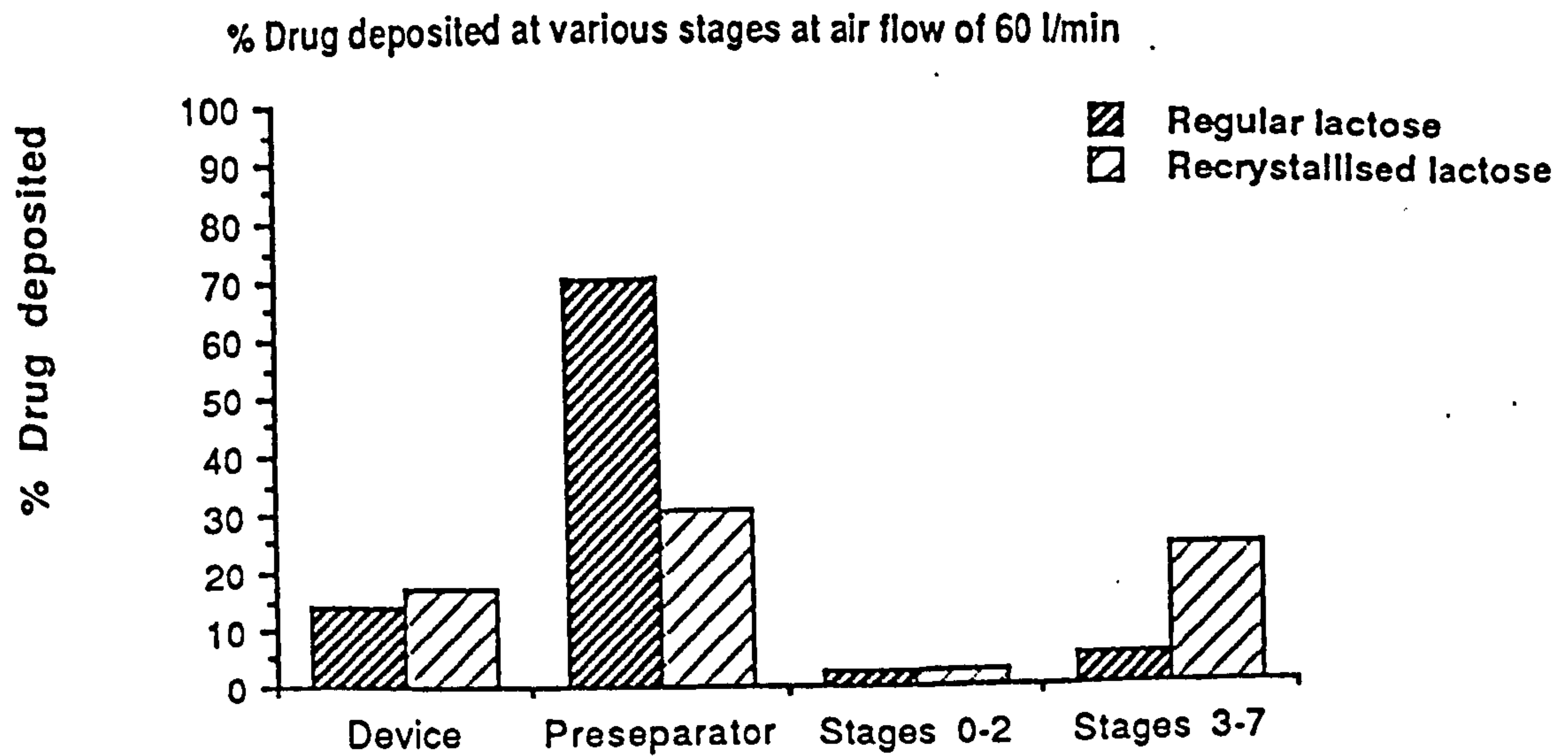


Fig 3.9

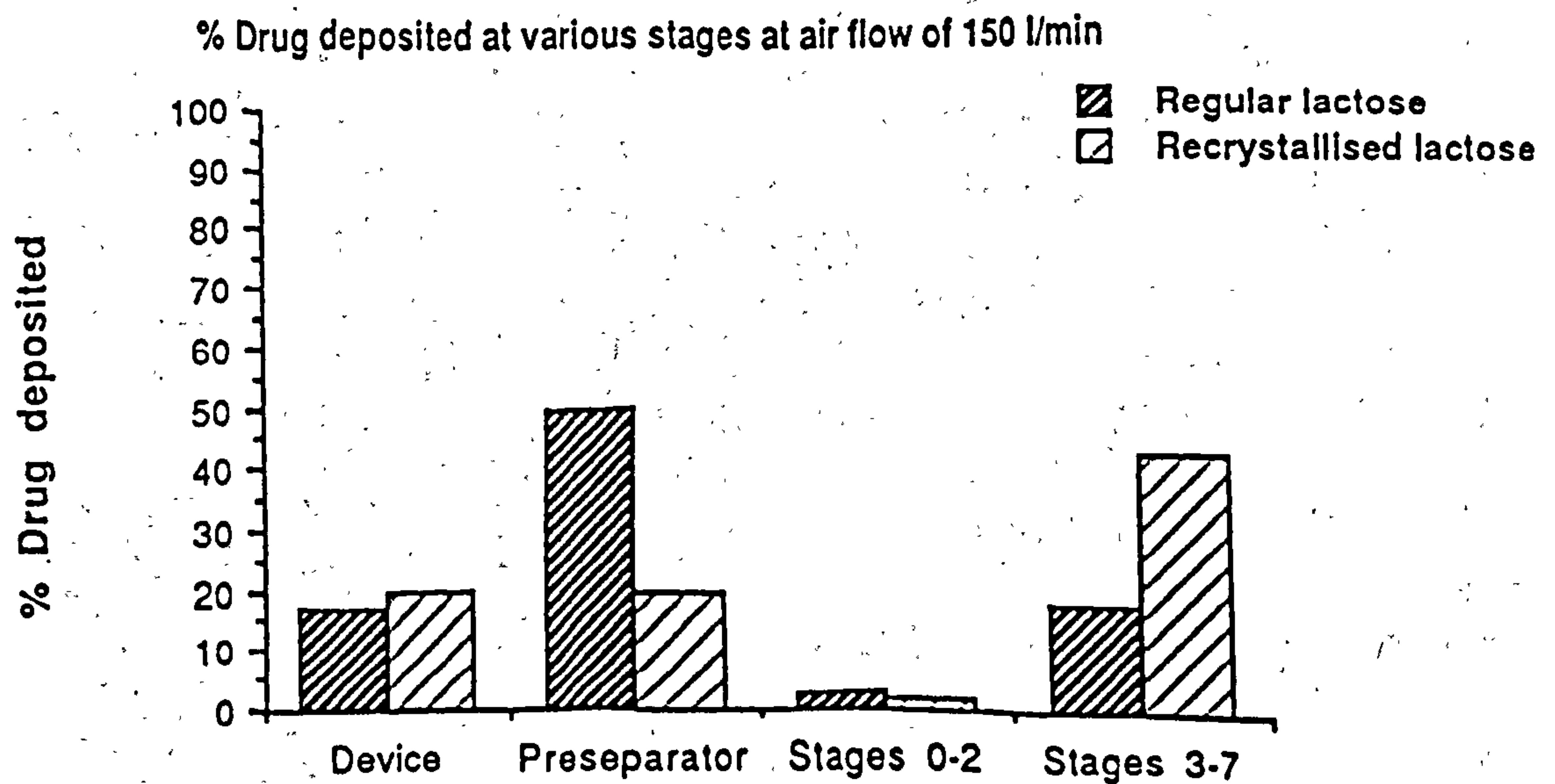


Fig 3.10

**Fig 3.11 Scanning electron micrographs of**

**A mixture of salbutamol sulphate and  
recrystallized lactose**



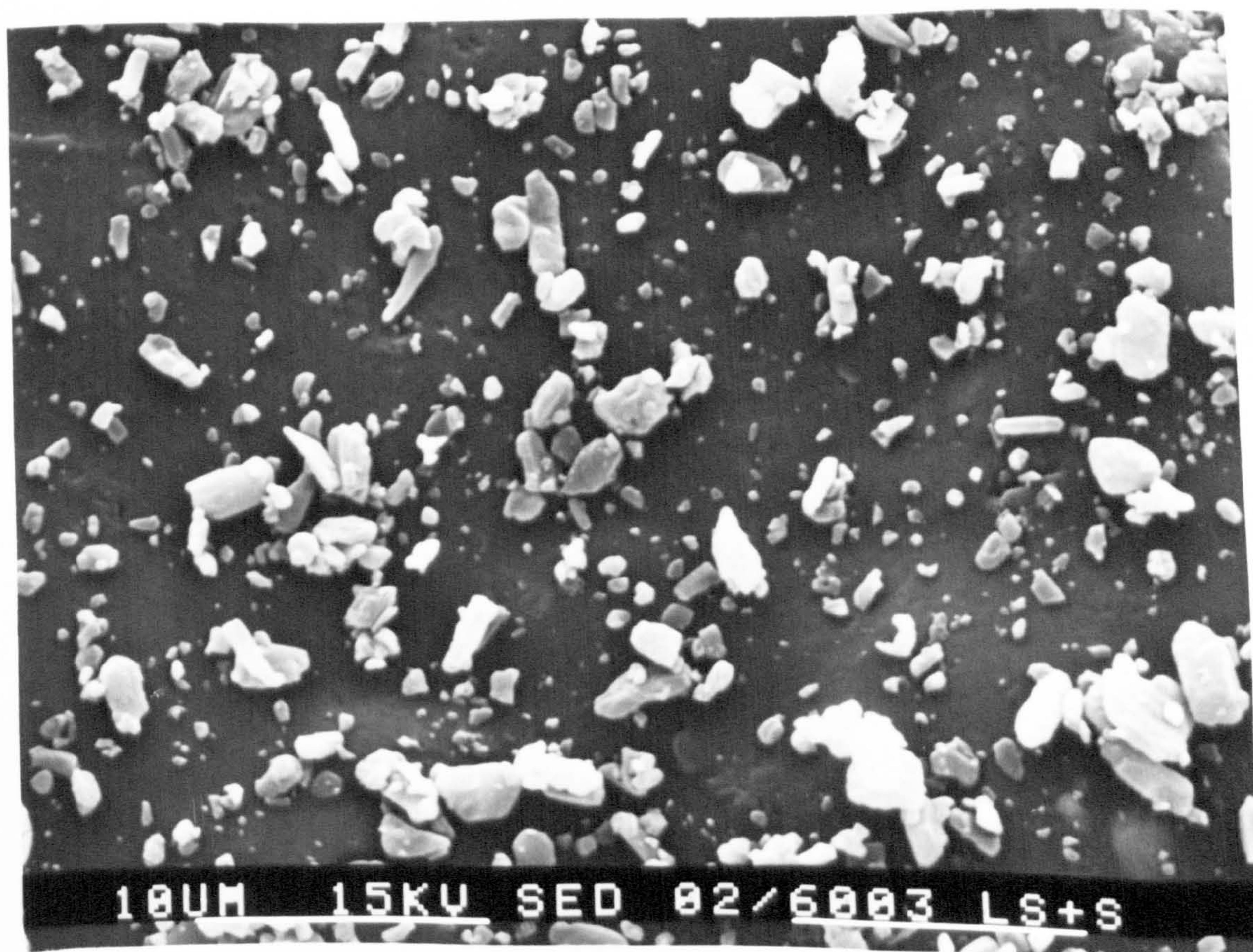
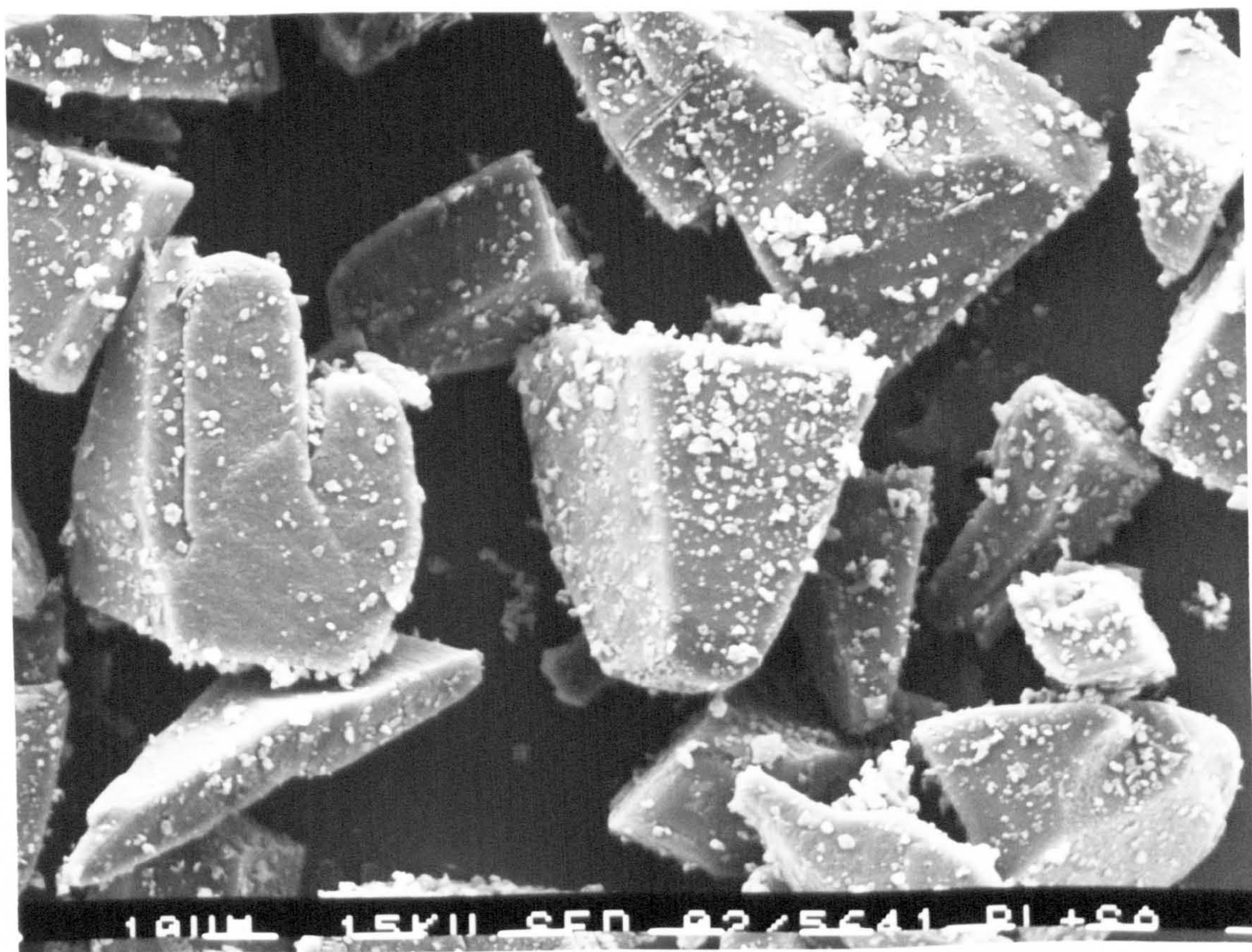
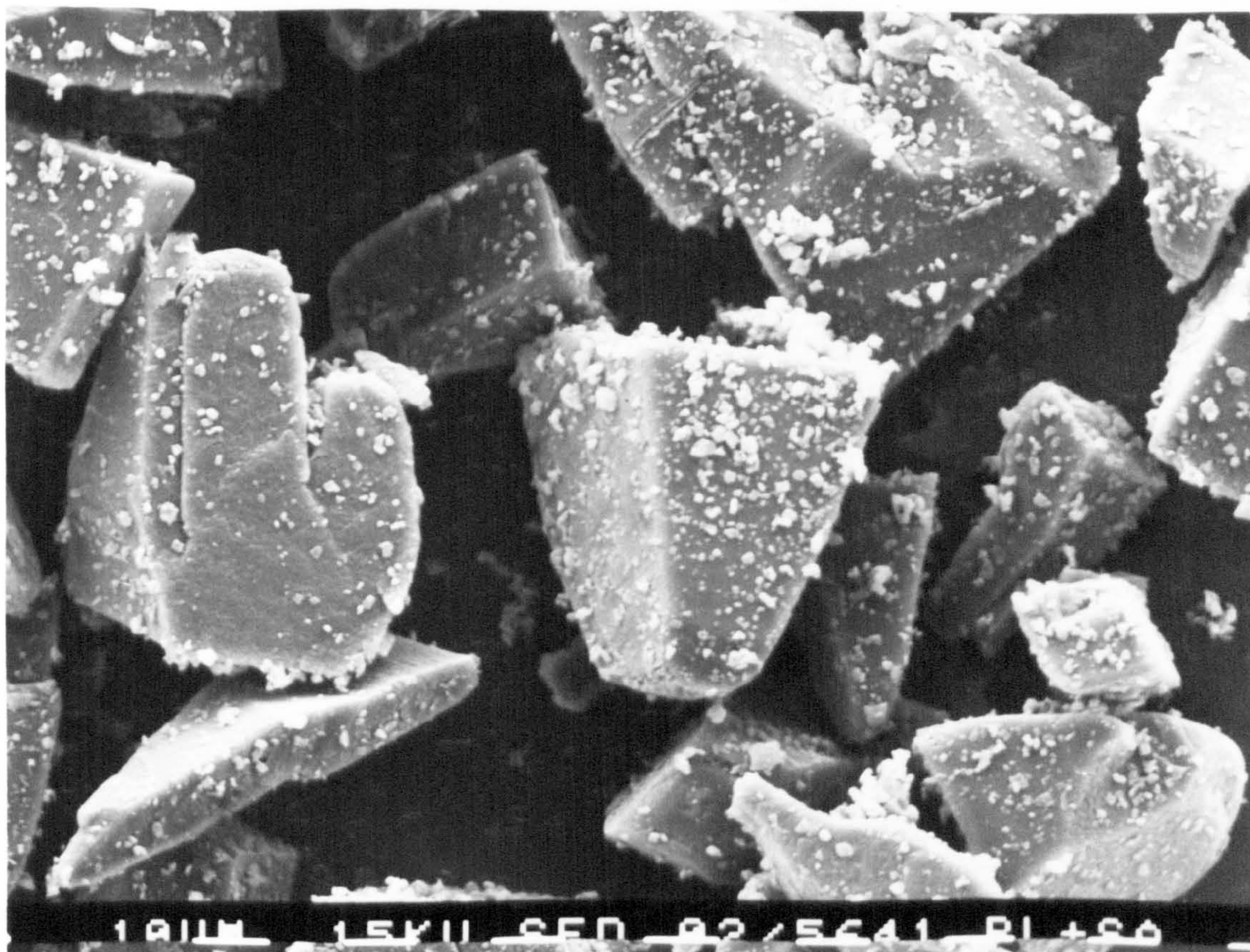
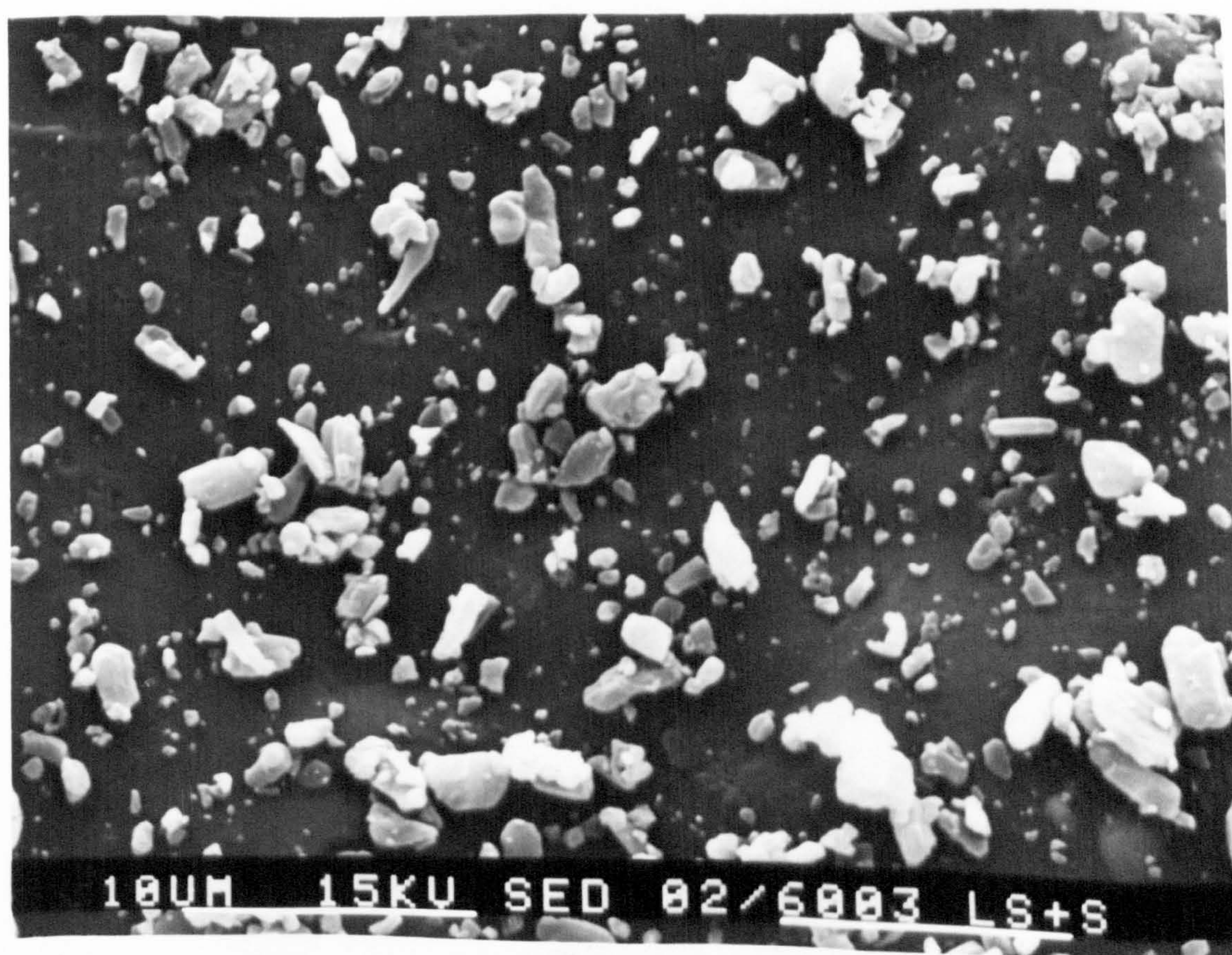




Fig 3.11 Scanning electron micrographs of



A mixture of salbutamol sulphate and  
recrystallized lactose





minimized the effect of surface asperities which could prevent drug particle detachment by mechanical interlocking.

However, although the release of the adherent particles is more likely to occur with the smooth surface carrier, the amount of drug retained in the inhaler was similar to that when regular lactose was used. This indicates that the adhesion was sufficiently strong to prevent drug particle detachment under low forces but allowed a high proportion of the particles to separate during "inhalation".

Therefore, the recrystallized lactose provided the ideal surface properties since a low amount of the drug was retained in the inhaler and an efficient redispersion of the drug particles was achieved during "inhalation".

Additionally, the improved efficiency at low air speeds suggests that this formulation can be effective even in patients with severe asthma and in children who cannot achieve high inspiratory flow rates.

This invention provided a carrier which is inert, soluble, non-toxic and sufficiently free flowing suitable for use in powder aerosols.

#### **3.4.2 The effect of particle size of the drug**

In dry powder aerosols a respirable particle size of the drug i.e  $<5\mu\text{m}$  must be used in the formulation. Therefore, to study the influence of the particle size of the drug on the inspirable characteristics of an aerosol cloud the range of sizes that can be employed is very narrow. However, an attempt was made to produce drug particles with different mass median diameter.

## **Materials and methods**

### **1. Micronization of salbutamol sulphate**

A batch of salbutamol sulphate was milled under conditions which differed from those described in Section 2.2.1 by micronizing at a powder feed rate of 5g/min and an air pressure of 3.5 bar.

An electronphotomicrograph of the micronized drug is shown in Figure 3.12.

### **2. Powder mixtures**

The micronized batch of salbutamol sulphate obtained by milling under the conditions described in section 2.2.1 (Batch 1) and the above batch (Batch 2) were mixed with lactose of 63-90 $\mu$ m size fraction in a ratio of 1:67.5.

### **3. Flow rates**

Experiments were conducted at air flow rates of 60 and 150 l/min.

## **Results and discussion**

### **1. Particle size of salbutamol sulphate**

The mass median diameter of Batch 1 of the micronized salbutamol sulphate was 2.8 $\mu$ m with a geometric standard deviation of 1.3 and for Batch 2, 3.5 $\mu$ m with a geometric standard deviation of 1.4.

The size distribution is shown in Figure 3.13.

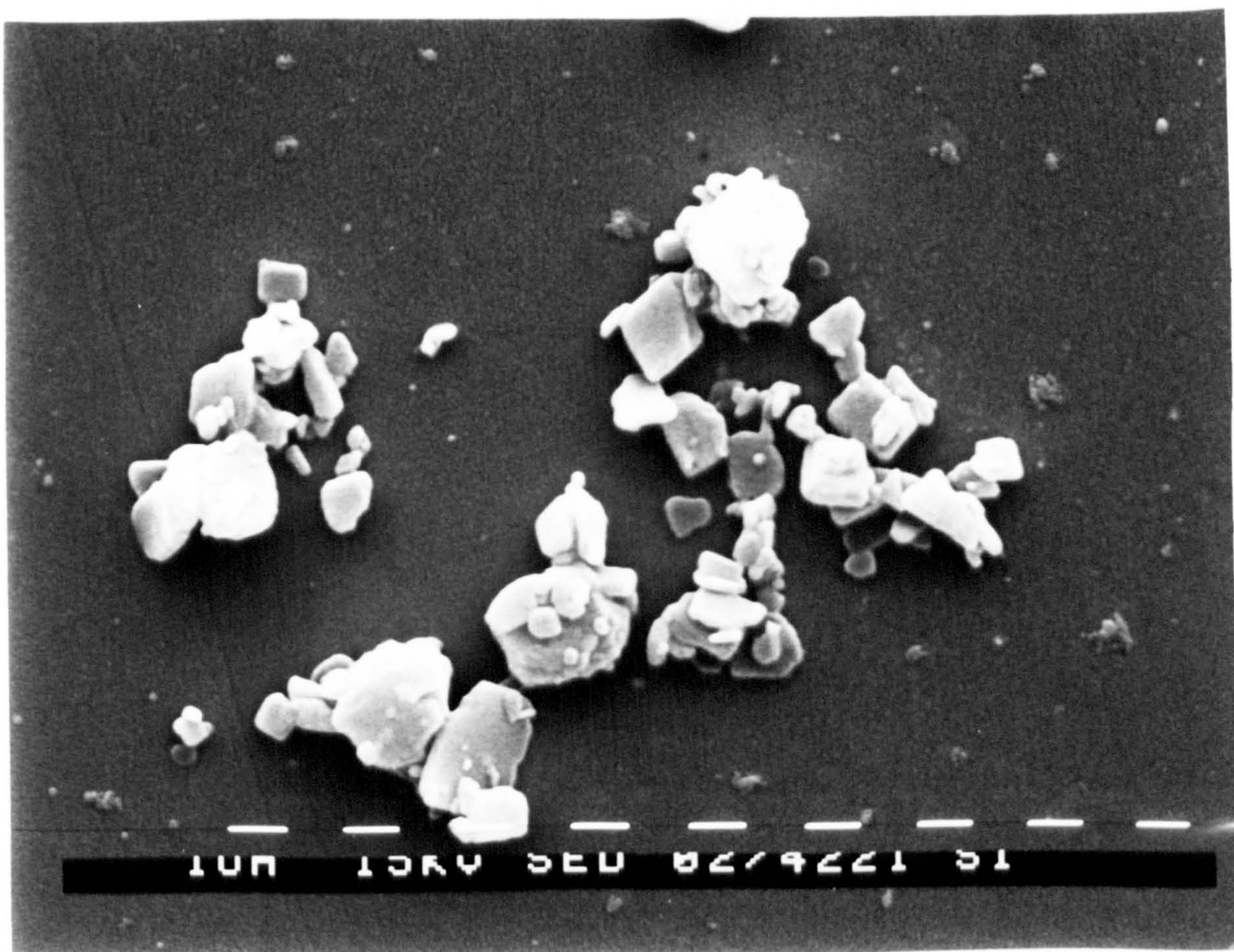
### **2. The effect of drug particle size on the characteristics of an inspirable cloud**

The results are given in Table 3.7. The use of drug particles



**Fig 3.12 Scanning electron micrographs of micronised  
salbutamol sulphate**







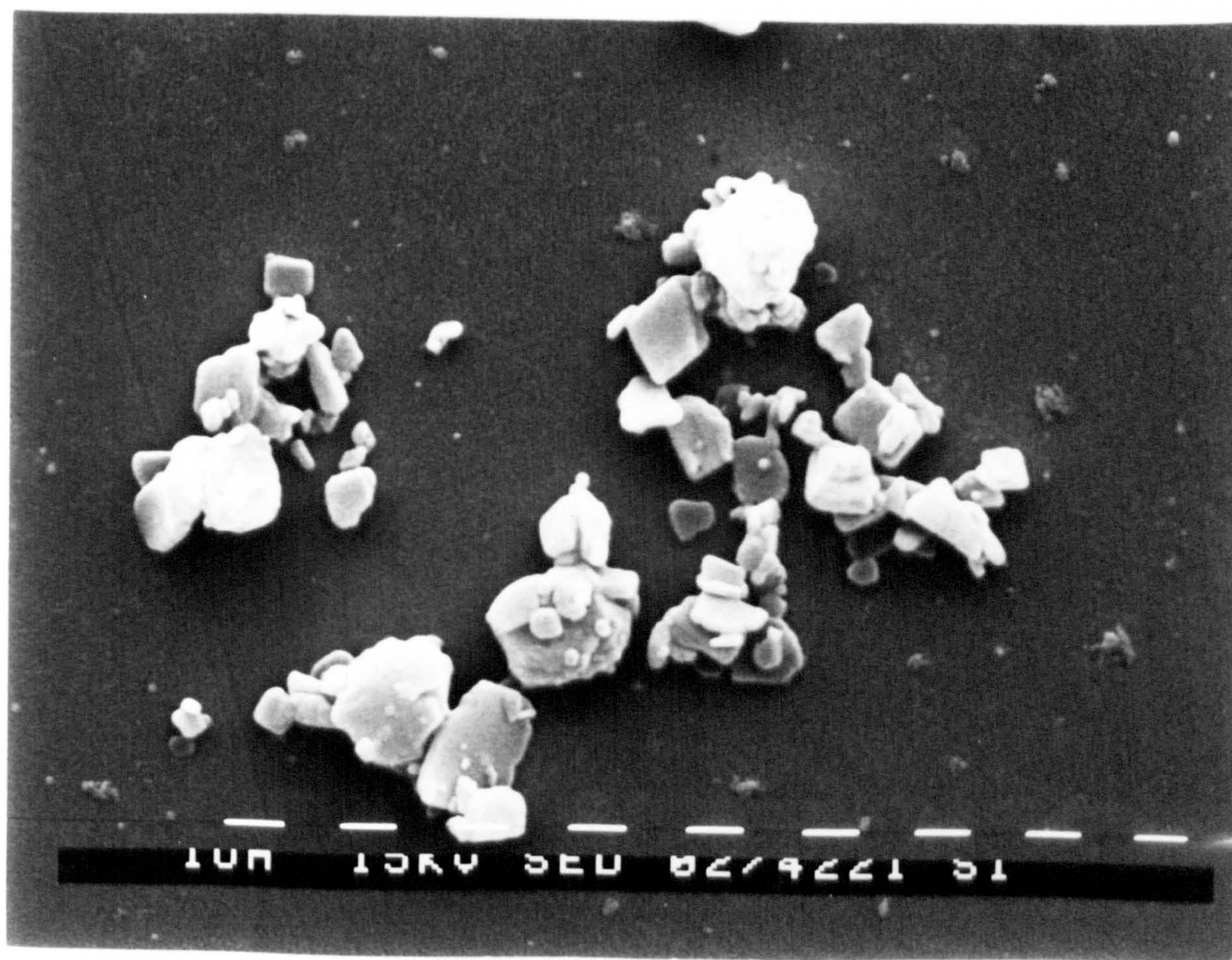
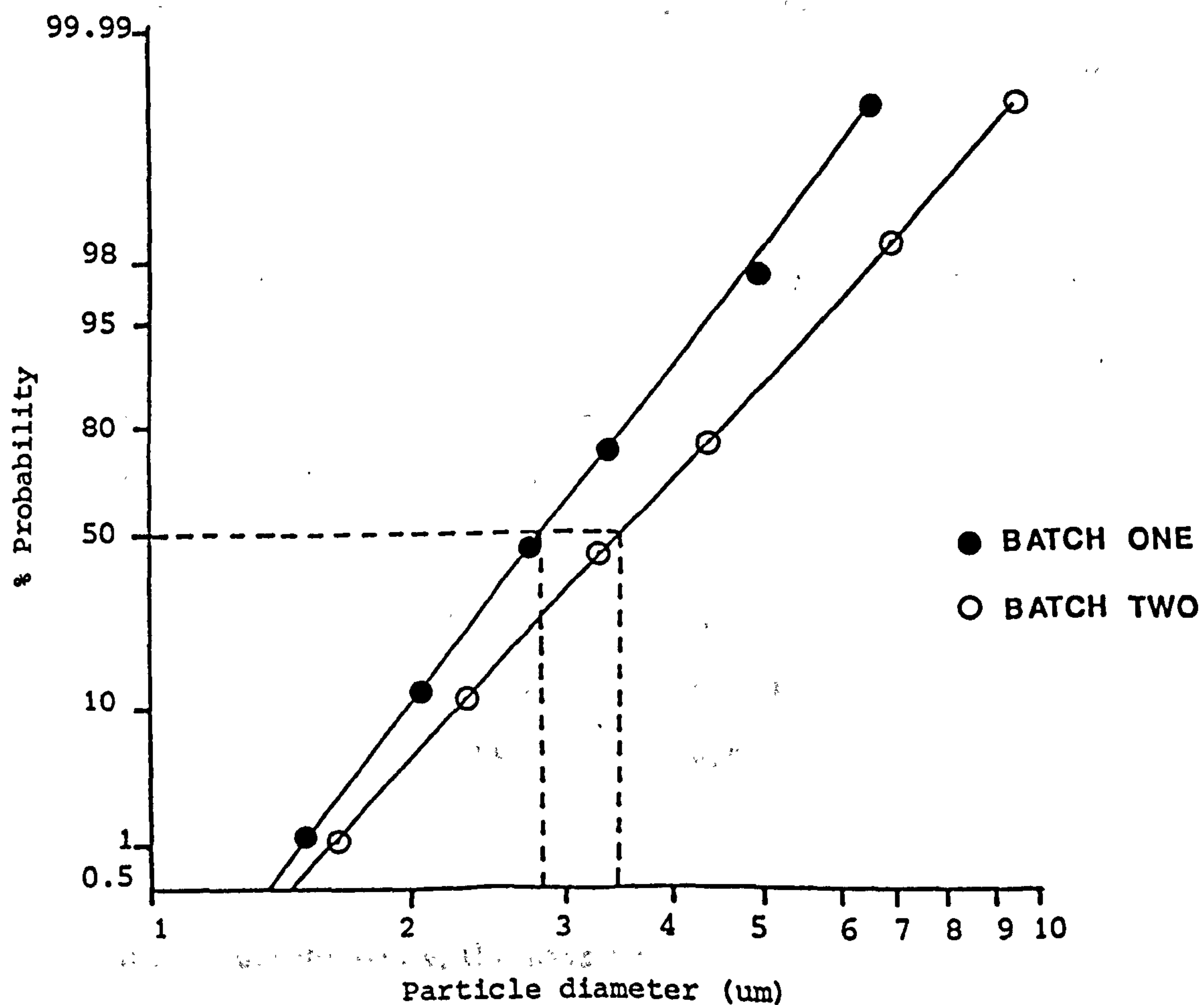


Fig 3.12 Scanning electron micrographs of micronised salbutamol sulphate





**Fig 3.13** Particle size distribution of the two micronized batches of salbutamol sulphate

with a different mass median diameter in the powder mixture had no significant influence on the pattern of drug deposition. This disagrees with previous investigations if the results are to be interpreted in terms of the effect of the adherent particle size on the adhesion characteristics.

The effect of the adherent size on the degree of adhesion was studied by several workers using different adhesive systems and techniques (Corn and Stein 1965, Kulvanich and Stewart 1987a). An increase in the adhesive force was observed with a reduction in the particle size.

However, the most relevant study to the present work is the one carried out by Corn and Stein (1965) who showed that the removal efficiency of a particle exposed to a bulk air stream velocity decreased with the reduction in particle size. This was explained by the fact that these small particles sink deeper into the boundary layer at the surface, until they are out of the range of the main stream eddies which could dislodge them. Therefore, once the particle is engulfed in the laminar sublayer, it requires a higher bulk air stream velocity to thin this layer in order to reach this particle.

In the current study, the assessment of the powder mixtures containing adherent particles of different sizes showed no increase in the respirable fraction when the larger drug particles were used, even at flow rates of 150 l/min. This reflects the fact that the variation in the adhesive forces was not significant for the two particle sizes used. Larger differences in the size distributions might have given different results. However, milling the powder to

**Table 3.7 Effect of drug size on the pattern of drug deposition at various flow rates**

Air flow rate (l/min)	Device	Preseparator	Stages 0-2	Stages 3-7
<b><u>Drug size 2.8<math>\mu</math>m</u></b>				
60	13.2	69.0	1.3	4.1
150	15.2	51.9	1.3	15.6
<b><u>Drug size 3.5<math>\mu</math>m</u></b>				
60	14.5	57.4	1.3	4.8
150	12.6	50.6	1.2	14.4



a mass median diameter of less than  $2.8\mu\text{m}$  is difficult. Moreover, for the particles to penetrate into the lung, their size should not exceed  $5\mu\text{m}$ . Therefore, this experiment was limited by the range of sizes that can be produced and used.

### 3.4.3 Effect of the concentration of drug powder

The concentration of the drug in the powder mixture was varied using different drug to carrier ratios.

The maximum salbutamol sulphate concentration that could be packed on the carrier surface was theoretically estimated by assuming that the drug particles formed a close-packed monolayer.

The amount of drug can be calculated from the following equation (Jones and Pilpel 1965):

$$\text{The amount of drug} = 2 \pi d (D+d)^2 / \sqrt{3} D^3$$

where  $D$  and  $d$  are the diameters of the carrier and drug, respectively.

## Materials and methods

### 1. Powder mixtures

Blends of salbutamol sulphate ( $2.8\mu\text{m}$ ) and lactose in the size fractions of  $63-90\mu\text{m}$  and  $<20\mu\text{m}$  were prepared in ratios of 1:135, 1:67.5 and 1:33.7. A ratio of 1:1 and 1:64 were prepared when the salbutamol was mixed with the carrier sizes of  $<20\mu\text{m}$  and  $63-90\mu\text{m}$ , respectively. The later ratios were required to saturate the carrier surface with the drug particles.

The use of a micronized drug without any carrier added to the formulation was also investigated.

## **2. Flow rate**

Experiments were conducted at flow rates of 60 and 150 l/min.

### **Results and discussion**

The deposition behaviour of a drug from powder mixtures containing different drug concentrations is compared in Figures 3.14 to 3.17. A similar pattern of deposition was observed at the two flow rates employed. The amount of the drug retained in the inhaler was inversely related to the proportion of lactose in the powder mix and it was greatest when salbutamol was used without any carrier. A lower deposition in the preseparator stage and a noticeable rise in the respirable fraction were observed as the proportion of lactose in the mix was reduced particularly at an air flow of 150 l/min.

No significant increase in the respirable fraction was observed when a high drug concentration was used at a flow rate of 60 l/min. This indicates that the separation force was not sufficient to overcome the interparticulate adhesive forces. However, the amount of the drug deposited on stages 3 to 7 was higher when the fine carrier ( $<20\mu\text{m}$ ) was used. This was attributed to the effect of the carrier size on the adhesion characteristics (see Section 3.4.9).

Additionally, when the fine carrier was used in a 1:1 ratio, a high percentage of the drug was retained in the preseparator at an air flow of 60 l/min. This might be explained by the formation of agglomerates at this concentration; the surface available for adhesion being not sufficient for the dispersion of the fine drug particle and the low air speed was not enough to break such agglomerates. However, as the proportion of lactose was increased

Effect of drug concentration in the powder mix on the characteristics of an inspirable cloud using a carrier size of 63-90um at different airflow rates

% Drug deposited at various stages at air flow of 60 l/min using carrier size of 63-90um.

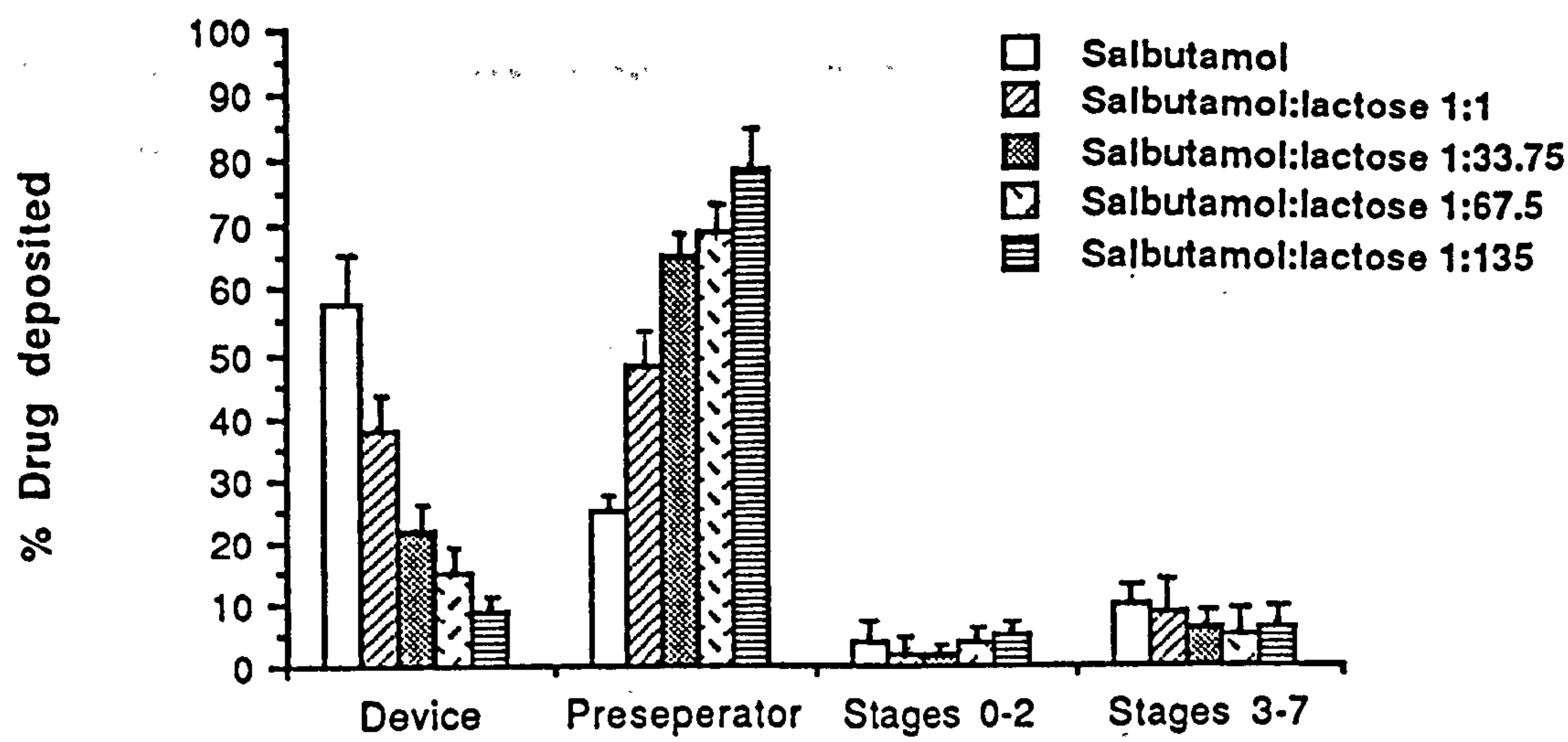


Fig 3.14

% Drug deposited at various stages at air flow rate of 150 l/min using carrier size of 63-90um

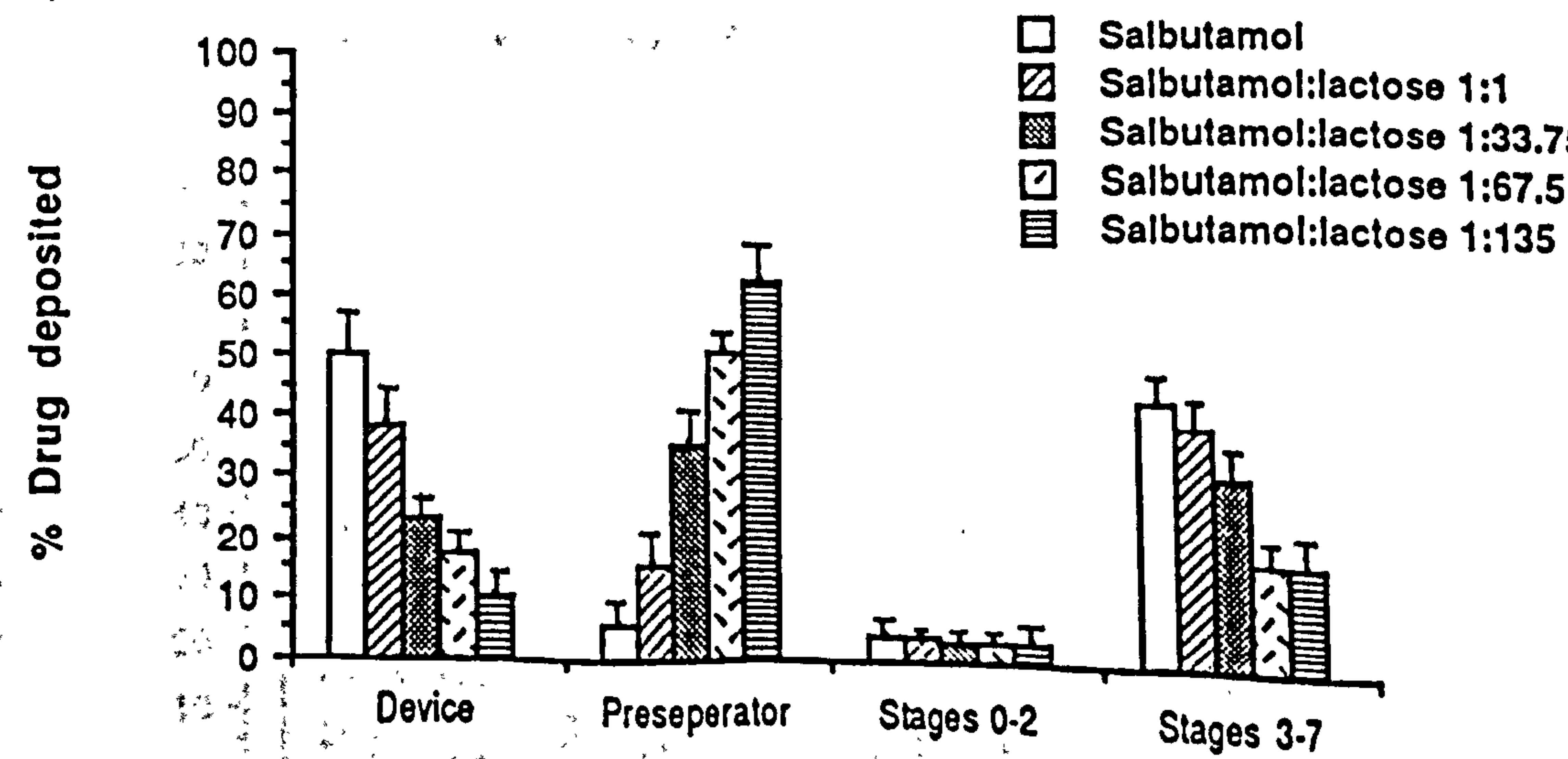


Fig 3.15



Effect of drug concentration in the powder mix on the characteristics of an inspirable cloud using a carrier size of <20um at different airflow rates

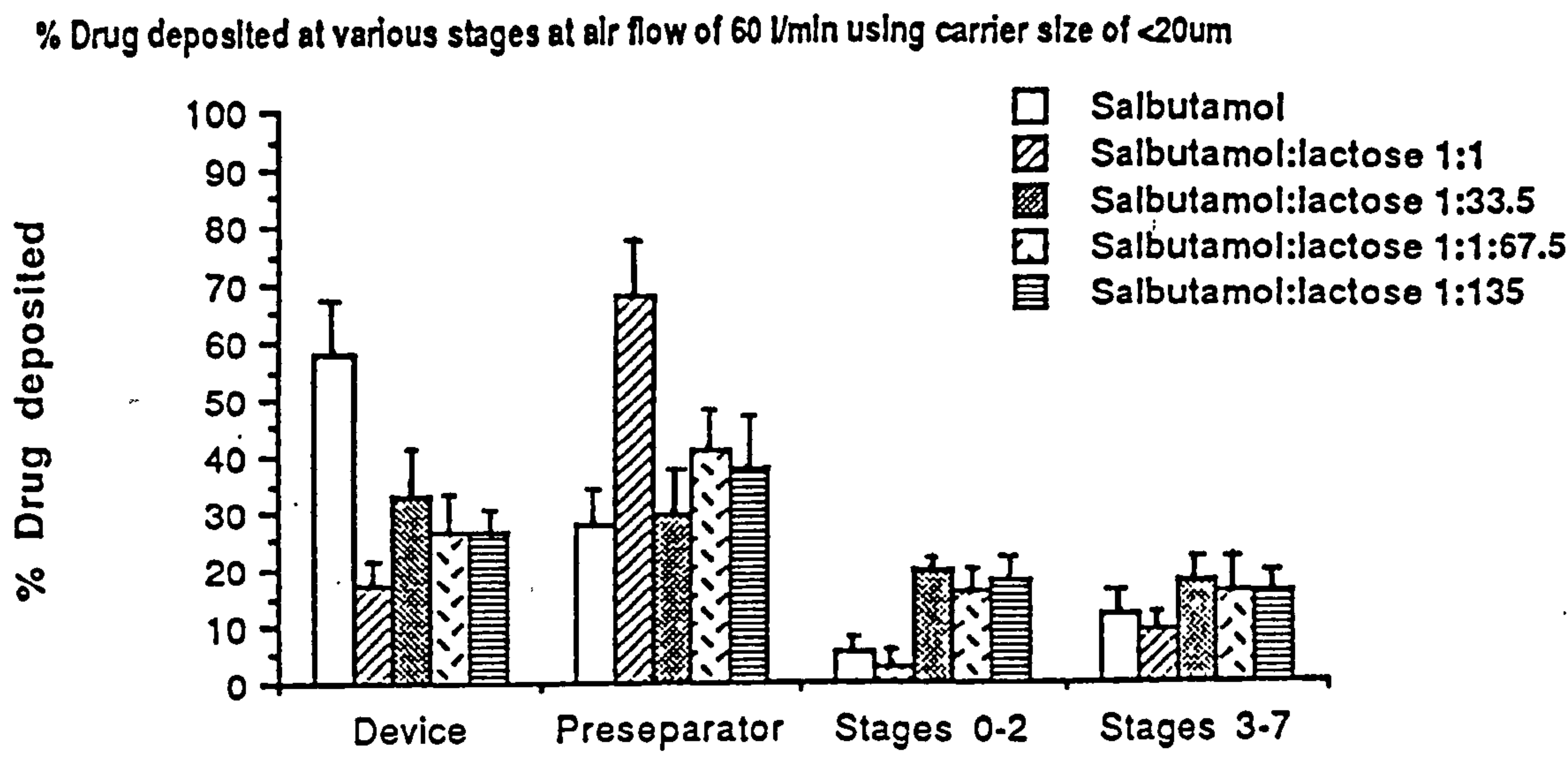


Fig 3.16

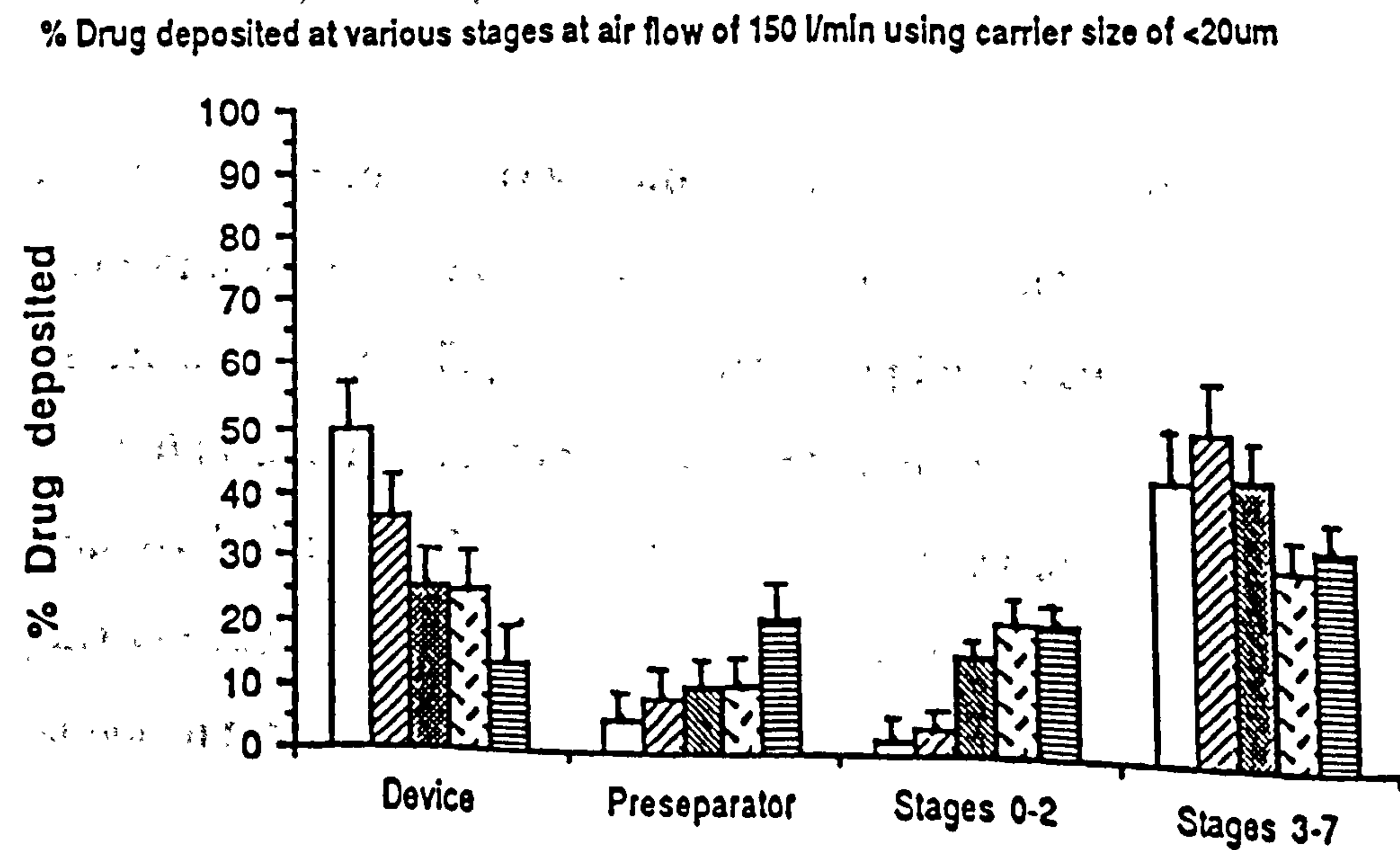


Fig 3.17

in the mix, more surface was available for particle distribution and looser or fewer agglomerates were formed.

No significant variation in the fraction deposited on stages 0 to 2 was observed with the different concentrations of the drug employed. However, more drug was recovered from these stages when a fine carrier was used since some of the lactose particles were in a size range comparable to that of the drug particles, thus forming aggregates.

The results show that the addition of lactose to the formulation improved emptying of the inhaler, thus more drug was made available for "inhalation". This has been reported by Bell *et al* (1971) who demonstrated the extensive coating of the interior walls of a capsule with the drug particles in the absence of a coarse carrier; they suggested the addition of a flow aid in any proportion. However, the results of this study suggest that the lactose cannot be added in any proportion since increasing the amount of lactose in the formulation resulted in a reduction in the respirable dose. Thus, when lactose is added, a compromise between powder fluidisation and lung penetration must be taken into consideration.

The increase in the respirable fraction at the higher drug concentrations can be explained in terms of adhesion of the drug to the carrier surface. Figure 3.18 shows the photomicrographs of the ordered mixtures formed at the different concentrations of the drug employed. The tendency of the adherent drug particles to form particle layers increased with the concentration of the drug. Although the amount of drug which could be accommodated on the

**1:135**

**1:33**

**1:1**



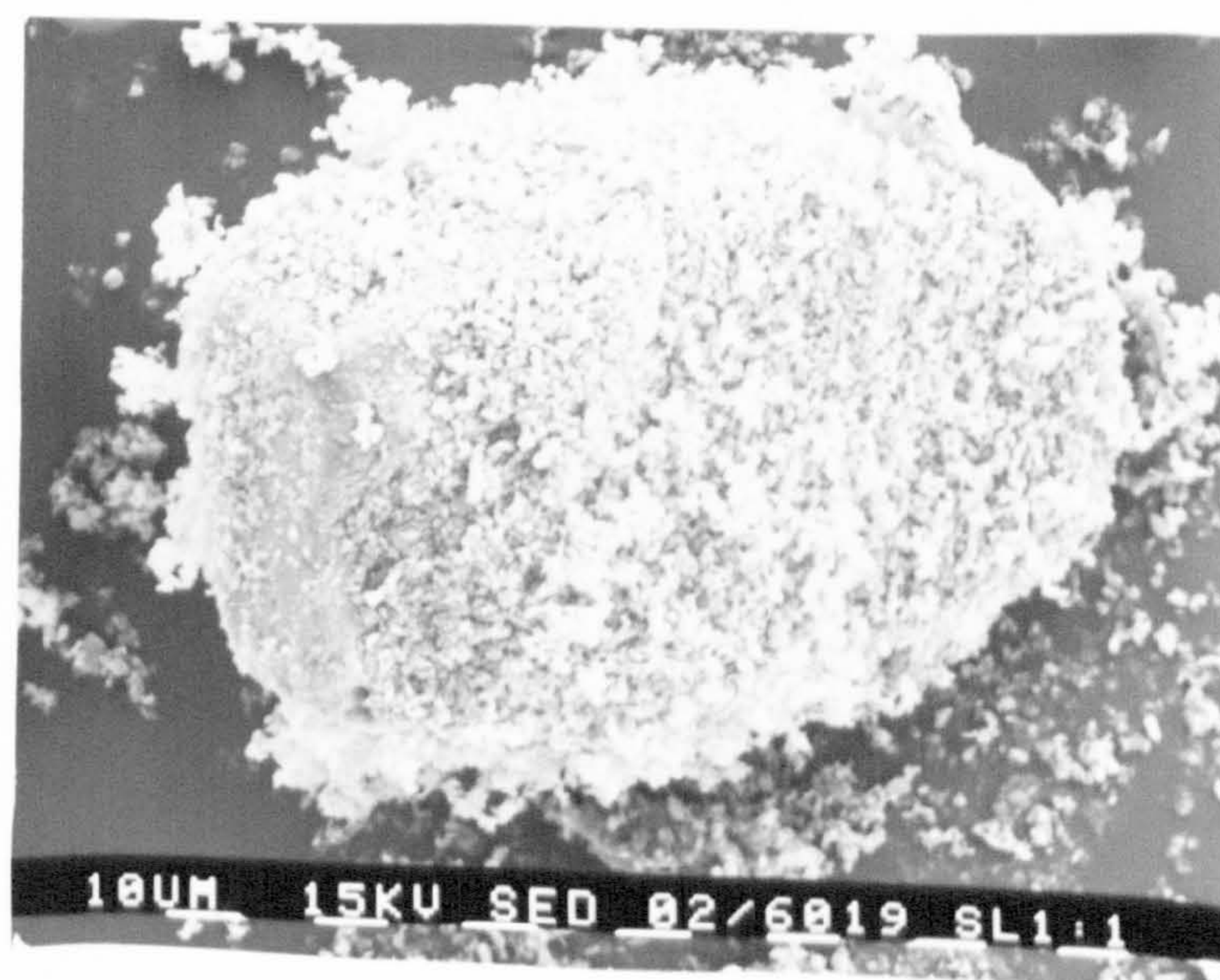
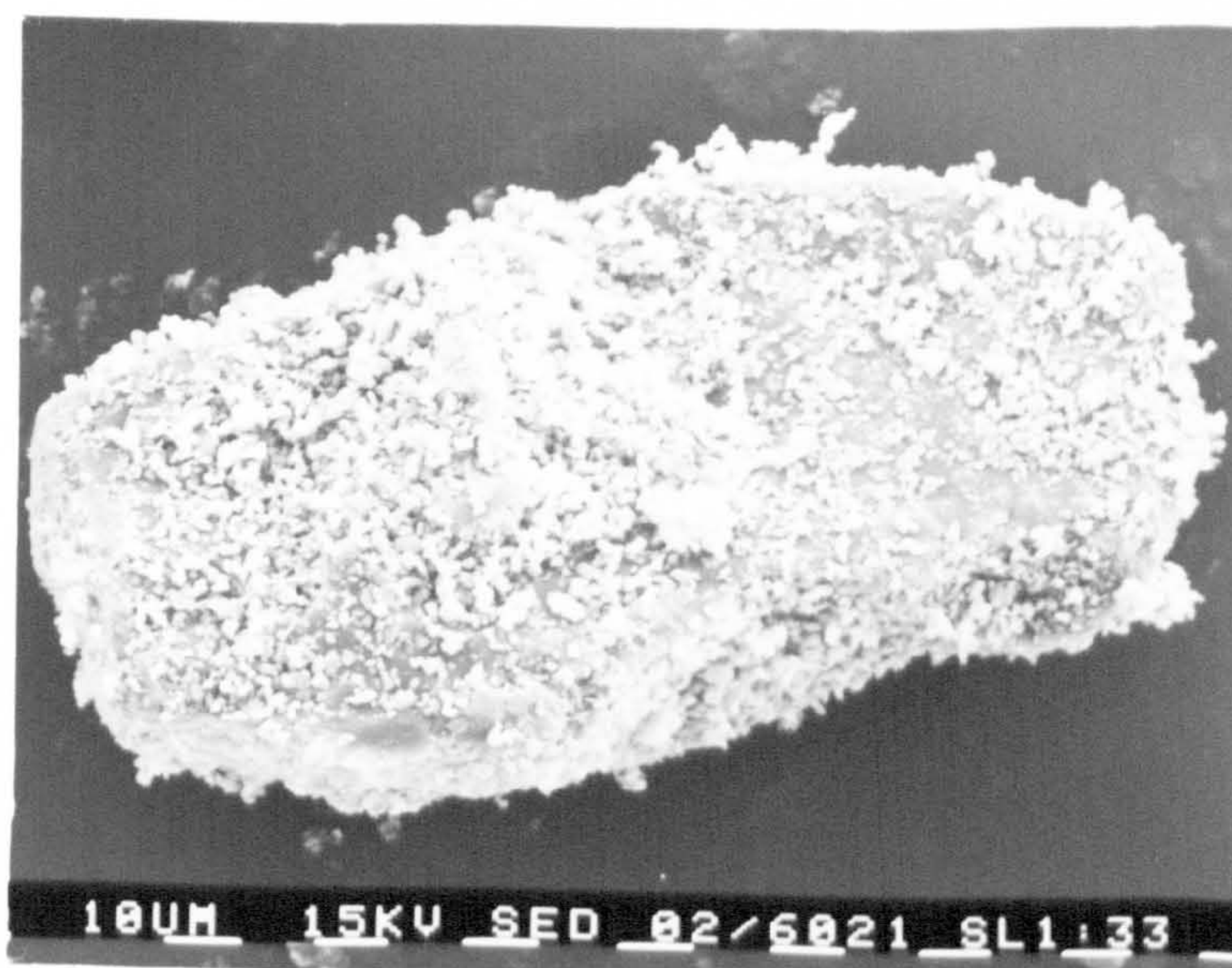
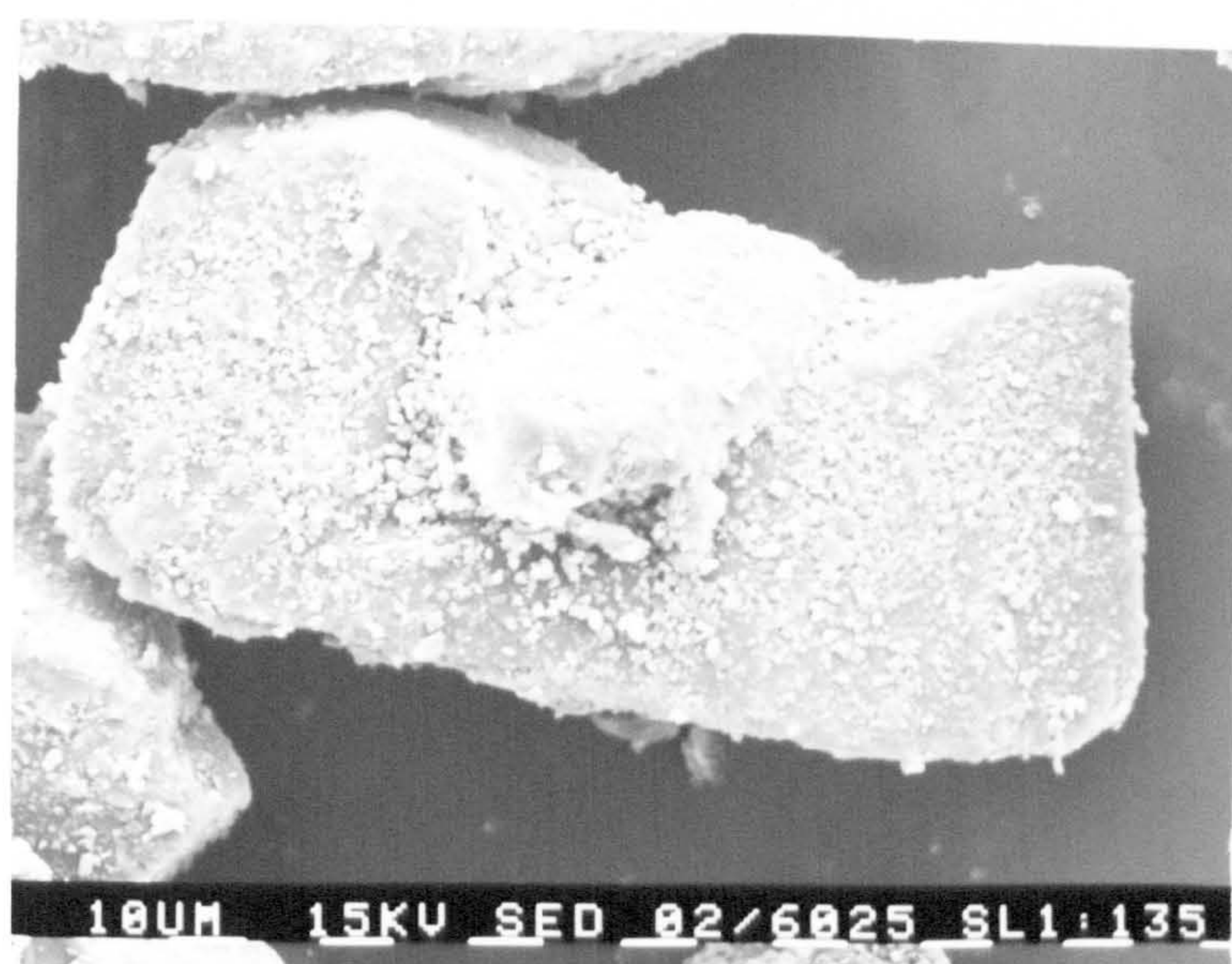
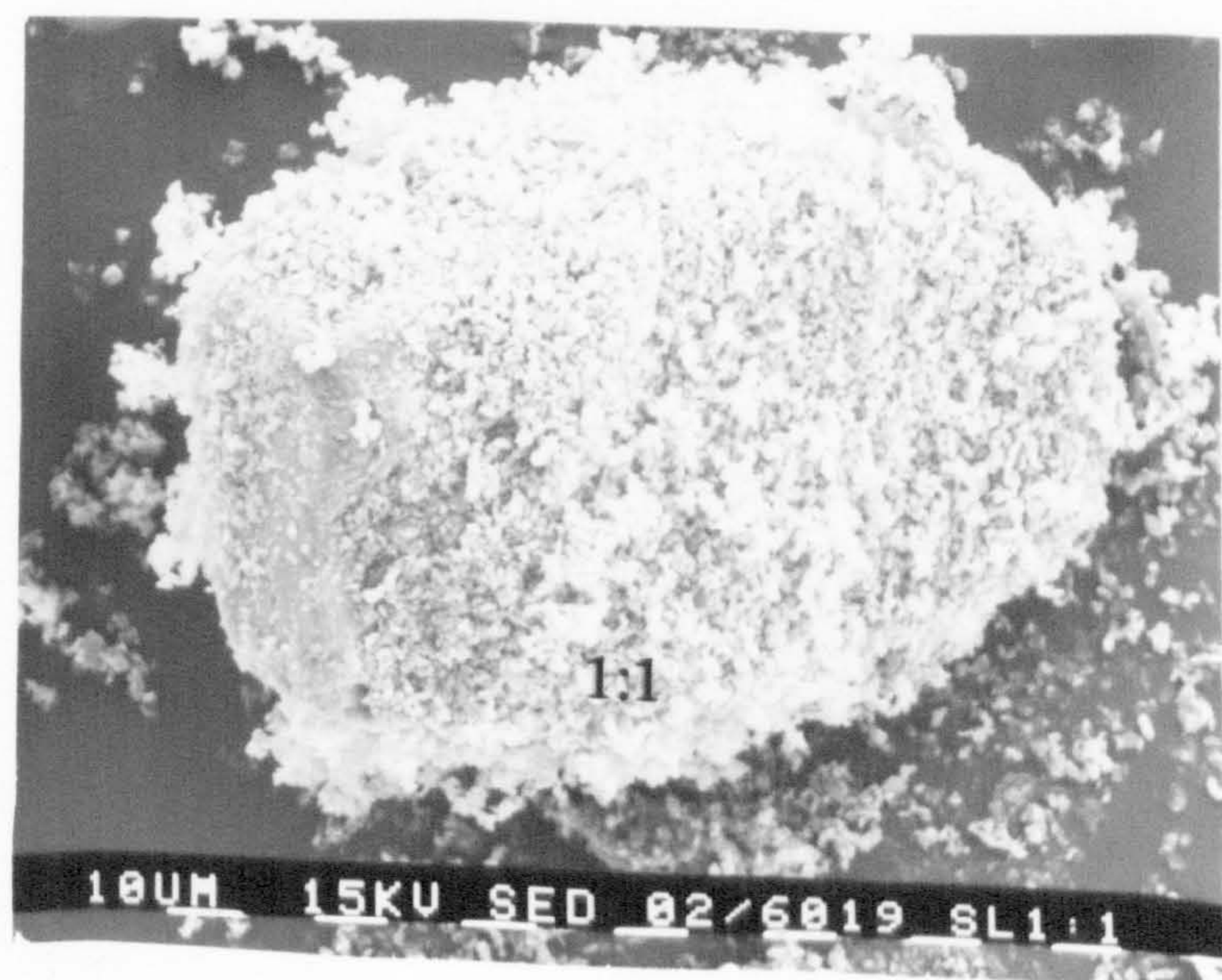
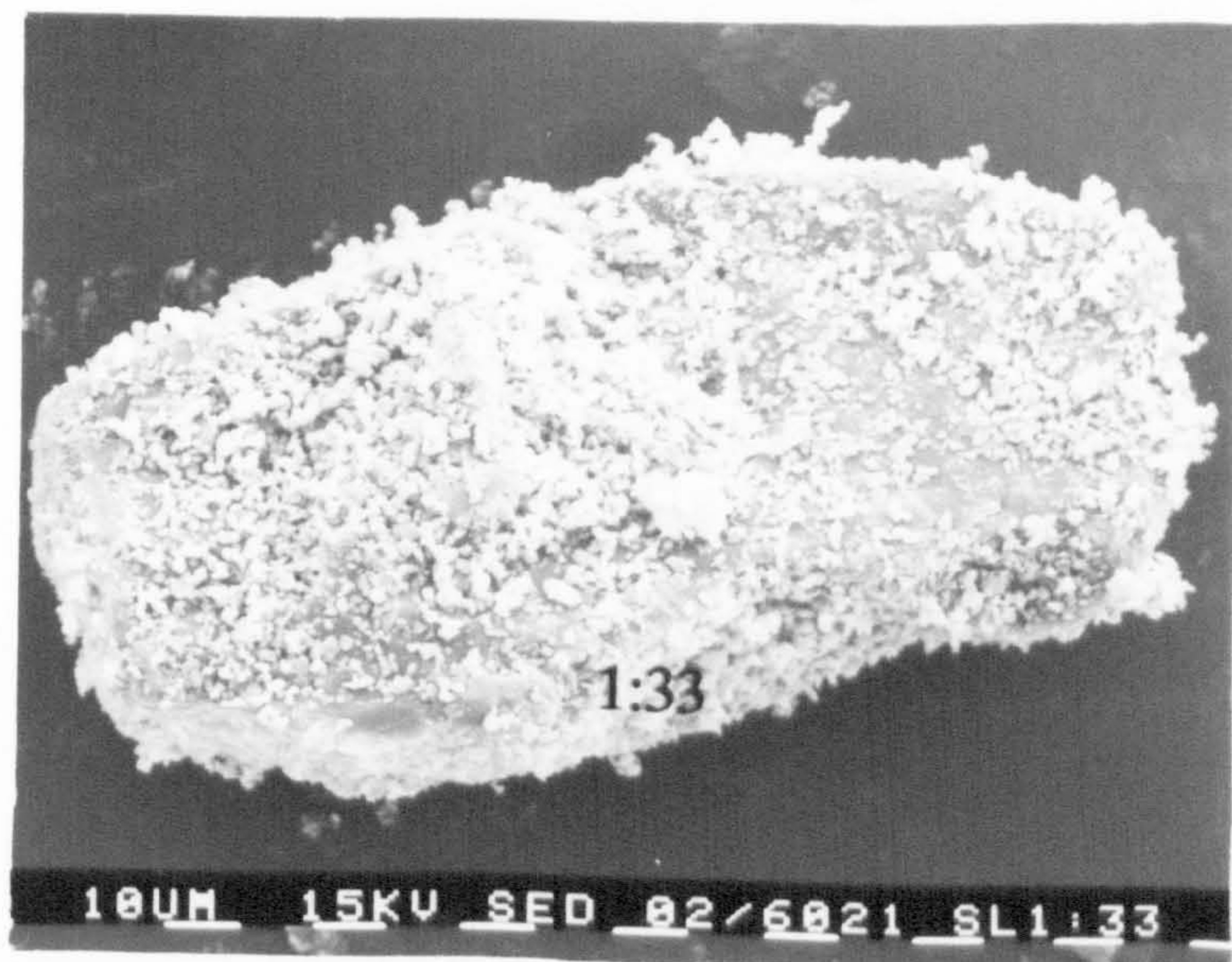
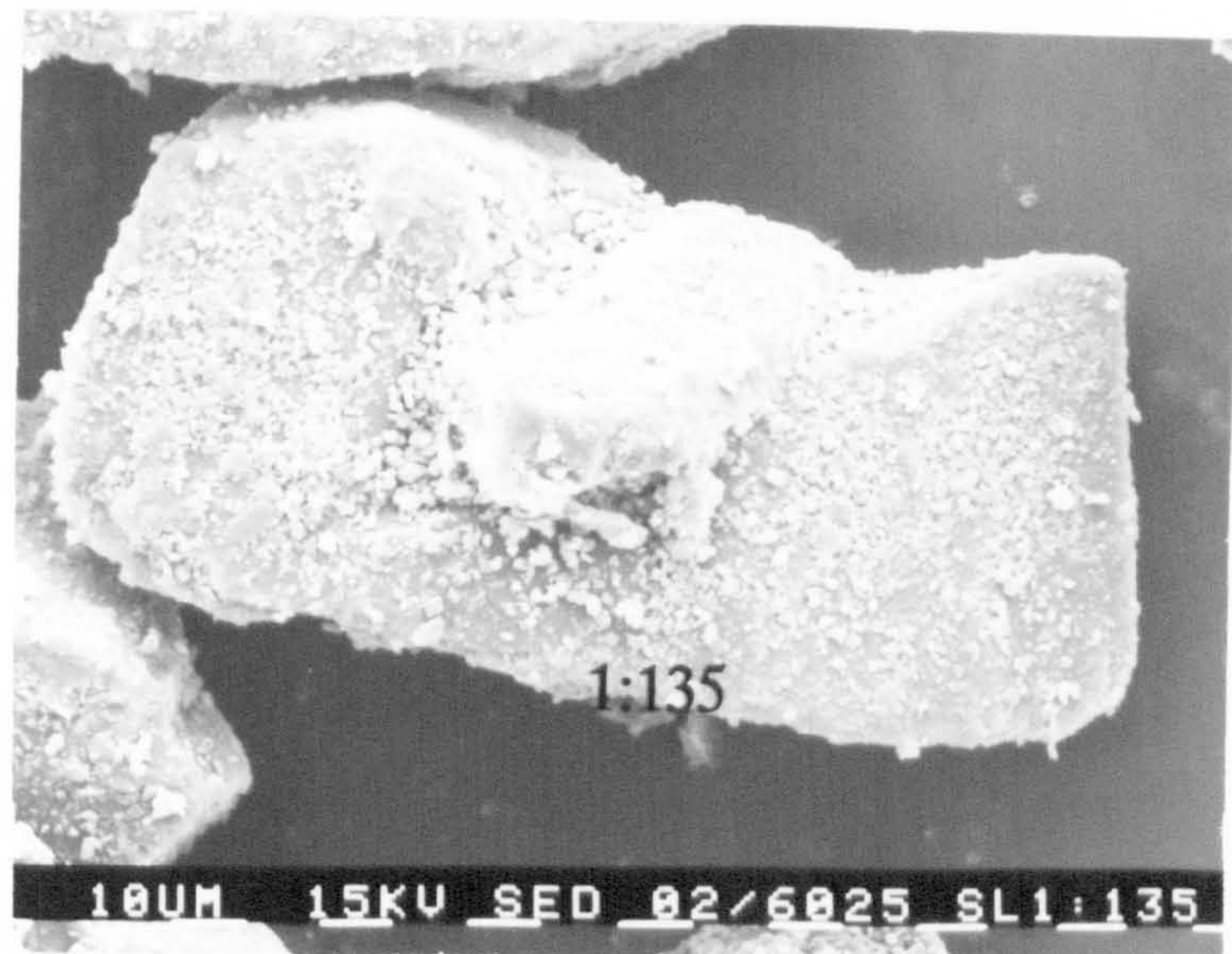




Fig 3.18 Scanning electron micrographs of mixtures of different drug to carrier ratios





carrier surface as a monolayer was theoretically estimated as 1:6.4 drug to carrier ratio for a carrier size of 63-90 $\mu$ m, particle layers were formed well below this value (Figure 3.18).

Therefore, the calculation of a monolayer produced an overestimate of the amount of particles covering the carrier surface.

Additionally, the particle layer formation observed at the high drug concentration occurred despite the availability of a free space on the carrier surface. These observations are supported by Hersey (1975) who suggested that some areas of the carrier surface are devoid of binding sites and some sites are stronger than others. Therefore, due to the limited number of active sites, as the concentration of the drug increases, the excess drug particles which are not capable of forming strong bonds with the carrier will either form weaker association or remain free in the bulk mixture. Another possible explanation is that a multiple detachment of drug particles might occur either due to a collision effect or a particle layer formation.

As the concentration of the drug in a mixture increases, the interparticle distance decreases with a greater chance for particle collisions to occur. The collision effect results from the impingement of the detached particles with neighbouring particles which were in their path as they leave the carrier. Particles detach from the carrier surface in a way which depends on the direction of the forces acting on the particle. They might be removed by sliding or rolling off the carrier. Consequently they tend to collide with other particles resulting in multiple detachment.

Furthermore, a rough surface of the carrier facilitates the formation



of particle layers. Fine powders tend to fill up the surface irregularities in agglomerates rather than in a particulate manner. Therefore, multiple detachment in the form of particle layers might occur if the binding force between the inner particles in contact with the carrier surface is less than the external force applied. These particle layers then break up into single particles at the high air speeds.

The results are at variance with the findings of Chowhan and Linn (1978) and Chowhan and Amero (1977) who reported that an increase in the lactose proportion in the formulation of powder aerosols would result in an increase in the respirable fraction.

However, their studies were carried out at an air flow of 29 l/min which may have been inadequate for complete fluidisation of the powder. Here, the influence of increasing the proportion of lactose in their powder mix would have overcome problems in powder flow. Consequently the possibility of drug penetration into the respiratory tract would have increased as a result of dispensing higher drug doses rather than an efficient redispersion of the drug particles from the carrier surface.

Therefore, it can be concluded from this study that the higher the drug concentration in the formulation, the more efficient is the drug delivery to the lungs. However, this is only true at high flow rates since a large force is required to breakup the aggregates and agglomerates.

#### **3.4.4 The effect of a ternary component in the mix**

It has been observed by Lai and Hersey (1979) and Staniforth and

Rees (1982) that the presence of a ternary component might stabilize or de-stabilize the powder mixture. The addition of magnesium stearate and colloidal silicas was reported to reduce the mechanical stability. Therefore in the following study, although dry powder aerosols are usually comprised of the drug and the carrier only, the effect of adding these two materials to the powder mix was investigated.

## **Materials and methods**

### **1. Powder mixtures**

The ternary mixtures were prepared by tumbling lactose in the size range of 63-90 $\mu$ m with 1.5% magnesium stearate or 1.5% "Aerosil" 200 for three days in a glass jar using a roller mill. These were then mixed with micronized salbutamol sulphate (2.8 $\mu$ m MMD) in a ratio of 1:67.5.

### **2. Flow rate**

The aerosol cloud was generated at air flow rates of 60 and 150 l/min.

## **Results and discussion**

The drug deposition behaviour of the powder mixtures containing magnesium stearate or "Aerosil" as the ternary component is shown in Figures 3.19 and 3.20. The pattern of deposition is compared with that obtained for a regular lactose.

When lactose tumbled with either magnesium stearate or "Aerosil" was used, a slightly higher amount of the drug was retained in the inhaler in comparison with regular lactose. As for the deposition on

Effect of the presence of ternary component in the powder mix on the characteristics of an inspirable cloud at different airflow rates

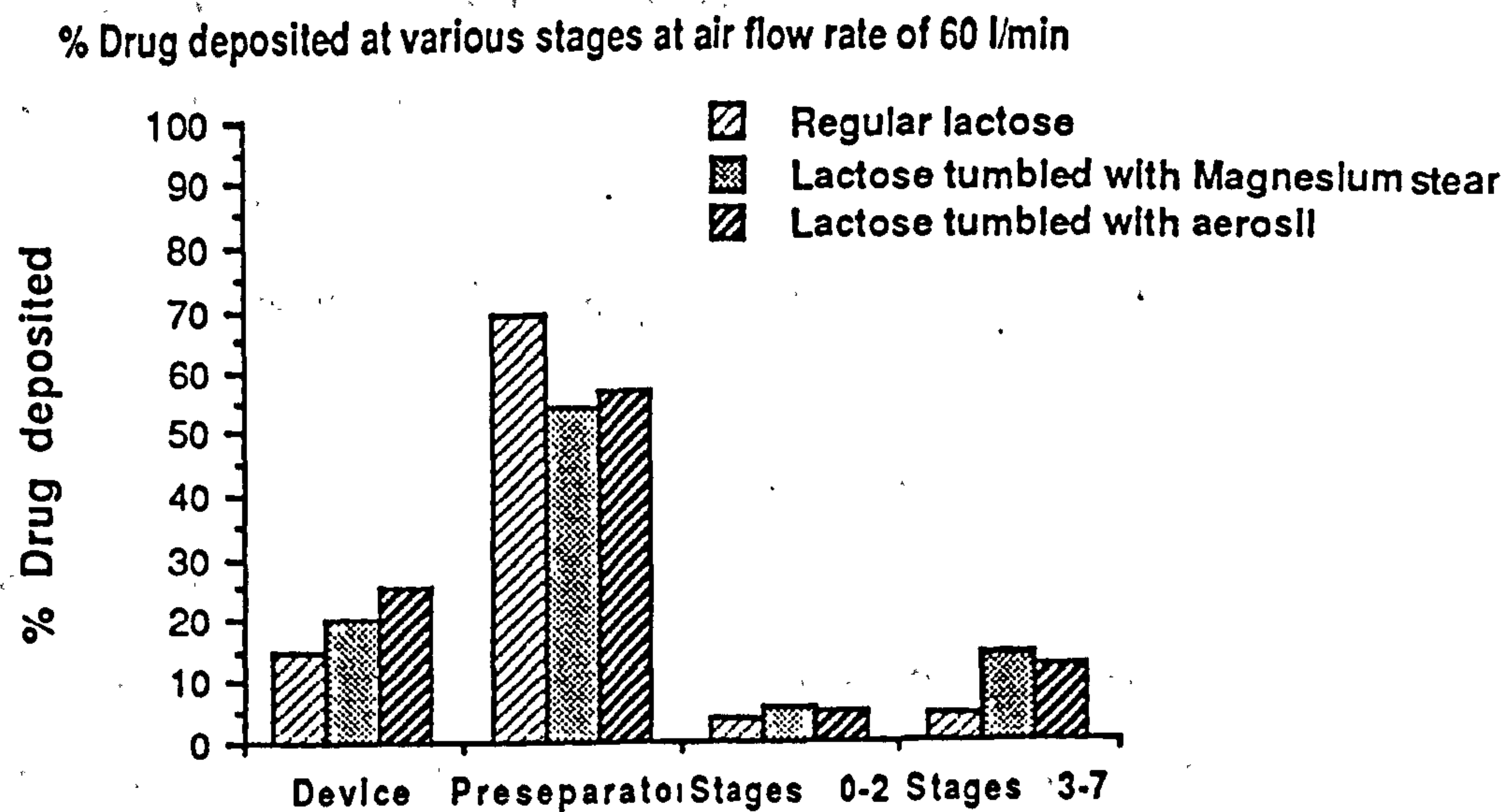


Fig 3.19

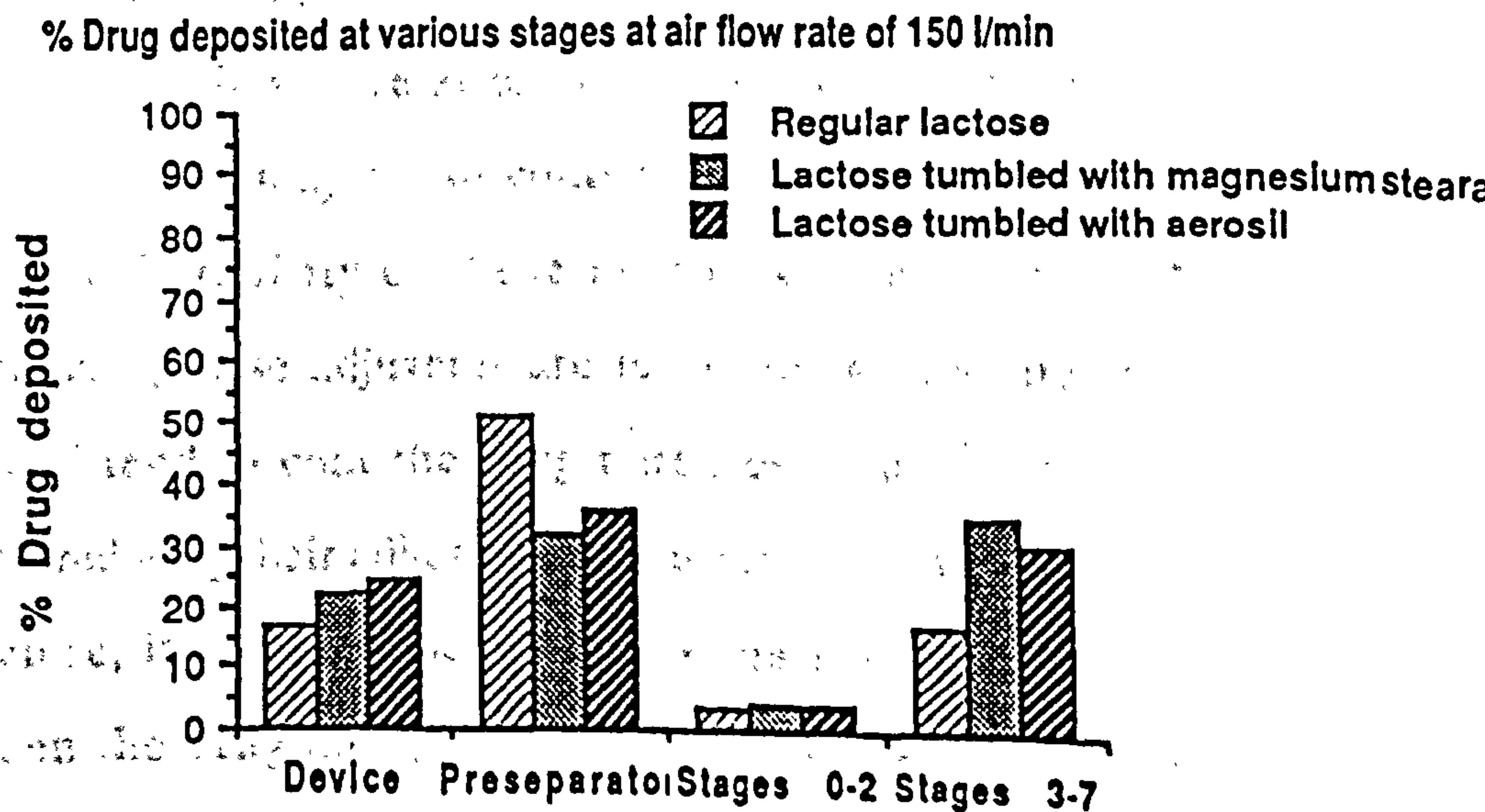


Fig 3.20



the other stages, the percentage of the drug recovered from the preseparator stage was significantly reduced when either magnesium stearate or "Aerosil" was present in the mixture. This was accompanied by an apparent increase in the respirable fraction. For instance, at an air flow of 150 l/min, the amount of drug retained in the preseparator decreased from 50% to 35% and the respirable fraction increased from 17% to 34% with regular lactose and lactose tumbled with magnesium stearate, respectively. When "Aerosil" was used, the respirable fraction was slightly lower (30%).

A similar pattern of deposition was observed at 60 l/min. However, only 14% of the drug was recovered from stages 3 to 7.

These results indicate that the characteristics of an inspirable cloud are highly influenced by the presence of a ternary component. These components may act by binding to the strong active sites and/or by filling the surface irregularities during the tumbling process. Another possible explanation is that these components act by stripping the drug particles from the carrier surface as described previously by Lai and Hersey (1979). The electrostatic behaviour of these materials in relation to the other components of the powder mixture might also contribute to the reduction of the mechanical stability of these mixtures (see Section 3.5.3). Additionally, these adjuvants are lubricants with a large surface area and tend to coat the drug particles with a lubricant film thereby reducing their adhesion tendency to the carrier surface.

Therefore, it can be concluded that the extent of association between the drug and the carrier was altered in the ternary mixtures by one or more of the above mechanisms. This resulted in a more efficient redispersion of the drug particles.

However, the effect of adding another component to the mixture is difficult to predict and is complicated by the behaviour of the powder constituents in relation to each other. Thus, three possibilities exist: the mechanical stability of the powder mixture may be enhanced, reduced or unaffected by the presence of other adjuvents.

Hence, although addition of both magnesium stearate and "Aerosil" resulted in a more highly respirable cloud from the powder mixtures employed in this study, these two adjuvents may behave differently when used with other powder mixture components.

#### **3.4.5 The effect of carrier size**

The choice of the carrier size in dry powder aerosols is based on two main aspects. First, a very large carrier i.e.,  $>200\mu\text{m}$ , is unsuitable as it is difficult for these particles to be carried by the inhalation air stream due to gravitational forces. Second, the use of very fine carrier particles is undesirable due to the poor flow properties of these mixtures which create problems of filling and dispensing. Therefore, the carrier size employed in the formulation of powder aerosols is mainly in the range of  $30\text{-}90\mu\text{m}$ , with a very limited fraction of finer and coarser particles. In the following investigation a range of carrier sizes from  $<10\mu\text{m}$  and up to  $180\mu\text{m}$  were employed to study the influence of carrier size on the inspirable characteristics of an aerosol cloud.

### **Materials and methods**

#### **1. The powder mixtures**

Blends of salbutamol sulphate ( $2.8\mu\text{m}$  MMD) and regular lactose in



size fractions of 125-180 $\mu$ m, 63-90 $\mu$ m, 20-40 $\mu$ m, <20 $\mu$ m and <10 $\mu$ m were prepared in a ratio of 1:67.5. Mixtures of the drug and unclassified lactose were also investigated.

## **2. Flow rate**

The aerosol cloud was generated at air flow rates of 60,100,150 and 200 l/min.

### **Results and discussion**

The influence of the flow rate on drug deposition on stages 3 to 7 with all the carrier sizes employed is shown in Figure 3.21.

The results show that an increase in the air flow rate resulted in an increase in the respirable fraction with all the carrier sizes used. For instance, at an air flow of 200 l/min and a carrier size of <10 $\mu$ m, 47% of the drug was deposited on stages 3 to 7 in comparison with 17% at a flow of 60 l/min.

The influence of the carrier size and flow rate on the fractional deposition of the drug is given in Table 3.8.

The data indicate that emptying the inhaler was more efficient at the higher flow rates and that more drug was retained when a fine carrier was used. The latter can be explained by the high cohesiveness of these powders as illustrated by their tensile strength values (Figure 3.1).

Drug deposition on the other stages was found to be highly dependent on the carrier size. When a coarse carrier was used, a high fraction of the drug was recovered from the preseparator stage indicating a high association with the carrier. For finer carriers, the



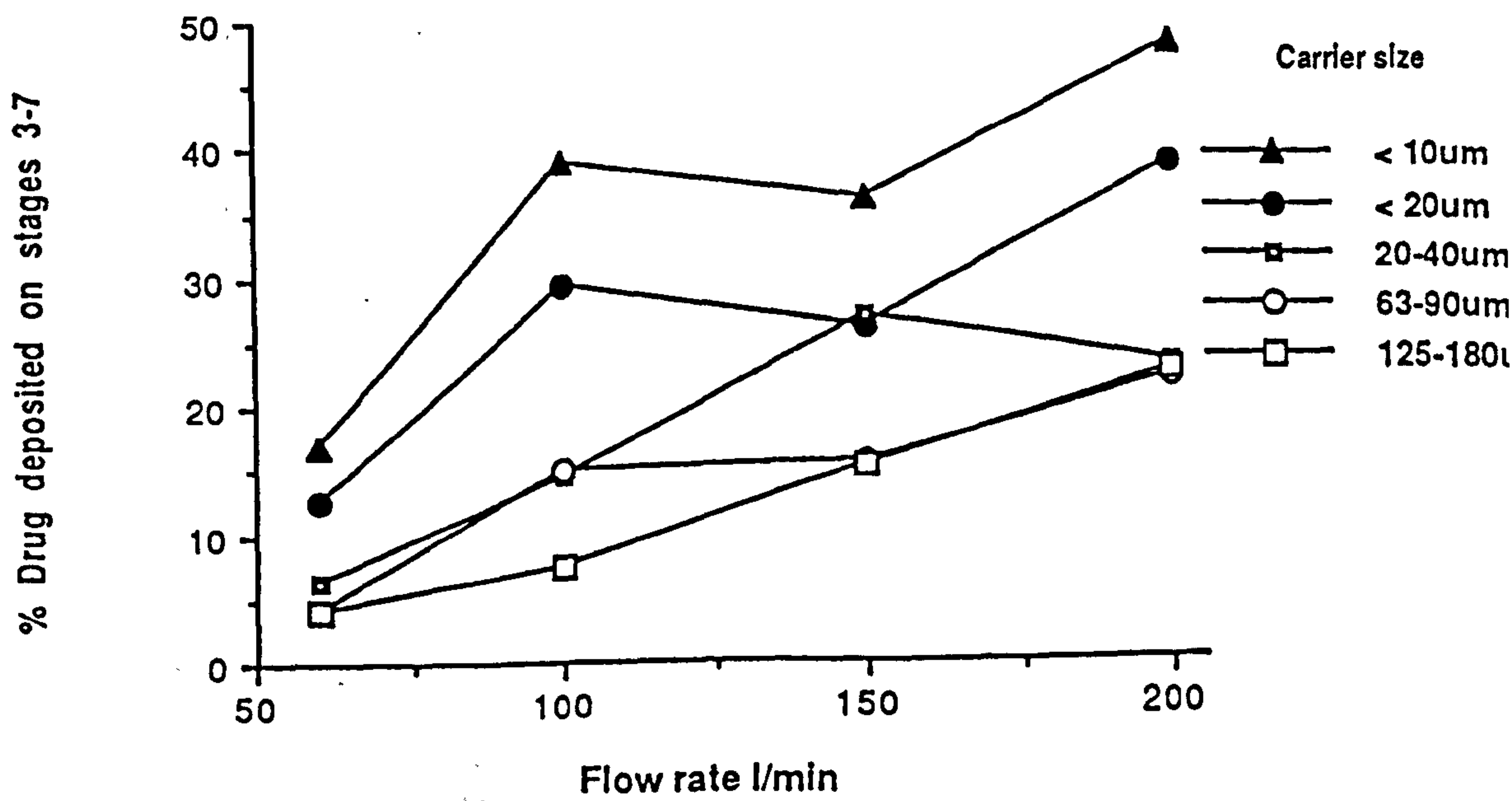


Fig 3.2] Effect of airflow rate on the amount of drug deposited on stages 3-

**Table 3.8** The percentage of dose deposited at various stages

Flow rate l/min	Device	Preseparator > 10um	Stages 0-2 5-10um	Stages 3-7 < 5um
<b>Carrier size &lt;10um</b>				
200	14.2	7.1	15.6	47.7
150	18.5	7.2	23.9	36.0
100	26.2	17.1	11.1	38.9
60	29.5	26.2	9.2	16.9
<b>Carrier size &lt;20um</b>				
200	13.7	9.2	14.7	38.4
150	22.8	9.1	16.6	26.0
100	19.8	20.0	19.3	29.5
60	27.2	40.7	10.9	12.7
<b>Carrier size 20-40um</b>				
200	17.7	26.3	2.3	23.0
150	17.6	22.0	2.3	27.0
100	21.2	32.8	2.9	14.5
60	20.1	46.0	2.1	6.4
<b>Carrier size 63-90um</b>				
200	14.5	50.2	1.2	22.0
150	15.2	51.9	1.3	15.6
100	15.1	61.0	1.3	15.2
60	13.2	69.0	1.3	4.1
<b>Carrier size 125-180um</b>				
200	13.0	55.2	2.0	22.5
150	14.3	64.5	1.5	15.4
100	15.6	73.9	0.9	7.5
60	10.3	82.2	0.5	4.0
<b>Unclassified lactose</b>				
200	19.3	22.0	8.4	27.7
150	19.9	22.4	8.5	26.4
100	19.9	26.4	11.9	21.5
60	20.3	46.0	10.9	13.2

low drug deposition in the preseparator and the high fraction deposited on stages 3 to 7 indicate that the interparticle adhesion forces were reduced. These effects were observed at all flow rates showing that the detachment of the fine drug particles from the surface of the carrier decreases as the particle size increases. This can be explained by examining the electron photomicrographs (Fig3.22) which indicate that the coarse lactose particles provide stronger adherence sites due to the more surface discontinuities shown by the increased surface roughness. This agrees with the findings of Staniforth *et al* (1982) who pointed out that the interparticle adhesion forces are much higher in ordered mixes based on large carrier particles. Smaller carriers release a higher fraction of the adhering particles due to the fewer strong adherence sites as can be seen from the photomicrograph (Figure 3.22). Another possible explanation is that the aerosol cloud comprising fine particles is more likely to be completely entrained by the air stream, thus responding to its acceleration and deceleration. Consequently the dislodgement of the fine drug particles from the carrier surface is more efficient. In comparison, the entrainment of a cloud comprising a coarser carrier by the air stream depends on the particle size distribution of the cloud i.e. the coarser the particles the lower the degree of entrainment.

As for the deposition on stages 0 to 2: when a coarse carrier was used, all the particles in the mixture were either larger or smaller than the cut-off size of these stages. Therefore, there can be virtually no material within this size range, unless formed by drug agglomerates. The small amount of deposition given in Table 3.8



**Fig 3.22 Scanning electron micrographs showing the surface details of**

**Fine lactose**

**Coarse lactose**



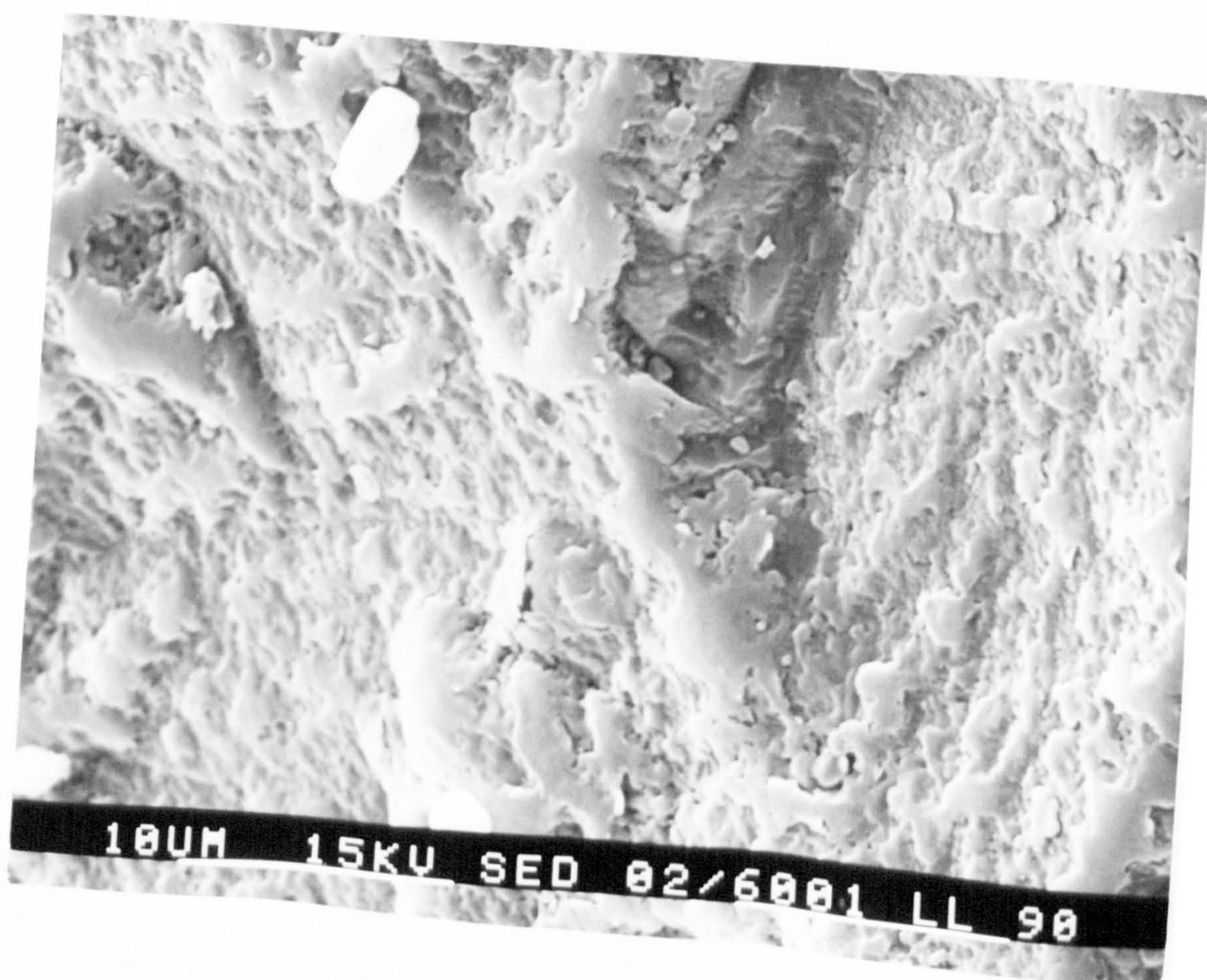
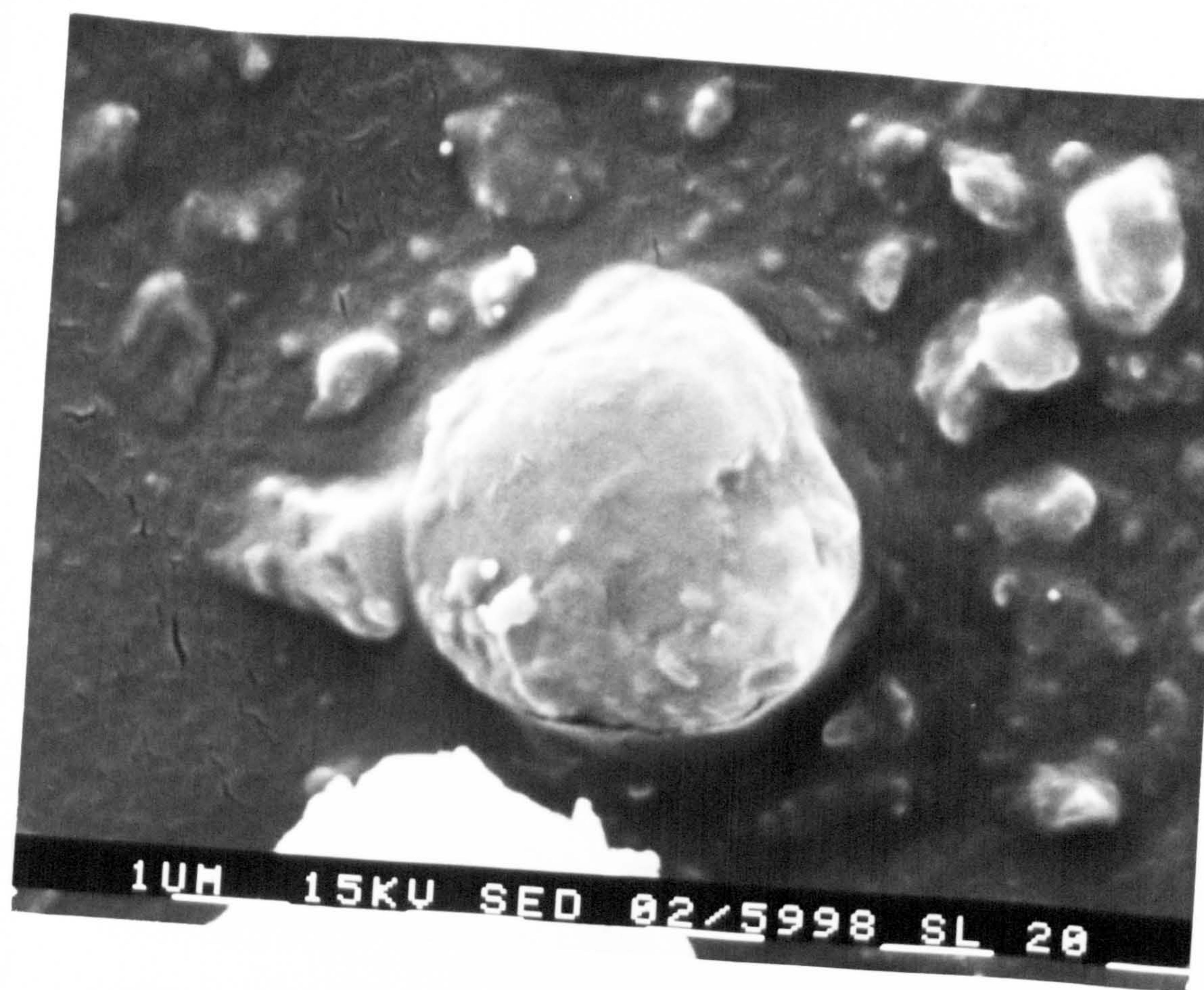
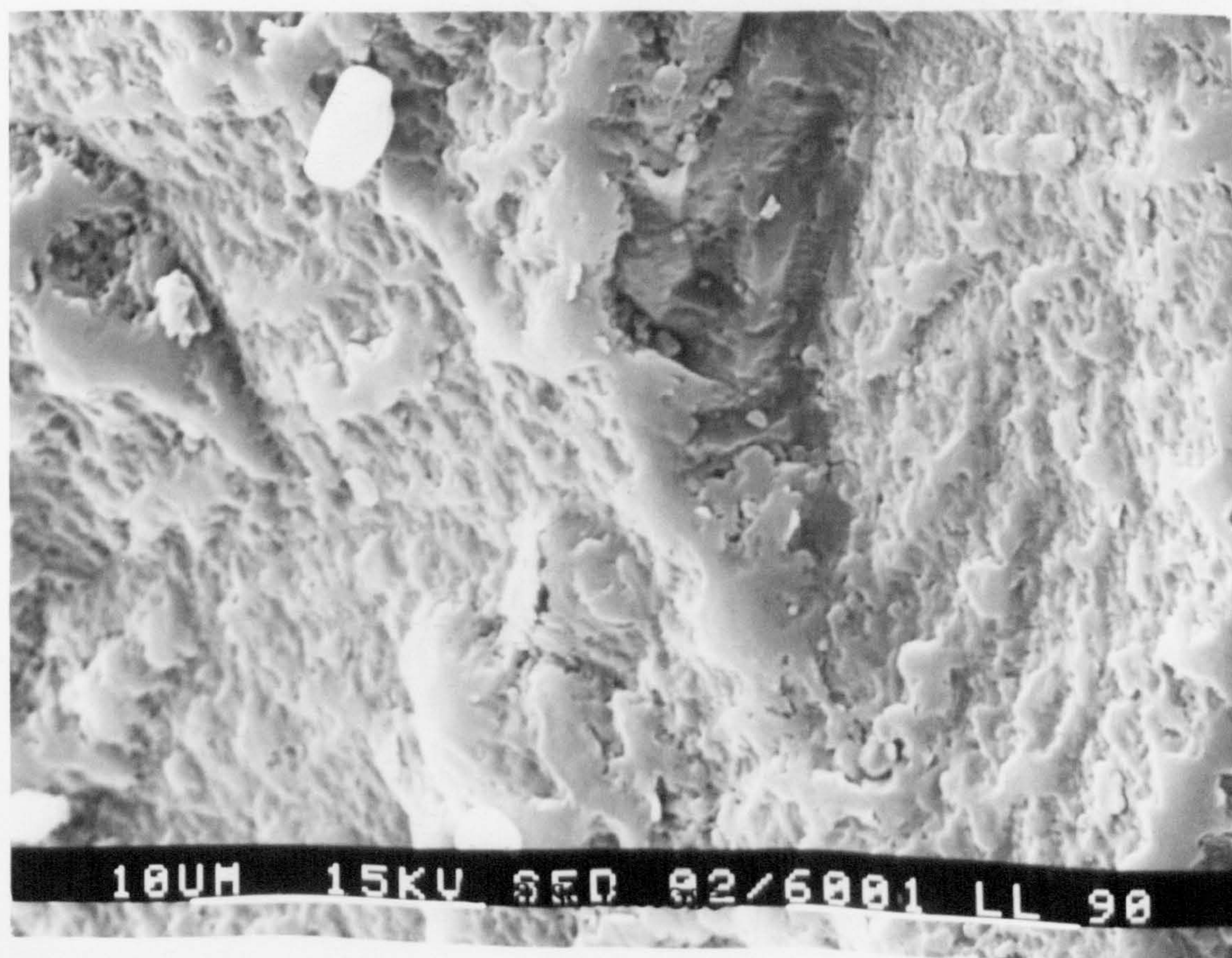




Fig 3.22 Scanning electron micrographs showing the surface details of





indicates that any such agglomerates would have been broken up during mixing by the mechanical action of the large particles. In formulations comprising a small carrier size, many particles were within the size range of these stages, therefore a high percentage of the drug was recovered as a coarse material, either as agglomerates or as drug adsorbed on the surface of the fine carrier.

When unclassified lactose was used in the formulation, intermediate results were obtained. For example, at an air flow of 150 l/min the amount of drug deposited on stages 3 to 7 was 26.4%. This is lower than that achieved by using the fine carrier (36.0%), but higher than that when the coarse carrier was used (15.4%). In such a mixture comprising coarse and fine particles, it is probable that the small particles release more of the adhering particles than the coarse ones, therefore contributing more to the effective delivery of the drug to the lungs.

Bell *et al* (1971) reported that the optimum carrier size in dry powder aerosols is in the range of 70-100 $\mu$ m, and that the use of finer or coarser carriers markedly reduces the respirable fraction. These observations were obtained with a "Spinhaler" and at airflow rates not exceeding 60 l/min. The use of a fine carrier limited the availability of the medicament due to the high retention of the drug in the capsule, since a flow rate of  $\leq 60$  l/min is insufficient for complete fluidisation of the powder. The use of coarser carriers resulted in an intermittent blocking of the holes drilled in the capsule wall, as dispensing occurs through these holes. A carrier size of 70-100 $\mu$ m provided optimum flow of the powder and avoided the problems observed with the coarser and finer carriers.

However, these observations are mainly applicable to the type of inhaler they used and the conditions of their experiment.

Thus, it can be concluded that the choice of the carrier size should not be based on the flow properties of the powder. The carrier size influences the characteristics of an inspirable cloud mainly by affecting the nature of the adhesive forces formed between the mixture components. A coarse carrier resulted in poor inspirable characteristics of a cloud, whereas a fine carrier was found to markedly improve the efficiency of a powder aerosol despite the poor flow properties.

However, if this carrier is to be used on a large industrial scale, several technical problems may be encountered. Therefore, the potential therapeutic advantages may have to be set against the possible production difficulties.

### **3.5 Electrostatic properties of powders**

Measurement of electrostatic charges provides useful information regarding the behaviour of particles forming the adhesive mix. In general, the larger the difference in magnitude of electropositive and negative charges of two sets of powder particles, the larger will be their mutual attraction.

Therefore, in dry powder aerosols, since the strength of the adhesive forces between the drug and the carrier is one of the major factors influencing the characteristics of an inspirable cloud, this investigation aimed to determine the sign and magnitude of the charge which develop on the powder mixture constituents.



### **3.5.1 Theoretical considerations**

Under normal handling, powders can become charged by contact, friction or impact against other surfaces, even in the absence of an externally applied electric field. Such charging is known as contact electrification or triboelectrification. The simple model of triboelectrification can be described by metal-metal contacts. The typical energy level diagram for a metal material is illustrated in Figure 3.23a. Electrons exist in the material within various energy levels up to the outermost level associated with the conduction of electrons, i.e. the Fermi level. The work function of a metal is the energy difference between the Fermi level and a reference level outside the molecule known as the vacuum energy level. On contact between metals possessing different work functions, electrons are transferred between surfaces until the Fermi levels are equal (Figure 3.23b). To reach this state, one material loses electrons to become electropositive, whereas the other material accepts the electrons thereby becoming electronegative. When the two surfaces are semiconductors or insulators, as in most pharmaceutical powders, the concept of work function is more complex. However, electrostatic charging will occur in a similar manner, although the charge transfer mechanisms are less well understood.

### **3.5.2 Electrostatic charge measurement**

The specific charge of powders was determined using a Faraday well connected to an electrometer (type 610C, Kiethley Instruments, Cleveland, USA).

The Faraday well, shown in Figure 3.24, is a double-walled vessel.



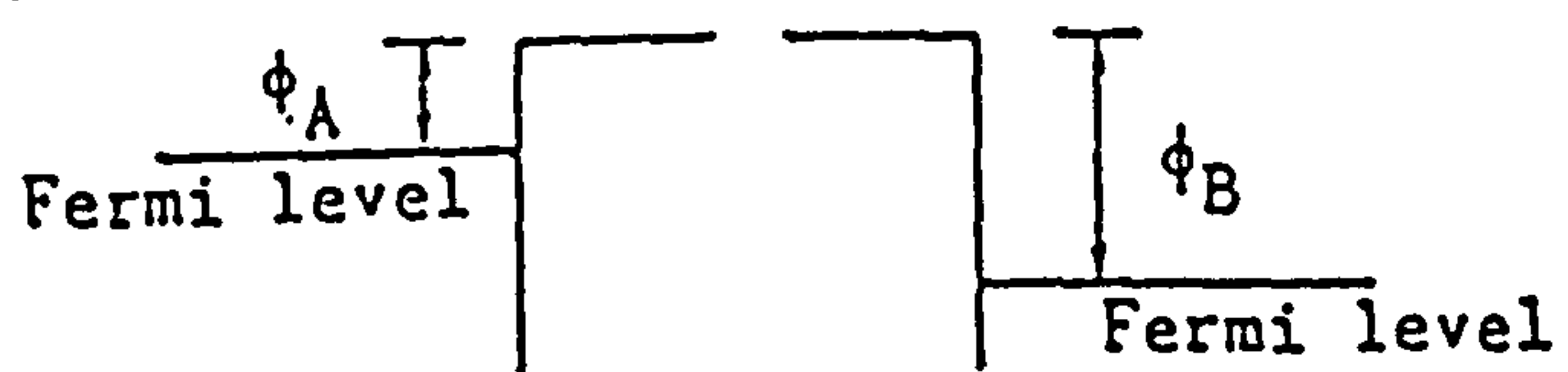
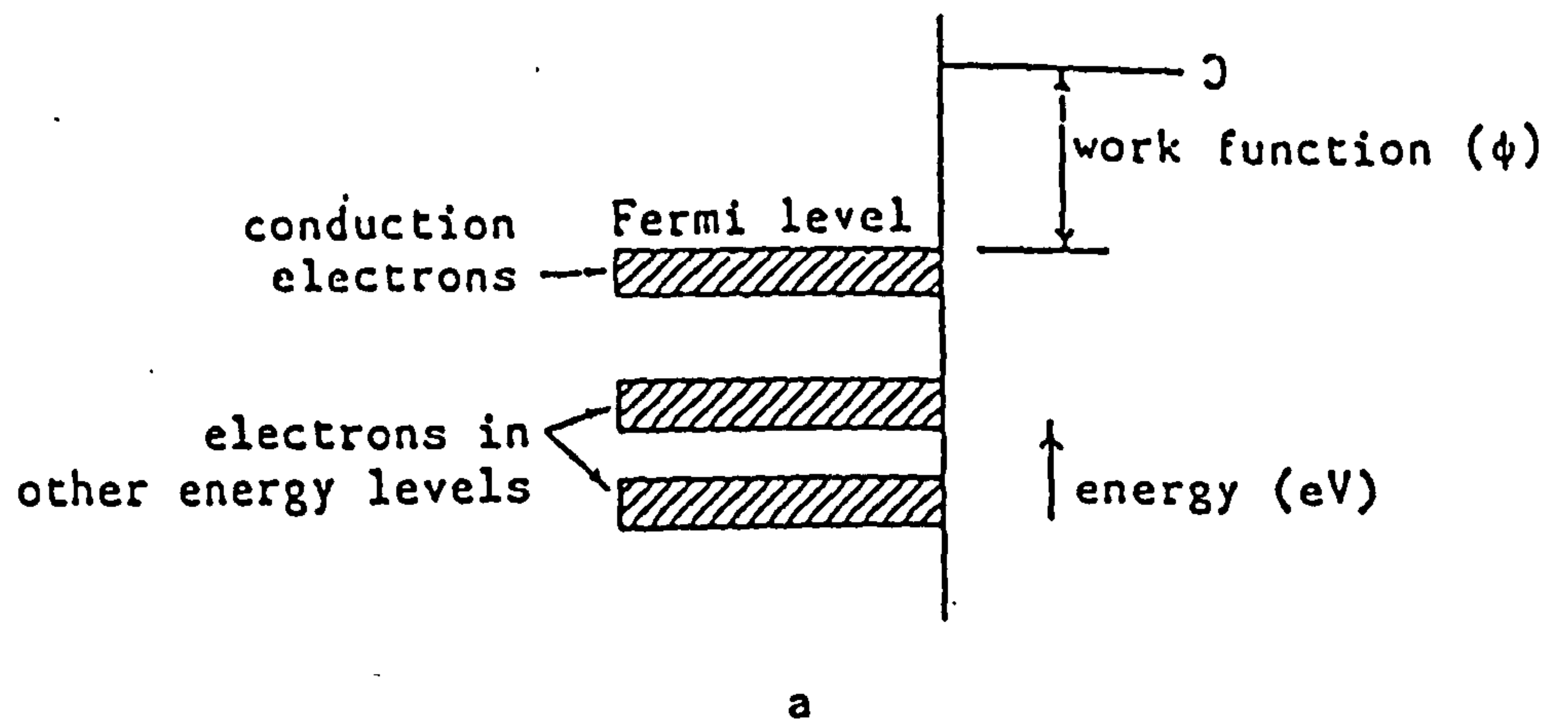


**Fig 3.23** a) Electron energy level of a metal material showing the Fermi level and work function  
b) Development of contact potential between material A and B

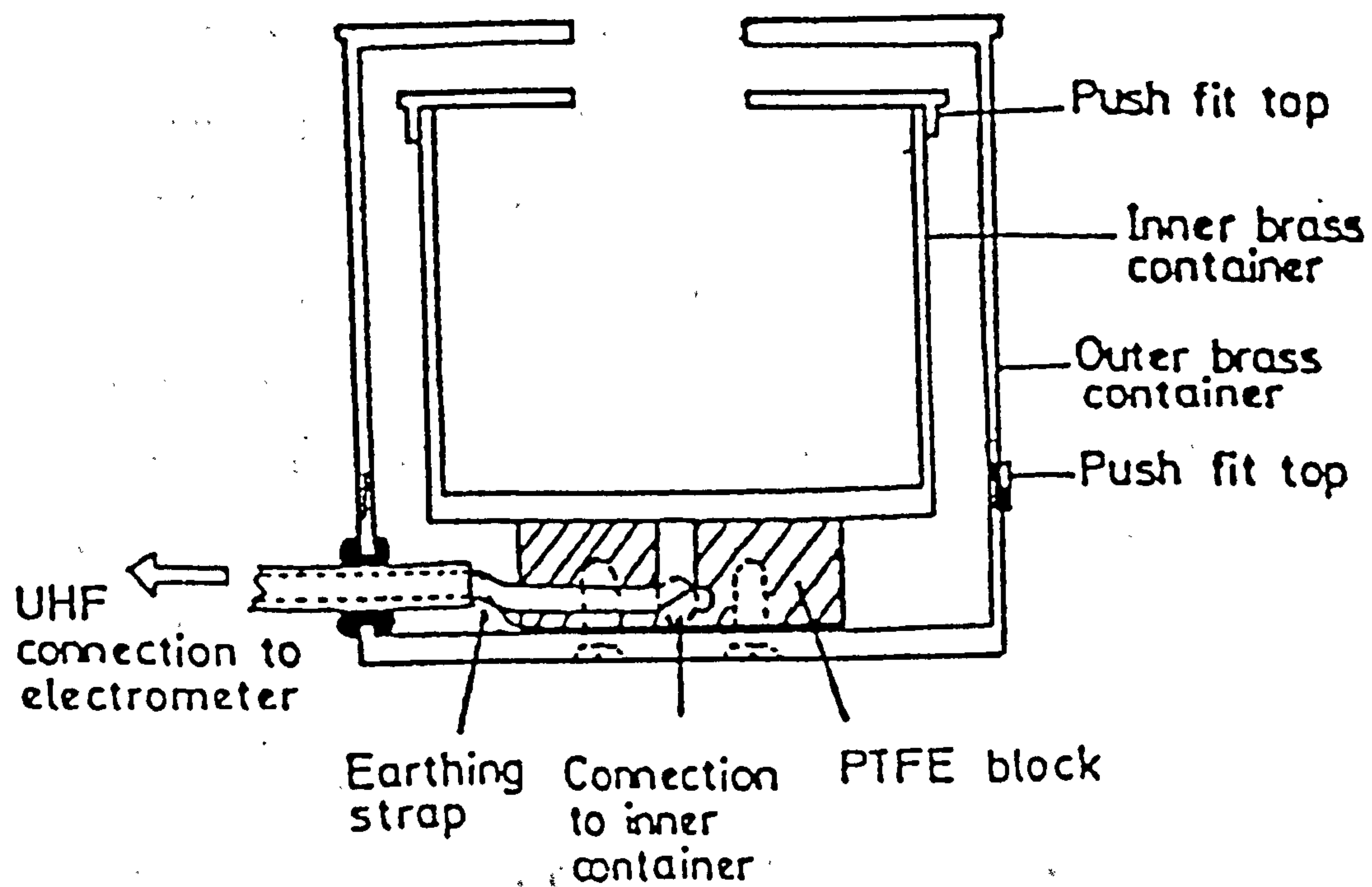


**Fig 3.24** Front elevation of Faraday well for determining static charge on powder particles

The outer wall is grounded and forms an electrical screen which prevents stray external charges from affecting the measurement. The inner wall is connected to an electrometer which detects the voltage built up across a known capacitance. Micronized salbutamol sulphate and other materials, which included: regular lactose in the size range of 63-90 $\mu$ m and <20 $\mu$ m, spray dried lactose (63-90 $\mu$ m), recrystallized lactose (60-90 $\mu$ m), glass beads (60 $\mu$ m), milled glass (63-90 $\mu$ m), magnesium stearate (<20 $\mu$ m) and "Aerosil" 200 (<10 $\mu$ m), were tested individually. Powder mixtures of, the drug and carriers, lactose and magnesium stearate and lactose and "Aerosil" were also tested.

The experiment was carried out by pouring a known weight of powder at a constant rate of approximately 0.5g/sec off a perspex or brass chute into the inner container of the Faraday well so that the base was uniformly covered. Four replicate determinations were made for each sample. Brass and perspex were used since different materials produce charges of different signs on the same powder depending on their position in the triboelectric series. The sign of the charge developed on the powders following contact with the walls of the "Rotahaler" was also tested by filling the inhaler with few grams of the powder sample and tumbling it to facilitate contact electrification. The charge magnitude was not recorded since it was not possible to pour the powder from the inhaler at a constant rate.

### **3.5.3 Results and discussion**

The mean static charges obtained with individual powders are shown in Tables 3.9 and 3.10.



Most of the powders acquired a positive electrostatic charge in contact with a perspex, whereas following contact with a brass some materials acquired either a positive or a negative charge. The magnitude of the charge was similar for all types of lactose used, however it differed significantly between other materials. Potential mutual attractiveness can be demonstrated qualitatively using a triboelectric series which is analogous to an electrochemical series (Staniforth and Rees, 1982b). Although the triboelectric series is specific to the conditions under which powders are tested, such a series nevertheless gives a useful indication of the possible interaction between different powders as well as a better understanding of contributing mechanisms.

Using the data shown in Tables 3.9 and 3.10, a triboelectric series were constructed for powders poured off a perspex or a brass chute (Tables 3.11 and 3.12). "Aerosil" 200 was found to be most electronegative following flow on either perspex or brass chutes. Magnesium stearate was the next most electronegative material when contacted with a perspex, but acquired a positive charge when poured off a brass chute.

The mean static charges for the powder mixtures are given in Tables 3.13 and 3.14. The sign and magnitude of the charge were dependent upon the constituents forming the adhesive mix and on their proportions. Thus the charge measured was a net charge acquired by the two components. Since the powder mixtures consisted of dissimilar sized particles, the number of rubbing contact events between the powders themselves and the powder and the surfaces will depend on the particle size distribution and unequal charging of the particles will therefore occur. Powders

**Table 3.9 Mean specific charges of different powders measured after flow on a perspex chute. (Values are the mean of four separate determinations  $\pm$  standard deviations)**

Powder sample	Mean specific charge $\text{Cg}^{-1} \times 10^{-9}$
Regular lactose (63-90 $\mu\text{m}$ )	+ 1.21 $\pm$ 0.42
Spray dried lactose (63-90 $\mu\text{m}$ )	+ 3.80 $\pm$ 0.31
Recrystallized lactose (60-90 $\mu\text{m}$ )	+ 1.02 $\pm$ 0.03
Regular lactose (<20 $\mu\text{m}$ )	+ 4.40 $\pm$ 0.80
Glass beads (60 $\mu\text{m}$ )	+ 0.35 $\pm$ 0.07
Milled glass (63-90 $\mu\text{m}$ )	+ 0.25 $\pm$ 0.02
Salbutamol sulphate (<5 $\mu\text{m}$ )	+ 1.55 $\pm$ 0.36
Magnesium stearate (<20 $\mu\text{m}$ )	- 2.42 $\pm$ 0.36
Aerosil 200 (<10 $\mu\text{m}$ )	- 51.10 $\pm$ 5.90

**Table 3.10 Mean specific charges of different powders measured after flow on a brass chute. (Values are the mean of four separate determinations  $\pm$  standard deviation)**

Powder sample	Mean specific charge $\text{Cg}^{-1} \times 10^{-9}$
Regular lactose (63-90 $\mu\text{m}$ )	- 5.36 $\pm$ 0.17
Spray dried lactose (63-90 $\mu\text{m}$ )	- 3.50 $\pm$ 0.26
Recrystallized lactose (63-90 $\mu\text{m}$ )	- 4.80 $\pm$ 0.41
Regular lactose (<20 $\mu\text{m}$ )	- 7.40 $\pm$ 1.20
Glass beads (60 $\mu\text{m}$ )	+ 0.70 $\pm$ 0.06
Milled glass (63-90 $\mu\text{m}$ )	+ 1.10 $\pm$ 0.10
Salbutamol sulphate (<5 $\mu\text{m}$ )	+ 5.70 $\pm$ 1.80
Magnesium stearate (<20 $\mu\text{m}$ )	+ 2.30 $\pm$ 0.71
Aerosil 200 (<10 $\mu\text{m}$ )	- 37.00 $\pm$ 3.60



**Table 3.11** Triboelectric series of different powders flow on a perspex chute

State	Powder
Electronegative	Aerosil 200 Magnesium stearate
Electropositive	Salbutamol sulphate Lactose Glass

**Table 3.12** Triboelectric series of different powders flow on a brass chute

State	Powder
Electronegative	Aerosil Lactose
Electropositive	Salbutamol sulphate Magnesium stearate Glass

**Table 3.13** Mean specific charges of mixtures of powders measured after flow on a perspex chute. (Values are the mean of four separate determinations  $\pm$  standard deviation)

Powder sample	Mean specific charge $\text{Cg}^{-1} \times 10^{-9}$
Regular lactose (63-90 $\mu\text{m}$ ) + Salbutamol sulphate (<5 $\mu\text{m}$ ) 67.5:1	+ 4.52 $\pm$ 0.25
Regular lactose (63-90 $\mu\text{m}$ ) + Salbutamol sulphate (<5 $\mu\text{m}$ ) 1:1	+ 0.45 $\pm$ 0.14
Spray dried lactose (63-90 $\mu\text{m}$ ) + Salbutamol sulphate (<5 $\mu\text{m}$ ) 67.5:1	+ 6.60 $\pm$ 0.16
Recrystallized lactose (60-90 $\mu\text{m}$ ) + Salbutamol sulphate (<5 $\mu\text{m}$ ) 67.5:1	+ 4.82 $\pm$ 0.06
Regular lactose (<20 $\mu\text{m}$ ) + Salbutamol sulphate (<5 $\mu\text{m}$ ) 67.5:1	+ 3.70 $\pm$ 0.70
Regular lactose (<20 $\mu\text{m}$ ) + Salbutamol sulphate (<5 $\mu\text{m}$ ) 1:1	+ 2.14 $\pm$ 0.34
Regular lactose (63-90 $\mu\text{m}$ ) + Magnesium stearate (1.5%)	- 0.44 $\pm$ 0.20
Regular lactose (63-90 $\mu\text{m}$ ) + Aerosil 200 (1.5%)	- 12.5 $\pm$ 3.10

**Table 3.14 Mean specific charges of mixtures of powders measured after flow on a brass chute. (Values are the mean of four separate determinations  $\pm$  standard deviation)**

Powder sample	Mean specific charge $\text{Cg}^{-1} \times 10^{-9}$
Regular lactose (63-90 $\mu\text{m}$ ) + Salbutamol sulphate (<5 $\mu\text{m}$ ) 67.5:1	+ 0.43 $\pm$ 0.03
Regular lactose (63-90 $\mu\text{m}$ ) + Salbutamol sulphate (<5 $\mu\text{m}$ ) 1:1	+ 1.80 $\pm$ 0.09
Spray dried lactose (63-90 $\mu\text{m}$ ) + Salbutamol sulphate (<5 $\mu\text{m}$ ) 67.5:1	- 0.80 $\pm$ 0.04
Recrystallized lactose (60-90 $\mu\text{m}$ ) + Salbutamol sulphate (<5 $\mu\text{m}$ ) 67.5:1	+ 0.48 $\pm$ 0.10
Regular lactose (<20 $\mu\text{m}$ ) + Salbutamol sulphate (<5 $\mu\text{m}$ ) 67.5:1	- 1.40 $\pm$ 0.13
Regular lactose (<20 $\mu\text{m}$ ) + Salbutamol sulphate (<5 $\mu\text{m}$ ) 1:1	+ 0.60 $\pm$ 0.08
Regular lactose (63-90 $\mu\text{m}$ ) + Magnesium stearate (1.5%)	- 1.10 $\pm$ 0.30
Regular lactose (63-90 $\mu\text{m}$ ) + Aerosil 200 (1.5%)	- 5.60 $\pm$ 1.80



**Table 3.15 The sign of the charge produced on the surface of different powders after flow on different materials**

Powder sample	Perspex	Brass	Inhaler
Lactose	+	-	-
Glass	+	+	+
Magnesium stearate	-	+	+
Aerosil 200	-	-	-
Salbutamol sulphate	+	+	+

having fine particle size distribution are expected to acquire higher charge magnitudes due to increased surface area facilitating contact electrification. However, the results in Tables 3.9, 3.10, 3.13 and 3.14 underestimate the surface charge density of the fine powders due to the formation of agglomerates which reduces direct contacts between the powder and the surfaces.

Table 3.15 shows the sign of the surface charge produced on different powders following contact with the walls of the "Rotahaler". The charge developed is compared with that obtained following contact with perspex or brass. The charge sign acquired by the powders was similar to that acquired after contact with brass.

The above method used for electrostatic charge determination produced great variations in the magnitude of charge. This has been previously reported by Staniforth and Rees (1982b) who used the same technique; variations of up to 50-90% were observed in some determinations. In this study, despite these variations the data obtained provided useful information about the electrostatic behaviour of powders in relation to other surfaces.

The fact that surfaces produce different charge properties has significant implications in the context of mixing and fluidisation. The dependence of ordered mix stability on the triboelectric properties of the surface with which the powders are in contact has been demonstrated by Staniforth and Rees (1982b,c). Since the further apart powders with different charge signs are in the series the greater is their mutual attraction, the surface charges can be optimized to facilitate the formation of ordered mixes with desirable adhesive properties. Boschung and Glor (1980) pointed

out that the specific charge on different drug and excipient powders can be increased or decreased according to the triboelectrification conditions.

The behaviour of some of the powder mixtures used in this study can be explained by the electrostatic properties of the constituents. For example, the use of lactose tumbled with magnesium stearate resulted in a higher respirable fractions which was explained in terms of the reduced association between the drug and the carrier. The above results indicate that lactose developed a charge opposite to that of magnesium stearate during tumbling. Thus magnesium stearate would be strongly attracted to the active adherence sites on the oppositely charged carrier. When salbutamol sulphate was added to the mix, it would have been located at weaker adherence sites and the dislodgement from the carrier surface will be enhanced.

The electrostatic phenomenon also explains the high segregation tendency observed for powder mixtures containing glass as a model carrier. In such a mixture, in addition to the smooth surface contribution to the weak adhesive forces, the similar charges developed on both the drug and the glass particles played a role in facilitating the redispersion of the drug particles.

This study also demonstrates that by a proper selection of the material of the inhaler, similar charges can be produced on the powder surfaces upon fluidisation during inhalation. Consequently, the segregation of the constituents can be enhanced and more efficient drug penetration into the lungs can be achieved.

Therefore, electrostatic charging can be utilized to produce highly



respirable powder mixtures by adjusting the type of charge induced on the particles.

Induction of opposite charges on the constituents will be valuable during mixing to produce stable powder mixtures for filling and handling, whereas induction of similar charges during inhalation is necessary to facilitate efficient redispersion of the fine drug particles from the carrier surface.

### **3.6 Conclusions**

The factors influencing the adhesion characteristics between the drug and the carrier, and the force employed to generate the powder cloud were found to highly influence the performance of powder inhalation aerosols.

In these studies, the powder properties and their behaviour in a turbulent air stream were investigated. The results demonstrated that redispersion of the drug particles can be enhanced by several methods. A proper choice of the carrier size, the carrier surface properties which facilitate drug particle detachment but resist segregation under normal handling and processing, the presence of ternary components in the mix, the use of an appropriate proportion of the carrier in the mix and controlling the surface charge induced on the powder surfaces, all improve the availability of the medicament to the lungs.

However, although the use of ternary components in the mix resulted in highly inspirable clouds, the addition of these components to powder mixtures for inhalation is undesirable as it is not advisable to deliver these foreign particles to the delicate tissues of the lungs.

The use of a smooth surface carrier seems to be the most appropriate method to increase the inspirability of a powder aerosol cloud. The use of such a carrier will overcome the problem of cohesive powder fluidisation which is a major drawback to the use of fine carriers . Additionally, this will limit the proportion of the carrier that can penetrate into the lungs.

These studies also demonstrated that when formulating dry powders for inhalation by mixing the fine drug particles with a coarser component, the factors affecting the adhesion properties can be employed to modify the relationship between the drug and the carrier thus improving the efficiency of these aerosols.

Moreover, the influence of air flow rate demonstrated throughout this chapter indicated that with all the formulation variables, greater efficiencies were obtained at high flow rates. Therefore, in such a dosage form, even if a good formulation is developed, generation of deeply inspirable cloud cannot be achieved unless combined with both the use of an inhalation device which produces high de-aggregation of the powder, and a proper inhalation manoeuvre by the patient.

**Chapter four**

**Clinical assessment of a novel powder formulation  
and a newly designed inhalation device**



#### 4.1 Introduction

The efficiency of dry powder aerosols depends on three major factors: the patient, the powder formulation and the inhalation device. The patient plays an essential role since redispersion of the fine drug particles is limited by the energy available from the inspiratory flow. However, controlling the force provided by the patient is difficult. Therefore, the development process of a powder inhalation product should involve the design of a formulation and a delivery device which provides a maximum redispersion with minimum effort on the part of the user.

The *in vitro* studies in Chapter 3 suggest that this approach is possible to achieve by modifying the relationship between the drug and the carrier. The invention of a carrier with low surface rugosity provided a formulation which can be redispersed efficiently even at low air flow rates.

The construction of the inhaler can also provide efficient de-aggregation of the powder mixture if high levels of turbulence are attained. The design of the inhaler described in Chapter 3 has an additional advantage of low resistance to air flow, therefore patients can achieve high inspiratory flow rates with minimum exertion.

However, the respiratory tract is a system of branching tubes of progressively decreasing size. This complexity acts as a barrier to the penetration of drug particles and none of the *in vitro* experiments can predict the exact behaviour of the aerosol cloud once inhaled by human lungs. Therefore, preliminary *in vitro*

findings should be followed by *in vivo* evaluation of the developed inhalation products.

For inhaled products, the best method which describes the fate of the inhaled particles is gamma-scintigraphy. However, labelling micronized drug particles has not yet been achieved due to technical reasons. Physical labelling of the particles as described by Vidgren *et al* (1987b) and Newman *et al* (1989) alter the physical properties of micronized particles. Therefore the latter technique can not be applied to the novel formulation since the inspirable characteristics of this formulation are highly dependent on the relationship between the drug and the carrier. Therefore, since the model drug employed throughout this study is a bronchodilator, one of the methods which can be applied to detect the penetration of the drug particles into the lungs is by assessing the lung function before and after administration of the medicament.

The commonly accepted criteria for a positive bronchodilator response is an improvement in lung functions. Lung functions can be described in the following way (Figure 4.1): the volume of gas in the lungs at the end of a normal exhalation during quiet breathing is termed the functional residual capacity (FRC). The volume of air inhaled or exhaled with each breath during quiet breathing is the tidal volume (TV). The maximum volume of air that can be drawn into the lungs from FRC is the inspiratory capacity (IC), whereas the maximum volume that can be exhaled from FRC is the expiratory reserve volume (ERV). The volume of gas in the lungs after a maximum inspiration is termed the total lung capacity (TLC). The vital capacity (VC) is the maximum volume that can be exhaled following a maximum inspiration to total lung capacity.

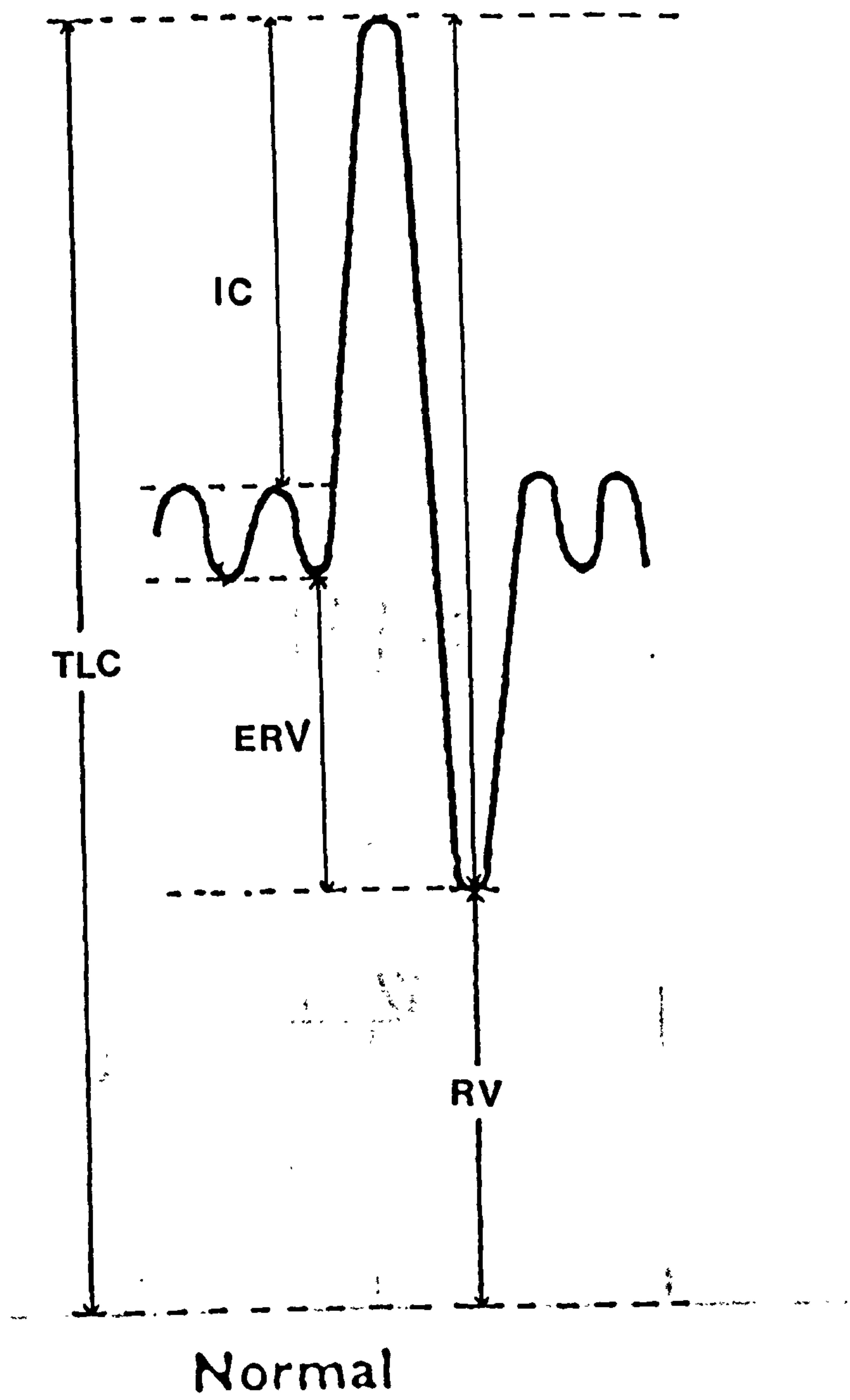


Fig 4.1 Lung function spirogram



The volume of gas remaining in the lung after a maximum expiratory effort is the residual volume (RV).

The gas volume moving into and out of the lungs is commonly measured in the laboratory using a closed circuit spirometer.

The rate of air flow or the volume inhaled or exhaled over specific time intervals serve as indirect measure of the flow-resistive properties of the airways. In measuring a forced expiratory vital capacity, the patient takes a full inspiration to total lung capacity followed by a maximum, rapid, forceful exhalation into a spirometer.

The measurements require the patient to breathe with his nose clipped. The volume exhaled in the first second of expiratory manoeuvre from total lung capacity is a forced expiratory volume in one second (FEV1). Figure 4.2 shows typical spirometric trace of expiratory volume- time curve.

FEV1 reflects air flow resistance in the large airways as limitation of expiratory flow rates occur in these airways which become constricted by increasing the expiratory effort. Other measurements characterizing small airway can be performed.

Using an instrument which measures flow and volume simultaneously, it is possible to draw a flow-volume curve as shown in Figure 4.3, which displays the instantaneous air flow rate as a function of lung volume.

The vital capacity delivered from total lung capacity (TLC) to residual volume (RV) is associated with a reduction in flow towards residual volume. In the latter half of the exhalation (Figure 4.3) the flow is independent of effort and reflects small airways ( $\leq 2\text{mm}$ ) resistance. Direct measurement of maximum expiratory flow rates

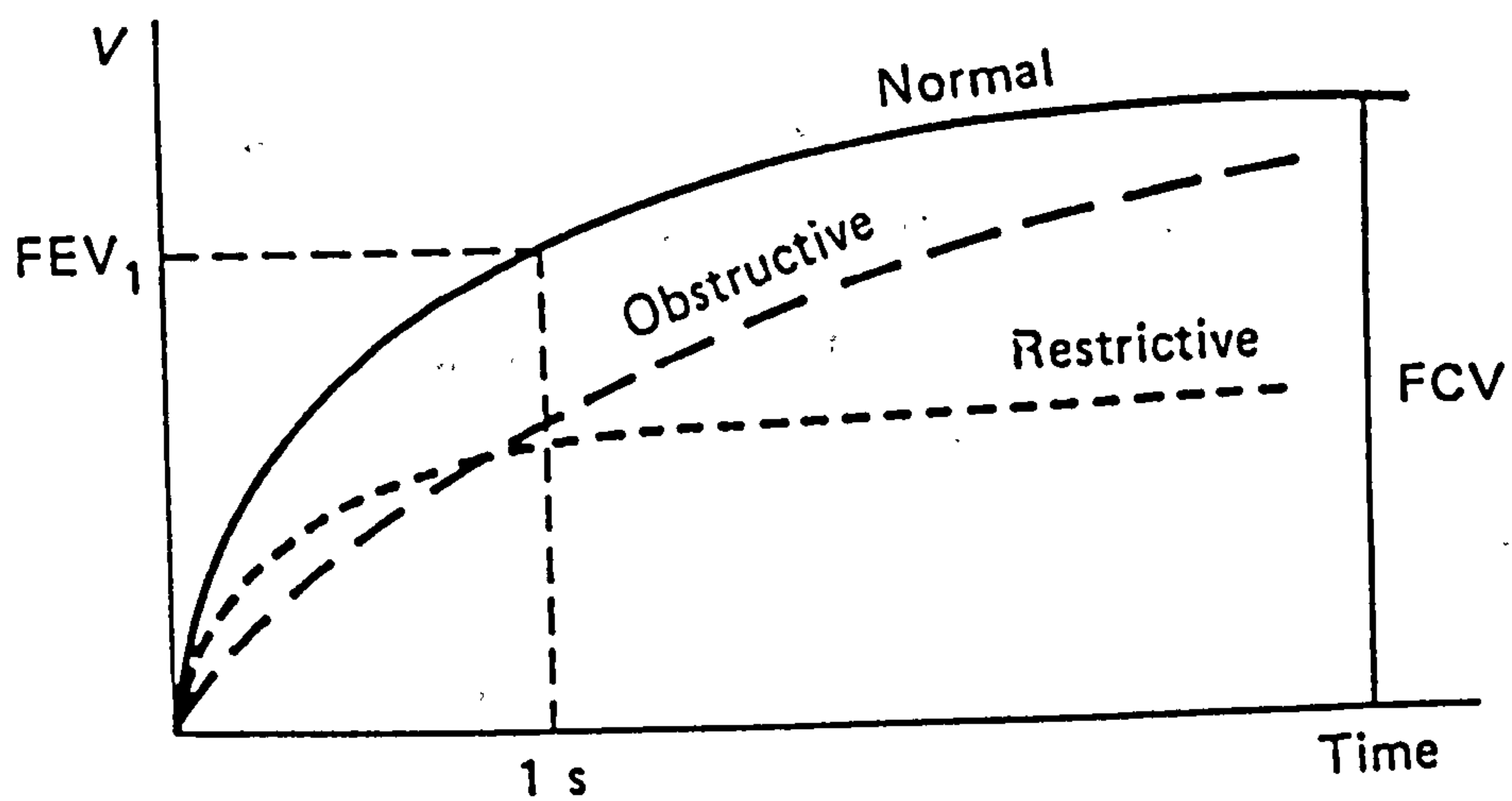


**Fig 4.2** Spirometric trace of expiratory volume-time curve

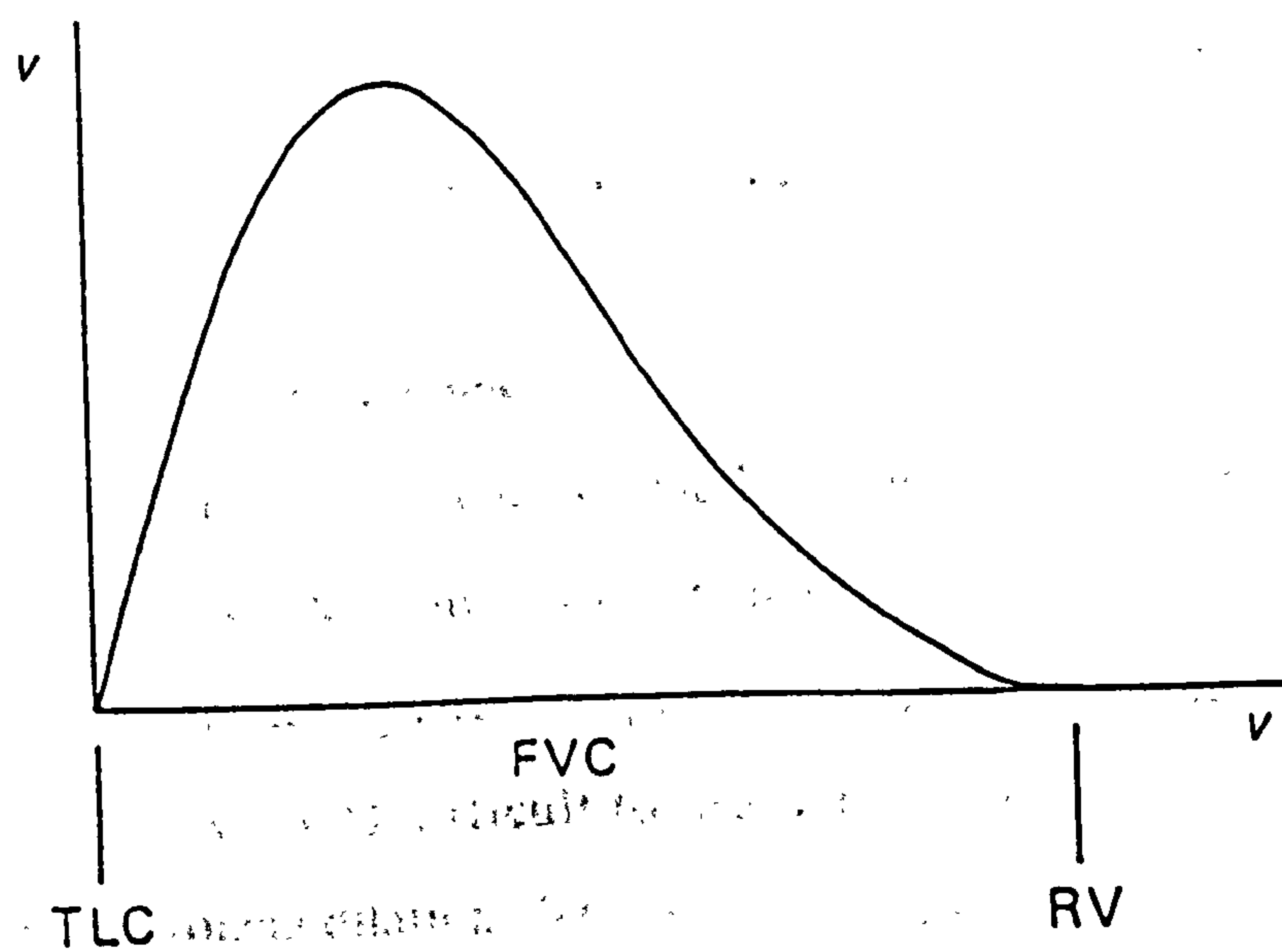


**Fig 4.3** Spirometric trace of expiratory flow-volume curve

( $V_{\max}$ ) at certain percentage of the vital capacity in the latter half of the exhalation can be made from the flow-volume curve.

Since the reversibility of airway obstruction in patients with asthma and chronic obstructive pulmonary disease can be detected by simple measurements such as FEV1 and  $V_{\max}$  at certain percentage of the vital capacity following inhalation of a bronchodilator, these two measurements were considered sufficient for *in vivo* evaluation of the developed inhalation products.

The following study consists of two parts and was designed to:

- (a) Compare the bronchodilator response achieved following inhalation of the novel formulation, which was shown to be highly respirable *in vitro*, with that of a commercially available powder aerosol formulation.
- (b) Compare the response to the bronchodilator inhaled with a newly designed inhaler and a "Rotahaler".

## 4.2 Materials and methods

Since salbutamol was used as a model drug throughout the study, a commercially available salbutamol formulation was chosen to compare the therapeutic response. A dose of 200 $\mu$ g drug was employed as it was difficult to predict the dose which produces maximal bronchodilation. The two formulations were administered with both the new inhaler and the "Rotahaler" to double blind the study.



#### **4.2.1 Formulations**

##### **1. Preparation of the novel powder aerosol formulation**

A powder blend of salbutamol sulphate ( $2.8\mu\text{m}$  MMD) and lactose was prepared in a ratio of 1:67 by mixing the micronized drug and the recrystallized lactose with a spatula.  $13.5 \pm 0.68\text{mg}$  of the mixture was filled into off-white opaque hard gelatin capsules (size 3) so that each capsule contained  $200\mu\text{g}$  drug. The content uniformity of the capsules was confirmed by the assay of 10 capsules using the HPLC method described in Section 2.2.2.

##### **2. A commercial salbutamol formulation**

"Ventolin Rotacaps"  $200\mu\text{g}$  (Allen and Hanbury's Limited, Batch Number S7439MA) were employed. To blind the study, the capsule contents were transferred into matching hard gelatin capsules. The inspirable characteristics of Ventolin were not affected by the transfer of the contents as was confirmed by an in vitro experiment.

##### **3. Microbiological test**

Since these powders are intended for inhalation by asthmatic patients, it was necessary to ensure that they are free from any bacterial contamination since some pathogenic bacteria can apparently survive in dry pharmaceutical raw materials.

Both micronized salbutamol sulphate and recrystallized lactose were tested for total viable count.

A 0.5g samples of each material was dissolved in 5ml nutrient broth. The solutions were incubated for 3-4 hours at  $37^{\circ}\text{C}$ . After incubation, triplicate  $50\mu\text{l}$  samples were plated out onto tryptone soya agar plates. The plates were then incubated at  $37^{\circ}\text{C}$  and

examined for bacterial growth after 18-24 and 48 hours.

No microbial growth was detected in either material.

#### **4.2.2 Inhalation devices**

##### **1. New inhaler**

The inhaler is shown in Figure 4.4. It was made of glass and its design is described in Section 3.2.

Dispensing is performed by inserting the capsule containing the drug into the inhaler and turning this end to separate the capsule into two halves. The part of the capsule containing the powder drops and is retained by a grid inserted at position A. As the patient inhales, the powder is dispensed from the capsule into the inhaled stream through a nozzle fitted with a grid on the top (position B).

##### **2. "Rotahaler" (Allen and Hanbury's Limited)**

The design of this inhaler and its mode of use is described in section 1.5.3

#### **4.2.3 Patient selection**

Eleven moderate asthmatic patients (six males and five females) volunteered for the study. The mean age of the patients was 38 years and their clinical condition was stable. The patients characteristics are shown in Table 4.1.

Patients were entered into the study if their forced expiratory volume in one second (FEV1) was less than 80% of predicted normal value and increased by more than 15% of the initial value after inhalation of a bronchodilator. A 15% increase in FEV1 was the minimum change required to demonstrate that a patient





a



b

**Fig 4.4** The inhalers used for the in vivo studies :  
(a) the newly designed inhaler , ( b) the Rotahaler



respond to a bronchodilator therapy since this exceeds spontaneous within-day variations in patients with reversible airway obstruction. All patients were non-smokers.

The study was carried out at King's College Hospital, and the protocol was approved by the Hospital Ethical Committee. Informed consent was obtained from all subjects.

#### **4.2.4 Study design**

Patients were enrolled in a four day, double blind cross-over study. Patients were randomly allocated to one of the two formulations, so that they inhaled either the novel formulation or "Ventolin" using a "Rotahaler" in the first two visits, with cross-over of the formulations using the new inhaler in visits three and four of the study. All bronchodilator therapy was withheld for at least 6 hours prior to the study.

Patients were instructed to inhale as fast as possible. However, the peak inspiratory flow rate (PIFR) and the total inspired volume were not registered. Some patients inhaled twice from the inhaler to ensure complete emptying of the powder. Each inhalation was followed by a 10 seconds breath-holding pause.

The patients had never previously used powder inhalation aerosols as a method of treatment except one who used a "Diskhaler" (Allen and Hanbury's Ltd).

Each patient attended the clinic at the same time on the test day. The procedure on all four days was the same: the patient was allowed to rest for 10 minutes after which baseline measurements of lung function as assessed by FEV1 and maximum expiratory

volume at 30% of the vital capacity ( $V_{\max 30}$ ) were recorded using a spirometer (Vitalograph). These measurements were made at each visit to ensure that the baseline values did not differ by more than 15% between the treatment days. Following baseline measurements, the subject inhaled one of the randomly allocated formulations and subsequently spirometric measurements were repeated at 5, 10, 15 and 30 minutes after inhalation. Each measurement was made in triplicate and the results were expressed as the increment of each measurement above the individual's pre-administration baseline for that day. Four patients were excluded after the first two visits as their basal FEV1 and  $V_{\max 30}$  was varied by more than 15% from the first two days of the study. Seven patients completed the study.

#### **4.2.5 Determination of the amount of drug retained in the inhalers**

After inhalation, the inhaler and the capsule were rinsed with 20ml of methanol and water (65:35 v/v) and the washings were assayed by HPLC as described in Section 2.2.2. The amount of salbutamol sulphate recovered was calculated and the percentage of the dose delivered was determined in relation to the administered dose.

#### **4.2.6 Analysis of results**

A paired t-test was used;  $P < 0.05$  was considered statistically significant.

**Table 4.1 Patient's characteristics**

Patient	Sex	Age (yrs)	Concurrent medication	FEV1 (L)	V <sub>max</sub> <sup>30</sup> (L)
1	M	31	β <sub>2</sub> -agonists corticosteroids	1.73	0.42
2	M	24	β <sub>2</sub> -agonist corticosteroid	3.73	1.19
3	F	57	β <sub>2</sub> -agonist corticosteroids	1.33	0.56
4	F	24	β <sub>2</sub> -agonist corticosteroids Aminophyllin	1.37	0.41
5	M	26	β <sub>2</sub> -agonist corticosteroid	2.54	1.22
6	F	33	β <sub>2</sub> -agonist corticosteroid	2.34	0.97
7	M	45	β <sub>2</sub> -agonist corticosteroid	2.52	1.41
8	F	32	β <sub>2</sub> -agonist corticosteroids	2.29	1.38
9	M	46	β <sub>2</sub> -agonist corticosteroid theophylline Anti-cholinergic	0.98	0.19
10	F	36	corticosteroids	1.49	0.53
11	M	63	β <sub>2</sub> -agonist	2.12	0.27
M:F 6:5 x=38 range:24-63				2.04 ±0.77	0.78 ±0.46



## **4.3 Results and discussion**

### **4.3.1 Formulation**

The two formulations were inhaled by 11 patients using a "Rotahaler" and 7 patients using the new inhaler.

The mean changes in FEV1 and  $V_{\max}^{30}$  after drug inhalation with both devices are shown in Figures 4.5 to 4.8.

The percentage mean increase in FEV1 above the pretreatment baseline was significantly greater for the novel formulation (27.5%) than for "Ventolin" (21.4%) ( $P < 0.05$ ). However, for  $V_{\max}^{30}$ , although the percent mean increase was higher for the novel formulation (36.6%) than "Ventolin" (29.8%), this was not statistically significant ( $P = 0.26$ ) due to the large scatter of the values around the mean.

When the new inhaler was employed, no significant difference between the therapeutic responses to these two formulations was observed ( $P > 0.05$ ).

### **4.3.2 Inhalers**

The present study showed that with regard to clinical effect, the two inhalers are comparable. The lung function results obtained with both inhalers are illustrated in Figures 4.9 to 4.12. No statistically significant difference in the mean increase of FEV1 or  $V_{\max}^{30}$  was demonstrated ( $P < 0.05$ ).

### **4.3.3 The amount of drug retained in the inhalers**

By analysing the amount of drug retained in the inhalers following inhalation, it was found that the dose delivered to the patients was less than  $200\mu\text{g}$  in the four treatment days and with all subjects.

The mean changes in FEV1 following Inhalation of the novel formulation and Ventolin

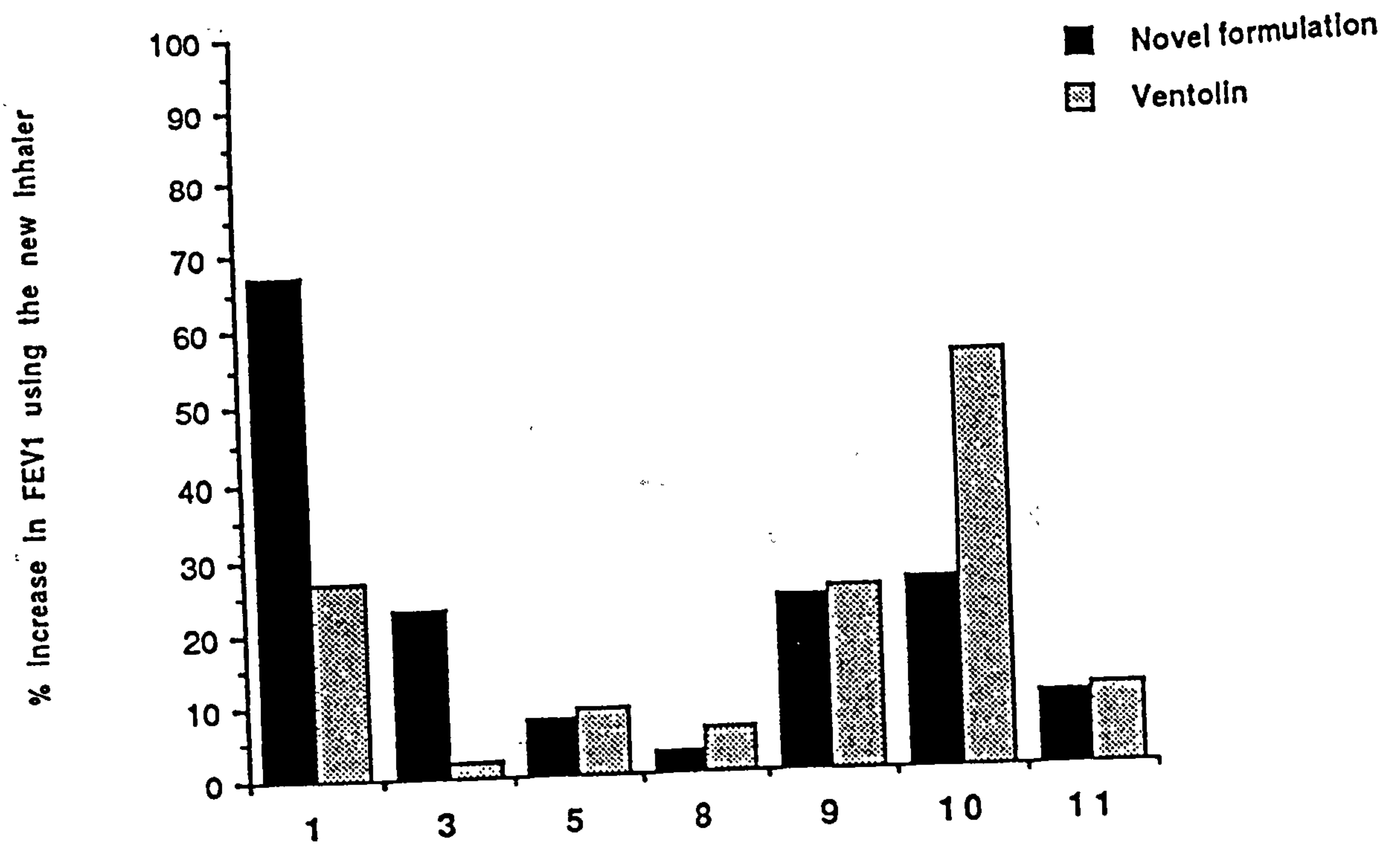


Fig 4.5

Patients

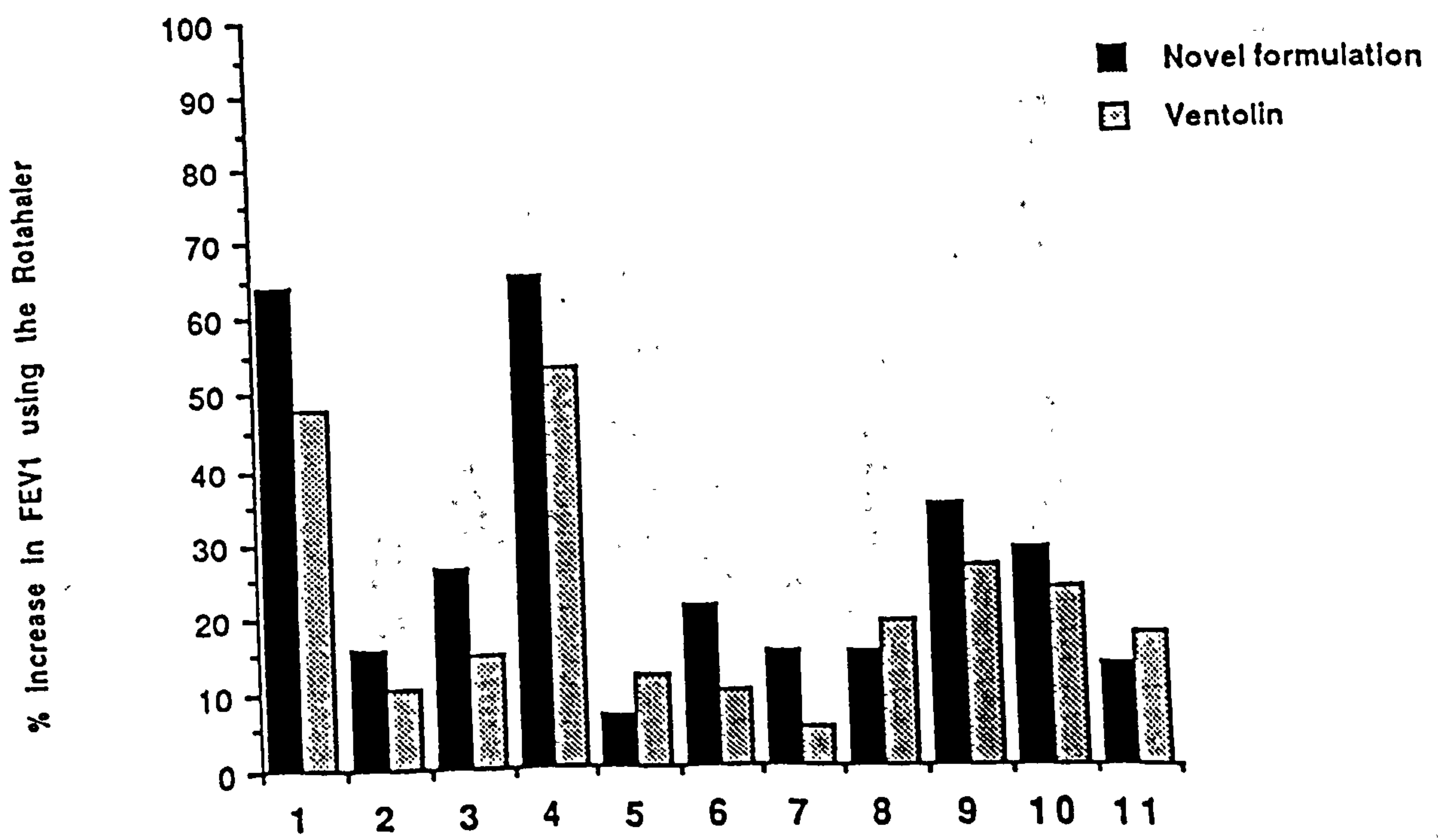


Fig 4.6

Patients

The mean changes in Vmax30 following inhalation of the novel formulation and Ventolin

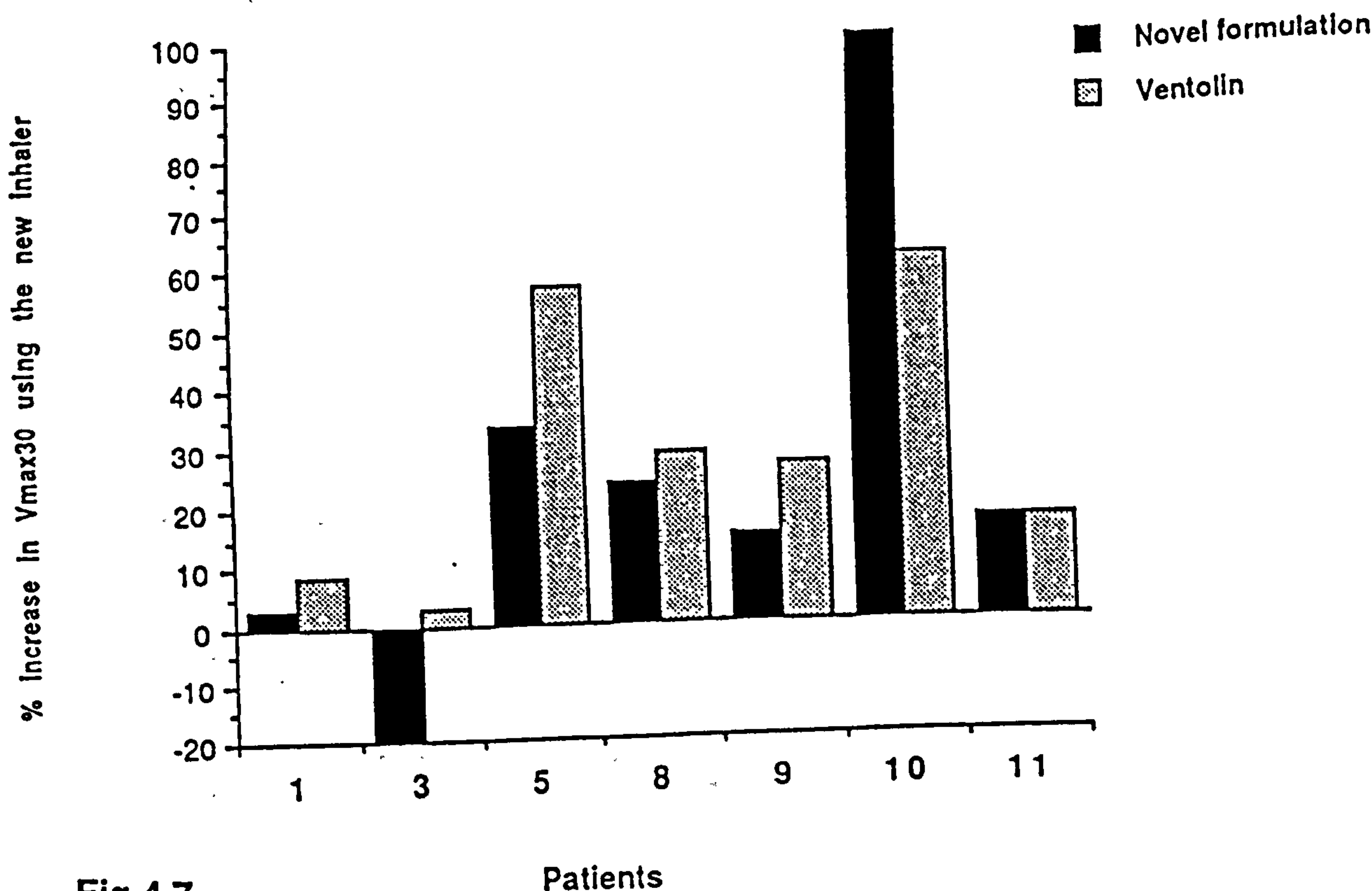


Fig 4.7

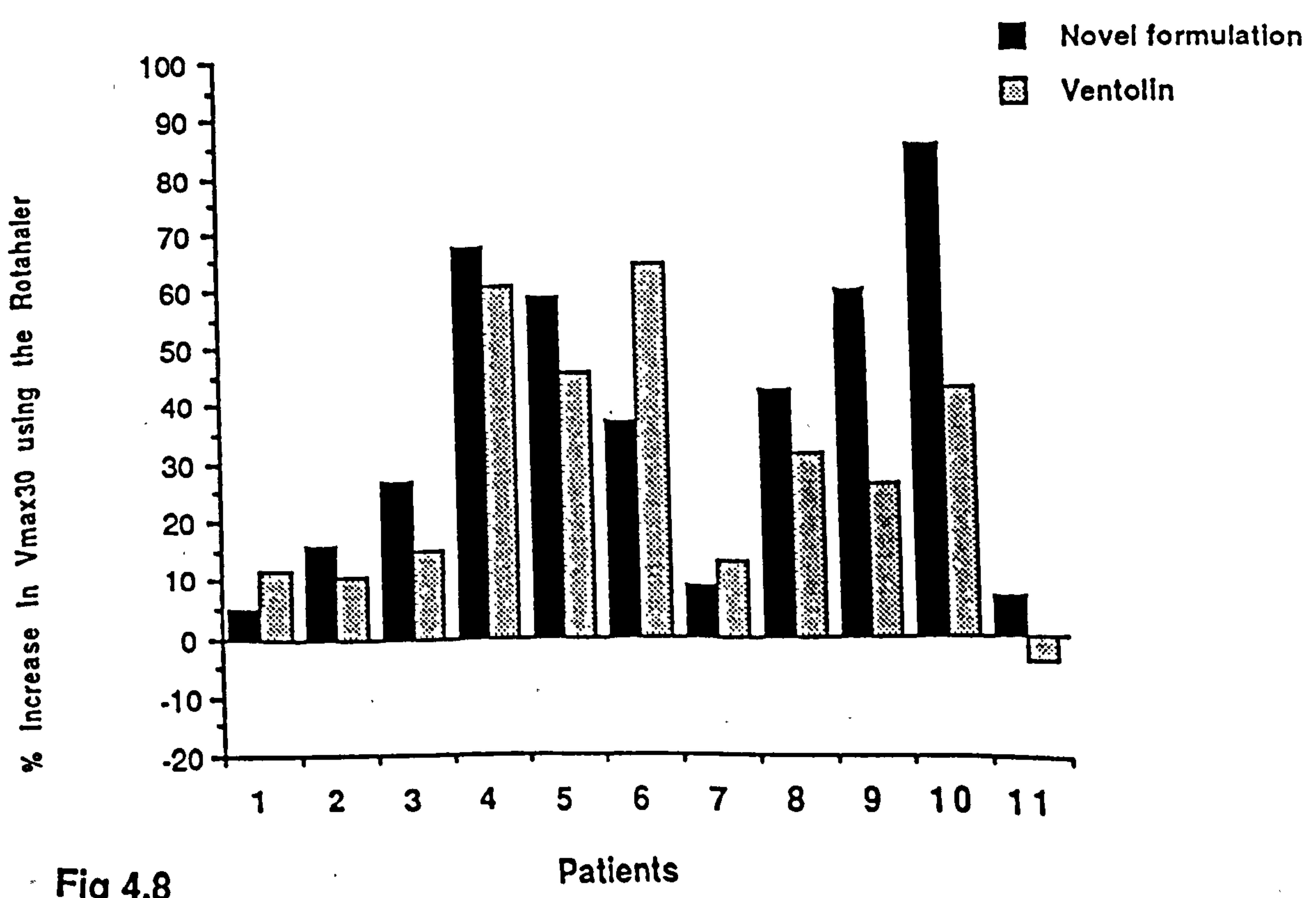


Fig 4.8



The mean changes in FEV1 following inhalation with the new inhaler and the Rotahaler

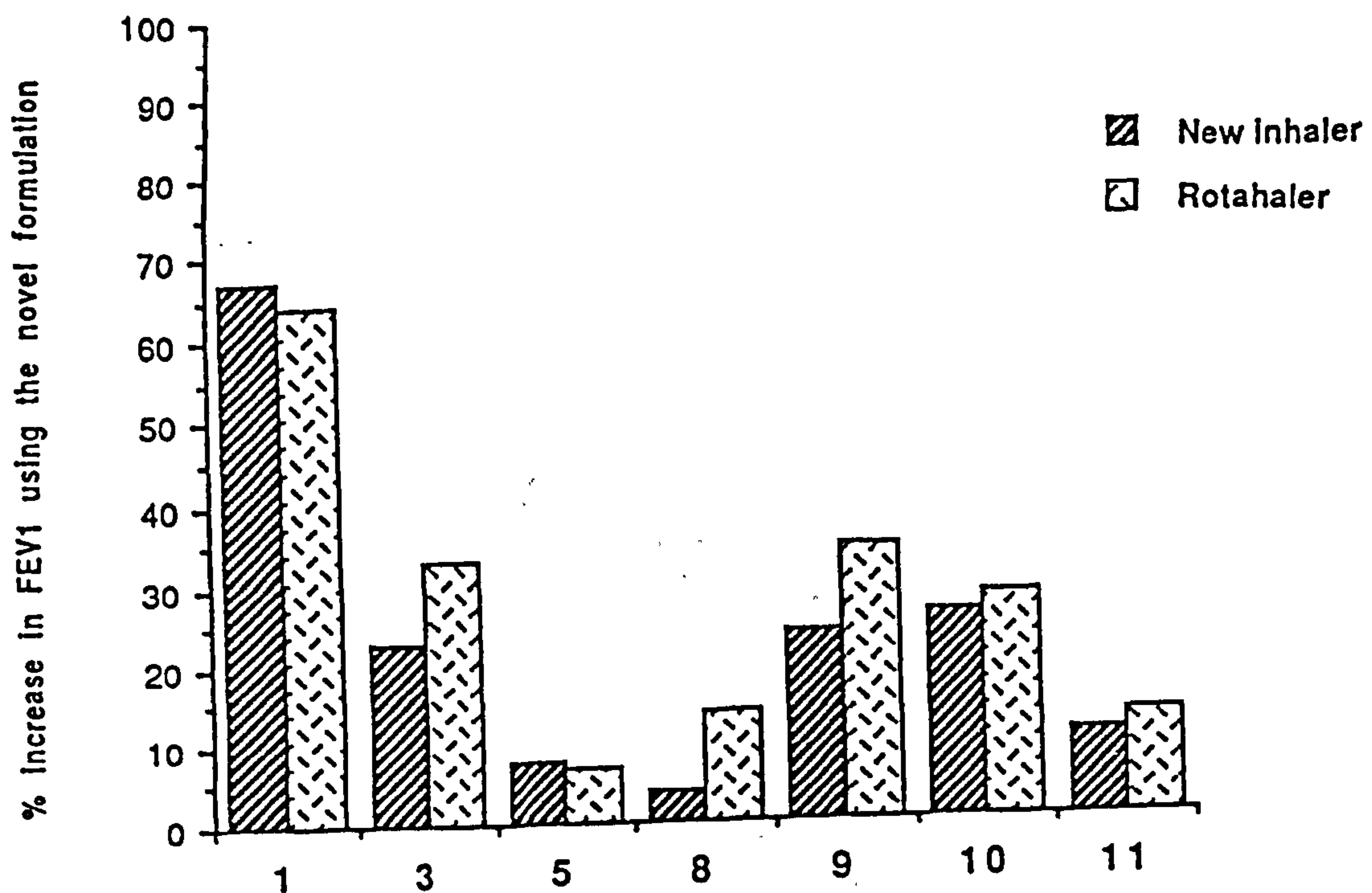


Fig 4.9

Patients

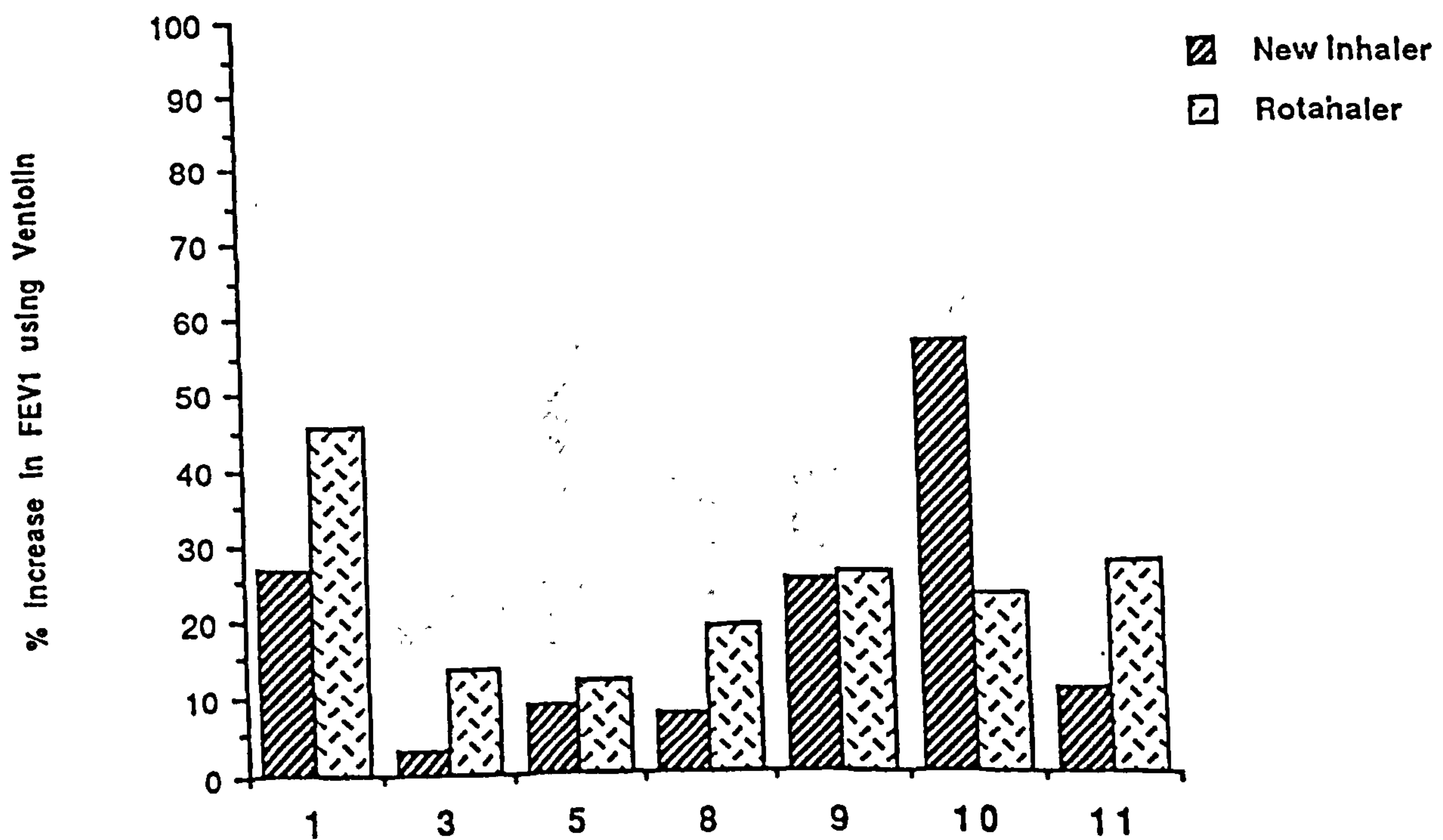
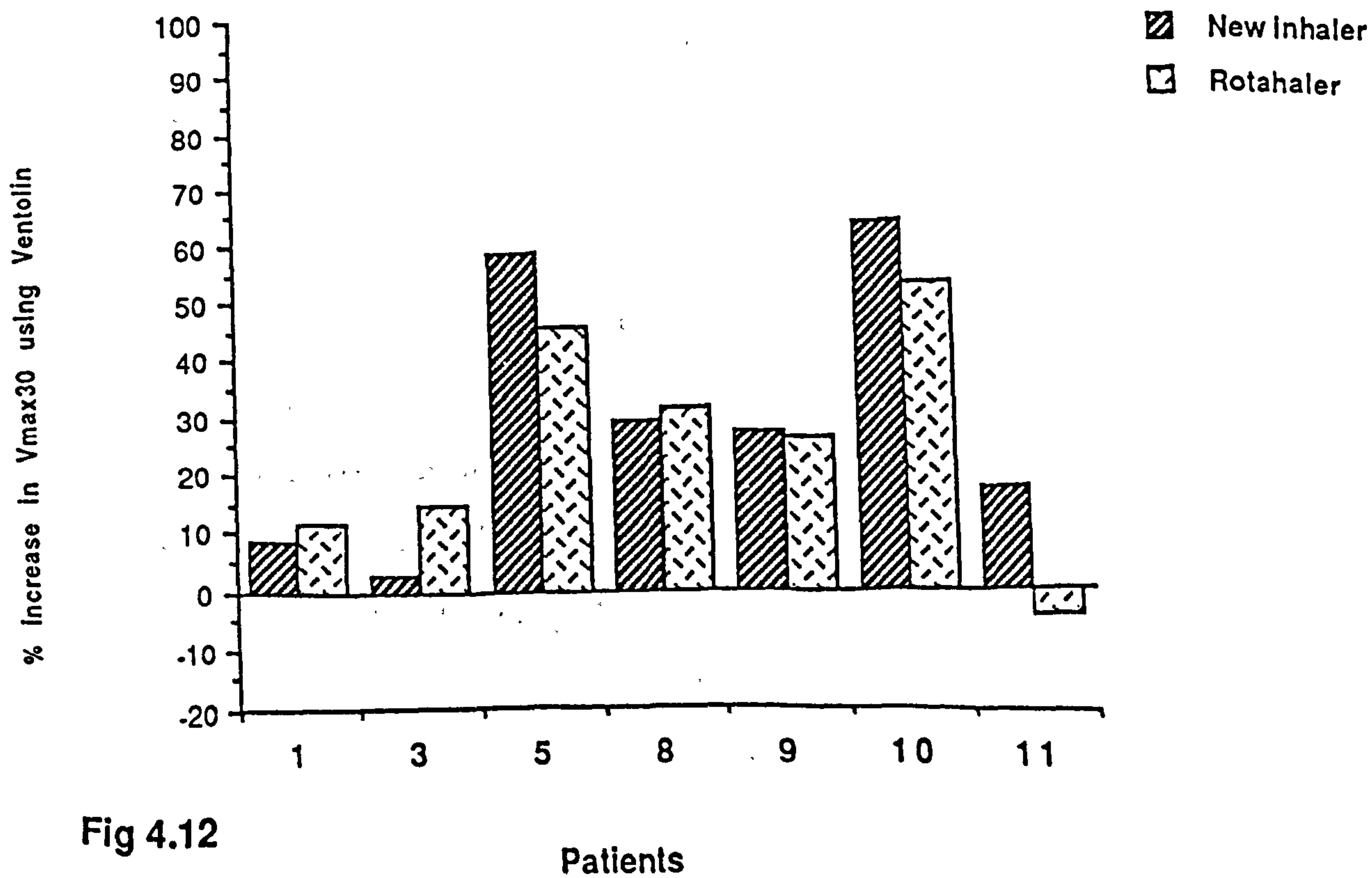
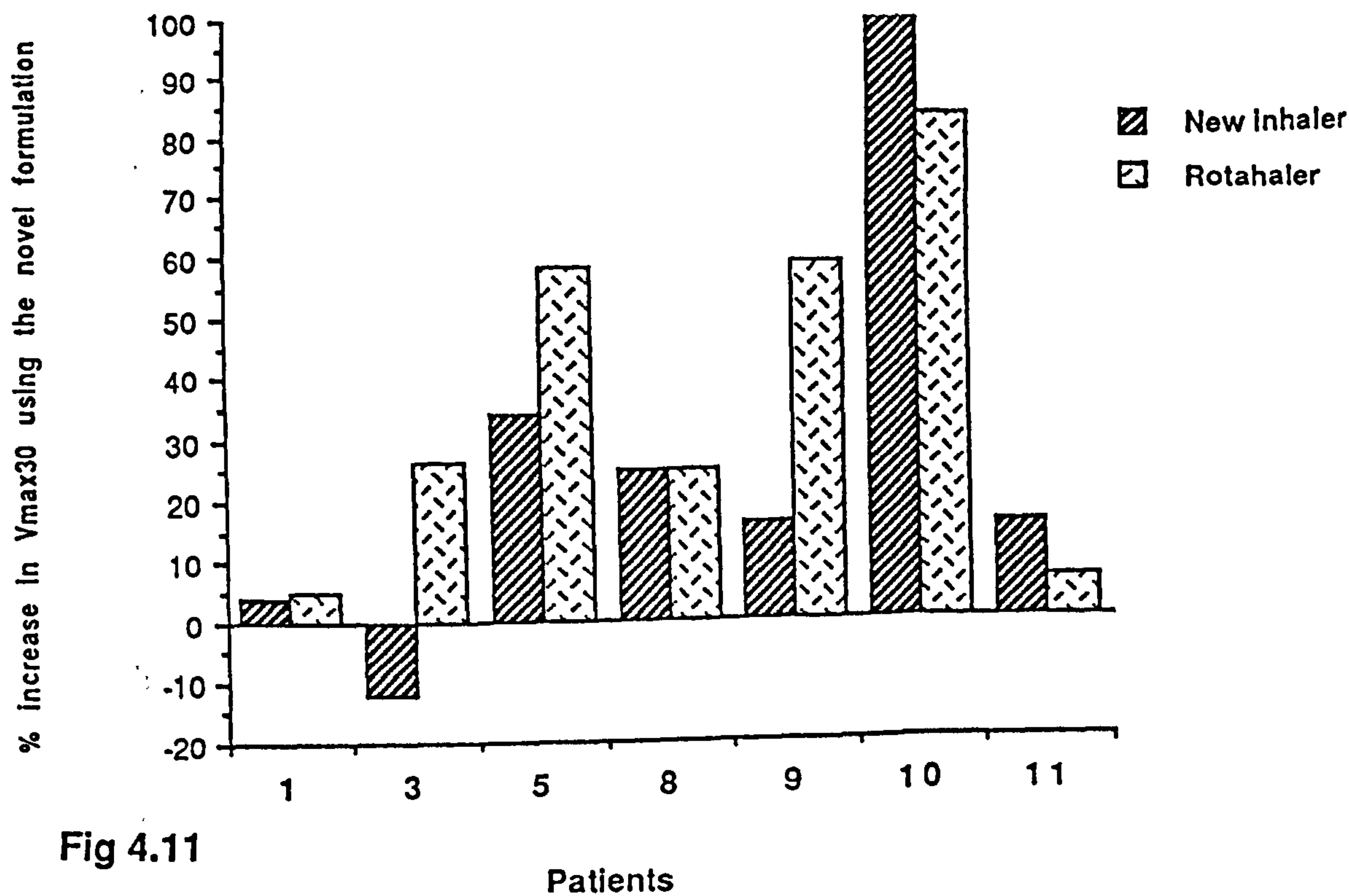


Fig 4.10

Patients

The mean changes in Vmax30 following inhalation with the new inhaler and the Rotahaler



This was expected since the fine drug particles tend to adhere to the walls of the inhaler and the capsule following contact. However, marked variations between individuals and within individuals in each visit were observed. The overall dose of salbutamol delivered from both formulations and with both inhalers differed significantly.

The actual doses delivered per actuation to each individual patient are compared in Figures 4.13 and 4.14. The "Rotahaler" delivered a mean dose of 58.9% and 79.3%, whereas the new inhaler delivered a mean dose of 28.7% and 46.6% of the novel formulation and "Ventolin", respectively.

These figures also indicate that the mean dose delivered from the new formulation was lower than the mean dose delivered from "Ventolin" with both inhalers (Figures 4.15 and 4.16). Therefore, the subjects participating in the study received very much less of the drug on the treatment days where the novel formulation and the new inhaler were used than they did when "Ventolin" and the "Rotahaler" were used.

Therefore, it can be concluded that the novel formulation has proved to be better than "Ventolin" as judged by FEV1 values and equivalent improvement in lung function following the use of the new inhaler.

However, considering the large variations in the amount of drug delivered to each individual patient, it is not possible by comparing the mean FEV1 and  $V_{\max}^{30}$  of all subjects to confirm whether the difference between the two formulations was highly significant or whether any difference between the two inhalers exist. Comparing the results individually, i.e. for each patient, might give a clearer evaluation.



A comparison between the actual dose delivered from the new inhaler and the Rotahaler

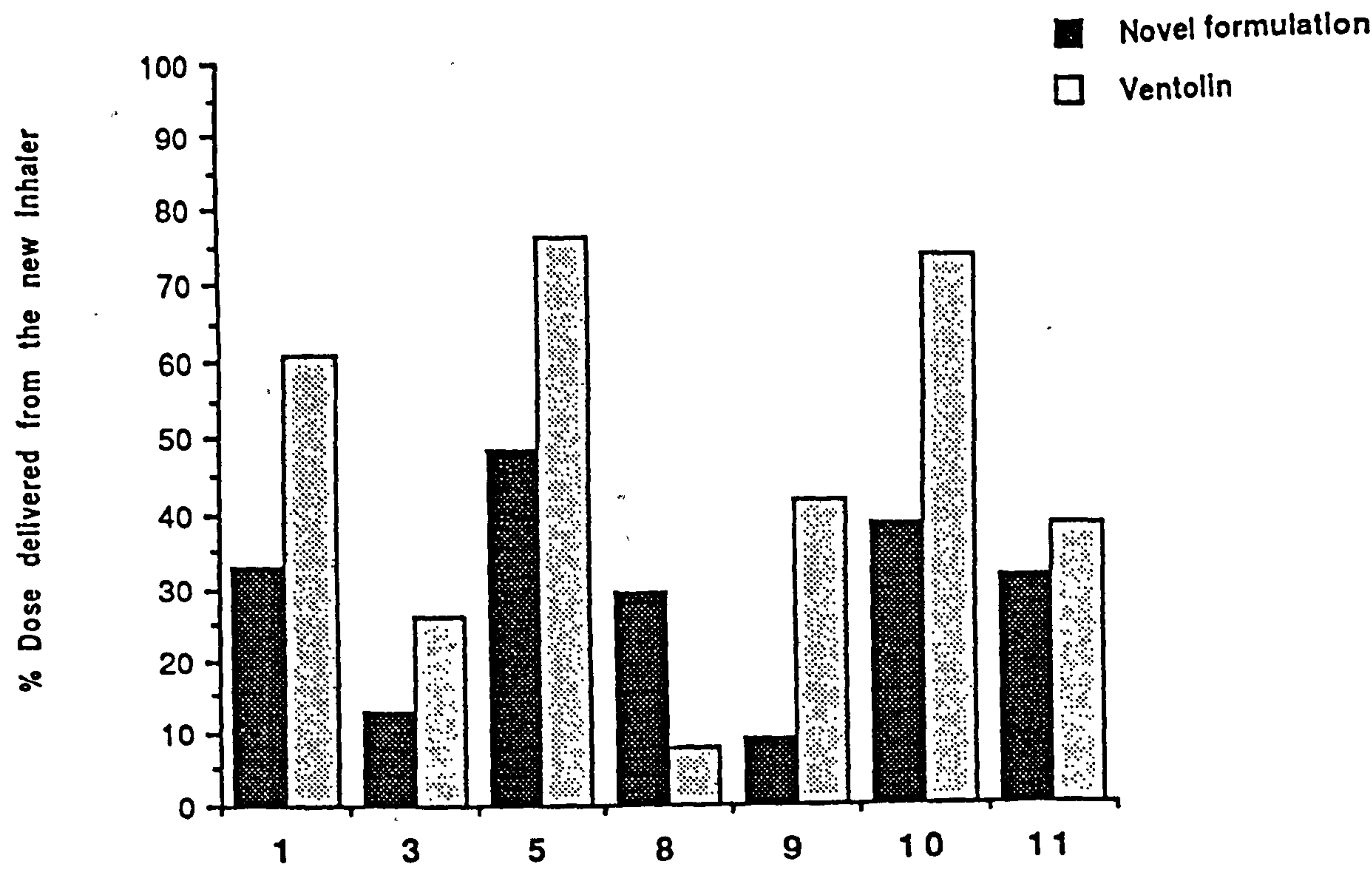


Fig 4.13

Patients

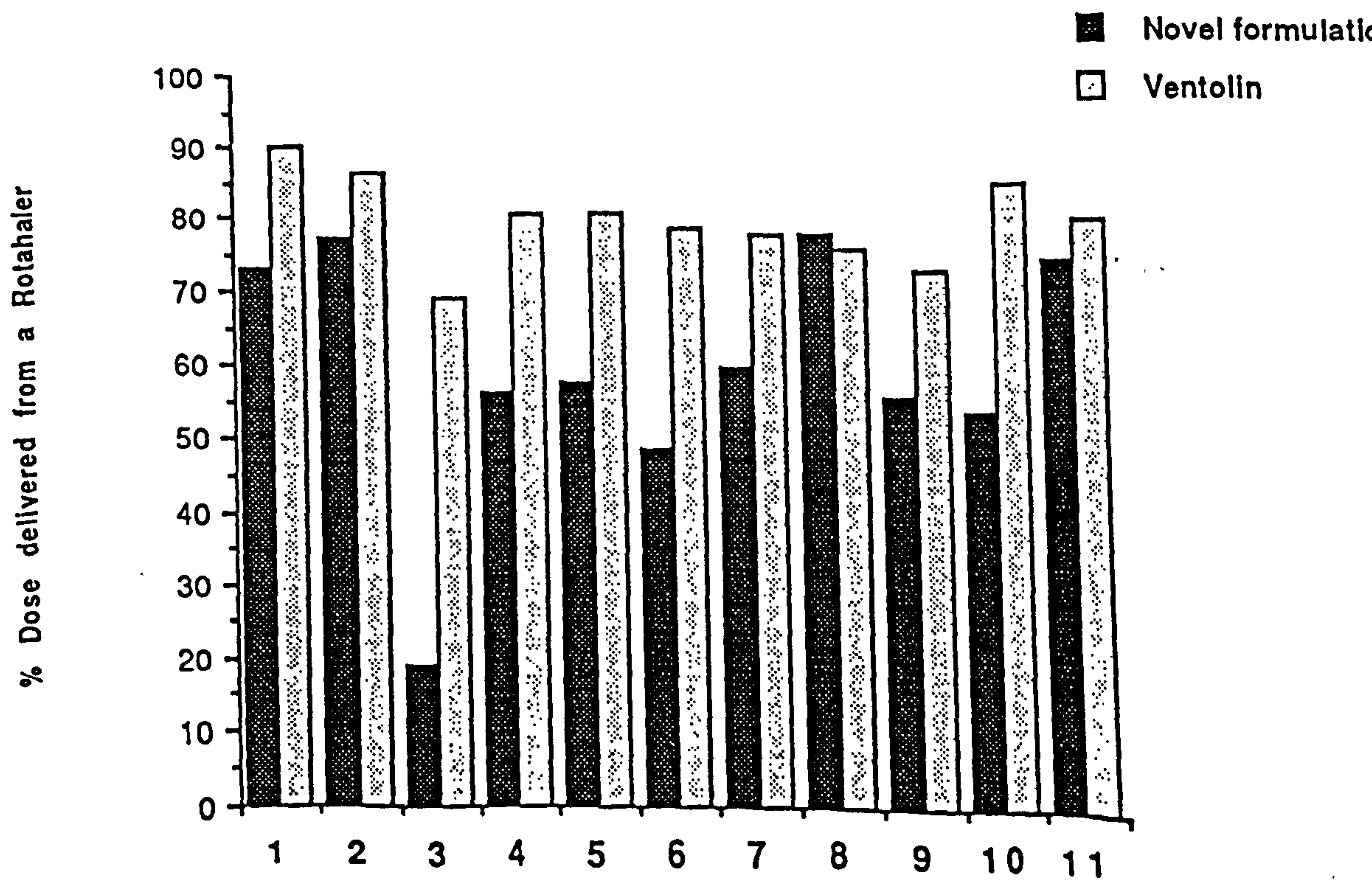


Fig 4.14

Patients

A comparison between the actual dose delivered of the novel formulation and Ventolin

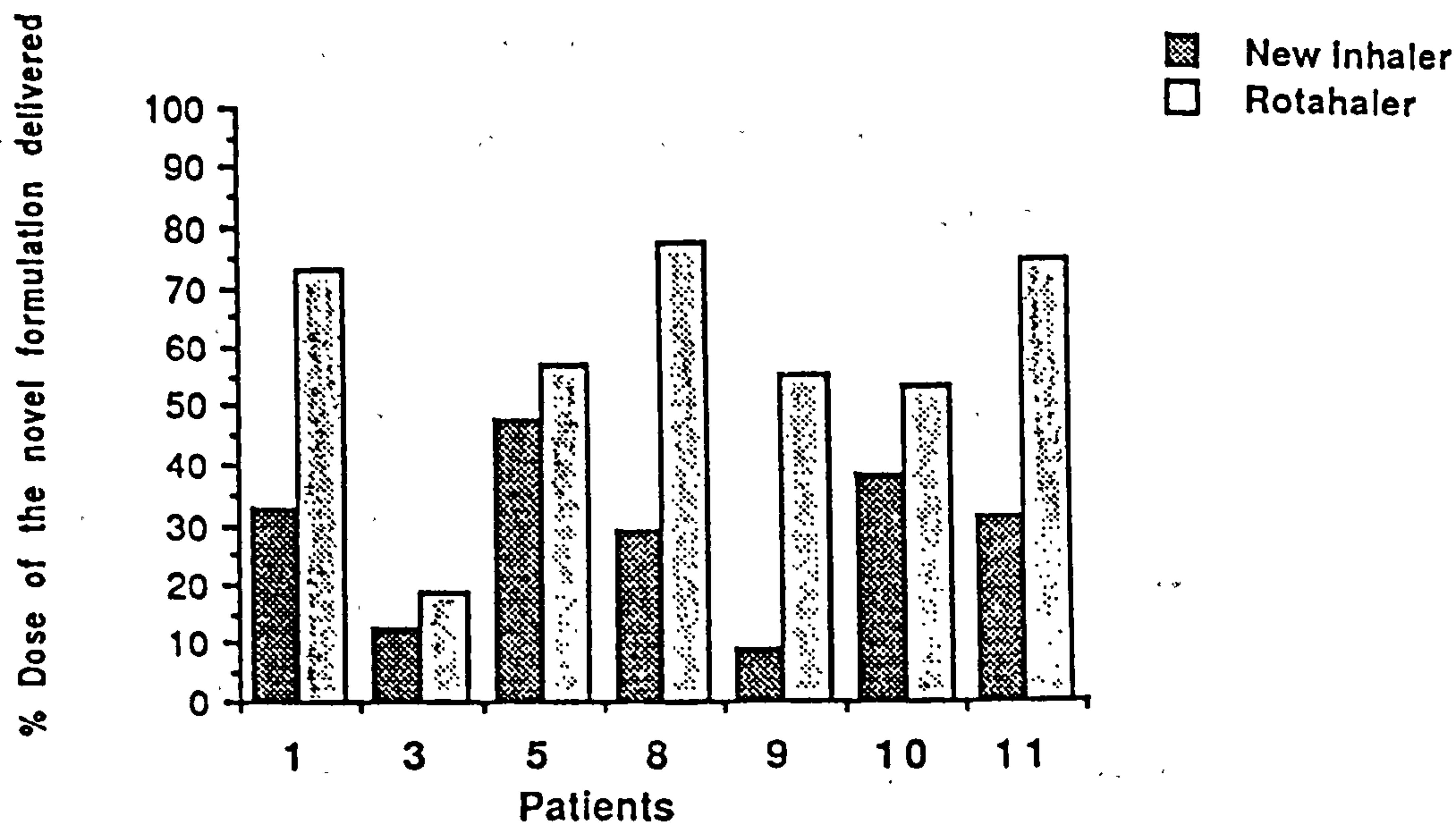


Fig 4.15

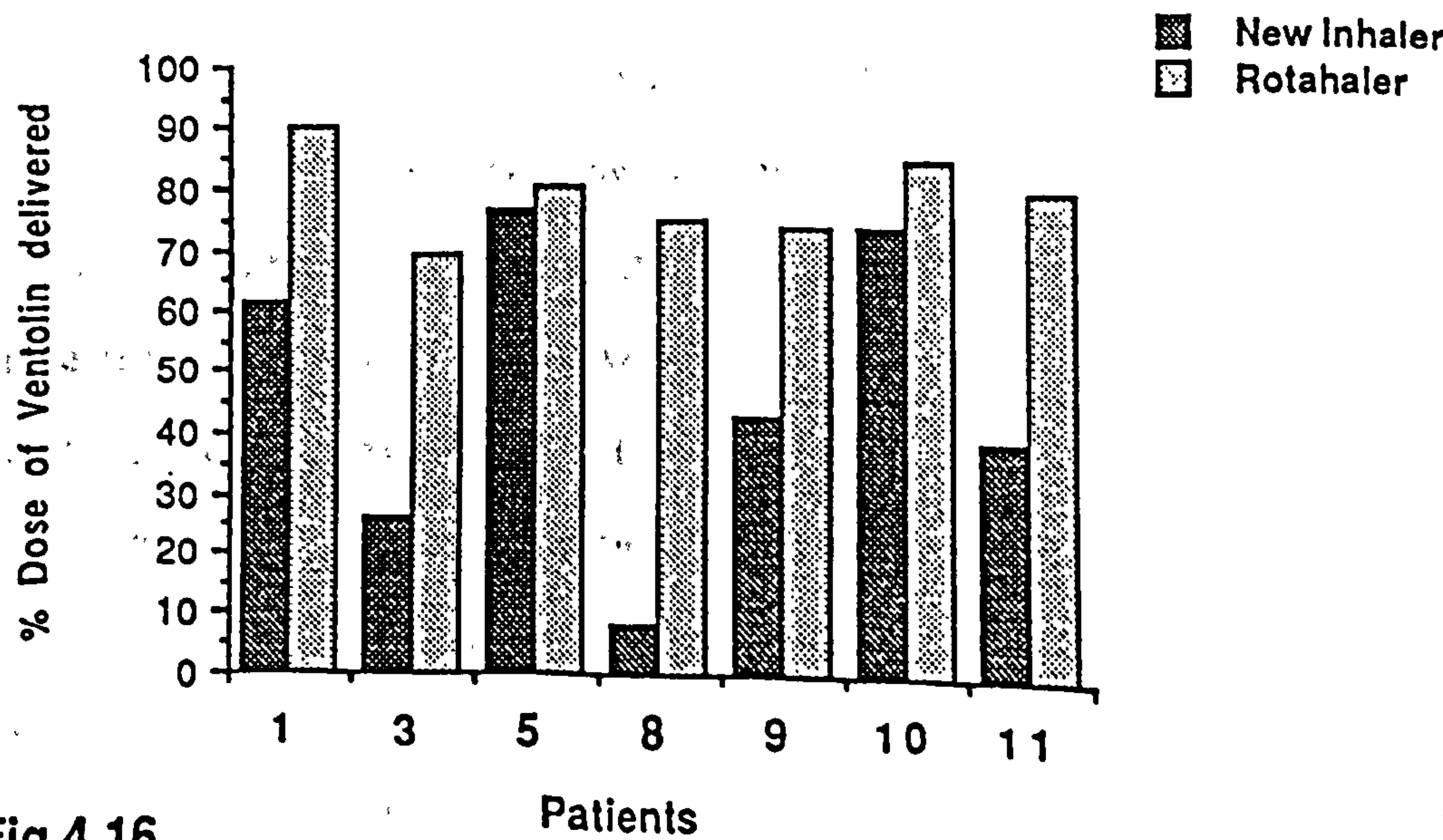


Fig 4.16



The percentage increase in FEV1 and  $V_{\max}^{30}$  from baseline at 5, 10, 15 and 30 minutes for each individual patient is shown in Figures 4.17 to 4.24.

FEV1 values for each patient following administration of either the novel formulation or "Ventolin" using the "Rotahaler" are shown in Figure 4.17.

Despite the substantially lower doses of the novel formulation delivered to each subject, a higher percentage increase in FEV1 was observed for 8 patients (1, 2, 3, 4, 6, 7, 9 and 10) whereas only three patients were slightly better on "Ventolin".

For  $V_{\max}^{30}$  values (Figure 4.18) there was more scatter in the results, three patients (8, 9, and 10) achieving higher values following administration of the novel formulation and three (4, 5 and 7) showing similar response with both formulations.

Only two patients (2 and 6) achieved higher response following inhalation of "Ventolin". Patients 1 and 11 showed no clinical response since the increase over baseline value did not exceed 15% and values even below the pre-treatment baseline were observed for patient 3.

Figures 4.19 and 4.20 compare the lung function measurements for each patient following the use of the new inhaler to deliver the two formulations. The results show a similar trend as that observed with the "Rotahaler". However the number of patients who showed more improvement on the new formulation was less since they received a dose lower than that delivered by the "Rotahaler", and more patients showed no response to the bronchodilator. Two patients (1 and 3) out of seven demonstrated a greater increase in FEV1 over the pre-treatment baseline although they received a dose half of that of "Ventolin".



One patient (9) showed a comparable FEV1 values with both formulations although 41% of the dose was delivered when inhaling "Ventolin" compared to only 9% with the novel formulation.

Patient (10) who achieved higher FEV1 values when inhaling "Ventolin", showed higher  $V_{\max 30}$  values with the novel formulation indicating that more of the drug had penetrated into the small airways.

When comparing the performance of the two inhalers in individual patients following inhalation of either the novel formulation or "Ventolin" (Figures 4.21 to 4.24), it can be observed that many patients achieved either similar or better response. For example, in four patients (1, 3, 10 and 11) the increase in FEV1 over baseline values following inhalation of the novel formulation was similar with both the new inhaler and the "Rotahaler". One patient (9) showed a higher response when using the "Rotahaler". However, this response was only 10% higher than that achieved by the new inhaler although 51% and 9% of the dose was delivered by the "Rotahaler" and the new inhaler, respectively.

Similar results were observed with  $V_{\max 30}$  measurements. For instance, when "Ventolin" was administered by the new inhaler three patients showed a higher response (5, 10 and 11) and 3 patients showed a similar response (1, 8 and 9), although the amount of drug received by each respective patient was less. Patient 11, for example, showed an increase in  $V_{\max 30}$  of 233% above baseline values when using the new inhaler, compared to an increase of 94% when using the "Rotahaler" although a dose of 52% and 74% was delivered via the new inhaler and the "Rotahaler", respectively.

The above results suggest that although the mean improvement in

lung function was not significantly higher for the new inhaler and for the novel formulation as assessed by  $V_{\max}^{30}$ , the variation between individuals was quite large. Such variations have been generally reported by similar studies and are partially due to differences in respiratory anatomy and the disease state of the patient.

In the present investigation an additional reason is the wide variation in the amount of drug retained in the inhalers following inhalation. One cause for these variations is that these two inhalers were used for the first time by the subjects participating in the study and no previous training was given on the correct use. Moreover, the use of a specific inhalation technique was not practiced by the patients. For instance, the number of inhalations from the inhaler was not standardized, some patients used two consecutive inhalations and some inhaled once only. Additionally, there was both intra-individual and inter-individual differences in the velocity of the inspiratory air flow. The influence of the inhalation manoeuvre on lung function has been demonstrated by several workers (Groth and Dirksen, 1983; Auty *et al*, 1987; Richard *et al*, 1988; Dolovich *et al*, 1989 and Pedersen *et al*, 1990) and found to highly affect the performance of a powder inhalation product.

Therefore, it can be concluded that since the inhalation technique was not standardized, comparing the two inhalation devices in the present study might not be reliable even if done individually. In a study carried out by Vidgren *et al* (1987) to compare the performance of different commercially available inhalers, patients were trained to inhale at air flow between 55-70 l/min.

However, comparing the results individually illustrates that the



novel formulation and the new inhaler may prove to be more efficient if the same dose was delivered to the patients during the study. For instance,  $V_{\max}30$ , which indicates drug penetration into the small airways ( $\leq 2\text{mm}$ ), was either higher or similar in most patients using the new inhaler despite the smaller amount of drug inhaled, demonstrating that a deeply and highly inspirable cloud can be generated if the dispensing efficiency of the inhaler is improved.

The high retention of the drug in the new inhaler was observed in the *in vitro* experiments (Section 3.3.2), it did not exceed 34%. Fractions of up to 92% were retained when the inhaler was used by the patients.

Variations in the amount of drug recovered from the inhaler following use by the patient was reported by Vidgren *et al* (1987d) and was found to be dependent on the inspiratory effort. In one investigation a mean retention of 43.8% was observed when inhaling from a "Rotahaler" at an air flow of 55-70 l/min. In another investigation (Vidgren *et al* , 1990) where the inspiratory flow rate was not standardized, 25.8% was recovered from the same inhaler indicating that patients inhaled faster.

The high retention of the drug in the new inhaler was mainly attributed to its complicated design compared to that of the "Rotahaler". Additionally, the glass material of the inhaler may influence the nature of the electrostatic charges induced on the powder particles upon fluidisation and hence the electrostatic attraction to the walls of the inhaler.

The length of the inhaler might also affect its emptying efficiency since the powder particles travel a longer distance before they reach the mouth piece and thus they may settle due to gravitational



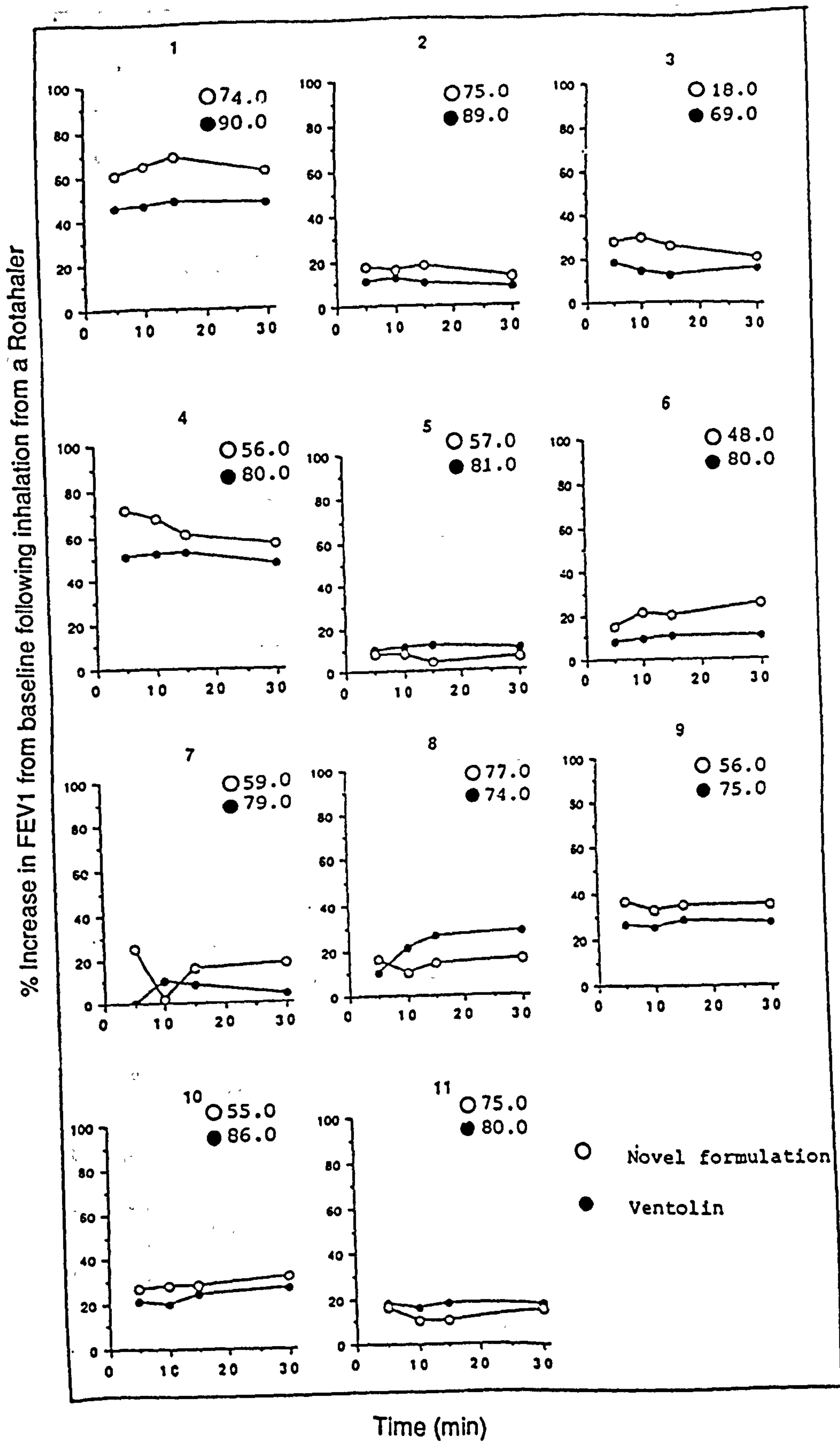


**Fig 4.17** FEV1 values for each patient following inhalation of either the novel formulation or Ventolin using the Rotahaler

The percentage of the dose delivered to each numbered patient is indicated by the symbols next to each diagram.

% Increase in Vmax30 from baseline following inhalation from a Rotahaler

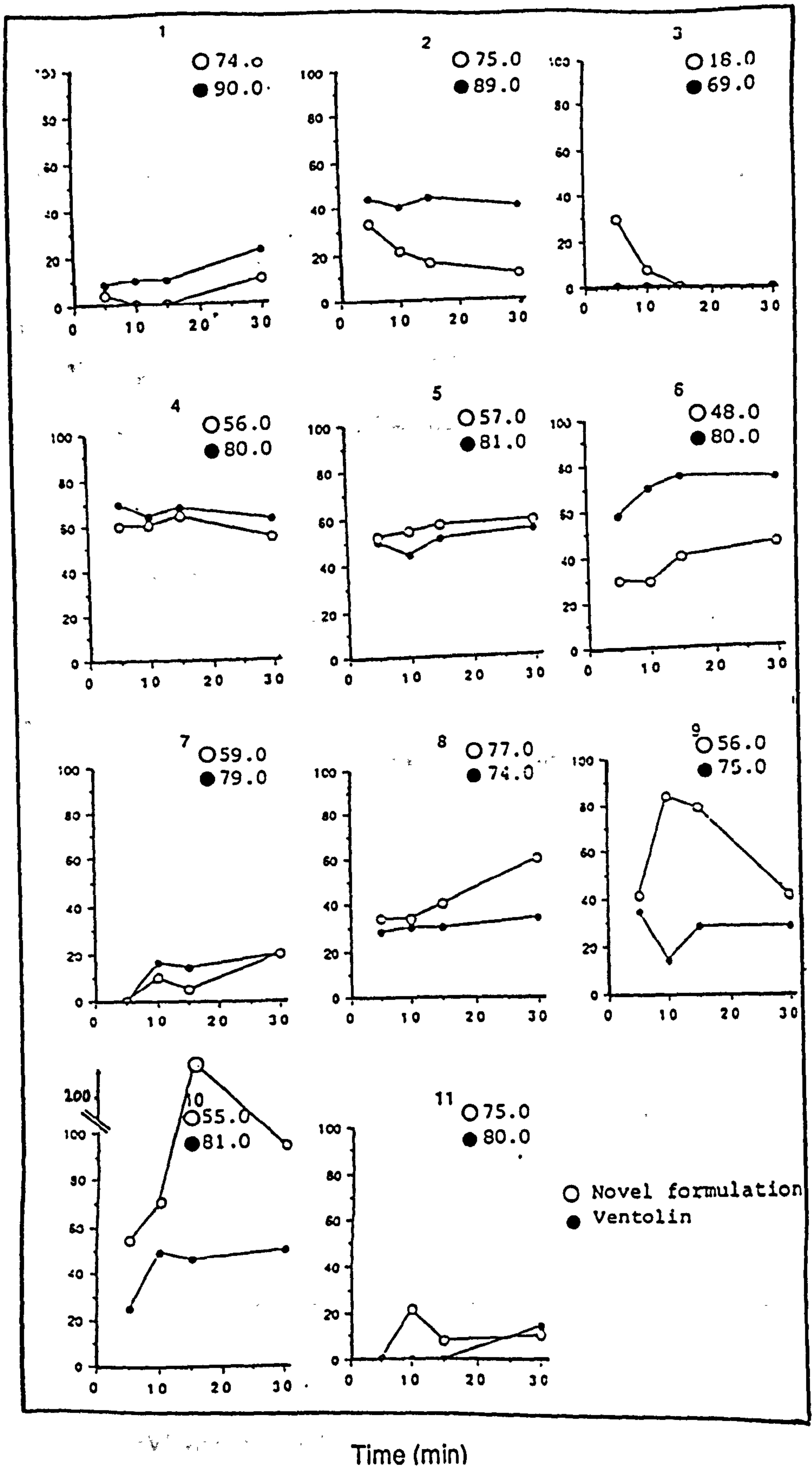


**Fig 4.18** Vmax30 values for each patient following inhalation of either the novel formulation or Ventolin using the Rotahaler

The percentage of the dose delivered to each numbered patient is indicated by symbols next to each diagram.

% Increase in FEV1 from baseline following inhalation from a new inhaler

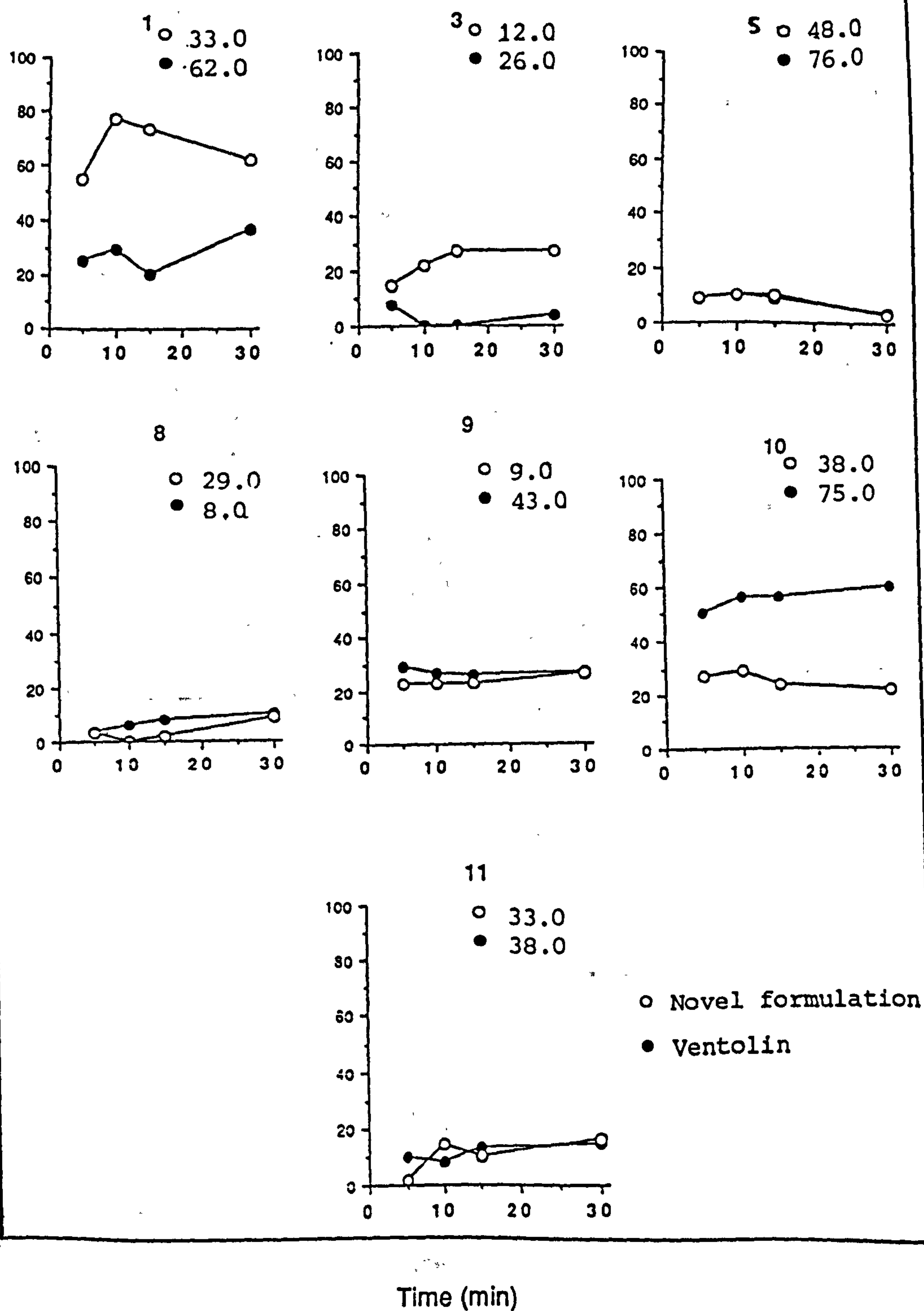


**Fig 4.19** FEV1 values for each patient following inhalation of either the novel formulation or Ventolin using the new inhaler

The percentage of the dose delivered to each numbered patient is indicated by the symbols next to each diagram.



% increase in Vmax30 from baseline following inhalation from a new inhaler

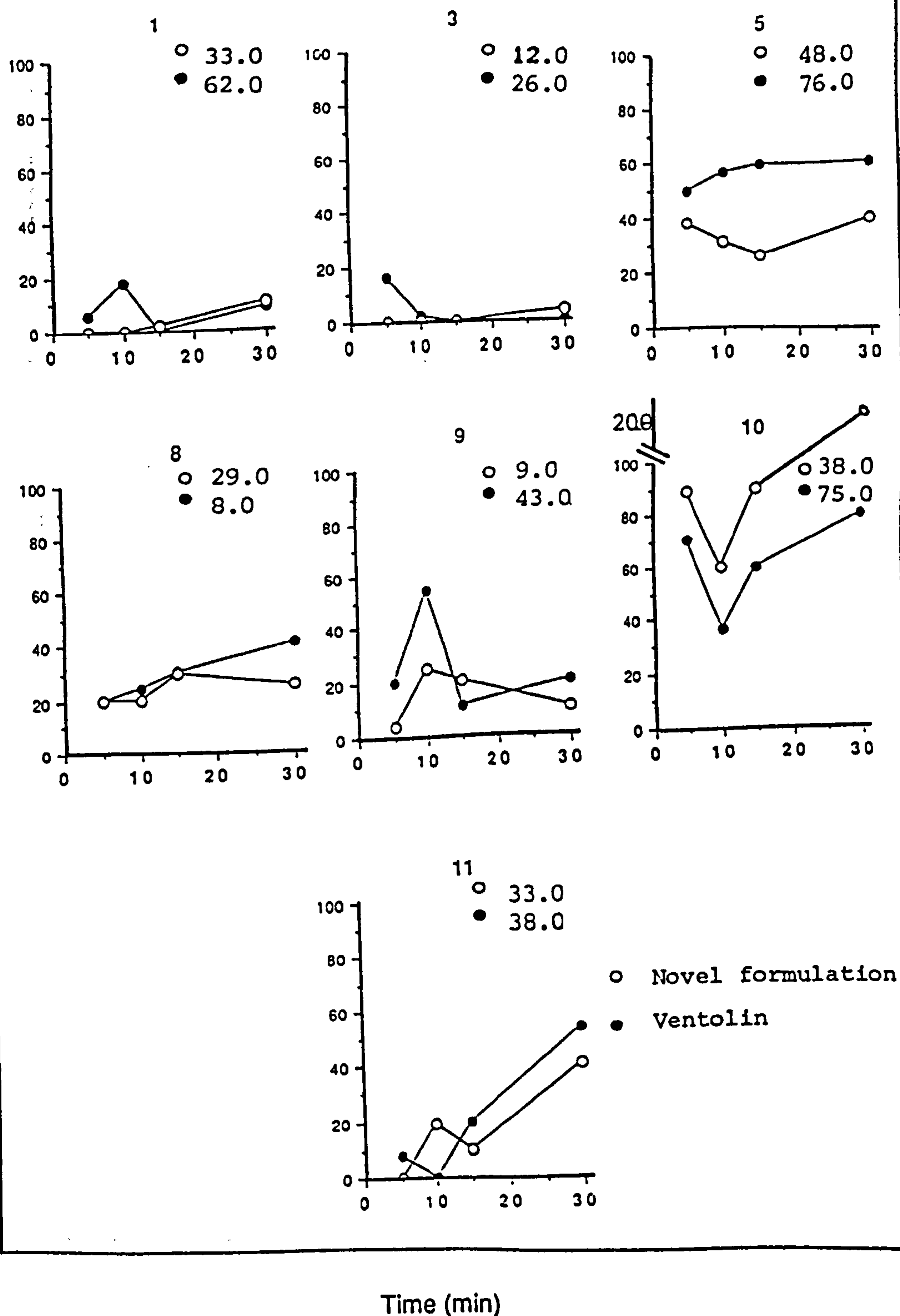


**Fig 4.20** Vmax30 values for each patient following inhalation of either the novel formulation or Ventolin using the new inhaler

The percentage of the dose delivered to each numbered patient is indicated by the symbols next to each diagram.

% Increase in Vmax30 from baseline following inhalation of the novel formulation

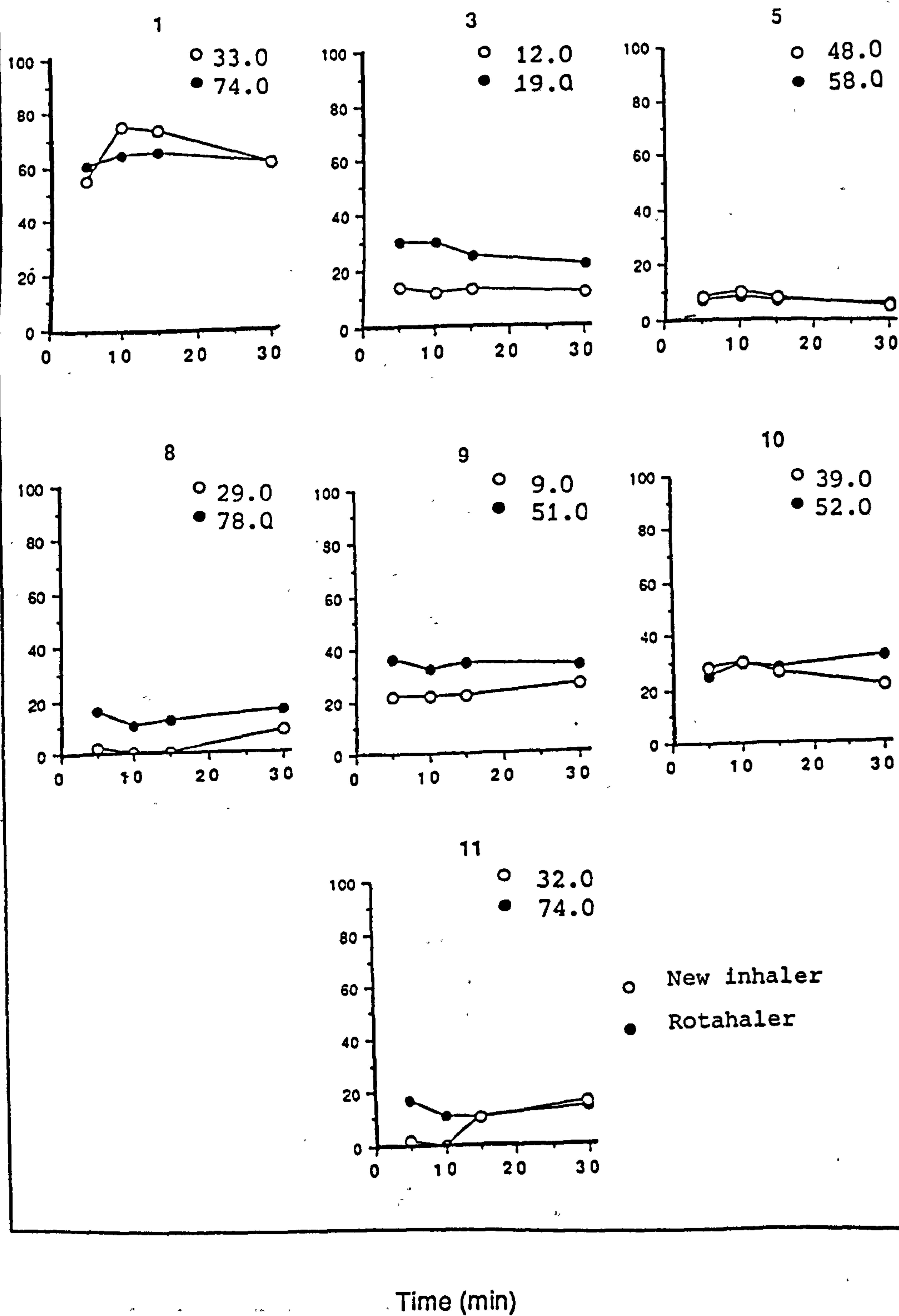


**Fig 4.21** FEV1 values for each patient following inhalation of the novel formulation using either the new inhaler or the Rotahaler

The percentage of the dose delivered to each numbered patient is indicated by the symbols next to each diagram.

% Increase in FEV1 from baseline following inhalation of the novel formulation

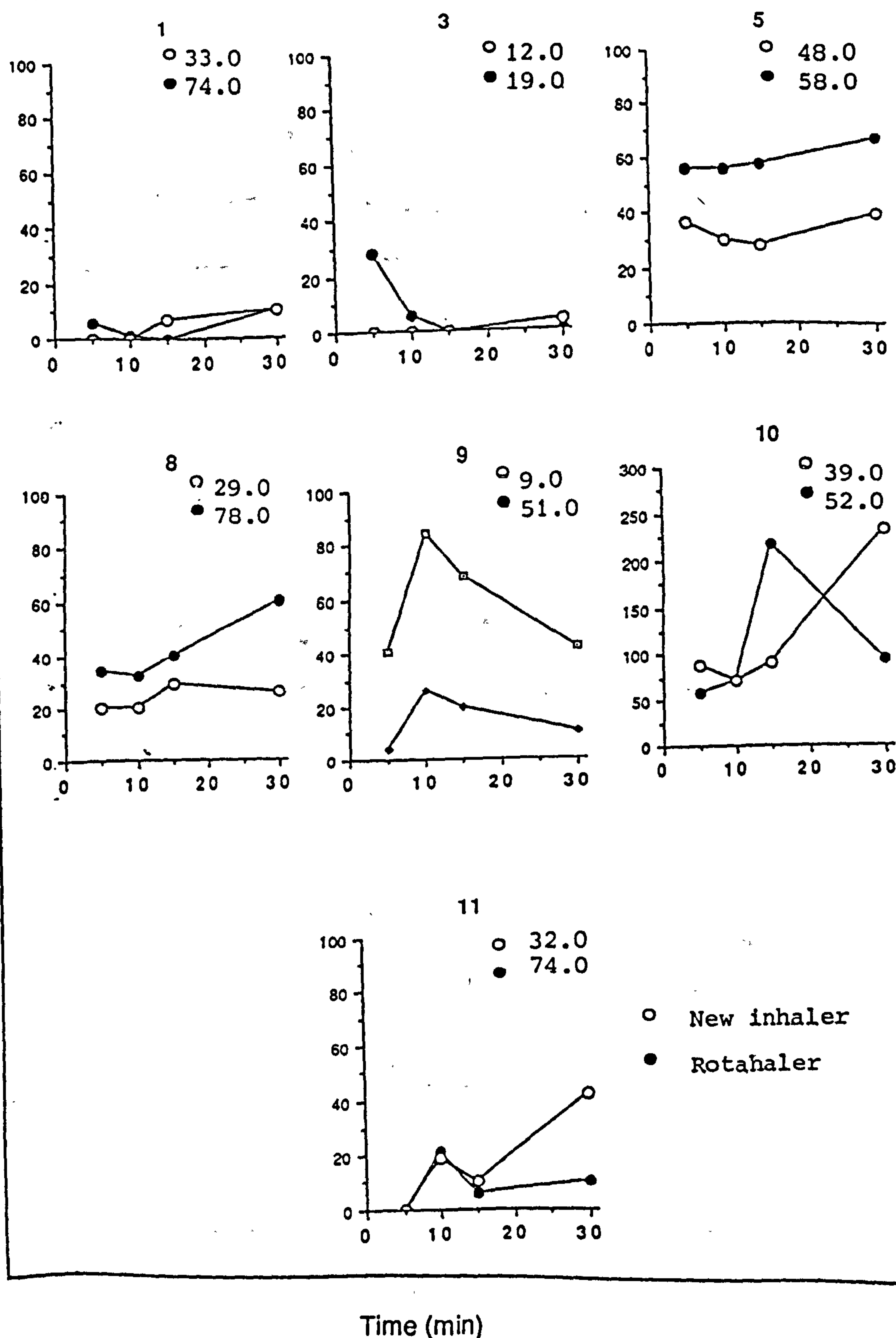


**Fig 4.22** Vmax30 values for each patient following inhalation of the novel formulation using either the new inhaler or the Rotahaler

The percentage of the dose delivered to each numbered patient is indicated by the symbols next to each diagram.



% increase in FEV1 from baseline following inhalation of Ventolin

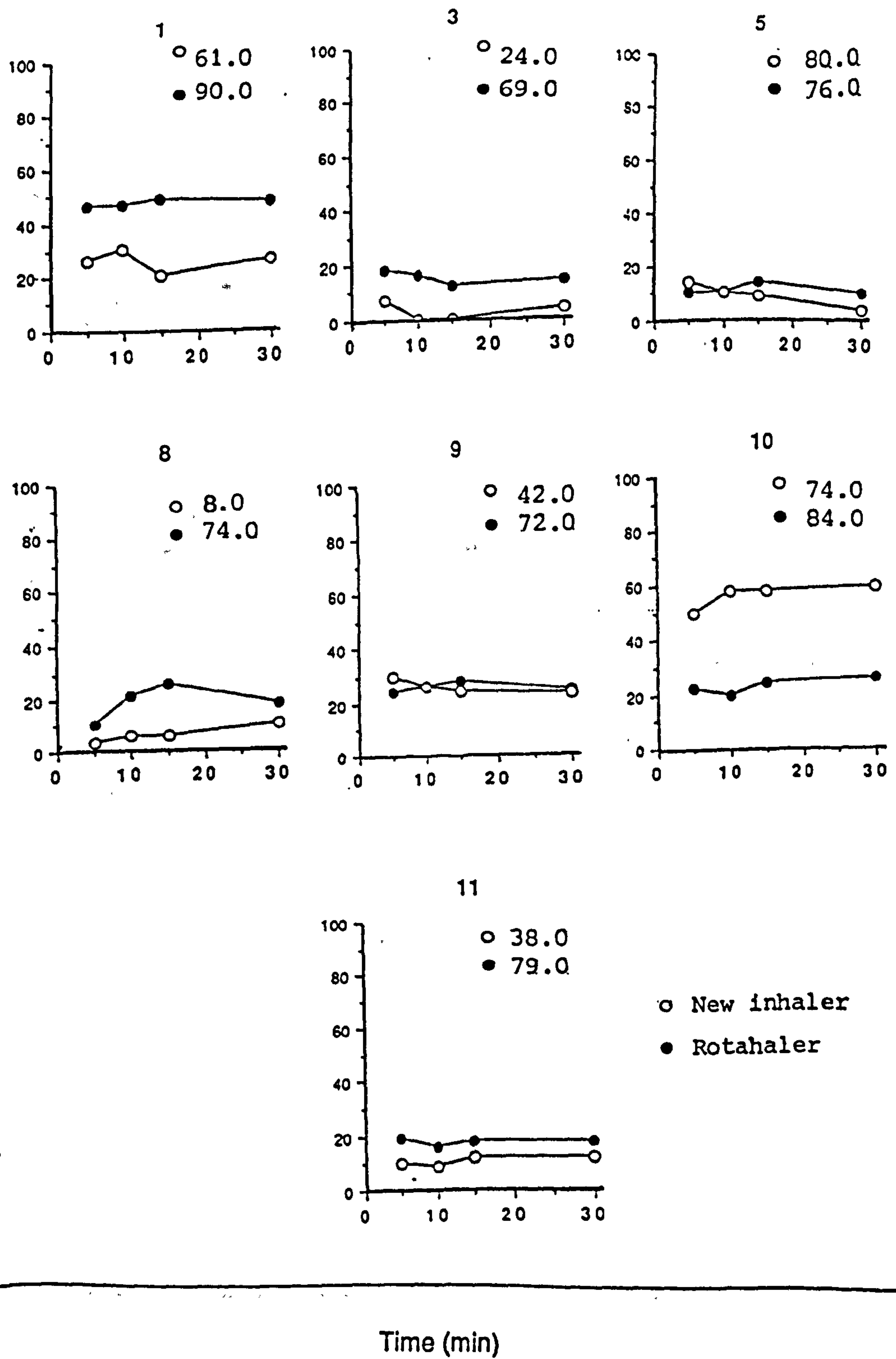


**Fig 4.23** FEV1 values for each patient following inhalation of Ventolin using either the new inhaler or the Rotahaler

The percentage of the dose delivered to each numbered patient is indicated by the symbols next to each diagram.

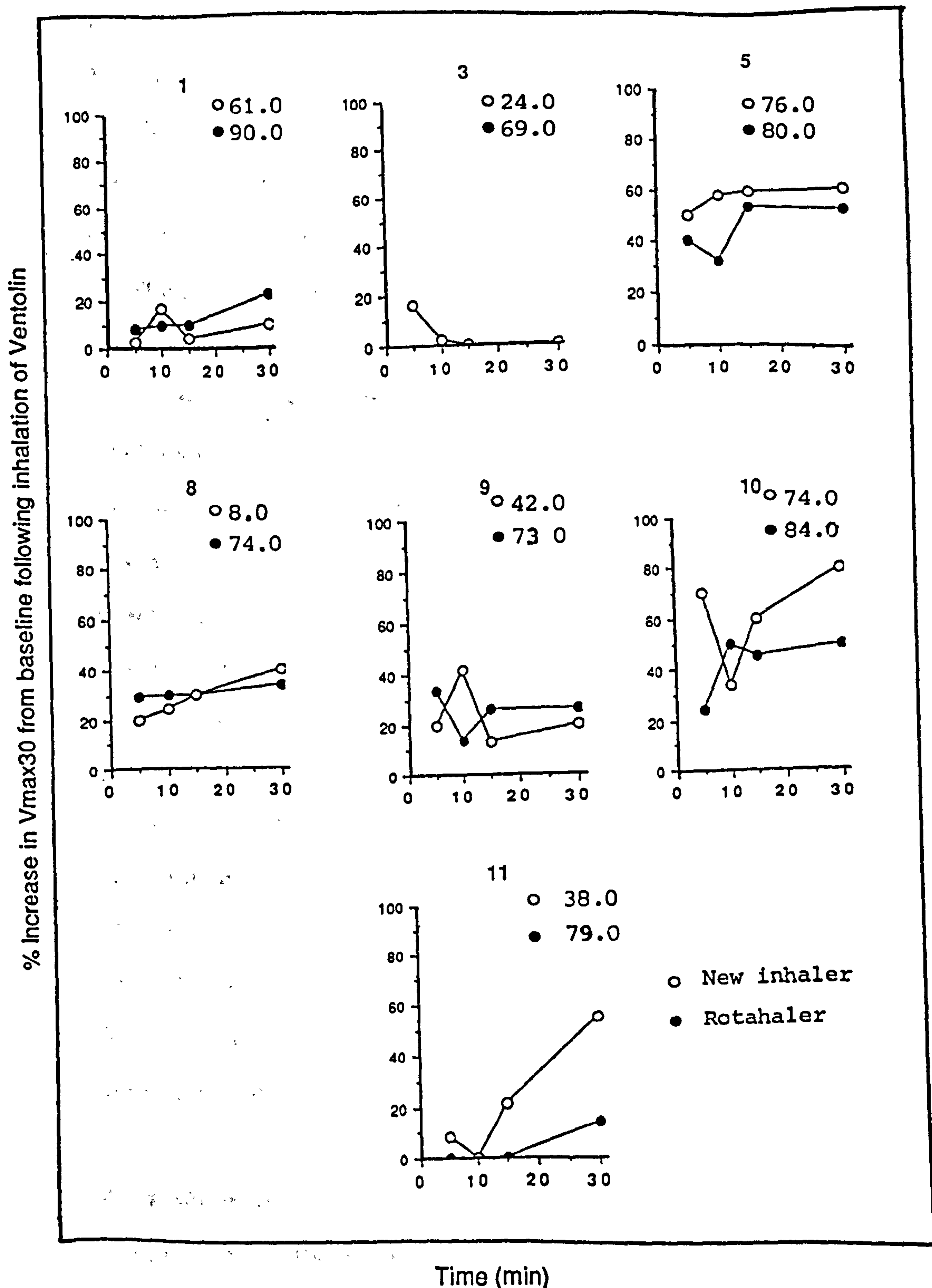


**Fig 4.24** Vmax30 values for each patient following inhalation of Ventolin using either the new inhaler or the Rotahaler

The percentage of the dose delivered to each numbered patient is indicated by the symbols next to each diagram.

influence. It was not possible to construct a shorter version of the inhaler from glass due to technical difficulties.

Another contributing factor to the inefficient emptying of the inhaler, is failure of the capsule part, which drops during dispensing, to rotate upon inhalation and consequently most of the powder remains in the capsule. This problem can be attributed to the insufficient inspiratory effort which is the only energy source for rotation of the capsule. It has been established that the effect of the "Rotahaler" is reduced at inspiratory flow rates below 50 l/min (Pedersen , 1990). However, it is not clear how sensitive is the new inhaler to a reduction in inspiratory flow below 60 l/min and it is possible that there is a critical air flow rate below which the effect will be reduced.

These observed problems with the new inhaler suggest that some modifications are required to facilitate more efficient emptying. However the results of this investigation indicate that the basic design of the inhaler offers an advantage of generating a deeply inspirable cloud.

The reason for the higher drug retention in the inhaler observed when the novel formulation was used is unclear since a comparable fraction of the drug was recovered with both formulations in the *in vitro* experiments.

#### 4.3.4 Subjective results

Comments on the sensation and taste of both treatments are summarized in Figure 4.25. Some patients verbally reported an improvement in their symptoms following the administration of the drug particularly the novel formulation and when using the new inhaler although their lung function tests showed no difference.

Patients also reported the feeling of powder on the tongue in all



Questionnaire response to

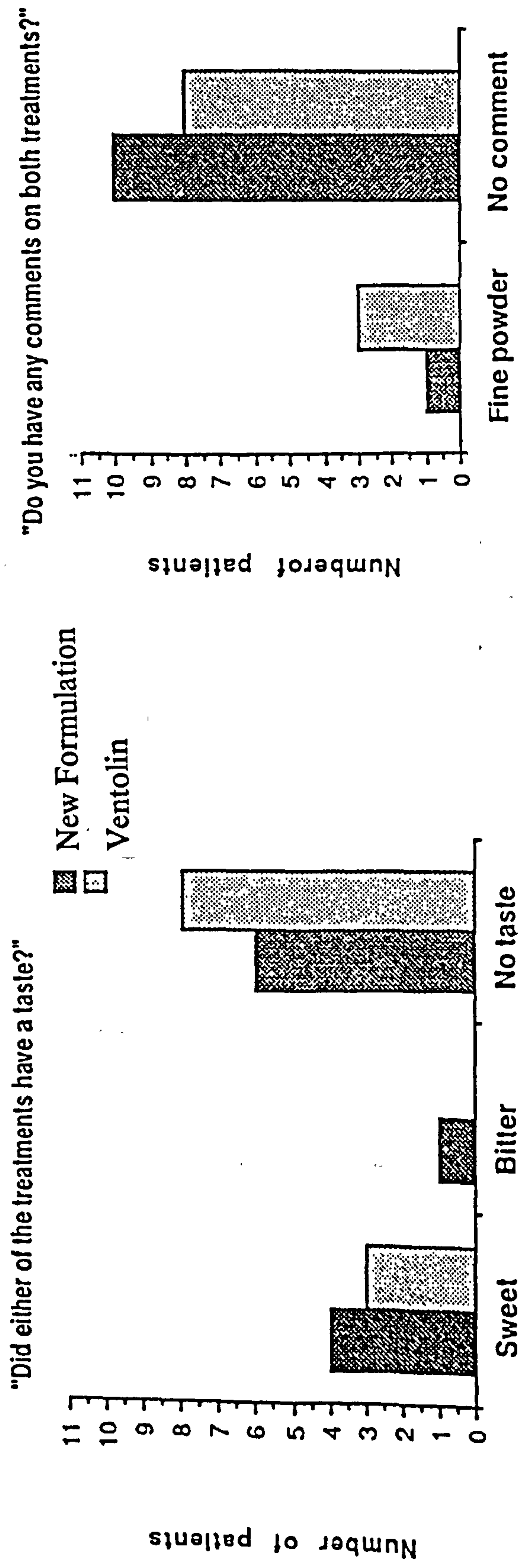


Fig 4.25

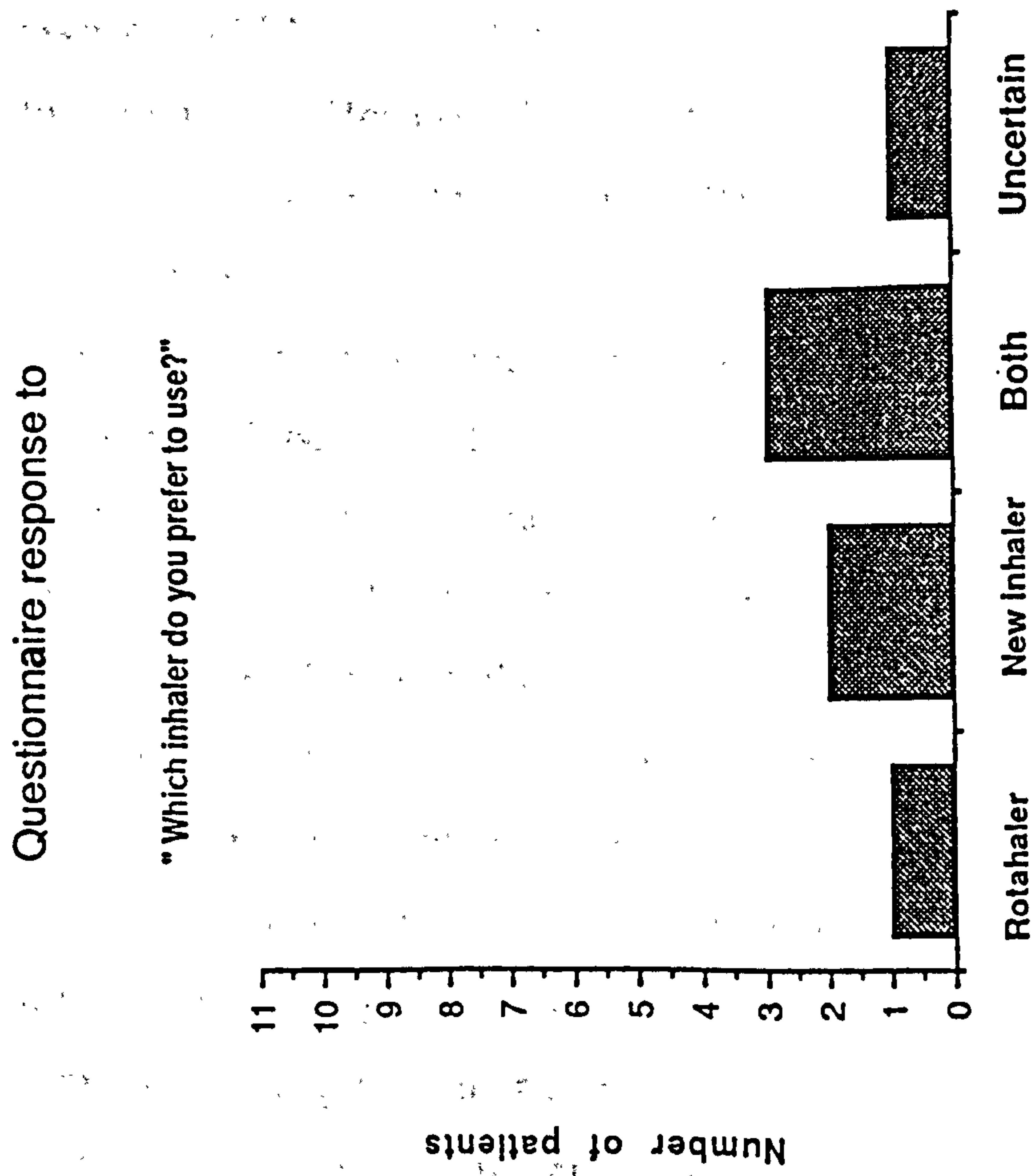


Fig 4.26

cases.

Patient acceptability of the inhalers is shown in Figure 4.26. The results indicate a high degree of patient acceptability to both inhalers which also indicate patient acceptability to this type of inhalation delivery system since they were using it for the first time.

#### **4.4 Conclusions**

This preliminary study showed that the novel formulation with a modified carrier was clinically more efficient than "Ventolin" as assessed by FEV1 despite the large difference in the dose delivered to the patient. However, it failed to confirm whether the new inhaler was more effective than the "Rotahaler" in redispersing the aerosol cloud.

The results suggest that modifying the construction of the inhaler to improve its dispensing efficiency, while keeping the same principle for generating high turbulence, is essential. Additionally, avoiding the shortcomings of this study in future work may result in a more constructive evaluation of the new inhaler.

Standardization of the inspiratory manoeuvre is essential and patients should train on the correct use of the inhaler prior to the study and practice a specific inspiratory flow rate. The number of inhalations through the inhaler should also be standardized. Moreover, a larger number of patients should be involved since seven patients are not sufficient to compare two delivery devices. A more suitable design would be an open randomized, cross-over study in which more patients are enrolled. Another study design which can be used is a cumulative dose response comparison between the two formulations with both inhalers. This type of study requires a small number of patients all of which must show a



response at a certain dose level. Another advantage with this study design is that differences in response can be more obvious at higher doses. Moreover, an indication of the dose required to achieve a maximal response can be established; this could be different for both formulations. The formulation requiring a smaller dose to achieve a maximal response being the more efficient.

In conclusion, further clinical studies would be valuable.

## References

Agnese, D.S. and Anderson, D.A., 1946, Celiac syndrome. *Am. J. Dis. Child.*, 72: 17-61.

Agnew, J.W., 1984, Physical properties and mechanisms of deposition of aerosols. In: Clarke, S.W. and Pavia, D. eds. *Aerosols and the lung: Clinical and experimental aspects*, Butterworths, London.

Allen, T., 1981, Sampling of dusty gases in gas streams. In: *Particle size measurement* (3rd ed.), Chapman and Hall, London.

Assoufi, B.K. and Hodson, M.E., 1989, High dose salbutamol in chronic air flow obstruction: comparison of nebulizer with rotacaps. *Resp. Med.*, 83: 415-420.

Auty, R.M., Brown, K., Neale, M.G. and Snashall, P.D., 1987, Respiratory tract deposition of sodium cromoglycate is highly dependent upon technique of inhalation using the Spinhaler. *Br.J. Dis. Chest*, 88 : 371-378.

Bell, J.H., Hartley, P.S. and Cox, J.S.F., 1971, Dry powder aerosols I: A new powder inhalation device. *J. Pharm. Sci.*, 60: 1555-1563.

Benoy, C.I., El-Fellam, M.S., Scheneida, R. and Wade, O.L., 1975, Tolerance to sympathomimetic bronchodilators in guinea-pig isolated lungs following chronic administration *in vivo*. *Br. J. Pharmacol.*, 55: 547-554.

Bogaard, J.M., Slingeland, R. and Verbreak A., 1989, Dose-effect relationship of terbutaline using a multidose powder inhalation system (Turbohaler) and salbutamol administered by powder inhalation (Rotahaler) in asthmatics. *Pharmatherapeutica*, 5: 400-406.

Boschung, P. and Glor, M., 1980, Methods for investigating the electrostatic behaviour of powders. *J. Electrostat.*, 8: 205-219.

Bouchikhi, A., Becquemin, M.H., Bignon, J. and Teillac, A., 1988, Particle size study of nine metered dose inhalers, and their deposition probabilities in the airways. *Eur. Resp. J.*, 1: 547-552.

British pharmacopoeia, 1988, Vol II, Appendix XVIIC, A 204-207.

British pharmacopoeia, 1988, Vol II: 875.

Brogdan, R.N., Speight, T.M. and Avery, G., 1974, Sodium cromoglycate (cromolyn sodium): A review of its mode of action, pharmacology, therapeutic efficacy and use. *Drugs*, 7: 164-282.

Brompton Hospital/Medical Research Council Collaborative Trial, 1972, Long-term study of disodium cromoglycate in treatment of severe extrinsic or intrinsic bronchial asthma in adults. *Br. Med. J.*, 2: 383-388.

Carmicheal, J., Duncan, D. and Crompton, G.K., 1978, Beclomethesone dipropionate dry powder inhalation compared



with conventional aerosol in chronic asthma. Br. Med. J., 2:657-658

Chambers, S., Dunbar, J. and Taylor, B., 1980, Inhaled powder compared with aerosol administration of fenoterol in asthmatic children. Arch. Dis. Child, 55: 73-74.

Chan, T.L. and Yu, C.P., 1982, Charge effects on particle deposition in the human tracheobronchial tree. In: Inhaled particles, V. Ed: Walton, W.H., Pergamon, Oxford, 65.

Chowhan, Z.T. and Amaro, A.A., 1977, Powder inhalation studies I: Selection of a suitable drug entity for bronchial delivery of new drugs. J. Pharm. Sci., 66: 1254-1258.

Chowhan, Z.T. and Linn, E.E., 1979, Powder inhalation studies II. *In vitro* rat lung model and its comparison with the air sampler. Int. J. Pharm., 3: 117-126.

Clark, T.J.H., 1979, Small airways in health and disease. Excerpta Medica, Amsterdam: 170-178.

Clay, M.M., Pavia, D., Newman, S.P. and Clarke, S.W., 1983, Factors influencing the size distribution of aerosols from jet nebulizers. Thorax, 38: 755-759.

Conolly, M.E., Davies, D.S., Dollery, C.T. and George, C.F., 1971, Resistance to  $\beta$ -adrenoceptor stimulants (A possible explanation for the rise in asthma deaths). Br. J. Pharmacol., 43: 389-402.

Corn, M. and Stein, F., 1965, Re-entrainment of particles from a plane surface. *Am. Ind. Hyg. Assoc. J.*, 26: 325-336.

Crompton, G.K., 1988, New inhalation devices. *Eur. Resp. J.*, 1: 679-680.

Crompton, G.K., 1982a, Inhalation devices. *Eur. J. Resp. Dis.*, 63: 489-492

Crompton, G.K., 1982b, Problems patients have using pressurized aerosol inhalers. *Eur. J. Resp. Dis.*, 63, Suppl. 119: 101-104.

Curry, S.H., Taylor, A.J. and Evans, S., 1975, Deposition of disodium cromoglycate administered in three particle sizes. *Br. J. Clin. Pharmacol.*, 2: 257-270.

Davis, C.N., 1979, Particle-fluid interactions. *J. Aerosol Sci.*, 10: 477-513.

Davies, D.S., 1975, Pharmacokinetics of inhaled substances. *Postgraduate Med. J.*, 51: 69-75.

Davies, P.J., Amin, K.K. and Mott, G.A., 1980a, Particle size of inhalation systems II: Uniformity of delivery of some commercial inhalation aerosols. *Drug Develop. Ind. Pharm.*, 6: 653-658.

Davies, P.J., Amin, K.K. and Mott, G.A., 1980b, Particle size of inhalation aerosol systems I: Production of homogenous dispersions. *Drug Develop. Ind. Pharm.*, 6: 645-651.

Davies, P.J., Hanlon, G.W. and Molyneux, A.J., 1976, An Investigation into the deposition of inhalation aerosol particles as a function of air flow rate in a modified 'Kirk lung'. J. Pharm. Pharmacol., 28: 908-911.

Davis , S.S., 1978, Physico-chemical studies on aerosol solutions for drug delivery I. Water-propylene glycol systems. Int. J. Pharm., 1: 71-83.

Davies, S.E., 1968, Effect of disodium cromoglycate on exercise-induced asthma. Br. Med. J., 3: 593-594.

Deckers, W., 1975, The chemistry of new derivatives of tropane alkaloids and the pharmacokinetics of a new quaternary compound. Postgrad. Med. J., 5, Suppl. 7: 76-78.

Dolovich, M., Vanzielegem, M., Hidingier, K.G. and Newhouse, M.T., 1989, Influence of inspiratory flow rate on the response to terbutaline sulphate inhaled via the Turbohaler. Am. Rev. Resp. Dis., 137: 433.

Douglas, N.J., Davidson, I., Sudlow, M.F. and Flenley, D.C., 1979, Bronchodilation and the site of airway resistance in severe chronic bronchitis. Thorax, 34: 51-56.

Duncan, D., Paterson, I.C. Harris, D. and Crompton, G.K., 1977, Comparison of the bronchodilator effects of salbutamol inhaled as a dry powder and by conventional pressurized aerosol. Br. J. Clin. Pharmacol., 4: 669-671.



Fissan, H. and Schioientek, G., 1987, Sampling and transport of aerosols. TSI J. of Particle Instrumentation, 2: 3-10.

Foreman, J.C. and Garland, L.G., 1976, Cromoglycate and other antiallergic drugs: A possible mechanism of action. Br. Med. J., 1: 820-821.

Francis, P.W.J., Kelly, C.A. and Zimmerman, P.V., 1983, Comparison of salbutamol powder with terbutaline aerosol administered with tube spacers in asthmatic children. Aust. Paed. J., 19: 245-247.

Fuller, R.W. and Collier, J.G., 1983, The pharmacokinetic assessment of sodium cromogylcate. J. Pharm. Pharmacol., 35: 289-292.

Fuchs, 1964, The mechanics of aerosols. Pergamon Press, Oxford.

Godfrey, S., Balfour-Lynn, L. and König, P., 1975, The place of cromolyn sodium in the long-term management of childhood asthma based on a 3- to 5-year follow up. J. Paediatr., 87: 465-473.

Gonda, I. and Byron. P.R., 1978, Perspectives on the biopharmacy of inhalation aerosols. Drug Dev. Ind. Pharm., 4: 243-259.

Grimwood, K., Johnson-Barrett, J.J. and Taylor, B., 1981, Salbutamol: Tablets, inhalation powder, or nebulizer? Brit. Med. J., 282: 105-106.

Groth, S. and Dirksen, H., 1983, Optimal inhalation procedure for the fenotenol powder inhaler. *Eur. J. Resp. Dis.*, 64: 17-24.

Hale, F.C., Olsen, C.R. and Mickey, J.R., 1968, The measurement of bronchial wall components. *Am. Rev. Resp. Dis.*, 98: 978-987.

Hallworth, G.W., 1977, An improved design of powder inhaler. *Br. J. Clin. Pharmacol.*, 4: 689-690.

Hallworth, G.W. and Andrews, U.G., 1976, Size analysis of suspension inhalation aerosols by inertial separation methods. *J. Pharm. Pharmacol.*, 28: 898-907.

Hallworth, G.W., Clough, D., Newnham, T. and Andrews, U.G., 1978, A simple impinger device for rapid quality control of the particle size of inhalation aerosols delivered by pressurised aerosols and powder inhalers. *J. Pharm. Pharmacol.*, 30: 31P.

Hallworth, G.W. and Westmoreland, D.G., 1987, The twin impinger: A simple device for assessing the delivery of drugs from metered dose pressurized aerosol inhalers. *J. Pharm. Pharmacol.*, 39: 966-972.

Heel, R.C., Brogden, R.N., Speight, T.M., 1978, Fenoterol: A review of its pharmacological properties and therapeutic efficacy in asthma. *Drugs*, 15: 39-43.

Hersey, J.A., 1975, Ordered mixing: A new concept in powder mixing practice. *Powder Technol.*, 11: 41-44.

Hetzel, M.R. and Clark, T.J.H., 1976, Comparison of intravenous and aerosol salbutamol. *Br. Med. J.*, 2: 919.

Hetzel, M.R. and Clark, T.J.H., 1977, Comparison of salbutamol Rotahaler with conventional pressurized aerosol. *Clin. Allergy*, 7: 563-568.

Heyder, J., Gebhart, J., Stahlhofen, W. and Stuck, R., 1982, Biological variability of particle deposition in the human respiratory tract during controlled and spontaneous mouth-breathing. *Ann. Occup. Hyg.*, 26: 137-147.

Hiller, F.C., Mazumder, M.K., Wilson, J.D., and Bone, R-G., 1980, Effect of low and high relative humidity on metered-dose bronchodilator solution and powder aerosols. *J. Pharm. Sci.*, 69: 334-337.

Hiller, F.C., Mazumder, M.K., Wilson, J.D. and Bone, R.G., 1978, Aerodynamic size distribution of metered dose bronchodilator aerosols. *Am. Rev. Resp. Dis.*, 118: 311-317.

Ho, K.K.L., 1988, An *in vitro* and *in vivo* evaluation of venturi nebulizers. PhD Thesis, University of Wales.

Hodson, M.E., 1988, Antibiotic treatment: Aerosol therapy. *Chest*, 94: 1565-1615.

Hogg, J.C., 1982, The pathophysiology of asthma. *Chest*, 82, Suppl.: 85-115.



Jaques, L.B., Mahadoo, J. and Kavanagh, L.W., 1976, Intrapulmonary heparin: A new procedure for anticoagulant therapy. *Lancet*,: 1157-1161.

Jenkins, S.C., Richard, W.H., Fultern, T.J., and Moxham, J., 1987, Comparison of domiciliary nebulized salbutamol and salbutamol from a metered dose inhaler in stable chronic air flow limitation. *Chest*, 91: 804-807.

John, W., 1980, Particle charge effects. In: Generation of aerosols and facilities for exposure experiments. Ed. : Willeke, K. , Ann Arbor Science Publishers Inc., 141-151.

Jones, T.M. and Pilpel, N., 1965, Some physical properties of lactose and magnesia. *J. Pharm. Pharmacol.*, 17: 440-448.

Jones, A.L., Kellaway, I.W. and Taylor, G., 1988. Pulmonary absorption of aerosolised Insulin in the rabbit, *J. Pharm. Pharmacol.*, 40: 99P.

Karig, A.W., Peck, G.E. and Sperandio, G.J., 1973, Evaluation of inhalation aerosols using a simulated lung apparatus. *J. Pharm. Sci.*, 62: 811-815.

Kim, C.S., Trizillo, D. and Sakner, M.A., 1985, Size aspects of metered-dose inhaler aerosols. *Am. Rev. Resp. Dis.*, 132: 137-142.

Kirk, W.F., 1972, *In vitro* method of comparing clouds produced

from inhalation aerosols for efficiency in penetration of airways. J. Pharm. Sci., 61: 262-264.

Köhler, D., Fleischer, W. and Ma thyo, 4, 1988, New method for easy labelling of Beta-2-agonists in the metered dose inhaler with Tc- 99m. Respiration, 53: 65-73.

Koing, P, 1985, Spacer devices used with metered dose inhalers: breakthrough or gimmick. Chest, 88: 276-283.

Kulvanich, P. and Stewart, P.J., 1987, The effect of particle size and concentrations on the adhesive characteristics of a model drug-carrier interactive system. J. Pharm. Pharmacol., 39: 673-678.

Kulvanich, P. and Stewart, P.J., 1987, Fundamental considerations in the measurement of adhesional forces between particles using the centrifuge method. Int. J. Pharm., 35: 111-120.

Lai, F.K. and Hersey, J.A., 1979, A cautionary note on the use of ordered powder mixtures in pharmaceutical dosage forms. J. Pharm. Pharmacol., 31: 800.

Lam, T.P., Martin, G.P., Bell, A.T. and Marriot, C., 1984, The effect of humidity on the particle size distribution of salbutamol measured over realistic deposition time intervals. J. Pharm. Pharmacol., 36: 84P.

Larson, S. and Svedmyr, N., 1977, Bronchodilating effect and side effects of Beta<sub>2</sub>-adrenoceptor stimulants by different modes of

administration. *Am. Rev. Resp. Dis.*, 116: 861-869.

Lauber, B.L., Swift, D.L., Wagner, H.N., Norman, P.S. and Adams, G.K., 1986, The effect of bronchial obstruction on central airway deposition of a saline aerosol in patients with asthma. *Am. Rev. Resp. Dis.*, 133: 740-743.

Lawford, P. and McKenzie, D., 1981, Does inspiratory flow rate affect bronchodilator response to an aerosol  $\beta_2$ -agonist? *Thorax*, 36: 714.

Lee, S.L., 1985, Particle drag in turbulent two-phase suspension flow. Second workshop on two-phase flow predictions, Erlangen, Germany.

Lourenco, R.V. Loddenkemper, R. and Carton, R.W., 1972, Pattern of distribution and clearance of aerosols in patients with bronchiectasis. *Am. Rev. Resp. Dis.*, 106: 857-866.

Lourenco, R.V. and Cotromanes, E., 1982, Clinical aerosols I: characterization of aerosols and their diagnostic uses. *Arch. Intern. Med.*, 142: 2163-2172.

Maugh, T.H., 1984, What is the risk from chlorofluorocarbons? *Science*, 223: 1051-1052.

McPhillips, J.J., 1985, In: *Modern pharmacology*. 2nd Edition, Pharmacological control of asthma: 1014-1027.



McFarland, A.R., Wedding, J.B. and Cermak, J.E., 1977, Wind tunnel evaluation of a modified Andersen impactor and an all-weather sampler inlet, *Atm. Env.*, 11: 535-539.

Mercer, T.T., 1973, In: *Aerosol technology in hazard evaluation*, Academic Press, New York.

Miller, W.F., 1973, Aerosol therapy in acute and chronic respiratory disease. *Arch. Intern. Med.*, 131: 148-155.

Mitchell, R.I. 1960. Retention of aerosol particles in the respiratory tract. *Am. Rev. Resp. Dis.*, 82: 627-639.

Molina, M.J. and Rowlands, F.S., 1974, Stratospheric sink for chlorofluoromethanes: chlorine atom catalyzed destruction of ozone. *Nature*, 249: 810-812.

Muittari, M. and Ahonen, A., 1979, Comparison of the bronchodilator effect of inhaled salbutamol powder and pressurized salbutamol aerosol. *Current Therapeutic Research*, 25: 804-808.

Nadel, J.A. and Barnes P.J. 1984, Autonomic regulation of the airways. *Ann. Rev. Med.*, 35: 451-467.

Newman, S.P. and Clark, S.W., 1985, *Aerosols in medicine*. Elsevier, Amsterdam.

Newman, S.P. and Clark, S.W., 1983, Therapeutic aerosols: I. Physical and practical considerations. *Thorax*, 38: 881-886.

Newman, S.P., Pavia, D., Garland, N. and Clarke, S.W., 1982, Effects of various inhalation modes on the deposition of radioactive pressurized aerosols. *Eur. J. Resp. Dis.*, 63, Suppl. 119: 57-65.

Newman, S.P., Pavia, D. and Clarke, S.W., 1981, How should a pressurized  $\beta$ -adrenergic bronchodilator be inhaled? *Eur. J. Resp. Dis.*, 62: 3-21.

Newman, S.P., Killip, M., Pavia, D., Moren, F. and Clarke, S.W., 1984, The effect of changes in particle size on the deposition of pressurized inhalation aerosols. *Int. J. Pharm.*, 19: 333-337.

Newman, S.P., Moren, F., Trofast, E., Talaei, N. and Clarke, S.W., 1989, Deposition and clinical efficacy of terbutaline sulphate from Turbohaler, a new multi-dose powder inhaler. *Eur. Resp. J.*, 2: 247-252.

Newman, S.P., Pellow, P.G.D. and Clarke, S.W., 1986, Choice of nebulizers and compressors for delivery of carbenicillin aerosol. *Eur. J. Resp. Dis.*, 69: 160-168.

Nelson, H.S., 1982, Beta adrenergic agonists. *Chest*, 82, Suppl.: 335-385.

Nouri, J.M., Whitelaw, J.H. and Yianneskis, M., 1987, Particle

motion and turbulence in dense two-phase flow. *Int. J. Multiphase Flow*, 13: 729-739.

Nurtan, A., Esmen, and Lee, T.C., 1980, Distortion of cascade impactor measured size distribution due to bounce and blow off. *Am. Ind. Hyg. Ass. J.*, 41: 410-419.

Padersen, S. and Steffensen, G., 1986, Fenoterol powder inhaler technique in children: Influence of inspiratory flow rate and breath-holding. *Eur. J. Resp. Dis.*, 68: 207-241.

Padfield, J.M., Winterborn, I.K., Pover, G.M. and Tattersfield, A., 1983, Correlation between inertial impactor performance and clinical performance of a bronchodilator aerosol. *J. Pharm. Pharmacol.*, 35: 10P.

Paterson, J.W., Woolcock, A.J. and Shenfield, G.M., 1979, Bronchodilator drugs. *Am. Rev. Resp. Dis.*, 120: 1149-1188.

Pedersen, S., Hansen, O.R. and Fuglsang, G., 1990, Influence of inspiratory flow rate upon the effect of a Turbohaler. *Archives of Disease in Childhood*, 65: 308-319.

Petersen, L.N. and Petersen, B.N., 1983, Fenoterol inhalation powder Aerosol. *Eur. J. Resp. Dis.*, 64, Suppl. 130: 1-5.

Pitchard, J.N., Jefferies, S.J. and Black, A., 1986, Sex differences in the regional deposition of inhaled particles in the 2.5-7.5 $\mu$ m size range. *J. Aerosol. Sci.*, 17: 385-389.



Persson, G., Gruvstad, E. and Stahl, E., 1988, A new multiple dose powder inhaler (Turbohaler) compared with a pressurized inhaler in a study of terbutaline in asthmatics. *Eur. Resp. J.*, 1: 681-684.

Rao, A.K. and Whitby, K.T., 1978, Non-ideal collection characteristics of inertial impactors I. Single stage impactors and solid particles. *J. Aerosol. Sci.*, 9: 77-86.

Rees, P.J., Clarke, T.J.H. and Moren, F., 1982, The importance of particle size in response to inhaled bronchodilators. *Eur. J. Resp. Dis.*, 63 Suppl. 119: 73-78.

Richards, R., Simpson, S.F., Renwick, A.G. and Holgate, S.T., 1988, Inhalation rate of sodium cromoglycate determines plasma pharmacokinetics and protection against AMP-induced bronchoconstriction in asthma. *Eur. Resp. J.*, 1: 896-901.

Riley, D.J., Weitz, B.W. and Edelman, N.H. 1976, The response of asthmatic subjects to isoproterenol inhaled at differing lung volumes. *Am. Rev. Resp. Dis.*, 114: 509-515.

Riley, D.J., Lin, R.T. and Edelman, N.H., 1979, Enhanced responses to aerosolized bronchodilator therapy in asthma using respiratory manouevres. *Chest*, 76: 501-507.

Rose, H.D., Pendharder, M.B., Sinder, G.L. and Kery, R.C., 1970, Evaluation of sodium colistimethate aerosol in gram-negative infections of the respiratory tract. *J. Clin. Pharmacol.*, 10: 274-281.

Salorinne, Y. and Ahoene, A., 1988, Comparison of the bronchodilator effect of ipratropium bromide powder and two doses of ipratropium bromide aerosol in the treatment of asthma. *Current Therapeutic Research*, 43: 1073-1081.

Scadding, J.G., 1987, Asthma and bronchial reactivity. *Br. Med. J.*, 294: 1115-1116.

Sciarra, J.J. and Cutrie, A., 1978, Simulated respiratory system for *in vitro* evaluation of two inhalation delivery systems using selected steroids. *J. Pharm. Sci.*, 67: 1428-1431.

Shenfield, G.M. and Paterson, J.W., 1973, Clinical assessment of bronchodilator drugs delivered by aerosols. *Thorax*, 28: 124-128.

Speed, W.G., 1960, Ergotamine tartrate inhalation: A new approach to the management of recurrent vascular headaches. *Amer. J. Med. Sci.*, 240: 327.

Speizer, F.E., Doll, R., Heaf, P.J. and Strang, L.B., 1968, Investigations into use of drugs preceding death from asthma. *Brit. Med. J.*, 1: 335-339.

Spiro, S.G., Singh, C.A., Tolfree, S.E.J., Partridge, M.R. and Short, M.D., 1984, Direct labelling of ipratropium bromide aerosol and its deposition pattern in normal subjects and patients with chronic bronchitis. *Thorax*, 39: 432-435.

Staniforth, J.N. and Rees, J.E., 1982<sup>a</sup> Effect of vibration time, frequency and acceleration on drug content uniformity. J. Pharm. Pharmacol., 34: 700-706.

Staniforth, J.N. and Rees, J.E., 1982<sup>b</sup>, Electrostatic charge interactions in ordered powder mixes. J. Pharm, Pharmacol., 34: 69-76.

Staniforth, J.N. and Rees, J.E., 1982<sup>c</sup> Investigation of triboelectric and ionisation methods for electrostatic charging of powder particles. Int. J. Pharm. Tech and Prod. Mfr., 3: 69-72.

Staniforth, J.N., Rees, J.F., Lai, F.K. and Hersey, J.A., 1981, Determination of interparticulate forces in ordered powder mixtures. J. Pharm. Pharmacol., 33: 485-490.

Staniforth, J.N., Rees, J.F. and Hersey, J.A., 1982, Interparticle forces in binary and ternary ordered powder mixes. J. Pharm. Pharmacol., 34: 141-145.

Summers, Q.A., Clark, A.R., Hollingsworth, A., Flemming, J. and Holgate, S.T., 1989, Preparation of a radio-labelled aerosol for administration by metered-dose inhaler that preserves the aerosol size distribution of the drug. In: Drug delivery to the lung. Aerosol Society meeting , Ware.

Svartengren, M., Philipson, K. and Camner, P., 1989, Individual differences in regional deposition of 6 $\mu$ m particles in humans with



induced bronchoconstriction. *Experimental Lung Research*, 15: 139-149.

Svedmyr, N., Lofdahl, C.G. and Svedmyr, K., 1982, The effect of powder aerosol compared to a pressurized aerosol. *Eur. J. Resp. Dis.*, 63, Suppl. 119: 81-88.

The Task Group on Lung Dynamics, 1966, Deposition and retention models for internal dosimetry of the human respiratory tract. *Health Physics.*, 12: 173.

Thiessen, B. and Pedersen, O.F., 1980, Effect of freon inhalation on maximal expiratory flows and heart rhythm after treatment with salbutamol and ipratropium bromide. *Eur. J. Resp. Dis.*, 61: 156-161.

Turner, J.R. and Hering, V., 1987, Greased and oiled substrates as bounce-free impaction surfaces. *J. Aerosol Sci.*, 18: 215-224.

Vidgren, M.T., Vidgren, P.A. and Peronen, T.P., 1987<sup>a</sup> Comparison of physical and inhalation properties of spray-dried and mechanically micronized disodium cromoglycate. *Int. J. Pharm.*, 35: 139-144.

Vidgren, M., Karkkainen, A., Karjalainen, P. and Paronen, P., 1987<sup>b</sup>, A novel labelling method for measuring the deposition of inhalation aerosols. *Int. J. Pharm.*, 37: 239-244.

Vidgren, M.T., Karkkainen, A., Paronen, T.P. and Karjalainen, P., 1987, Respiratory tract deposition of Tc 99m-labelled drug particles administered via a dry powder inhaler. *Int. J. Pharm.*, 39: 101-105.

Vidgren, M.T., Karkkainen, A., Karjalainen, P., Paronen, T.P. and Nuutinen, J., 1987, Effect of powder inhaler design on drug deposition in the respiratory tract. *Int. J. Pharm.*, 42: 211-216.

Vidgren, M., Paronen, P. and Vidgren, P., 1990, *In vivo* evaluation of the new multiple dose powder inhaler and the Rotahaler using gamma scintigraphy. *Acta. Pharm. Nord.*, 2: 3-10.

Vincent, J.H., Hutson, D. and Mark, D., 1982, The nature of air flow near the inlets of blunt dust sampling probes. *Atm. Env.*, 16: 1243-1249.

Vincent, J.H., Emmett, P.C. and Mark, D., 1985, The effect of turbulence on the entry of airborne particles into a blunt dust sampler. *Aerosol Sci. Technol.*, 4: 17-29.

Vincent, J.H., 1988, Aerosol sampling: The state of the art. *J. Aerosol Sci.*, 19: 899-901.

Walker, S.R., Evans, M.E., Richards, A.J. and Paterson, J.W., 1972, The fate of [ $^{14}\text{C}$ ] disodium cromoglycate in man. *J. Pharm. Pharmacol.*, 24: 525-531.

Wetterlin, K., 1988, Turbohaler: A new powder inhaler for administration of drugs to the airways. *Pharmaceutical Research*, 5: 506-508.

Wienner, R.W., Okazaki, K. and Willeke, K., 1988, Influence of turbulence on aerosol sampling efficiency. *Atm. Env.*, 22: 917-928.

Woolcock, A.J., 1977, Inhaled drugs in the prevention of asthma. *Am. Rev. Resp. Dis.*, 115: 191-194.

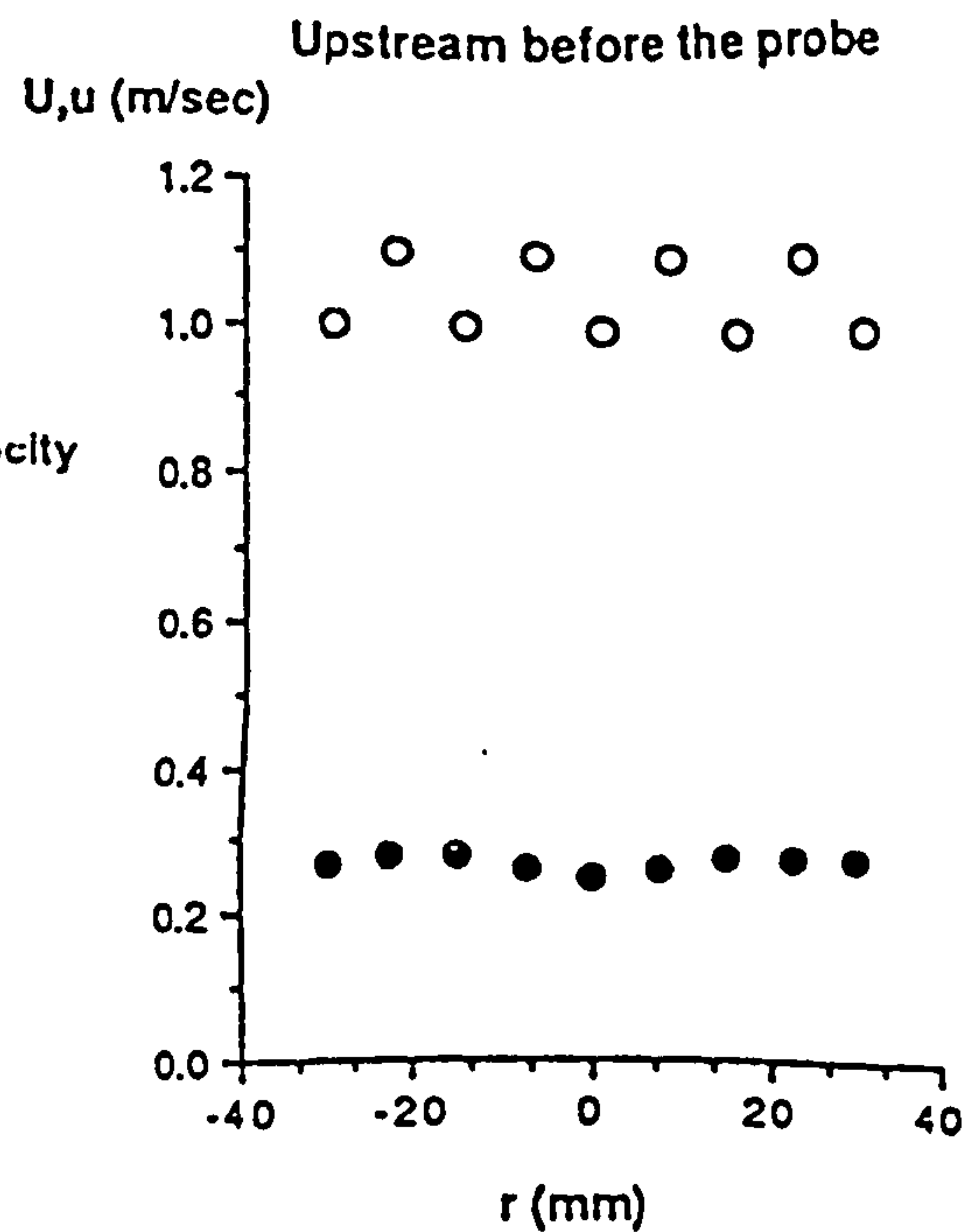
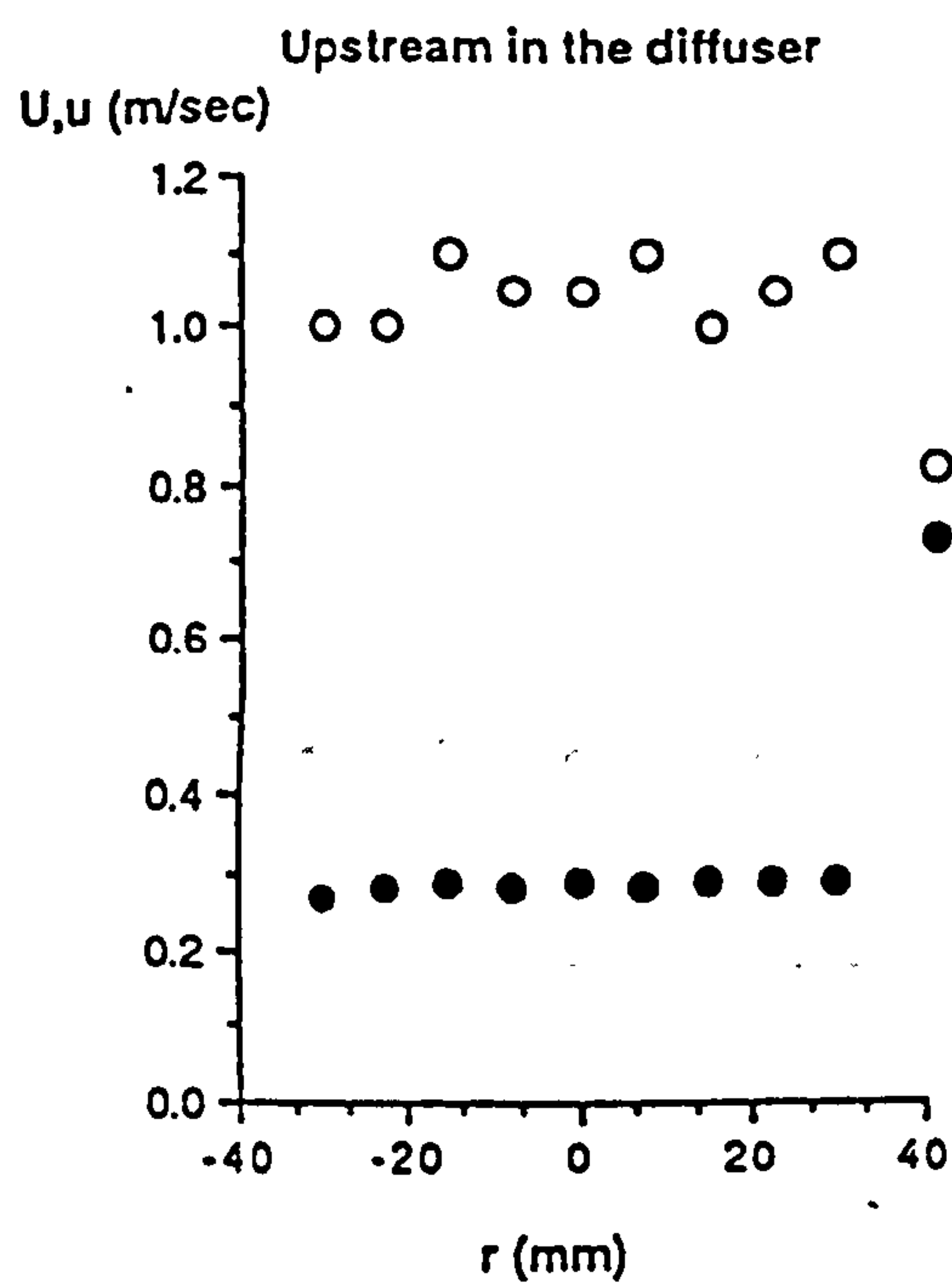
Yianneskis, M., 1987, Velocity, particle sizing and concentration measurement techniques for multiphase flow. *Powder Technology*, 49: 47-51.

Yianneskis, M and Whitelaw, I.H., 1984, Velocity characteristics of pipe and jet flows with high particle concentrations. *Int. Symp. on liquid solid flow and erosion wear in industrial equipment (ASME Fluids Engineering Conf.)*, London.

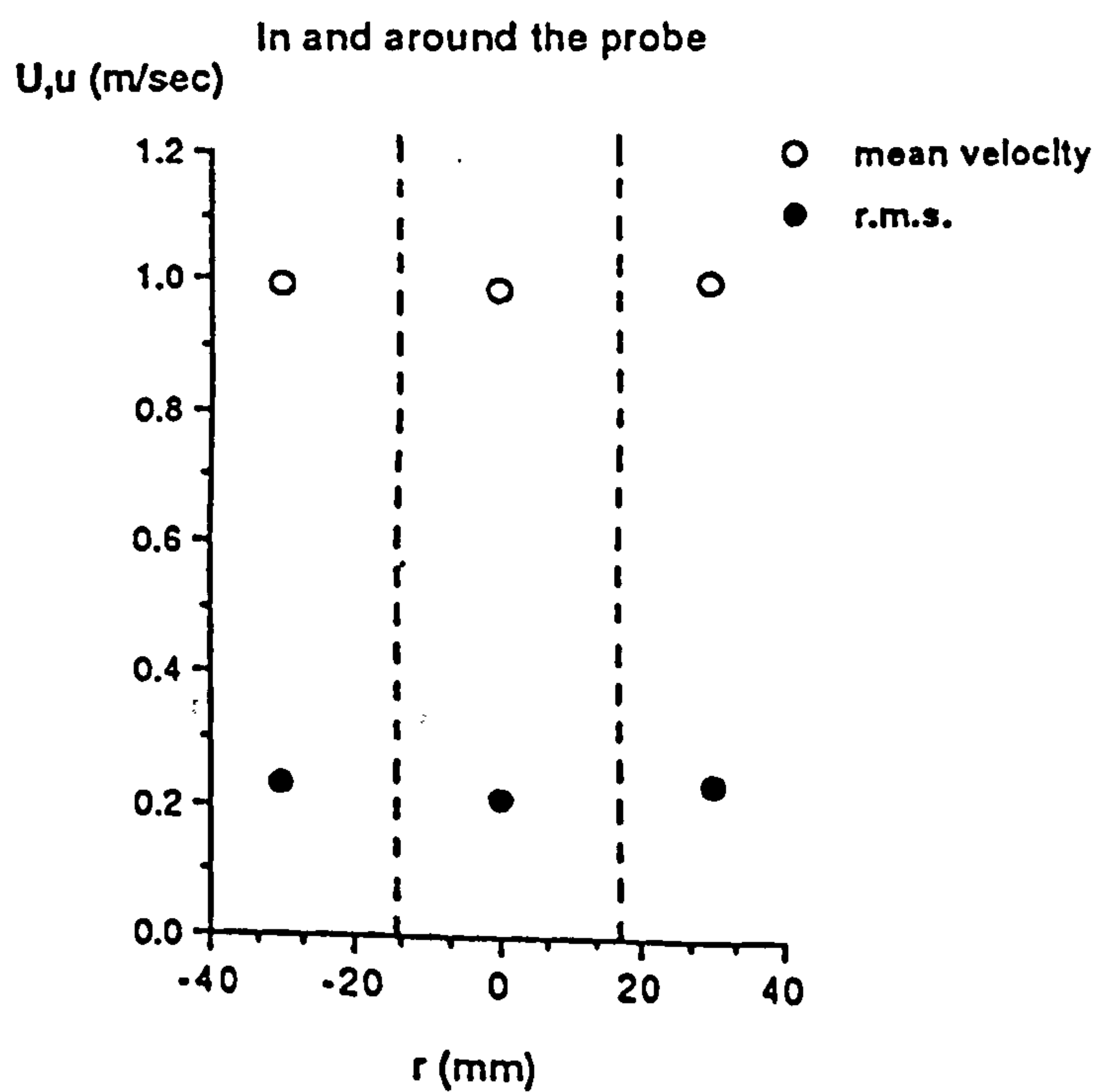
Yu, D.Y.C., Galant, S.P. and Gold, W.M., 1972, Inhibition of antigen - induced bronchoconstriction by atropine in asthmatic patients. *J. Appl. Physiol.*, 32: 823-828.



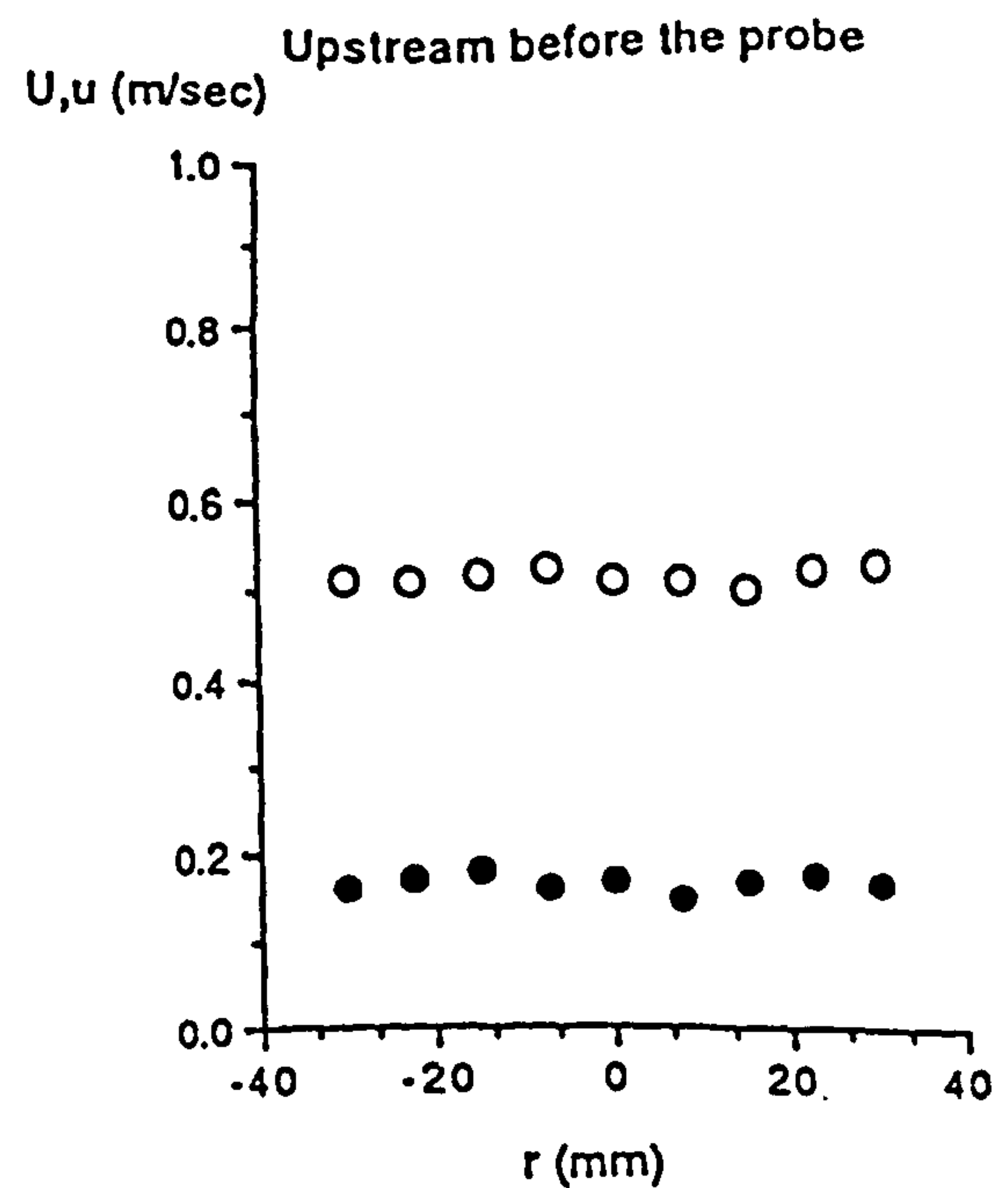
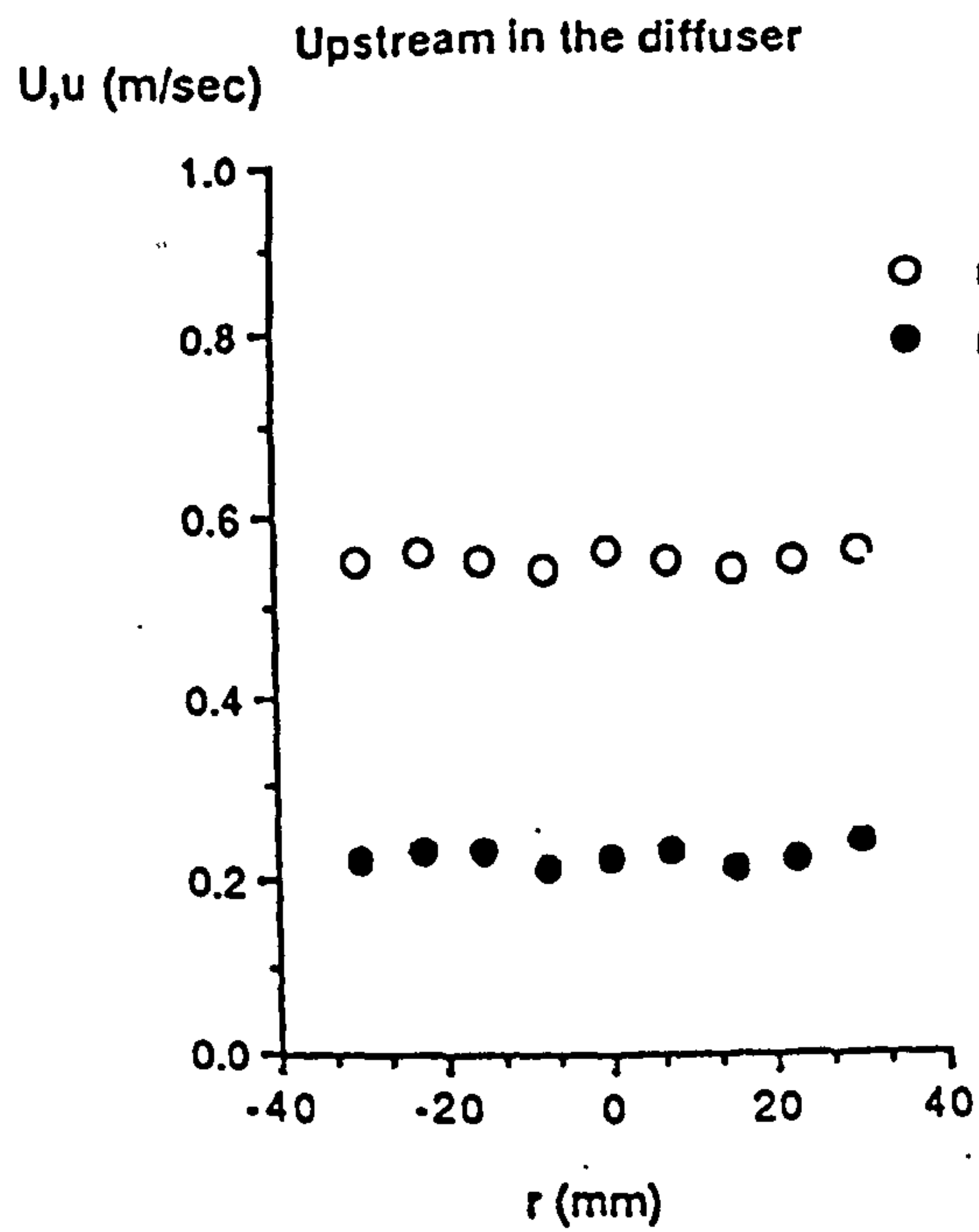
## Appendix



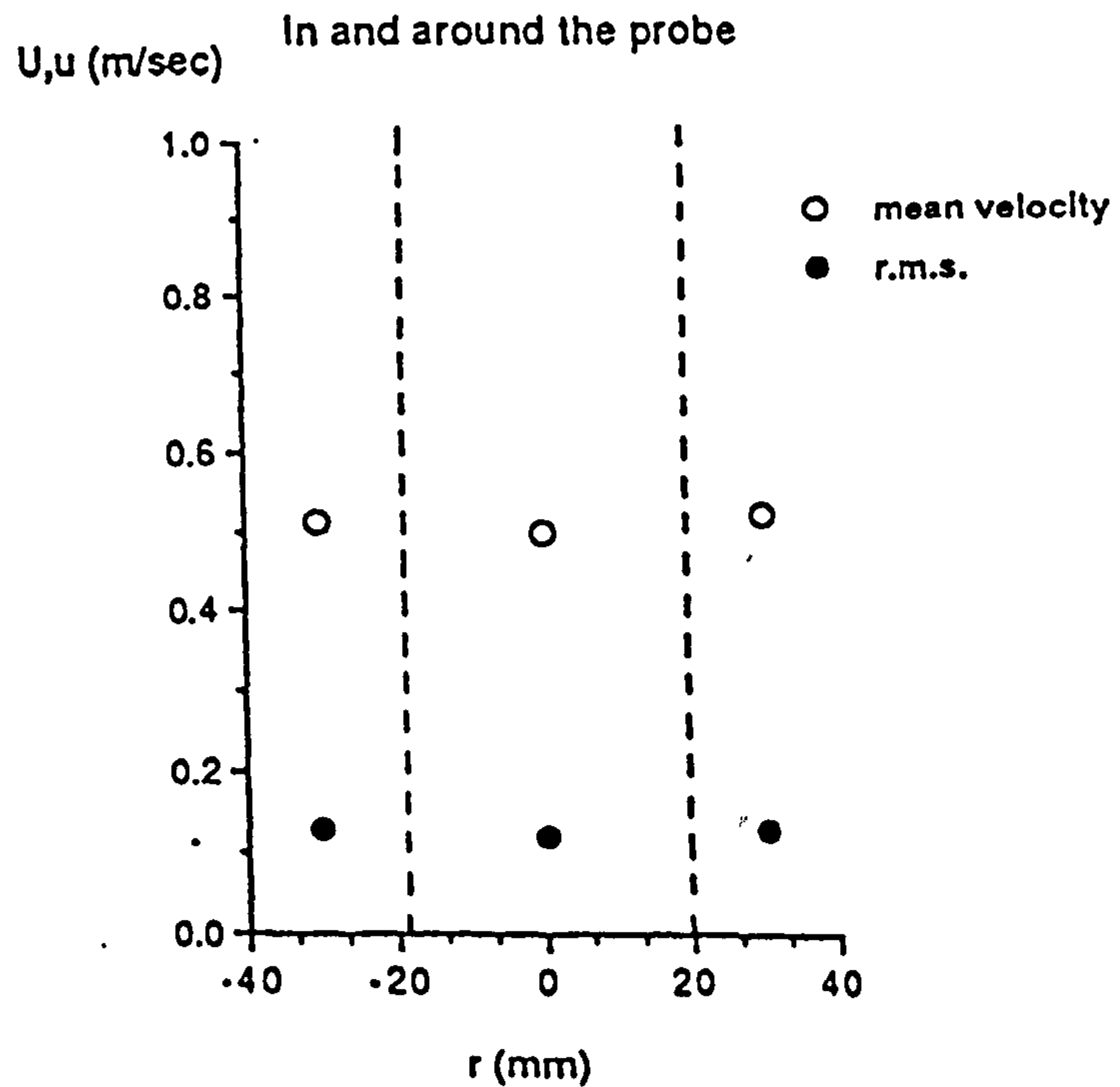
U Mean velocity  
u r.m.s. velocity  
r Distance from the centre



Profiles of axial mean and r.m.s. velocities of the gas at an airflow of 200l/min

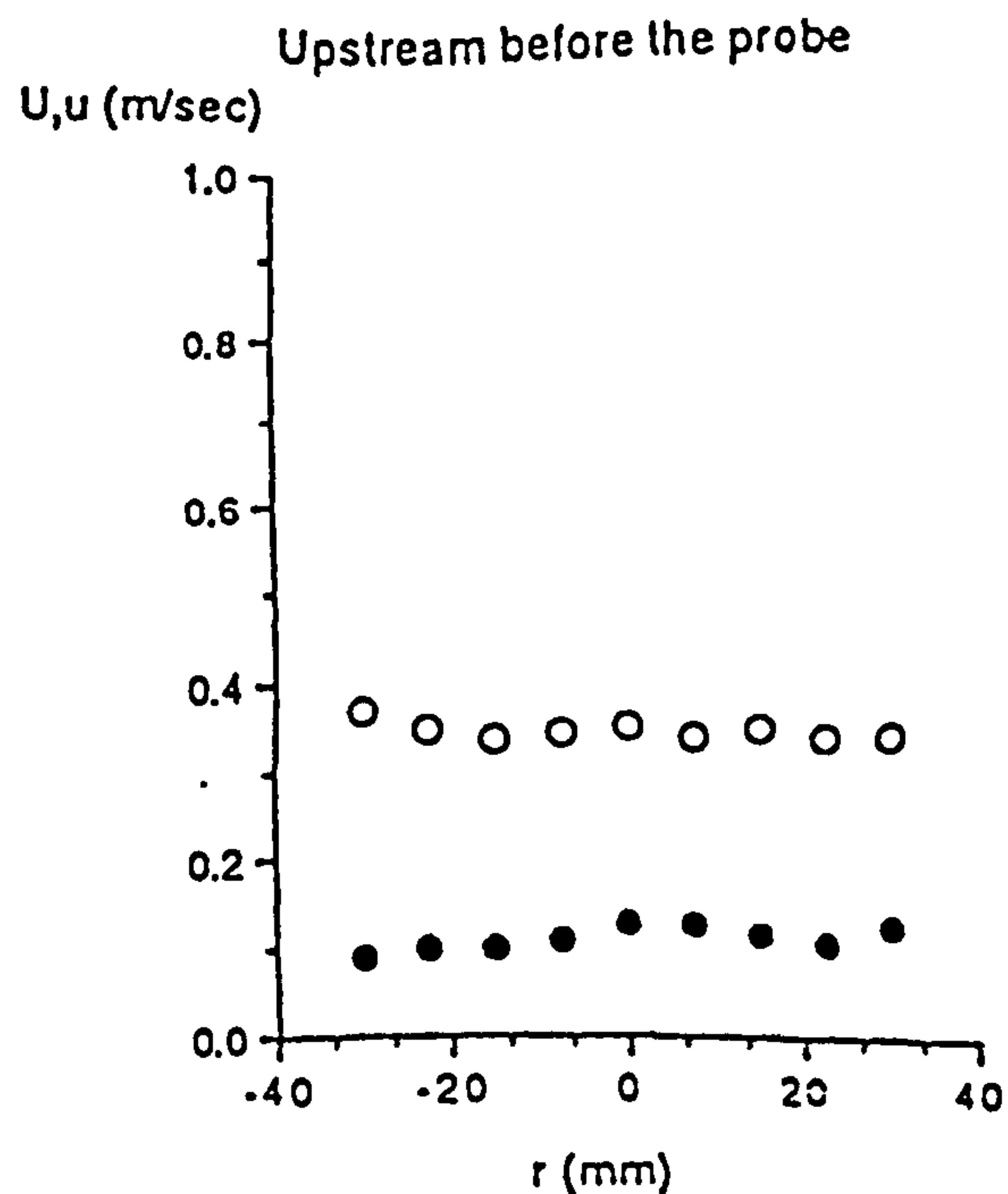
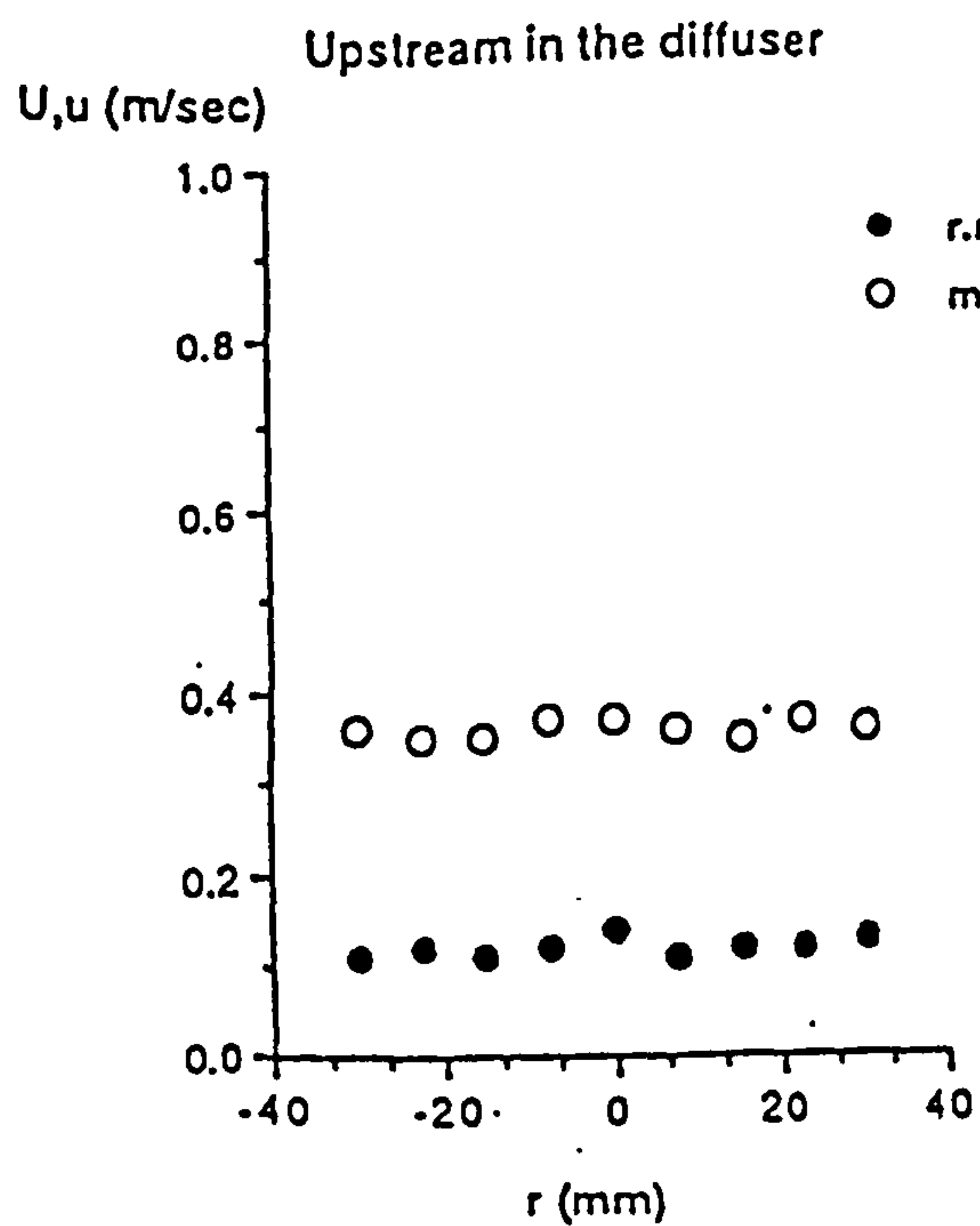


**U** Mean velocity  
**u** r.m.s. velocity  
**r** Distance from the centre

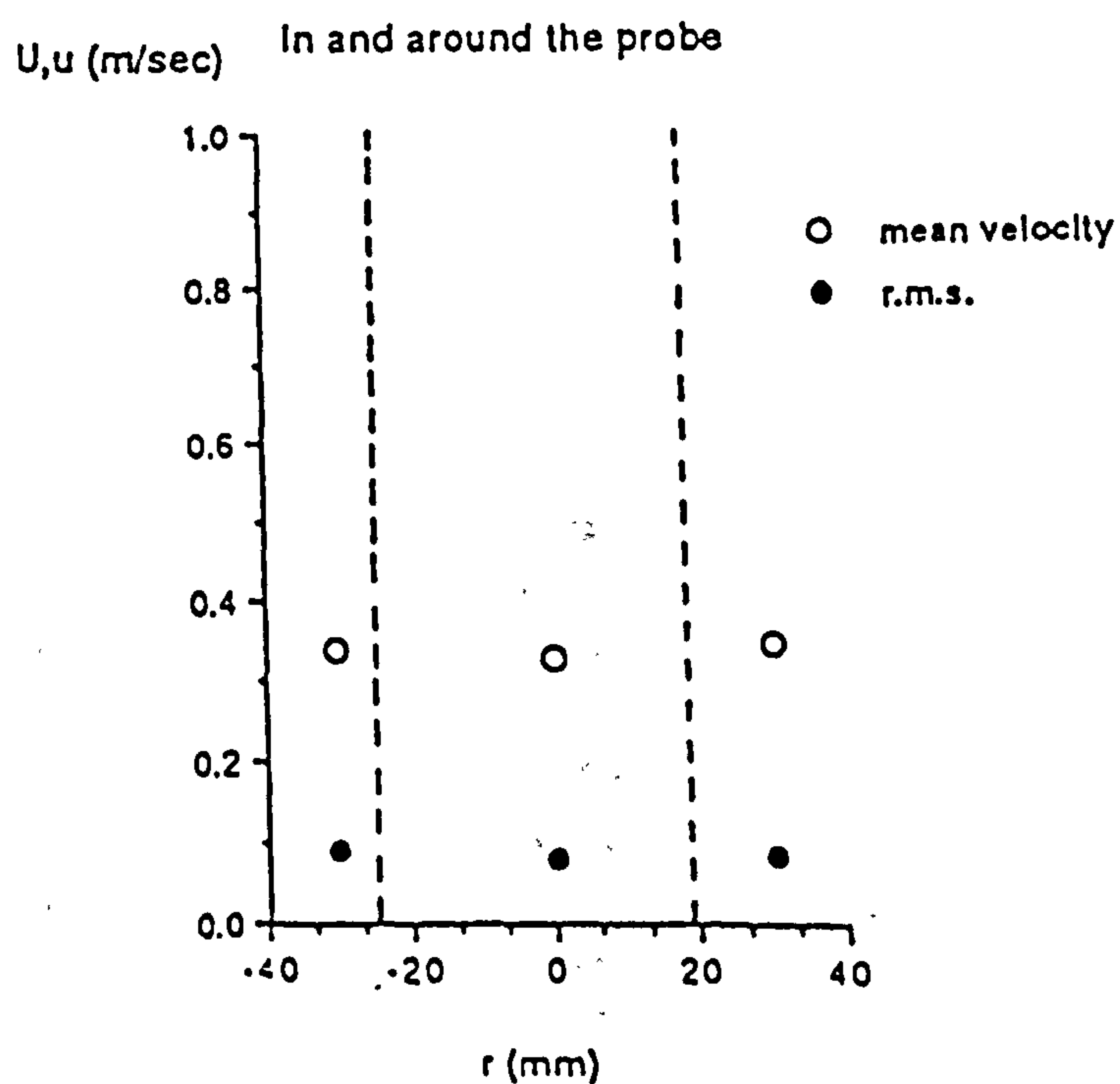


Profiles of axial mean and r.m.s. velocities of the gas at an airflow of 100 l/min

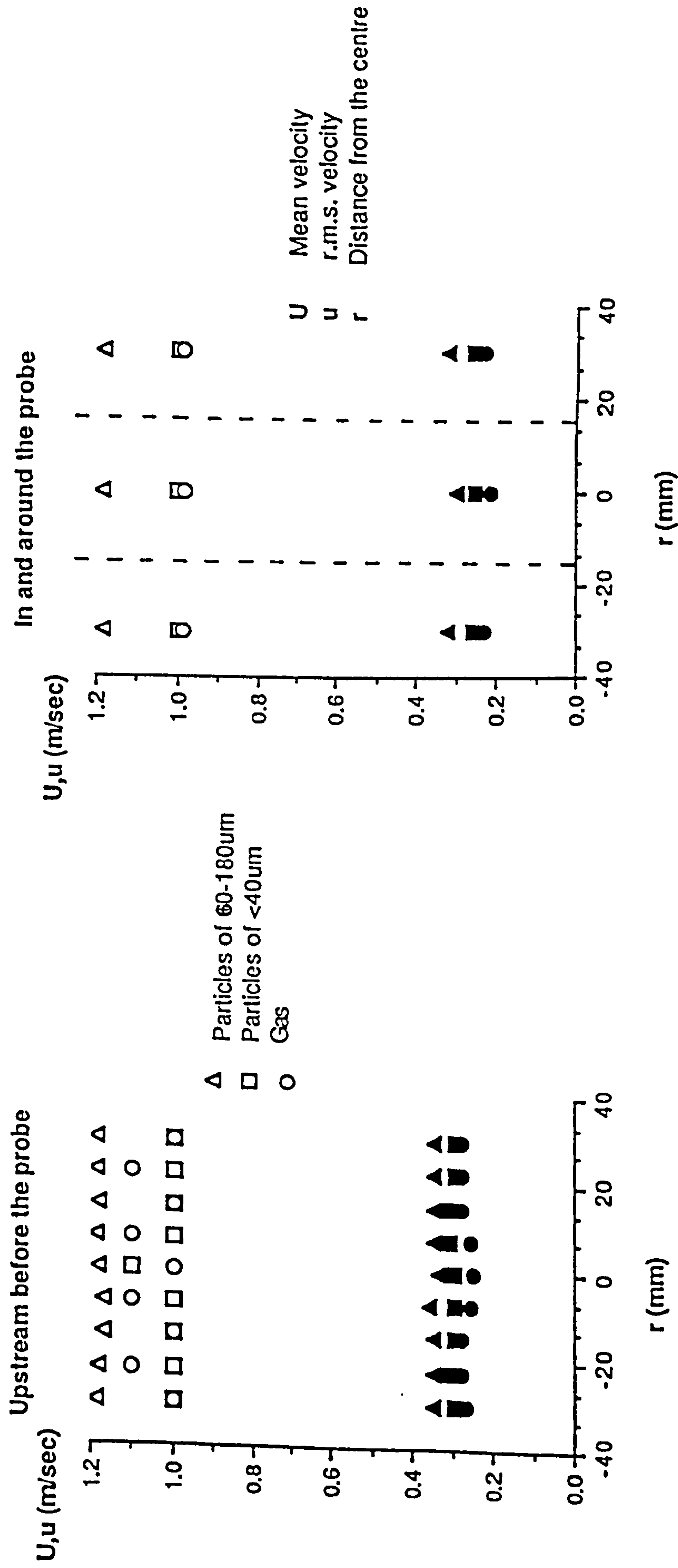




U Mean velocity  
 u r.m.s. velocity  
 r Distance from the centre



Profiles of axial mean and r.m.s. velocities of the gas at an airflow of 60 l/min



Profiles of axial mean (open symbols) and r.m.s. (solid symbols) velocities at an air flow of 200 l/min